

***To My Grandmother
and my Father***

Acknowledgments

I want to address my first words of gratitude to my supervisors, who turned this challenge into a wonderful journey and inspired me as a researcher but most of all, as a person. First and foremost, I would like to thank Professor Fernanda Borges for her unrivalled guidance, enthusiasm, kindness, and most importantly for the unconditional friendship. I also would like to thank Professor Eugenio Uriarte for his support, encouragement and friendliness.

I would also like to thank the FCT for its financial support, to Faculty of Sciences of the University of Porto and CIQ-("Centro de Investigação em Química"), for providing me the means for the execution of the experimental work.

I want to express my gratitude to all the research groups that collaborated in the execution of the work described in this thesis, namely the Department of Pharmacology of Faculty of the Pharmacy, University of Santiago de Compostela, Spain, the Institute of Pharmacology and Toxicology, University of Wuzburg, Germany, Department of Pharmacology of the Faculty of Pharmacy, University "Magna Græcia", Catanzaro, Italy and the Molecular Modeling Section (MMS) of the Pharmaceutical Science Department, university of Padua, Italy.

To Professor Nuno Milhazes, my profound thanks for the invaluable brainstorming sessions, encouragement and his one of a kind humour, but above all for his precious friendship.

Thank you to Professor Jorge Garrido and Professor Manuela Garrido, for their support, companionship and for believing in me.

To all of my colleagues in the lab, whose names I will not discriminate to avoid of forgetting someone, a genuine thank you for all the good times shared in the lab.

I would also like to thank all my friends outside of the research group with whom I will forever share great memories and, undoubtedly, create new ones in the future.

Abstract

The last few decades have provided stunning progresses in the understanding of physiopathology of several diseases. The remarkable progress in research fields, like genetics, immunology, neurobiology, among others, as well as the advent of more powerful tools, have made it possible to characterize, monitor, and understand far more of the basis of physiology and disease. However, for some diseases the treatment remains a problematic issue as the efforts performed so far were not translated into therapeutic solutions. Notwithstanding the steady increase in the total amount of money spent on pharmaceutical research and development over the past decade, the number of new drug approvals has declined in recent years. Despite the advances in technology, drug discovery is still a lengthy, expensive, difficult, and inefficient process, with a low rate of success. Therefore, the search for new chemical entities is still an unmet need for the drug discovery process.

Application of new drug discovery approaches/concepts for multifactorial diseases, such as cancer and neurodegenerative diseases, have prompted a switch on the strategy of one-molecule one-target to a new one, the multi-target approach, where a single chemical entity may be able to modulate multiple targets simultaneously.

In the present project, the main challenges were the validation of chromones as a privileged structure for the design of new drug candidates for Parkinson disease and the development dual-target lead compounds. Accordingly, the design of a chromone library to attain structure-activity relationships and the development of concise and diversity-oriented synthetic strategies has been carried out along this project. The small but innovative chromone libraries were screened to ascertain their potential as MAO-B inhibitors as well as A_{2A} adenosine receptor ligands. The output of the biological screening assays gave rise to preliminary structure-activity relationship regarding both of the targets. The overall data showed that chromones are privileged structures for drug discovery and development processes in the field of Parkinson disease and that chromone-3-(3'-hydroxy-4'-methoxyphenyl)carboxamide and chromone-3-(4'-chlorophenyl)carboxamide, exhibiting a IC_{50} for *h*MAO- B in a nanomolar range and affinity towards A_{2A} ARs, can be regarded as putative leads for further optimisation. In addition, during the drug discovery process interesting A_3 AR ligands based on chromone scaffold have been found, namely chromone-2-carboxamides such as the chromone-2-(4'-methoxyphenyl)carboxamide which presented a K_i value for *hA*₃ AR of 9,580 nM and reasonable to good selective indexes regarding the other ARs ligands.

Complementarily, the work described along this thesis was sustained on molecular docking studies performed over MAOs isoforms and ARs, for the most active chromone derivatives.

Resumo

As últimas décadas têm sido pautadas por um impressionante progresso em áreas como a genética, imunologia, neurobiologia, entre outras. O crescente conhecimento científico, bem como o desenvolvimento de novas e mais potentes tecnologias, tornaram possível não só a caracterização e monitorização dos processos fisiológicos mas também uma maior compreensão dos processos patológicos de inúmeras doenças. No entanto, para algumas enfermidades os esforços até agora realizados não conseguiram ser traduzidos em soluções terapêuticas.

O processo de descoberta e desenvolvimento de novos fármacos é dispendioso, demorado e com uma baixa taxa de sucesso. De facto, e apesar do crescente investimento económico por parte da indústria farmacêutica, o número de novos fármacos tem diminuído ao longo das últimas décadas. Neste contexto, a descoberta de novas entidades químicas (NCEs), candidatas a novos fármacos, continua a ser um tópico da maior relevância na química medicinal.

No caso das doenças de natureza multifatorial, como cancro e eventos neurodegenerativos, o processo de descoberta e desenvolvimento de novos fármacos é ainda um desafio. Numa tentativa de acelerar o processo assiste-se actualmente a uma modificação da estratégia do desenho racional de fármacos com passagem do paradigma “uma molécula-um alvo terapêutico” para uma abordagem multi-alvo, onde uma única entidade química tem ser capaz de modular, simultaneamente, mais do que um alvo.

O presente projeto consistiu na validação da cromona como uma estrutura privilegiada para a descoberta de novos candidatos a fármacos para a doença de Parkinson e no desenvolvimento de compostos líder com um mecanismo de acção em dois alvos terapêuticos. Neste contexto procedeu-se à obtenção e desenvolvimento de estratégias sintéticas para a construção de pequenas e inovadoras bibliotecas baseadas no núcleo da cromona. Adicionalmente, foram efetuados estudos para avaliação do seu potencial como inibidores da MAO-B e ligandos do recetor A_{2A} da adenosina. Os resultados obtidos foram interpretados através do estabelecimento de relações de estrutura-atividade e em estudos de modelização molecular, envolvendo as isoformas da MAO e os recetores da adenosina, os quais foram realizados para os derivados de cromonas mais potentes.

Os dados obtidos até à data permitiram concluir que a cromona pode ser uma estrutura privilegiada para a descoberta e desenvolvimento de novos fármacos para doença de Parkinson. Do estudo efectuado salienta-se os resultados obtidos para dois derivados da cromona sintetizados, nomeadamente a cromona-3-(3'-hidroxi-4'-

metoxifenil)carboxamida e a cromona-3-(4'-clorofenil)carboxamida, os quais exibiram um CI_{50} para *h*MAO-B na ordem dos nanomolar e afinidade relevante para o recetor A_{2A} da adenosina. Estes compostos, após uma etapa subsequente de otimização, podem produzir candidatos inovadores, com um mecanismo de ação duplo-alvo, e uma nova solução terapêutica para a doença de Parkinson. Salienta-se ainda os resultados obtidos para uma biblioteca de cromonas (cromona-2-carboxamidas), as quais evidenciaram, de uma forma geral, uma afinidade relevante para os recetores A_3 da adenosina, nomeadamente a cromona-2-(4'-metoxifenil)carboxamida a qual apresentou um valor de $K_i = 9,580$ nM para o referido recetor. Os dados obtidos, assim como a seletividade apresentada, leva a considerar este tipo de derivados de cromonas compostos passíveis de ser otimizados para o desenvolvimento de novos anticancerígenos.

Abbreviations

Ach – Acetylcholine

AChE – Acetylcholinesterase

Amino acids:

Asn – Asparagine

Cys – Cysteine

Gln – Glutamine

Glu – Glutamic acid

His – Histidine

Ile – Isoleucine

Leu – Leucine

Phe – Phenylalanine

Ser – Serine

Thr – Threonine

Trp – tryptophan

Tyr – Tyrosine

Val – Valine

ARs – Adenosine receptors

BOP – *O*-Benzotriazol-1-yloxytris(dimethylamino)phosphonium hexafluorophosphate

CNS – Central nervous system

COMT – Catechol-*O*-methyltransferase

COSY – Correlation spectroscopy

DA – Dopamine

DBU – Diazabicyclo[5.4.0]undec-7-ene

DOPAC – Dihydroxyphenylacetic acid

EI/MS – Electron Impact Mass Spectrometry

EL – Extra loop

GABA – Gamma aminobutyric acid

GP – Globus pallidus,

GPCRs – G protein coupled receptors

GPe – Globus pallidus *pars externa*

GPi – Globus pallidus *pars interna*

*hA*₁ AR – Human adenosine subtype *A*₁ receptor

*hA*_{2A} AR – Human adenosine subtype *A*_{2A} receptor

*hA*_{2B} AR – Human adenosine subtype *A*_{2B} receptor

hA₃ AR – Human adenosine subtype A₃ receptor
*h*MAO-A – Human monoamine oxidase type A isoform
*h*MAO-B – Human monoamine oxidase type B isoform
 HMBC – Heteronuclear multiple bond correlation
 HMPA – Hexamethylphosphoramide
 HMQC – Heteronuclear multiple quantum coherence
 HTS – High-throughput screening
 HVA – Homovanillic acid
 IL – Intra loop
 L-AAD – L-Aromatic amino acid decarboxylase or dopa decarboxylase
 L-dopa – L-Dihydroxyphenylalanine
 MAO-A – Monoamine oxidase type A isoform
 MAO-B – Monoamine oxidase type B isoform
 MPP⁺ – 1-Methyl-4-phenylpyridinium ion
 MPTP – 1-Methyl-4-phenyl-1,2,3,6-tetrahydropyridine
 NCEs – New chemical entities
 NMR – Nuclear magnetic resonance
 PD – Parkinson's disease
 PyBOP – *O*-Benzotriazol-1-yloxytris(pyrrolidino)phosphonium hexafluorophosphate
 PyBrOP – Bromotripyrrolidinophosphonium hexafluorophosphate
 SARs – Structure–activity relationships
 SN – Substantia nigra
 SNr – Substantia nigra pars reticulata
 STN – Subthalamic nucleus
 TH – Tyrosine hydroxylase

Metric units

µg – Microgram
 µL – Microliter
 µM – Micromolar
 g – Gram
 K – Degrees Kelvin
 L – Litre
 M – Molar
 mg – Milligram
 min – Minute
 mL – Mililiter

mM – Milimolar

ng – Nanogram

nL – Nanoliter

nM – Nanomolar

°C – Degrees Celsius

ppm – Parts per million

Symbols

δ – Chemical shift in ppm

d – Duplet

dd – Double duplet

ddd – Double double duplet

J – Coupling constant

m – Multiplet

m/z – mass charge ratio

s – Singulet

t – Triplet

Index

ACKNOWLEDGMENTS	II
ABSTRACT	III
RESUMO	V
ABBREVIATIONS	VII
METRIC UNITS	VIII
SYMBOLS	IX
INDEX	X
FIGURE INDEX	XIII
SCHEME INDEX	XV
TABLE INDEX	XVI
CHAPTER 1	17
INTRODUCTION	17
1.1 INTRODUCTION	18
1.2 SCOPE OF THE THESIS	20
CHAPTER 2	21
LITERATURE REVIEW	21
2.1 PARKINSON'S DISEASE	22
2.2 DOPAMINE BIOSYNTHESIS AND NIGROSTRIATAL PATHWAYS	23
2.3 PARKINSON'S DISEASE THERAPY THE CURRENT STATUS	26
2.3.1 <i>Dopaminergic treatments for Parkinson's disease</i>	26
2.3.1.1 L-Dopa	26
2.3.1.2 Dopamine agonists	27
2.3.1.3 Catechol-O-methyltransferase inhibitors	28
2.3.1.4 Monoamine oxidase-B inhibitors	31
2.3.2 <i>Non-dopaminergic treatments for Parkinson's disease</i>	33
2.3.2.1 Anticholinergic drugs	33
2.3.2.2 Glutamate antagonists	34
2.4 LOOKING FOR NEW TARGETS: ADENOSINE A _{2A} RECEPTORS AND PARKINSON'S DISEASE	35
2.4.1 <i>G Protein-coupled receptors and adenosine receptors: a general outlook</i>	35
2.4.2 <i>Adenosine, adenosine receptors and neurodegenerative diseases</i>	37
2.4.2.1 A _{2A} AR antagonists	38
2.5 CHROMONE AS A PRIVILEGED SCAFFOLD	39
2.5.1 <i>Privileged structures for lead discovery</i>	39

2.5.2	<i>Simple chromones</i>	40
2.5.3	<i>Chromones in therapy</i>	41
2.5.4	<i>Biological activity of simple chromones and derivatives</i>	41
2.5.4.1	Anti-inflammatory activity	42
2.5.4.2	Antimicrobial activity	44
2.5.4.3	Anticancer activity	45
2.5.4.4	Drugs for neurodegenerative diseases	47
2.6	METHODS OF SYNTHESIS OF SIMPLE CHROMONES	48
2.6.1	<i>Chromones from 2-hydroxyarylalkyl ketones</i>	48
2.6.2	<i>Synthesis of chromones from phenols</i>	52
2.6.3	<i>Synthesis of chromones from salicylic acids and derivatives</i>	53
2.6.4	<i>Synthesis of chromones via C-C cross coupling reactions</i>	54
2.6.5	<i>Synthesis of chromones from chromanones</i>	56
2.6.6	<i>Synthesis of chromones from other chromones</i>	56
CHAPTER 3		60
RESULTS		60
3.1	CHROMONE-2- AND -3-CARBOXYLIC ACIDS INHIBIT DIFFERENTLY MONOAMINE OXIDASES A AND B	61
3.2	CHROMONE, A PRIVILEGED SCAFFOLD FOR THE DEVELOPMENT OF MONOAMINE OXIDASE INHIBITORS	66
3.3	TOWARDS THE DISCOVERY OF A NOVEL CLASS OF MONOAMINE OXIDASE INHIBITORS: STRUCTURE–PROPERTY–ACTIVITY AND DOCKING STUDIES ON CHROMONE AMIDES	76
3.4	CHROMONE 3-PHENYLCARBOXAMIDES AS POTENT AND SELECTIVE MAO-B INHIBITORS	82
3.5	IN SEARCH FOR NEW CHEMICAL ENTITIES AS ADENOSINE RECEPTOR LIGANDS: DEVELOPMENT OF AGENTS BASED ON BENZO-F-PYRONE SKELETON	86
3.6	DISCOVERY OF NOVEL A3 ADENOSINE RECEPTOR LIGANDS BASED ON CHROMONE SCAFFOLD	92
3.7	COMBINING QSAR CLASSIFICATION MODELS FOR PREDICTIVE MODELING OF HUMAN MONOAMINE OXIDASE INHIBITORS.	102
3.8	SYNTHESIS AND NMR STUDIES OF NOVEL CHROMONE-2-CARBOXAMIDE DERIVATIVES.	119
CHAPTER 4		124
INTEGRATED OVERVIEW OF THE PERFORMED STUDIES		124
4.1	DESIGN, SYNTHESIS AND STRUCTURAL CHARACTERISATION OF THE DIVERSE FUNCTIONALIZED CHROMONE LIBRARIES	125
4.1.1	<i>Synthesis of ester, carboxylic acid and formylchromone derivatives</i>	129
4.1.2	<i>Synthesis of hydroxymethylchromone derivatives</i>	131

4.1.3	<i>Synthesis of amide chromone derivatives</i>	131
4.1.4	<i>Structural characterization of the chromone derivatives</i>	133
4.2	CHROMONE A VALID SCAFFOLD FOR THE DEVELOPMENT OF MAO-B INHIBITORS.....	133
4.3	CHROMONE A VALID SCAFFOLD FOR THE DEVELOPMENT OF ADENOSINE RECEPTORS	
LIGANDS	138	
4.4	CHROMONE-2-CARBOXAMIDE A VALID SCAFFOLD FOR THE DEVELOPMENT OF A ₃ AR	
LIGANDS	143	
CHAPTER 5	151
CONCLUDING REMARKS AND FUTURE PERSPECTIVES	151
5.1	CONCLUDING REMARKS AND FUTURE PERSPECTIVES	152
BIBLIOGRAPHY	154

Figure Index

FIGURE 2.1 SCHEMATIC REPRESENTATION OF THE BASAL GANGLIA ANATOMY	22
FIGURE 2.2 SCHEMATIC REPRESENTATION OF DOPAMINE METABOLISM. L-AAD: L-AROMATIC AMINO ACID DECARBOXYLASE AD: ALDEHYDE DEHYDROGENASE, COMT: CATECHOL-O-METHYLTRANSFERASE, DOPAC: DIHYDROXYPHENYLACETIC ACID, DOPAL: 3,4-DIHYDROXYPHENYLACETALDEHYDE, HVA: HOMOVANILLIC ACID, MAO-B: MONOAMINE OXIDASE-B, TH: TYROSINE HYDROXYLASE.....	24
FIGURE 2.3 SCHEMATIC REPRESENTATION OF BASAL GANGLIA DIRECT AND INDIRECT PATHWAYS. GPE: GLOBUS PALLIDUS PARS EXTERNA, GPI: GLOBUS PALLIDUS PARS INTERNA, SNC: SUBSTANTIA NIGRA PARS COMPACTA, SNR: SUBSTANTIA NIGRA PARS RETICULATA STN: SUBTHALAMIC NUCLEUS.	25
FIGURE 2.4 CHEMICAL STRUCTURE OF L-DOPA.....	26
FIGURE 2.5 CHEMICAL STRUCTURES OF L-AAD INHIBITORS.....	27
FIGURE 2.6 CHEMICAL STRUCTURES OF ERGOT AND NON-ERGOT DOPAMINE AGONISTS.....	28
FIGURE 2.7 PERIPHERAL BIOTRANSFORMATION OF L-DOPA BY ACTION OF COMT. COMT: CATECHOL-O- METHYLTRANSFERASE AND 3-OMD: 3-O-METHYLDOPA.	29
FIGURE 2.8 CHEMICAL STRUCTURES OF COMT INHIBITORS.	30
FIGURE 2.9 MAOS CATALYSED REACTIONS.....	31
FIGURE 2.10 CHEMICAL STRUCTURES OF MAO-B INHIBITORS IN CLINICAL PRACTICE.....	32
FIGURE 2.11 CHEMICAL STRUCTURES OF MULTITARGET DRUGS IN CLINICAL TRIALS.....	33
FIGURE 2.12 CHEMICAL STRUCTURES OF ANTICHOLINERGIC DRUGS.....	34
FIGURE 2.13 CHEMICAL STRUCTURE OF AMANTADINE.....	34
FIGURE 2.14 SCHEMATIC REPRESENTATION OF G PROTEIN-COUPLED ADENOSINE RECEPTORS. ATP: ADENOSINE-TRIPHOSPHATE; Ca^{2+} : ION CALCIUM (II); CAMP: CYCLIC ADENOSINE MONOPHOSPHATE; G _i /G _o : INHIBITORY G PROTEIN; G _s /G _q STIMULATORY G PROTEIN; K: POTASSIUM; P: PHOSPHORUS; PLC: PHOSPHOLIPASE C.....	36
FIGURE 2.15 CO-LOCALIZATION OF A _{2A} AR AND D2 RECEPTORS	38
FIGURE 2.16 CHEMICAL STRUCTURES OF ISTRADEFYLLINE AND PRELADENANT.	38
FIGURE 2.17 CHROMONE AND (ISO)FLAVONOIDS BACKBONE.	40
FIGURE 2.18 EXAMPLES OF CHROMONE DERIVATIVES IN THERAPY	41
FIGURE 2.19 CHEMICAL STRUCTURES OF (1): 7-METHANESULFONYLAMINO-6-PHENOXYCHROMONE AND (2): T-614.	42
FIGURE 2.20 CHEMICAL STRUCTURES OF STELLATIN AND ITS DERIVATIVES.	43
FIGURE 2.21 CHEMICAL STRUCTURES OF PRANLUKAST, FPL 55712 AND RG 12553.....	43
FIGURE 2.22 LT RECEPTOR ANTAGONISTS BASED ON (PIPERIDINYALKOXY)CHROMONE SCAFFOLD.	44
FIGURE 2.23 CHEMICAL STRUCTURES OF A: SULFONAMIDE CHROMONE DERIVATIVE AND B: DITHIAZOLE CHROMONE DERIVATIVE.	45
FIGURE 2.24 CHROMONE DERIVATIVES WITH ANTIVIRAL ACTIVITY. A) 2-STYRYLCHROMONES; B) 5- HYDROXY CHROMONE SCAFFOLD.	45
FIGURE 2.25 CHROMONE SCAFFOLDS FOR THE DEVELOPMENT OF NCE WITH ANTICANCER ACTIVITY....	46

FIGURE 2.26 2-STYRYLCHROMONES WITH ANTIPROLIFERATIVE ACTIVITY ON A PANEL OF CARCINOMA CELLS.....	46
FIGURE 2.27 CHEMICAL CORE OF CHROMONE DERIVATIVES TESTED AS A: ACHE AND MAO INHIBITORS AND B: DOPAMINE D ₂ AGONISTS.....	48
FIGURE 4.1. PHOSPHONIUM COUPLING AGENTS.....	132
FIGURE 4.2. VIRTUAL DOCKING OF CHROMONE-3-CARBOXYLIC ACID INTO THE HMAO-B CATALYTIC SITE (FIGURE EXTRACTED FROM ARTICLE IN SECTION 3.1).	135
FIGURE 4.3. CHEMICAL STRUCTURES OF FIVE OF THE BEST CHROMONE-3 CARBOXAMIDES AND THEIR INHIBITORY ACTIVITY TOWARDS HMAO-B.	136
FIGURE 4.4 CHEMICAL STRUCTURES OF N-PHENYL (COMPOUND 20), N-CYCLOHEXYL (COMPOUND 91) AND N-PROPYL (COMPOUND 105) CHROMONE-3-CARBOXAMIDES AND THEIR INHIBITORY ACTIVITY TOWARDS HMAO-B.	137
FIGURE 4.5 VIRTUAL DOCKING OF N-(4-(CHLOROPHENYL)-CHROMONE-3-CARBOXAMIDE INTO THE HMAO-B CATALYTIC SITE (FIGURE EXTRACTED FROM ARTICLE IN SECTION 3.2).....	137
FIGURE 4.6. CHEMICAL STRUCTURES OF THREE OF THE BEST CHROMONE-3 CARBOXAMIDES AS A _{2A} AR LIGANDS.	140
FIGURE 4.7. HYPOTHETICAL BINDING MODES OF ONE OF OUR MOST ACTIVE COMPOUND OBTAINED AFTER DOCKING SIMULATIONS: (A) INSIDE THE HA _{2A} AR BINDING SITE; (B) INSIDE THE HA ₃ AR BINDING SITE. (FIGURE EXTRACTED FROM ARTICLE IN SECTION 3.6)	141
FIGURE 4.8. CHEMICAL STRUCTURE OF ZM241385.....	141
FIGURE 4.9. CHEMICAL STRUCTURES OF MONO SUBSTITUTED CHROMONE-2-CARBOXAMIDES, THEIR CORRESPONDING HA ₃ KI AND SELECTIVE INDEX (SI).....	144
FIGURE 4.10. CHEMICAL STRUCTURES OF DI-EXOCYCLIC SUBSTITUTED CHROMONE-2-CARBOXAMIDES, THEIR CORRESPONDING HA ₃ KI AND SELECTIVE INDEX (SI).	146
FIGURE 5.1. CHEMICAL STRUCTURES OF TWO OF THE BEST CHROMONE-3-CARBOXAMIDES AS INHIBITORS OF HMAO-B ISOFORM AND AS LIGANDS OF HA _{2A} ARS.....	152

scheme index

SCHEME 2.1 SYNTHESIS OF CHROMONES VIA BAKER-VENKATAMARAN REARRANGEMENT.....	49
SCHEME 2.2 SYNTHESIS OF CHROMONES VIA CLAISEN CONDENSATION.....	49
SCHEME 2.3 PROPOSAL MECHANISM OF KOSTANECKI- ROBINSON REACTION ADAPTED FROM ^[248]	51
SCHEME 2.4 SYNTHESIS OF CHROMONES VIA.....	51
SCHEME 2.5 SYNTHESIS OF CHROMONES VIA BENZOPYRYLIUM SALT INTERMEDIATES.....	52
SCHEME 2.6 SYNTHESIS OF CHROMONES VIA SIMONIS AND RUHEMANN REACTIONS.....	53
SCHEME 2.7 SYNTHESIS OF CHROMONES FROM SALICYLIC ACIDS AND DERIVATIVES.....	54
SCHEME 2.8 SYNTHESIS OF CHROMONES VIA C-C CROSS COUPLING REACTIONS.....	54
SCHEME 2.9 SYNTHESIS OF CHROMONES CATALYSED BY NHCS.....	56
SCHEME 2.10 SYNTHESIS OF CHROMONES FROM HYDROXYL OR THIOCHROMONES.....	57
SCHEME 2.11 SYNTHESIS OF CHROMONES FROM CHROMONE CARBOXYLIC ACIDS.....	57
SCHEME 2.12 SYNTHESIS OF CHROMONES FROM 3-FORMYLCHROMONES.....	58
SCHEME 2.13 SYNTHESIS OF HETEROCYCLIC AND VINYL SUBSTITUTED CHROMONES.....	58
SCHEME 2.14 SYNTHESIS OF STYRYLCHROMONES FROM OTHER CHROMONES.....	59
SCHEME 4.1 SYNTHESIS OF ESTER CHROMONE DERIVATIVES BY FISHER ESTERIFICATION.....	129
SCHEME 4.2 SYNTHESIS OF ESTER CHROMONE DERIVATIVES BY CLAISEN CONDENSATION.....	130
SCHEME 4.3. SYNTHESIS OF 6-CHLORO-3-CHROMONE CARBOXYLIC ACID.....	130
SCHEME 4.4. SYNTHESIS OF HYDROXYMETHYLCHROMONE DERIVATIVES.....	131
SCHEME 4.5. SYNTHESIS OF AMIDE CHROMONE DERIVATIVES.....	132

table index

TABLE 4.1. CHROMONE LIBRARY I: ESTER, CARBOXYLIC ACID, HYDROXYMETHYL AND FORMYLCHROMONE DERIVATIVES.....	125
TABLE 4.2 CHROMONE LIBRARY II: PHENYLCARBOXAMIDE CHROMONE DERIVATIVES.	126
TABLE 4.3: CHROMONE LIBRARY III: ALKYL, PHENYL AND HETEROCYCLIC CHROMONE CARBOXAMIDE DERIVATIVES.....	128
TABLE 4.4. RADIOLIGANDS BINDING ASSAYS CONDITIONS.....	139
TABLE 4.5 AFFINITY (K _i , nM) OF MONOSUBSTITUTED CHROMONE-2-CARBOXAMIDES IN RADIOLIGAND BINDING ASSAYS AT HARS.	144
TABLE 4.5 (CONT.) AFFINITY (K _i , nM) OF MONOSUBSTITUTED CHROMONE-2-CARBOXAMIDES IN RADIOLIGAND BINDING ASSAYS AT HARS.	ERROR! BOOKMARK NOT DEFINED.
TABLE 4.6. AFFINITY (K _i , nM) OF DISUBSTITUTED CHROMONE-2-CARBOXAMIDES IN RADIOLIGAND BINDING ASSAYS AT HARS.	146
TABLE 4.7. AFFINITY (K _i , nM) OF MONOSUBSTITUTED CHROMONE-2-CARBOXAMIDES WITH WITHDRAWING GROUPS IN RADIOLIGAND BINDING ASSAYS AT HARS.	147
TABLE 4.8. AFFINITY (K _i , nM) OF MONOSUBSTITUTED CHROMONE-2-CARBOXAMIDES WITH DONATING GROUPS IN RADIOLIGAND BINDING ASSAYS AT HARS.	148
TABLE 4.9. AFFINITY (K _i , nM) OF TERTIARY CHROMONE-2-CARBOXAMIDES IN RADIOLIGAND BINDING ASSAYS AT HARS.....	148
TABLE 4.10. AFFINITY (K _i , nM) OF HETEROCYCLIC CHROMONE-2-CARBOXAMIDES IN RADIOLIGAND BINDING ASSAYS AT HARS.	149

Chapter 1

Introduction

1.1 Introduction

The Committee of the International Union of Pure and Applied Chemistry (IUPAC) defines medicinal chemistry as *“a chemistry-based discipline, also involving aspects of biological, medical and pharmaceutical sciences. It is concerned with the invention, discovery, design, identification and preparation of biologically active compounds, the interpretation of their mode of interaction at the molecular level, the construction of their structure-activity relationships, and the study of their metabolism”* ^[1]. The interdisciplinarity between Chemistry and Biology, essential for medicinal chemistry, was brilliantly recognized by Arthur Kornberg, a Nobel laureate, in 1959 who wrote: *“We have the paradox of the two cultures, chemistry and biology, growing further apart even as they discover more common ground.”* ^[2]. Due to the harmonization of these apparently distinct two sciences, conditions have been created for the growth of medicinal chemistry and consequently for drug discovery and development processes.

Nowadays, medicinal chemistry is seen as a science situated at the interface of organic chemistry and life sciences, encompassing the knowledge of biochemistry, pharmacology, molecular biology, genetics, immunology, pharmacokinetics and toxicology on one side, and chemistry based disciplines, such as organic and physical chemistry, crystallography, spectroscopy and computer-based techniques, data analysis and data imaging on the other side ^[3].

Medicinal chemistry is a dynamic science that changes as the drug discovery paradigms shifts. Before 1990 the lead generation in the drug discovery processes was based on natural ligands and massive synthesis ^[4-7]. Usually, the therapeutic purpose is fixed in advance and a large number (several thousands) of molecules is tested on a limited number of experimental models. This method, called as random screening, has been used for the discovery of several drugs, particularly antibiotics. The common criticism of this type of methodology is that it constitutes, by the absence of a rational lead, a sort of fishing.

The steep increase in the knowledge about biological processes, the factors leading to their misregulation and ultimately to disease as well as the development of new technologies, such as high-throughput screening (HTS), microwave assisted synthesis and parallel and combinatorial technology, have a tremendous impact on the methodologies of drug discovery, and correspond to the entrance of a new era - the so-called “rational drug design”. Classically, the drug discovery process embraces four stages of: i) target identification (enzyme, receptor, ion channel, signalling protein, transport protein or DNA.), ii) target validation, iii) (hit) lead identification and optimisation, iv) candidate(s) selection ^[8]. During the process it is essential to ensure

that the molecule is innovative (new chemical entities (NCEs)) and that it reaches its target effectively while also ensuring that it satisfies necessary safety requirements.

Drug design is a complex issue that still lacks a general approach that has proven reliability. There is still a need to select the appropriate structural series of compounds, to follow and pursue the SARs in order to identify suitable drug candidates for advancement to safety and clinical testing ^[5]. Furthermore, it has become increasingly clear that many effective drugs act by interactions with multiple receptors and/or enzymes, although they may have been designed to be highly selective.

For some time, scientists involved in drug discovery have been questioning the wisdom of the reductionist philosophy (one drug-one target.) of hitting single targets as the accurate approach to ameliorate complex disease states ^[9]. Although the strategy of one-molecule-one-target has led to the discovery of many successful drugs, this concept has been recently shifted to a new one, the multi-target approach, where a single chemical entity may be able to modulate simultaneously multiple targets. This new strategy seems to be of particular interest in areas that involve multiple pathogenic factors, like neurodegenerative diseases, diabetes, cardiovascular diseases, and cancer ^[9, 10]. One of the main limitations with this approach is the ability to define the set of targets that is causative of a particular disease state and design compounds that will hit the key targets with a desirable ratio of potencies. This is certainly a daunting challenge.

However, and despite the remarkable conceptual and technique differences of the earlier era of drug discovery, medicinal chemistry faces today many of the challenges that it confronted in the past. The accepted paradigm for drug discovery in the last 25 years has failed to provide a sufficient number of innovative and effective new drugs to continue to fuel the research and development (R&D) engine. Drug approvals by the US Food and Drug Administration (FDA) have continued to fall from the levels of the 1990's. The challenge to select the most druggable targets and to find the suitable drug-like molecules, substances that not only interact with the target but also have specific pharmacokinetic and toxicological properties, has generated more attrition in the process ^[11].

Now and again a remembrance of the past appears as a way out. Although natural products have been marginalized by major pharmaceutical companies over the last 20–30 years, the changing landscape of drug discovery now favours a greatly enhanced role for nature's privileged structures ^[12]. Advances in total synthesis, especially function-oriented syntheses and biosynthetic technologies offer new avenues to the identification and use of privileged structures and molecular fragments that are able to interact with more than one target. For nearly 20 years, privileged

structures have offered an optimal source of core scaffolds and fragments for the design of chemical libraries directed at a broad spectrum of targets ^[13].

In summary, although the drug discovery approaches have changed significantly over the past 50 years as the workflows have been reinvented, the same goals remain: find and test novel molecules that can reach and act on disease targets.

1.2 Scope of the thesis

The research program of the thesis was aimed at the discovery and development of new chemical entities skilled to be a therapeutic solution for Parkinson's disease. The main challenges were by one side the validation of the chromone scaffold as a privileged structure for the design of new drug candidates for Parkinson's disease and by the other the development of dual-target lead structures.

Therefore, the specific goals of this thesis were:

- i. Design of a library of structural related chromone derivatives suitable to achieve proper structure-activity relationships;
- ii. Establishment of concise and diversity-oriented synthetic strategies embedded with the benzopyran motif and development of efficient and less time consuming synthetic strategies;
- iii. Biological screening towards MAO-B;
- iv. Assessment of the binding affinities towards adenosine receptors.

Chapter 2

Literature Review

2.1 Parkinson's disease

Parkinson's disease (PD) is the second most prevalent neurodegenerative disorder, affecting up to 10 million people worldwide^[14, 15]. The cardinal neuropathological feature of PD is a dopaminergic cell loss within the substantia nigra (SN). Despite the enormous amount of research in the field, that reveal the implication of some molecular mechanisms such as mitochondrial dysfunction, production of free radicals and oxidative stress^[16, 17], protein aggregation^[18, 19], like α -synuclein aggregation^[20], neuroinflammation^[21], and impaired protein degradation^[22], the features and sequence of the events that generate the exact causes of cell death in PD remain unknown^[23]. It is also important to point out that some etiological factors have been associated with the disease, namely genetics^[24], aging^[15] and environmental toxins^[25, 26].

Classically, PD is considered a motor system pathological condition with an extensive degeneration of the dopaminergic neurons and subsequent dopamine (DA) depletion^[27]. The histopathological features of PD occur mainly on basal ganglia (Fig. 2.1), which comprises a group of interconnected deep brain nuclei, namely the striatum, formed by the caudate nucleus and putamen, the globus pallidus (GP), the substantia nigra and the subthalamic nucleus (STN). The dopaminergic nigrostriatal projections, by modulation of the thalamus and the cortex output, influence the generation and execution of voluntary movements. DA also plays a crucial role in modulation of other basal ganglia neurotransmitters associated with motor control, like γ -aminobutyric acid (GABA), acetylcholine (ACh), glutamate, enkephalin, and substance P^[27-29].

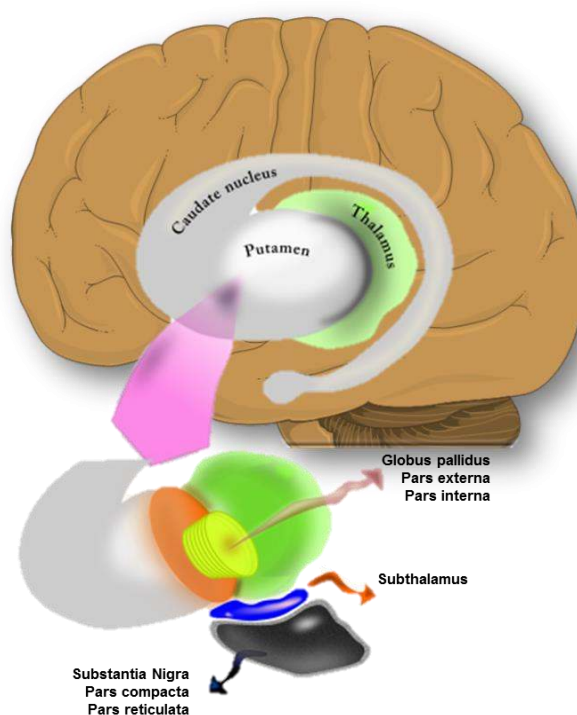


Figure 2.1 Schematic representation of the basal ganglia anatomy

The degeneration of the nigrostriatal dopaminergic neurons with the disruption of the complex circuitry mentioned above can culminate on movement disorders, such as those implied on PD^[30, 31]. This disease is clinical

translated into motor manifestations, such as bradykinesia, rigidity tremor and postural instability ^[27]. In addition to the degeneration and loss of the dopaminergic neurons, the neurodegenerative process is also associated with the loss of serotonergic, noradrenergic and cholinergic neurons and, consequently, with the depletion of the corresponding neurotransmitters ^[27, 32]. The latter described pathological processes are linked with the non-motor manifestations of PD, including cognitive decline, sleep abnormalities and depression as well as gastrointestinal and genitourinary disturbances ^[27, 32]. The advent of non-motor complications on PD is well documented although often under-recognised in clinical practice and diagnosis, which still relies on detection and evaluation of the cardinal motor symptoms ^[29].

2.2 Dopamine biosynthesis and nigrostriatal pathways

The biosynthesis of DA occurs in the dopaminergic neurons and starts with the conversion of the L-tyrosine to L-dihydroxyphenylalanine (L-dopa) by the action of the enzyme tyrosine hydroxylase (TH). L-Dopa is then converted into DA by the enzyme L-aromatic amino acid decarboxylase (L-AAD), also called dopa decarboxylase (Fig. 2.2) ^[33-36]. Once synthesised, DA is sequestered into vesicles and released into the synaptic cleft, where it exerts its role by interacting with specific receptors. The DA receptors are a class of G protein-coupled receptors (GPCRs), commonly divided in two major classes: D₁-like receptors, comprising D₁ and D₅ receptors, and D₂ like-receptors class formed by the D₂, D₃, and D₄ receptors subtypes ^[37]. The DA metabolism encompasses either its reuptake by the dopaminergic neurons or its uptake by glial cells. Briefly, after its reuptake by the neurons, DA can be recycled and stored in vesicles, or converted to dihydroxyphenylacetic acid (DOPAC) by the action of monoamine oxidase-B (MAO-B) and aldehyde dehydrogenase (AD) (Fig 2.2). On the other hand, within glial cells, DA is converted into homovanillic acid (HVA) by the action of catechol-*O*-methyltransferase (COMT), MAO-B and AD (Fig. 2.2) ^[33-36].

Through its innervation systems, DA acts as a relatively slow modulator of a faster neurotransmission mediated by glutamate and GABA, and it has been implied in several vital functions of the central nervous system (CNS) such as voluntary movement, appetite, affection, reward, sleep, attention, working memory and learning ^[38]. Accordingly, the typical movement disorders observed in PD have been linked with the degeneration and loss of basal ganglia dopaminergic projections, specially of the dopaminergic nigrostriatal neurons ^[28, 39, 40].

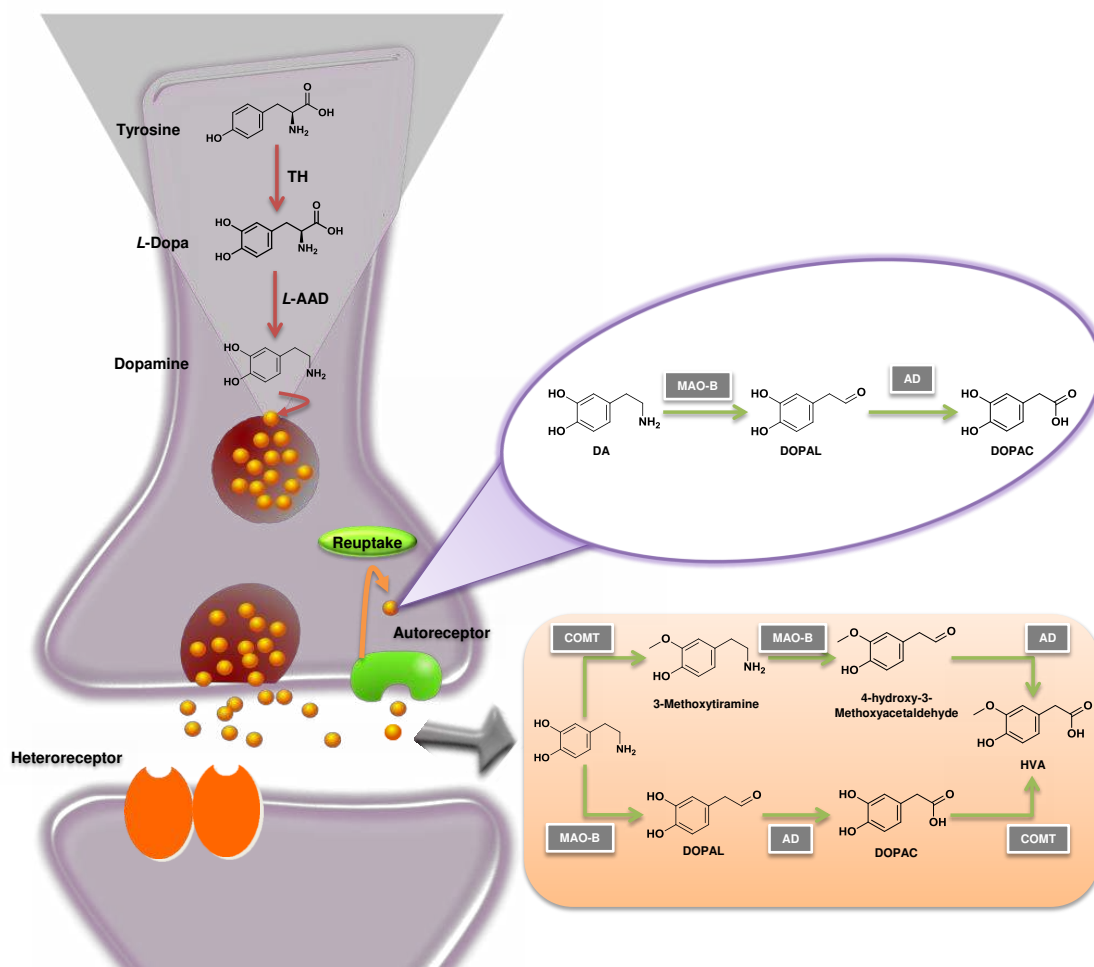


Figure 2.2 Schematic representation of dopamine metabolism. L-AAD: L-aromatic amino acid decarboxylase
AD: aldehyde dehydrogenase, COMT: catechol-O-methyltransferase, DOPAC: dihydroxyphenylacetic acid,
DOPAL: 3,4-Dihydroxyphenylacetaldehyde, HVA: homovanillic acid, MAO-B: monoamine oxidase-B, TH:
tyrosine hydroxylase.

The actual model of the basal ganglia circuitry is based in the existence of two major projection systems: the direct and indirect pathways. Concisely, the direct and indirect pathways arise from different populations of striatal projection neurons, whose activity is regulated by striatal dopamine, supplied via nigrostriatal projection from the *substantia nigra compacta* (SNc). The direct pathway (Fig.2.3) encloses D₁-like receptors, involving dopaminergic projections from the striatum to the *globus pallidus pars interna* (GPI) and *substantia nigra pars reticulata* (SNr). The indirect pathway (Fig.2.3) selectively expresses D₂-like receptors and involves the projections of the *striatum* to *globus pallidus pars externa* (GPe) [37, 39, 41, 42]. It has been postulated that movement control by basal ganglia involves both direct and indirect pathways, by modulation of the cortical afferent activity through *thalamus* output.

The direct pathway is triggered by the activation of D_1 receptors on neurons that project mainly to the GPi and SNr with subsequent inhibition of their GABAergic neurons, a process which seems to enhance thalamo cortical circuitry and, consequently, facilitate movement. The dopamine interaction with D_2 receptors triggers the indirect pathway by inhibiting the GPe GABAergic projections directly attached with STN. This inhibition, results in the activation of glutamatergic projections from STN to GPi/SNr enhancing the inhibitory effect of GPi/SNr over the thalamus [30, 39, 42]. Thus, the indirect pathway activation interferes with the thalamocortical circuitry resulting in a movement inhibition [43].

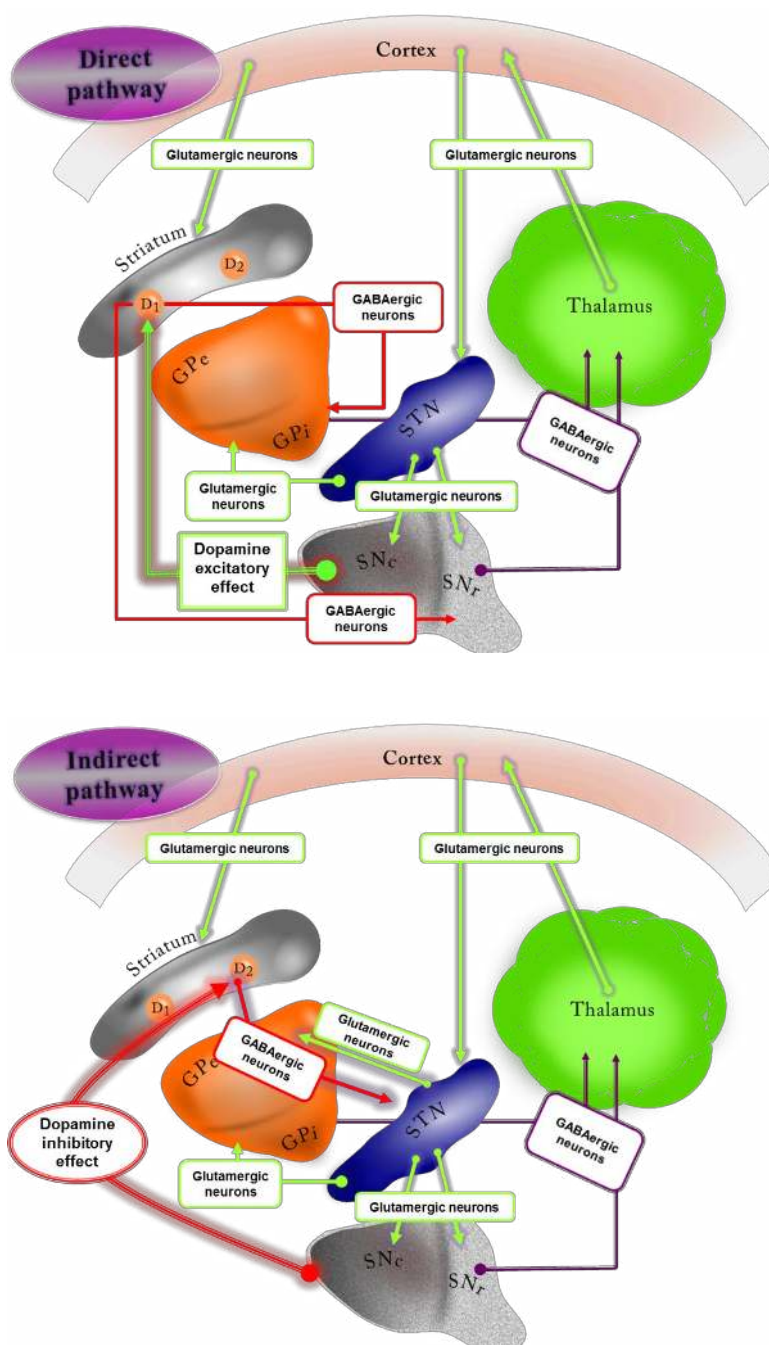


Figure 2.3 Schematic representation of basal ganglia direct and indirect pathways. GPe: *globus pallidus pars externa*, GPi: *globus pallidus pars interna*, SNc: *substantia nigra pars compacta*, SNr: *substantia nigra pars reticulata* STN: *subthalamic nucleus*.

More recently, controversial experimental data, led to questioning the consistency of the referred model. Although some of its features and hypotheses should be clearly reviewed [39, 44], significant assumptions of the basal ganglia circuitry model are still widely accepted (e.g. the basic connections between the basal ganglia nuclei and the

role of dopaminergic system in the striatum output) ^[39]. It is also important to point out its contribution to the study of the pathophysiology of movement disorders such as the ones observed in Parkinson's disease. In this neurodegenerative disease the regulatory role of DA in *striatum* is compromised ^[27, 29], which leads to a reduced activity of the direct nigrostriatal pathway, whereas the indirect nigrostriatal pathway activity is increased, resulting in an excessive GPi inhibitory output to the thalamus with a consequent movement disorders ^[28].

2.3 Parkinson's disease therapy the current status

Nowadays the pharmacological therapy available for Parkinson's disease (PD) aims to improve patients' life quality, slowing down the progression of symptoms, either through the delay of the physical and psychological morbidity inherent to of the disease or by diminishing the long-term complications associated with the therapy ^[45]. The main strategic developments for symptomatic treatment and discovery of new compounds to modify the course of PD were focused on the improvement of dopaminergic therapies and in the identification of non-dopaminergic drugs.

Despite all the recent research in the field, there are only a few classes of drugs approved for the treatment of the motor related symptoms of PD, namely the ones that act primarily on the dopaminergic system, such as L-dopa, dopamine agonists, MAO-B and COMT inhibitors, and the non-dopaminergic drugs like anticholinergic and glutamate antagonists ^[45, 46].

In the following sections it will be succinctly presented the current status of the available chemotherapy for the treatment of the motor afflictions of Parkinson's disease will be briefly discussed, as well as the importance of the discovery and development of new drugs for PD.

2.3.1 Dopaminergic treatments for Parkinson's disease

2.3.1.1 L-Dopa

The observation that dopamine levels in the basal ganglia of patients suffering from PD were much lower than those found in the brains of healthy persons, was the key information that boosted the drug discovery for PD that lead to the introduction of L-dopa (Fig.2.4) in the market from the late 1960's ^[47].

Almost 50 years later, L-dopa remains the most useful oral drug in PD therapy, showing real effectiveness in the reversibility of motor limitations of the disease.

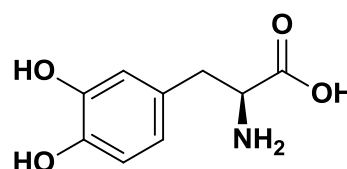
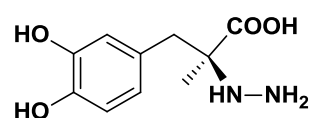


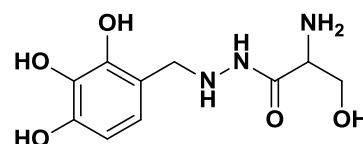
Figure 2.4 Chemical structure of L-dopa.

L-Dopa is a natural dopamine precursor that can cross the blood-brain barrier but has a relatively short half-life period of 60 to 90 min ^[48]. Once in the brain, exogenous L-dopa is taken up by dopaminergic neurons, thus mimetizing the endogenous one, and converted to DA by the dopa-decarboxylase and stored in vesicles with subsequent release into the synaptic cleft.

The PD progressive loss of dopaminergic neurons, which are required to the biosynthesis, metabolism, storage and release of dopamine, influence the beneficial effect of each dose of L-dopa by shorting the time of its effectiveness and so the daily scheduled dose must be adjusted ^[47]. The long-term usage of this drug can lead to a narrow therapeutic window as well as several complications ^[49]. Standard treatment of PD with L-dopa causes a number of typical peripheral and central dopaminergic adverse events, including nausea, vomiting, hypotension, hallucinosis, paranoid psychosis and particularly iatrogenic dyskinesias ^[50]. Some of the side effects are mainly due the peripheral metabolism of exogenous L-Dopa to DA in the liver and intestinal mucosa *via* peripheral L-AAD. In fact, less than 1% of administered L-dopa reaches the brain. To overcome this drawback a combination of L-dopa with L-AAD inhibitors such as carbidopa and benserazide (Fig. 2.5) is commonly prescribed. Thus, the L-dopa bioavailability is increased and the necessary dose to obtain effect reduced as well as the peripheral side effects ^[51].



Carbidopa



Benserazide

Figure 2.5 Chemical structures of L-AAD inhibitors.

2.3.1.2 Dopamine agonists

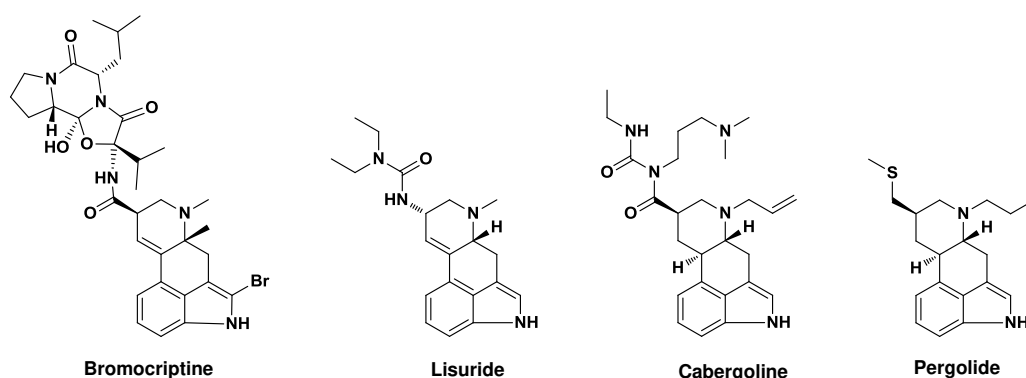
One of the strategies employed to minimize the side effects of L-dopa is related to the use of dopamine agonists. These drugs were launched as first-line effective drugs for monotherapy in the early stages of the disease, in order to postpone L-dopa introduction and its associated dyskinesia ^[52]. Furthermore, due to the fact that this class of compounds can delay the onset of dyskinesias and motor fluctuations, by one to three years, after L-dopa introduction DA agonists are also used as adjuvants to L-dopa in the later stages of the disease ^[53].

The main advantage associated with the use of dopamine agonists is the fact that they can act directly on dopamine receptors, bypassing the metabolic pathways in the degenerated nigrostriatal neurons ^[54-56]. It was also postulated that the antioxidant/free radical-scavenging activity demonstrated by this type of compounds, makes them good candidates for neuroprotection of the dopaminergic and non-

dopaminergic neurons ^[56-59]. These additional effects, although very important to the management of PD, still remain unproven and may not be significant for clinical practice as suggested for some authors ^[60, 61].

DA agonists are a heterogeneous group of drugs classically divided into ergot or non-ergot agonists. The ergot DA agonists (Fig. 2.6) are based on the structure of ergoline and include: bromocriptine, cabergoline, lisuride, and pergolide. The non-ergot DA agonists (Fig. 2.6) are a more diverse chemical group comprising apomorphine, piribedil, ropinirole, pramipexole, and rotigotine ^[54]. Due to several side effects, such as impulse control disorders (*e.g.* pathological gambling, hyper sexuality, or binge eating) the treatment with dopamine agonists must be initiated at low dosage and the titration period may be extended for months in order to improve tolerance to the peripheral side effects ^[62]. This dose escalation process may have direct implications in the patient's compliance to the treatment due to the time needed for beneficial effects to manifest.

Ergot Derivatives



Non-ergot Derivatives

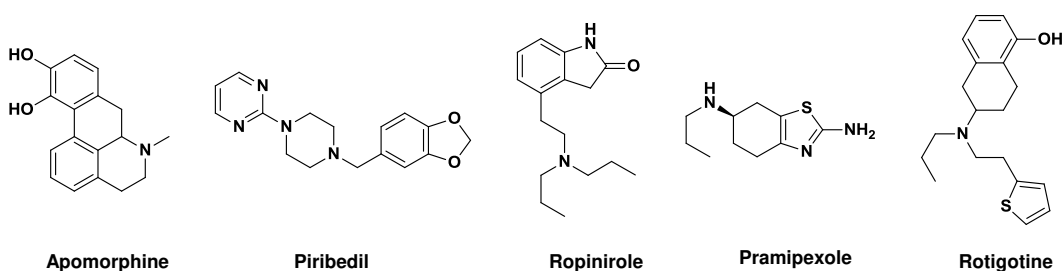


Figure 2.6 Chemical structures of ergot and non-ergot dopamine agonists.

2.3.1.3 Catechol-O-methyltransferase inhibitors

Catechol-O-methyltransferase (COMT) is an intracellular enzyme widely distributed in human tissues and highly active in liver, kidneys and gastrointestinal tract

[63]. This enzyme in presence of Mg^{2+} promotes the *O*-methylation of one of the hydroxyl groups present on the catechol substrate [63].

To understand the role of COMT inhibitors, as a valid resource for PD, it is important to highlight the role of this enzyme in the peripheral metabolism of L-dopa. Besides the peripheral conversion of L-dopa to dopamine via L-AAD, L-dopa is also peripherally metabolized to its inactive metabolite 3-*O*-methyldopa (3-OMD) (Fig. 2.7), by the action of COMT [63, 64]. The use of COMT inhibitors allows a prolonged maintenance of L-dopa serum levels, by increasing its half-life and boosting the central bioavailability of the drug. These drugs have the additional advantage of low motor fluctuations and less dependence on daily L-dopa [64].

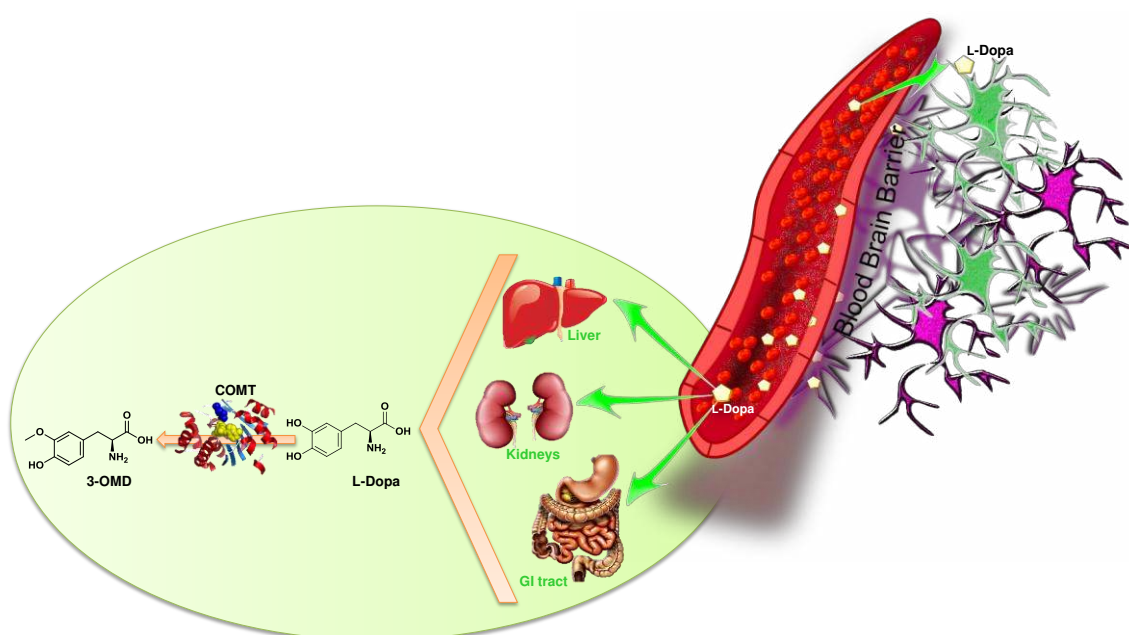


Figure 2.7 Peripheral biotransformation of L-dopa by action of COMT. COMT: Catechol-O-methyltransferase and 3-OMD: 3-*O*-methyldopa.

There are two COMT inhibitors, available since the mid-1990s, for clinical practice: tolcapone and entacapone (Fig. 2.8) [65]. Entacapone is a selective and reversible peripheral COMT inhibitor that does not cross the blood brain barrier (BBB) acting primarily in the increase and maintenance of plasmatic half-life of L-dopa [66]. Tolcapone has a half-life similar to entacapone but, as it has a greater bioavailability and smaller volume of distribution, thus resulting in higher potency for COMT inhibition [54]. Furthermore, tolcapone, unlike entacapone, may also inhibit central COMT brain [67, 68], increasing peripherally and central L-dopa availability, thus enhancing striatum dopamine neurotransmission [68]. However, the appearance of fatal acute hepatitis in some patients receiving tolcapone, raised several concerns about this

drug and the European Medicines Agency (EMA) has temporary suspended tolcapone in the European Union (EU) [67, 69]. In 2004, EMA lift the suspension but its use was substantially curtailed [67]. Comparatively, entacapone does not show the same tendency to cause hepatotoxicity, being the most common side effects related with the dopaminergic system. As reflex of the increased central dopaminergic activity, nausea, vomiting, orthostatic hypotension, and dyskinesia, can be experienced by the patients undergoing COMT inhibitors therapy. Additionally, it was reported the occurrence of diarrhoea in about 10% of cases, and in some patients it may be intractable and discontinuation of the drug may be required [70].

Recently, a novel catechol-O-methyltransferase (COMT) inhibitor, opicapone (Fig.2.8), was developed by BIAL and has been proposed as adjunctive therapy for PD patients treated with L-dopa. Opicapone is currently in phase III clinical trials and a license agreement was signed with Ono Pharmaceutical Co., Ltd. ("ONO") for the development and commercialization in Japan [71].

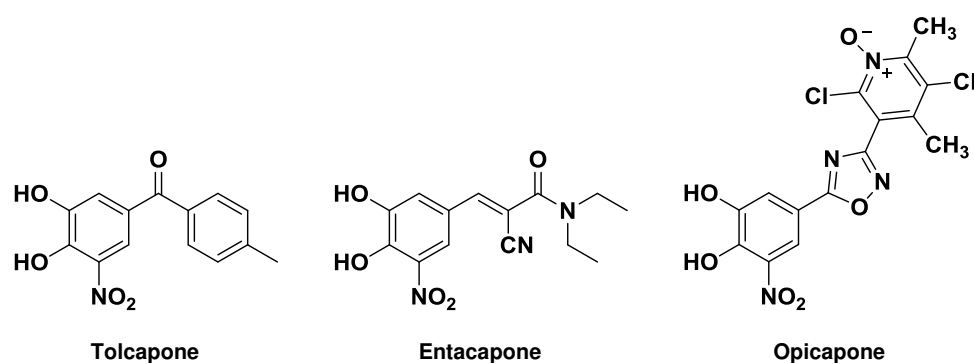


Figure 2.8 Chemical structures of COMT inhibitors.

2.3.1.4 Monoamine oxidase-B inhibitors

Monoamine oxidases (MAOs) are intracellular flavine-containing enzymes that play a major role in the *in vivo* inactivation of biogenic amines, both in peripheral and central neuronal tissues ^[72]. These enzymes are ubiquitously distributed on the body and are mainly located in the outer mitochondrial membrane. The biological role of MAOs is the catalysis of the oxidative deamination of endogenous monoamines (Fig. 2.9) by a process that involves the oxidation of the amine function, with the formation of an imine intermediate and simultaneous reduction of the flavin cofactor. The imine intermediate is then hydrolysed, yielding ammonia and the corresponding aldehyde. The cofactor is re-oxidized by molecular oxygen, with concomitant hydrogen peroxide release (Fig. 2.9) ^[73].

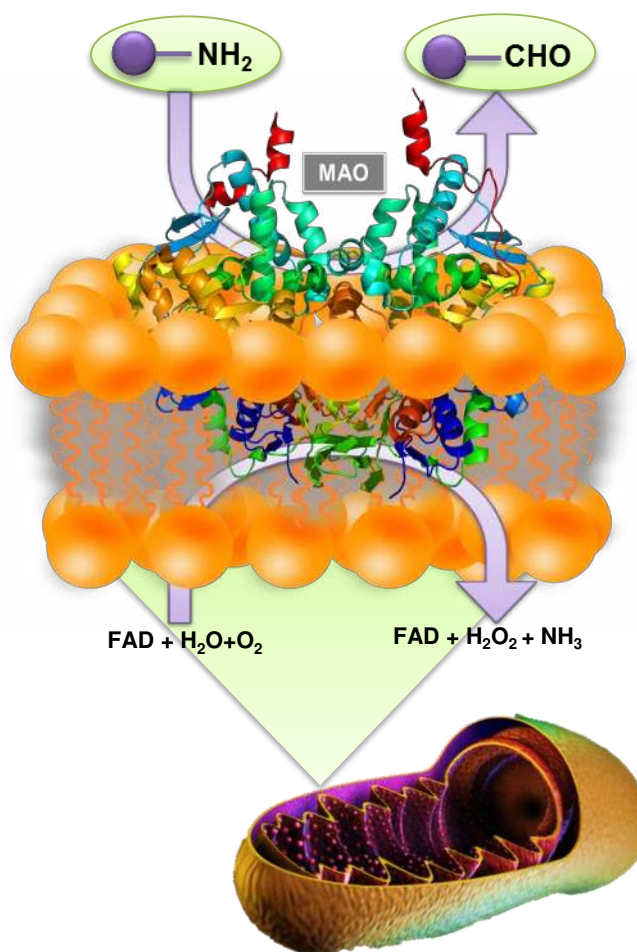


Figure 2.9 MAOs catalysed reactions

Two isoforms of MAOs are expressed in mammals: MAO-A and MAO-B, which can be distinguished based on their substrate preference for the substrate and their interaction with specific inhibitors ^[73, 74]. Within the CNS, the primary substrates of MAO are neurotransmitters, such as adrenaline, noradrenaline (NA), dopamine (DA), serotonin, also called 5-hydroxytryptamine (5-HT), and β -phenylethylamine (PEA). However, a variety of monoamines, like tyramine, octopamine, tryptamine and kynuramine, can be also metabolised by MAO. These substrates are deaminated by both isoforms of the enzyme, albeit with differing kinetic parameters, which are influenced by concentration, affinity and turnover rate of the substrate. Under normal physiologic conditions, NA and 5-HT are the preferred substrates of MAO-A, and PEA

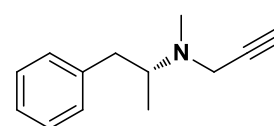
is preferentially metabolised by MAO-B. Both MAOs isoforms metabolise DA, although DA in human brain has higher affinity for MAO-B isoform ^[75].

These findings led to the development of selective inhibitors for each subtype of MAO, being MAO-A a target in the treatment of depression, whereas MAO-B inhibitors are used in therapy for neurodegenerative disorders, including PD ^[74]. MAO-B inhibition causes the blockade of the metabolism of dopamine and therefore could enhance both endogenous dopamine and the one produced from exogenously administered L-dopa.

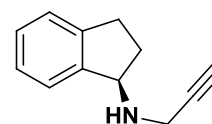
1-Methyl-4-phenyl-1,2,3,6-tetrahydropyridine (MPTP), a chemical compound, which was linked with parkinsonism by serendipity, had a significant impact on PD research and it was used since then as a tool to investigate the cause and treatment of the disease namely in the development of suitable PD animal models ^[76]. The neurotoxic effects are not caused by MPTP by itself, but by its bioactive metabolite, the 1-methyl-4-phenylpyridinium ion (MPP⁺), a metabolic process which can be MAO-B mediated. The active metabolite exerts its toxicity by acting as mitochondrial complex I inhibitor inducing cell death ^[77]. There are several studies suggesting that MAO-B inhibitors can block the conversion of MPTP to its active metabolite MPP⁺, thus giving rise to the thought that they can possess some neuroprotective properties ^[75, 78].

The MAO-B inhibitors currently in the market, selegiline (L-deprenyl) and rasagiline (Fig. 2.10) are both selective and irreversible inhibitors of MAO-B isoform. Selegiline in combination with L-dopa presents very successful results in the treatment of PD. First synthesised in 1962, the low potential of selegiline to produce the so-called "cheese effect", a common reaction following the usage of MAO inhibitors, had attracted attention even before MAO subtypes have been discovered. Additionally, selegiline may also display neuroprotective properties through the decrease of oxidative stress in neuronal striatal circuit ^[79]. A negative feature of selegiline is related to its biotransformation in amphetamine-like metabolites; two of them, L-amphetamine and L-methamphetamine, have shown to be potential neurotoxins. Despite the fact that the neurotoxicity mechanisms are not completely understood, it has been proposed that it involves damage in dopaminergic and serotonergic cells ^[80-82].

Rasagiline (Fig. 2.10) is a potent, selective and irreversible inhibitor of MAO-B. One of its main therapeutic advantages is related to its biotransformation, as no amphetamine-like metabolites are obtained ^[82-84]. Moreover, its major metabolite ((R)-1-



Selegiline



Rasagiline

Figure 2.10 Chemical structures of MAO-B inhibitors in clinical practice

aminoindan) exhibits neuroprotective activity in animal PD models ^[85]. Studies with patients, with moderate to severe symptoms of PD treated with L-dopa, showed that rasagiline improves the typical symptoms and motor fluctuations ^[86]. The key to the success of rasagiline seems to be its ability to limit the process of neurodegeneration in the early stages of the disease ^[87].

The multitarget drug discovery approach recently proposed for multifactorial diseases has already brought out encouraging results regarding PD. The development of new chemical entities (NCEs) with a MAO-B inhibitory activity allied to another relevant mechanism of action, culminated in synthesis of two new compounds: ladostigil and safinamide (Fig. 2.11).

The identification of the propargylamine moiety as a key structure related with the neuroprotective activity of MAO-B inhibitors was the inspiration for the design and development of ladostigil ^[10]. Ladostigil, is a NCE that combines the neuroprotective effects of the propargylamine moiety, the MAO-B inhibition profile of rasagiline and retains the acetylcholinesterase (AChE) inhibitory activity of rivastigmine ^[88].

Safinamide is an aminoamide derivative, currently in Phase III clinical trial for Parkinson's disease, which has been shown to be a reversible MAO-B inhibitor with the capacity to reduce dopamine reuptake and with antilutamatergic effects. This NCE may add a new dimension to PD treatment options, either as an adjuvant to current drugs for neuroprotection or motor symptomatic relief in PD, as it displays dopaminergic and non-dopaminergic effects ^[89].

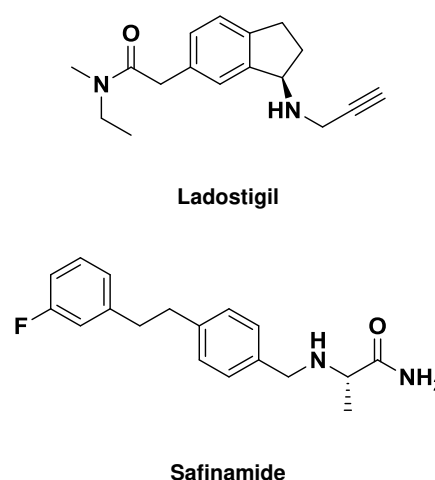


Figure 2.11 Chemical Structures of multitarget drugs in clinical trials.

2.3.2 Non-dopaminergic treatments for Parkinson's disease

2.3.2.1 Anticholinergic drugs

Before the discovery of L-dopa the therapy of choice for PD relied on anticholinergic drugs. The first's reports involving the use of anticholinergic drugs for ameliorating the motor symptoms of PD remount to the nineteen century (late 1860's, early 1870's) with use of the belladonna alkaloids, atropine and scopolamine. The synthetic anticholinergic agents, namely, trihexyphenidyl, Biperiden, procyclidine, benztropine and ethopropazine were only marketed for the treatment of PD in 1950's ^[90-92] (Fig. 2.12). Although the benefits were modest and inconsistent,

anticholinergic drugs remained the cornerstone of PD therapy for nearly one hundred years.

The rational use of anticholinergic agents in PD has been strengthened by the clear demonstration of dopaminergic-cholinergic antagonism in the striatal function [55]. The mechanism of action of the anticholinergic drugs in PD is not yet thoroughly known, but it is postulated that these drugs can antagonise overactive cholinergic transmission *via* blockade of postsynaptic muscarinic receptors, thereby restoring the balance between DA and ACh in the *striatum* [55, 93]. Although anticholinergics may be useful as monotherapy in early stages of PD, they are mainly used as adjuvants to L-dopa treatment. They are more effective in ameliorating the mild symptoms of tremor and rigidity, without significant changes in bradykinesia signals [94]. Anticholinergic agents can also block muscarinic ACh receptors peripherally leading to a myriad of side effects like xerostomia, sweating inhibition, blurred vision, and urinary retention as the most common ones. CNS side effects, such as confusion, dementia and other psychiatric symptoms are also frequent [95].

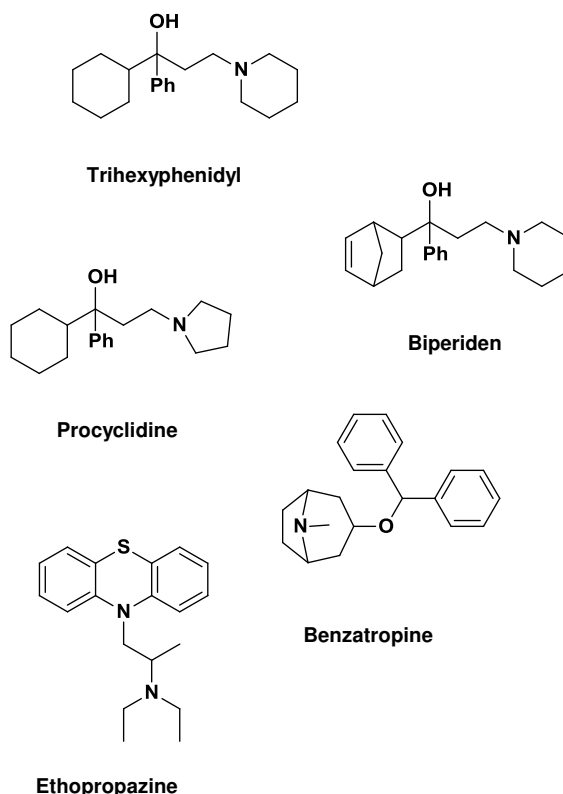


Figure 2.12 Chemical structures of anticholinergic drugs

2.3.2.2 Glutamate antagonists

Amantadine (Fig. 2.13) is a tricyclic amine that was firstly used as an antiviral agent. Its benefits in PD therapy were discovered by serendipity in 1969 by Schwab *et al.* [96]. Despite the lack of scientific evidence of its efficacy regarding the delay of PD progression, this drug has been used for the relief of PD motor since then [55]. Amantadine is

administered either in combination with L-dopa or in monotherapy, in patients that have less tolerance for L-dopa [97]. More recently, the interest on this drug has re-emerged

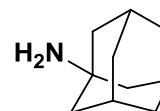


Figure 2.13 Chemical structure of amantadine.

due to its putative beneficial role in the treatment of motor fluctuations and dyskinesias^[98, 99]. The exact mechanism of action of amantadine remains unclear. The role of this drug in PD has been related to the antagonism exerted on N-methyl-D-aspartate (NMDA) receptor subtype, but other mechanisms have also been proposed, such as direct action over the dopaminergic system. None of the mechanisms so far proposed met the rigorous criteria for strength of evidence^[55, 100, 101].

However, the use of amantadine in therapy is limited due to its side effects, which are generally mild but may be severe, especially in elderly patients, and also due to the discovery of more effective therapeutic approaches. Adverse effects associated with amantadine usage are primarily central nervous system ones, like anxiety, hallucinations, depression, insomnia, somnolence/drowsiness, fatigue and impaired coordination, along with non-SNC effects, such as diarrhoea, nausea and vomiting, constipation, xerostomia, and *livedo reticularis*^[98].

2.4 Looking for new targets: adenosine A2A receptors and Parkinson's disease

To date, most of the currently available therapies in PD target the dopaminergic system and none of these therapeutic approaches have been proven to modify the course of the disease. To various extents, these drugs can also cause motor and non-motor complications^[102].

The need for potent and safe antiparkinsonian agents has been the motor of an intensive research towards the development of new therapeutic approaches for PD, preferentially one that can operate beyond the damaged dopaminergic system. In fact, in the last years a large number of medicinal chemistry programs have been focused in looking for new non-dopaminergic modulators of basal ganglia motor circuits^[103].

As mentioned previously in section 2.3.2, there are available medicines whose mechanisms of action operate via a non-dopaminergic pharmacological approach (e.g. anticholinergic drugs and amantadine) illustrating the viability and the problems of this type of therapeutic strategy for PD motor symptoms relief^[104]. So, the development of novel antiparkinsonian agents whose mechanisms of action are mediated by other specific CNS receptors, preferentially restricted to basal ganglia neurons, may have an intrinsic therapeutic advantages while reducing the occurrence of adverse CNS events.

2.4.1 G Protein-coupled receptors and adenosine receptors: a general outlook

Adenosine can act as neuromodulator and has been associated with the coordination responses to DA and other neurotransmitters, in areas of the brain that are responsible for motor function, mood, learning and memory^[105, 106]. The

physiological functions of adenosine are mediated by adenosine receptors (ARs). Briefly, these receptors are G protein-coupled receptors (GPCRs) consisting of a single polypeptide chain that transverses the membrane from the extracellular side, beginning at the N terminus, to form seven transmembranar helices (TMs), which are connected by three intracellular and three extracellular loops (ILs and ELs, respectively), leaving the N-terminus in the extracellular milieu and the C-terminus in the cytoplasm^[107] (Fig. 2.14).

There are four distinct ARs subtypes designated as A₁, A_{2A}, A_{2B} and A₃. Adenosine A₁ and A₃ receptors are coupled to inhibitory G proteins, while A_{2A} and A_{2B} receptors are coupled to stimulatory G proteins. The A_{2A} and A_{2B} ARs preferably interact with members of the G_s family of G proteins, with consequent activation of adenylyl cyclase and consequently the production of cyclic AMP (cAMP), and contrariwise, the A₁ and A₃ ARs inhibit the adenylyl cyclase activity by interaction with G_i proteins^[107] (Fig. 2.14).

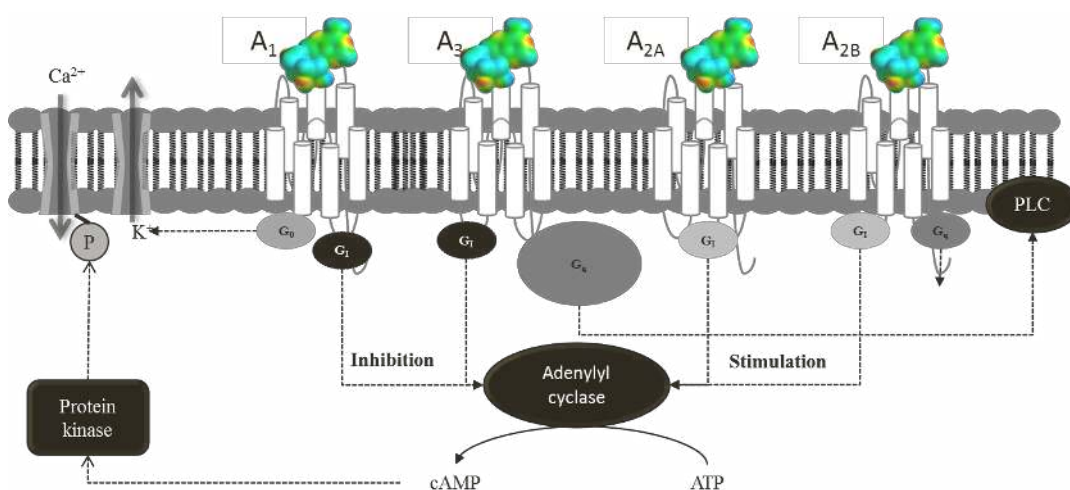


Figure 2.14 Schematic representation of G protein-coupled adenosine receptors. ATP: Adenosine-triphosphate; Ca²⁺: ion Calcium (II); cAMP: Cyclic adenosine monophosphate; G_i/G_o: inhibitory G protein; G_s/G_q stimulatory G protein; K: potassium; P: phosphorus; PLC: phospholipase C.

GPCRs have been implicated in a multitude of human disorders and numerous diseases as their signalling regulates an incredibly vast array of physiological functions and pathological conditions. Consequently, they have a high pharmaceutical appeal and constitute the target of a very large segment of the currently marketed drugs^[108]. It is estimated that nearly half of all modern drugs somehow regulate GPCR activity^[109].

Although GPCRs are among the most fruitful targets for marketed drugs, and while intense discovery efforts have been performed to find agents for GPCR subtypes, a selective drug candidate has not yet been reported. Particularly, ARs have long been

considered as targets for drug discovery programs of a variety of maladies, such as cerebral and cardiac ischaemia, immune and inflammatory disorders, and more recently for neurodegenerative and neoplastic events ^[108, 110, 111]. Consequently, numerous medicinal chemistry groups have made intense efforts to create selective agonists and antagonists for each AR subtype ^[112-115].

2.4.2 Adenosine, adenosine receptors and neurodegenerative diseases

Adenosine is a neuromodulator with several functions in the CNS, such as inhibition of neuronal activity in many signalling pathways ^[105,106,116,117]. Adenosine plays a major role in a diverse array of neural phenomena, which includes regulation of sleep and the level of arousal, neuroprotection, seizure susceptibility, locomotor effects, neuroprotection and modulation of various neurotransmitters, namely dopamine. The existence of an interaction between adenosine and dopamine within the basal ganglia, which could be correlated with the modulation of motor function, has been demonstrated ^[105, 116, 117]. Adenosine can also counteract the excitotoxicity associated with excessive glutamate release in the brain ^[118]. The overall findings support the hypothesis that adenosine plays an important role in the modulation of glutamatergic and GABAergic neurotransmission ^[28, 119, 120] of the basal ganglia indirect pathway ^[121].

The neuromodulation effect exerted by adenosine occurs probably through the activation of the A₁ and A_{2A} ARs, which are highly expressed in brain ^[122]. The A_{2A} AR in the CNS, distinguishes itself from the other adenosine receptors by its selective localization in striatum ^[107] (Fig. 2.15). In the striatum the A_{2A} AR are co-localize and physically associated with DA D₂ receptors. A_{2A} AR and D₂ receptors have opposing effects on adenylyl cyclase and cAMP production in cells. Interestingly, A_{2A} AR activation reduces the affinity of striatal D₂ receptor for dopamine and the blockade of A_{2A} AR with specific antagonists facilitates function of the D₂ receptor. Blockade of A_{2A} AR signalling by selective A_{2A} AR receptor antagonists was shown to be beneficial not only by enhancing the therapeutic effects of L-Dopa but also by reducing dyskinesia from long-term L-Dopa treatment.

The specific localization of A_{2A} ARs at basal ganglia, their biochemical and pharmacological properties, advocate that they will be effective targets in PD [120]. Therefore, A_{2A} AR antagonists will potentially reduce the effects associated

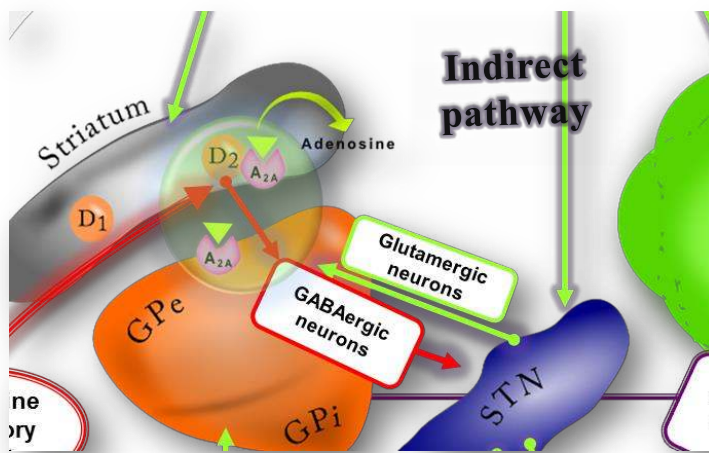


Figure 2.15 Co-localization of A_{2A} AR and D2 receptors

with dopamine depletion in PD. In fact this class of compounds have recently attracted considerable attention as they have shown potential effectiveness in counteracting motor dysfunctions, while displaying additional neuroprotective and anti-inflammatory effects in animal models of PD [60, 117, 118]. They have distinguished themselves over other antiparkinsonian agents in development, by the convergent epidemiological and preclinical evidence of their neuroprotective benefits as well as symptomatic relief [117, 118].

2.4.2.1 A_{2A} AR antagonists

The knowledge acquired over the last decades regarding the involvement of adenosine on motor functions, mainly through modulation of A_{2A} receptor, makes A_{2A} AR antagonists promising non-dopaminergic agents for the treatment of PD motor symptoms. A_{2A} AR antagonists developed do far have been traditionally categorized as xanthine based (e.g. caffeine and styrylxanthines) or non-xanthine based derivatives (e.g. pyrazolotriazolo pyrimidines, arylindeno pyrimidines, thiazolotriazolo pyrimidines). Excellent reviews have been published on this topic in the last five years [123-126]. However, until now only two A_{2A} AR antagonists have undergone clinical evaluation, namely, istradefylline (KW-6002) and preladenant (SCH 420814) (Fig.

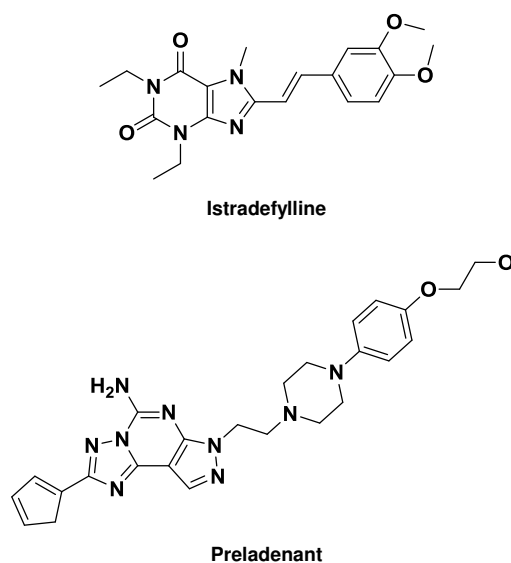


Figure 2.16 Chemical structures of istradefylline and preladenant.

2.16). The preclinical data demonstrates that istradefylline possesses beneficial effects on PD symptoms, and in clinical trials it has shown the ability to reduce the “off” time in patients with PD receiving dopaminergic therapy ^[117]. Istradefylline completed phase III clinical trials in 2009, but it was not approved by the FDA due to lack of efficacy in comparison with placebo ^[127]. Preladenant was being researched as a potential treatment for Parkinson's disease. Although positive results were reported in Phase II clinical trials it did not prove itself to be more effective than a placebo during Phase III trials, and so it was discontinued in May 2013.

2.5 Chromone as a privileged scaffold

2.5.1 Privileged structures for lead discovery

The term privileged structure was first introduced in 1988 by Evans and co-workers^[128] who have recognised the potential of certain regularly occurring structural motifs as templates for structural modification to expand the discovery of novel ligands for binding to proteins. Since then, the original concept definition has evolved and nowadays privileged structures (scaffolds or motifs) can be defined as molecular frameworks which are able of providing useful ligands for more than one type of receptor or enzyme targets by judicious structural modifications^[129]. Privileged structures typically exhibit drug-like properties and usually generate drug-like compound libraries and lead compounds. However, one should keep in mind that the presence of a privileged scaffold in a compound is no guarantee that all compounds in the library will be bioavailable and non-toxic.

Many of these frameworks have been used as templates for the design of libraries of molecules for drug discovery ^[130-134]. In fact, the privileged structure concept has emerged as a successful approach for the drug discovery process, *e.g.* as core structures for synthesis and optimal starting points for the library design of ligands with affinity to certain molecular targets ^[130-134]. The last decade has brought more popularity to this idea and numerous scaffolds have been claimed to be privileged: benzazepinone, diphenylmethane, piperidine, biphenyltetrazole, indole, biphenyl and benzopyrane ^[13, 130]. However, the prerequisites that make a structural motif a privileged one still remain unknown. Nevertheless, it is consensual that there are at least two important issues that can make a privileged structure suitable for fragment-based design: synthetic availability and ease of modifying its structure. The decoration of the privileged scaffolds using diversity-oriented synthesis has been proven to be an essential tool to rapidly discover biologically active small molecules. During the design of a synthetic library, it is advised to exploit simple one-pot approaches, *e.g.* condensation reactions that afford high yields. On the other hand, for building the

structure-activity matrix, usually guided by (bio)isosteric approaches, the tested compounds should be relatively versatile and cover a wide range of substituents^[135].

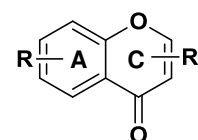
Privileged substructures from bioactive natural products are usually rigid heterocyclic based structures and have played and continue to play an invaluable role in the drug discovery process^[12]. In particular, benzopyrane is a privileged structural motif observed in many biologically active natural products that has been extensively studied by several research groups^[136], especially using as templates coumarin (2H-chromen-2-one) and flavonoid (2-phenyl-4H-chrome-4-one) or isoflavonoids (3-phenyl-4H-chrome-4-one) structure based scaffolds.

Although chromone has not been included so far as a benzopyrane privileged scaffold it is our believe that due to the number of natural chromone derivatives, the high degree of chemical diversity linked to the broad spectrum of pharmacological activities, they can be an important player in the medicinal chemistry drug discovery and development programs.

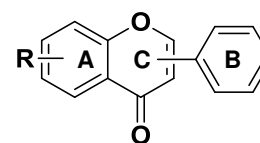
2.5.2 Simple chromones

Chromones are a group of naturally benzopyrone compounds that are ubiquitous in nature, especially in plants. Chromones are oxygen-containing heterocyclic compounds with a benzoannulated γ -pyrone ring (4*H*-chromen-4-one, 4*H*-1-benzopyran-4-one). Due to their structural diversity they are roughly divided into two different categories: simple chromone derivatives and fused chromones such as pyrano and furanochromones.

Simple chromones are a vast group of heterocyclic compounds of great biological and synthetic interest being (iso)flavonoids the most studied components of this group. Up till now, simple chromones have been progressively explored and, with the exception of (iso)flavonoids, and the literature in this area is rather diffuse. However, this type of compounds has attracted interest for a long time either from a biosynthetic and synthetic point of view and/or due to their interesting biological activities. In the present study our attention was focused on simple chromones, which do not have the characteristic B ring of the (iso)flavonoids (Fig. 2.17).



Chromone backbone



(Iso)flavonoids backbone

Figure 2.17 Chromone and (iso)flavonoids backbone.

2.5.3 Chromones in therapy

Chromones have been used in therapy since ancient times. One of the most charismatic examples of natural chromones in clinical practice is khellin (Fig. 2.18), a furanochromone, extracted from the seeds of the plant *Ammi visnaga*. Historically, khellin and its 9-demethoxy derivative, visnagin, were employed as herbal medicines in the treatment of angina, spasmolytic agents, and were also used for kidney stone treatment^[137], but the first clinical application of khellin in its pure form was as bronchodilator in asthma^[138, 139]. However, due to the unpleasant side effects (nausea and vomiting) the use of khellin for asthma events was abandoned^[138, 139]. Currently khellin is still used as a therapeutic agent in the treatment of vitiligo^[140].

The search for NCEs based on khellin with bronchodilation properties, without the inherent side effects and with a better water-solubility profile, led to the synthesis of a small molecule, the chromone-2-carboxylic acid (Fig. 2.18). This chromone was able to prevent bronchial spasms caused by antigens^[138] but unfortunately the effect was too short lived to be clinically useful^[141]. Further research has culminated in the development of the so-called bis-chromones, namely disodium cromoglycate (Fig. 2.18) a chromone that was largely employed for the treatment of bronchial asthma. Although nowadays the therapy for asthma relied on corticosteroids, sodium cromoglycate is still useful in the treatment of mild to moderate asthma, especially in children, mainly due to its lower risk profile compared to the inhaled corticosteroids and to its potent anti-inflammatory effect^[142].

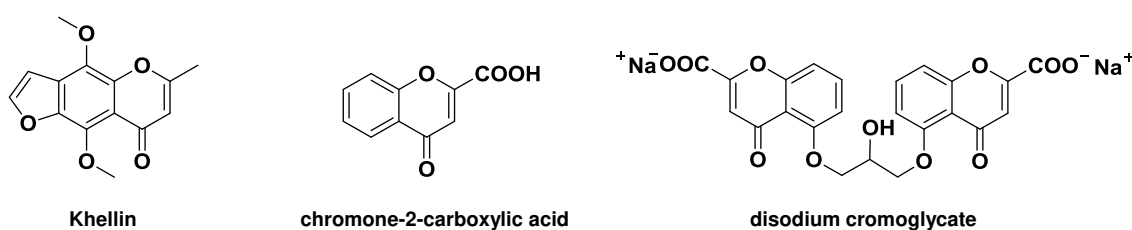


Figure 2.18 Examples of chromone derivatives in therapy

2.5.4 Biological activity of simple chromones and derivatives

Numerous biological activities have been attributed to simple chromones and their analogues, such as anticoagulants and antiplatelet^[143-146] as well as antidiabetics^[147] activities. Their ability to act as inhibitors of carbonic anhydrase^[148, 149], NADH:ubiquinonereductase (complex I)^[150, 151] and calpain^[152, 153] was also reported. However, in this work only the most illustrative properties, namely anti-inflammatory, antimicrobial, anticancer and those related with neurodegenerative diseases, will be further discussed.

The following subdivisions intend to summarise the developed medicinal chemistry artwork related with the potential therapeutic applications of simple chromones and their derivatives, with the exception of flavonoids.

2.5.4.1 Anti-inflammatory activity

The current mainstay treatment of inflammatory diseases, namely those related with rheumatoid (arthritis), respiratory (asthma), cutaneous (psoriasis) and irritable bowel syndrome (IBS) disorders, involve the use of corticosteroids and non-steroidal anti-inflammatory drugs (NSAIDs). However, both therapeutic approaches are linked with several side effects mainly related to a lack of drug target selectivity, among others factors. Despite some notable successes in the field, there is still a major unmet medical need for the treatment of inflammatory diseases. In addition, it has become clear over the last few years that inflammatory processes may also play a key role in other prevalent diseases, not previously considered to have inflammatory aetiologies, such as atherosclerosis, diabetes, cardiovascular, Alzheimer's and Parkinson's diseases as well as cancer.

Over the past 20 years in the modern era of target-based drug discovery, a relatively small number of pivotal targets have been identified and linked to inflammatory process. Most of these are antagonists of endogenous pro-inflammatory mediators, such as prostaglandins, leukotrienes (LTs) and histamine, exerting their biological role by interacting with enzymes, such cyclooxygenases 1 and 2 (COX-1 and COX-2 respectively) and with LT receptors. In this context, several studies aiming at the discovery and development of novel anti-inflammatory agents based on chromone scaffold were performed. Accordingly, 7-methanesulfonylamino-6-phenoxychromone (Fig. 2.19) and analogues were synthesised and evaluated for acute and chronic inflammation ^[154]. From the data a 3-formylamino derivative (T-614) (Fig. 2.19), has emerged as a prospective disease-modifying antirheumatic agent. Inspired by stellatin (Fig. 2.20), a natural chromone isolated from *Dysophylla stellata*s described as a cyclooxygenase inhibitor, Gautam *et al.* synthesised and evaluated several stellatin derivatives towards COX-1 and COX-2 ^[155].

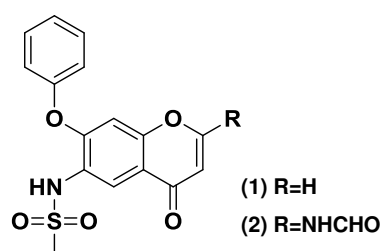


Figure 2.19 Chemical structures of (1): 7-methanesulfonylamino-6-phenoxychromone and (2): T-614.

From the SAR studies it is possible to highlight the compounds represented in Fig. 2.20. Compound 1 and 2 (Fig. 2.20) exhibited the highest COX-2 inhibitory activity off all the tested compounds and a significant anti-inflammatory outline in a TPA-induced mouse ear edema model. Furthermore, compounds 1 and 3 (Fig. 2.20) exhibited higher anti-inflammatory activity than indomethacin ^[155].

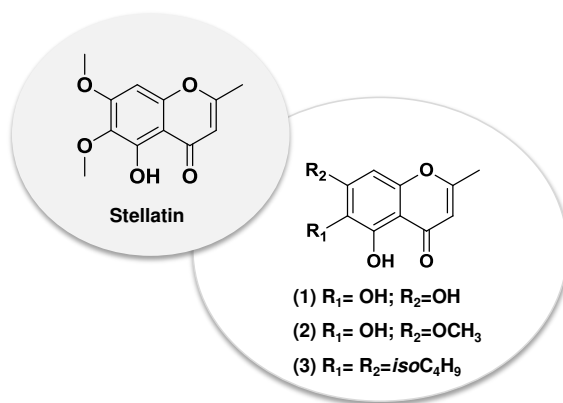


Figure 2.20 Chemical structures of stellatin and its derivatives.

In the 1980s and 1990s the discovery and development of novel LT receptor inhibitors based on the chromone nucleus prompted the emergence of pranlukast (Fig. 2.21). This drug was initially launched in the market for the management of asthma and in 2000 its license was extended for its use in allergic rhinitis. It is also worthy to mention, the discovery of one of the most potent leukotriene D4 (LTD4) antagonists so far reported RG 12553 (Fig. 2.21). RG 12553 was designed based on the combination of pranlukast and FPL 55712, a cromoglycate derivative previously described as LTD4 antagonist ^[156] (Fig. 2.21).

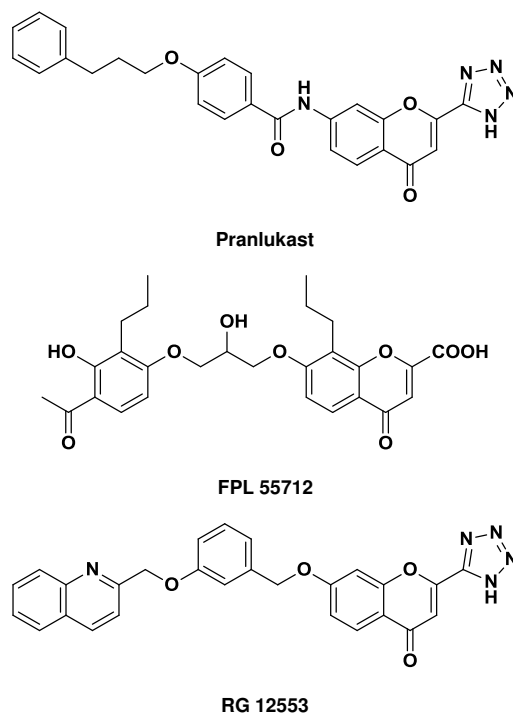


Figure 2.21 Chemical structures of pranlukast, FPL 55712 and RG 12553.

Additionally, the (piperidinylalkoxy) chromone derivatives (Fig. 2.22) have been also described as an important motif for the development of antihistaminic compounds with additional antagonistic activity against LTD4 ^[157].

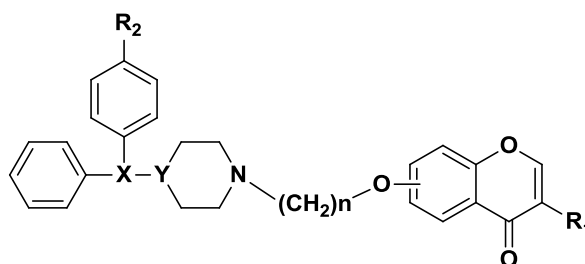


Figure 2.22 LT receptor antagonists based on (Piperidinylalkoxy)chromone scaffold.

Chromone derivatives were also described as potential anti-asthmatic and anti-allergic compounds by targeting mast cells and preventing the release of anaphylactic substances, such as the slow-reacting substance of anaphylaxis (SRS-A) ^[158], or stopping the allergic responses triggered by them, by the inhibition of the passive cutaneous anaphylactic (PCA) reaction ^[159-169].

2.5.4.2 Antimicrobial activity

Over the past 70 years, antimicrobial drugs, such as antibacterial, antifungal and antiviral agents, have been successfully used to treat patients with infectious diseases. Over the course of time, however, many infectious organisms have adapted to the available chemotherapy and the existing drugs became progressively less effective. The emergence of multidrug resistance in common pathogens and the rapid emergence of new infections are the main reasons to drive the discovery and development of new antimicrobial compounds forward. Some of the medicinal artwork in this particular field was based on the chromone structure. Several chromone derivatives, either of synthetic or natural origin, have been recognized to display valuable antibacterial and antifungal activity ^[170-173]. The usefully of the chromone nucleus as starting point to develop NCEs with potential antimicrobial activity is well demonstrated in the work of Chohan *et. al.* ^[174]. In this work several sulfonamide derived chromones were synthesised and their antibacterial activity evaluated against several Gram-negative (*Escherichia coli*, *Pseudomonas aeruginosa*, *Salmonella typhi* and *Shigella flexeneri*) and Gram-positive (*Bacillus subtilis* and *Staphylococcus aureus*) bacteria. Additionally, the same compounds were evaluated towards its antifungal activity against different fungi: *Trichophyton longifusus*, *Candida albicans*, *Candida glabrata*, *Aspergillus flavus*, *Microsporum canis*, *Fusarium solani*. From this work, the chromone derivative represented in Fig.2.23 A arises as the most promising compound of the tested library ^[174]. Other interesting chromone derivative with antimicrobial activity is the dithiazole represented in Fig. 2.23 B. This compound exhibited a better antifungal activity against *Geotrichum candidum* when compared to fluconazole and

also showed a significant antibacterial activity against *Shigella flexneri*^[175].

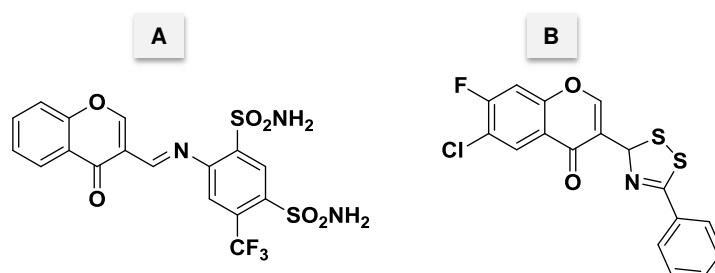


Figure 2.23 Chemical structures of A: sulfonamide chromone derivative and B: Dithiazole chromone derivative.

Others classes of chromone-based compounds, such as pyrazolydene, imidazolydene and pyrimidinyliden^[176], glucosides and aglycones^[177] as well as fused nitrogen heterocyclic systems^[178] and Chitosan derivatives^[179], have also been tested as putative antimicrobial agents, revealing themselves as promising lead compounds to further development in the area.

As an example of chromone derivatives with potential antiviral activity, it is possible to highlight the 2-styrylchromones shown in Fig. 2.24 A^[180, 181]. Furthermore, the (*E*)-5-hydroxy-2-styrylchromone and (*E*)-4'-methoxy-2-styrylchromone showed activity against human noroviruses. This study led the authors to propose the (*E*)-2-styrylchromone scaffold as a lead compound, for further development of new antiviral drugs^[182]. 5-Hydroxy chromones, like the one represented in Fig. 2.24 B, were also proposed as an interesting scaffold for the development of anti-hepatitis C virus drugs^[183]. The chromone moiety was also proposed as a putative scaffold for the development of NCEs against the human immunodeficiency virus (HIV), mainly due to their capacity to inhibit the reverse transcriptase^[184-186] and integrase-mediated strand transfer^[187] enzymes.

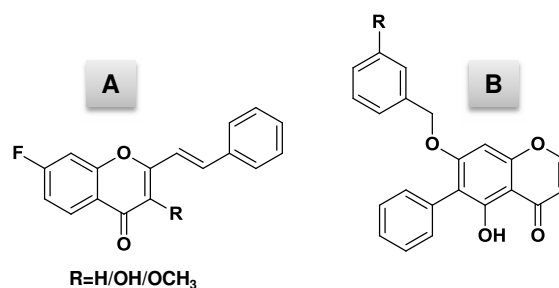


Figure 2.24 Chromone derivatives with antiviral activity. A) 2-styrylchromones; B) 5-hydroxy chromone scaffold.

2.5.4.3 Anticancer activity

The chromone backbone has also been used to discover and develop NCEs with anticancer potential. Accordingly, a number of chromone derivatives were screened toward a panel of cancer cell lines^[188-195]. Some of the obtained results are herein highlighted: i) Substituted-3-(5-phenyl-3*H*[1,2,4]dithiazol-3-yl)chromones and

substituted chromones with a *N*-phenylthioamide in position-3 (Fig. 2.25 A) have shown significant cytotoxic activity [196]; ii) Heterocyclic-substituted chromone derivatives have been screened and 6-chloro-2-(2-quinolyl) chromone (Fig. 2.25 B) emerged as the most promising compound, due to its significant activity towards Sarcoma 180 [197]. iii) Several chromone phosphorus hydrazides derivatives (Fig. 2.25 C) have been reported as having antineoplastic activity against P388 and L1210 leukemia either in monotherapy or in combination with methotrexate [190, 198, 199].

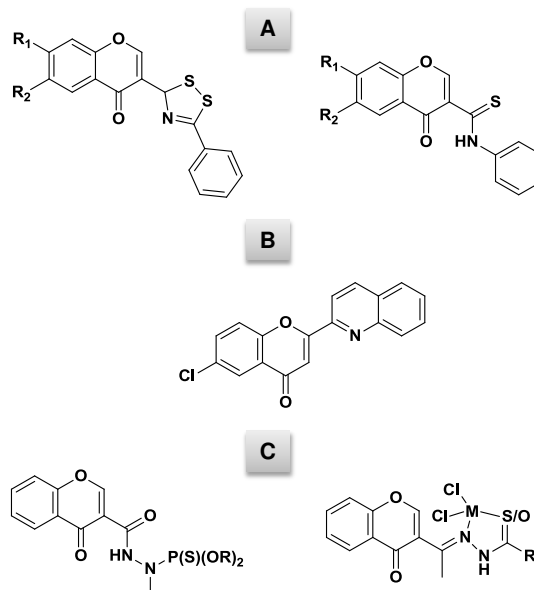


Figure 2.25 Chromone scaffolds for the development of NCE with anticancer activity.

Other works reported several chromone derivatives as potential inhibitors of enzymes implied on tumour growth, namely kinases [200-203], protein tyrosine phosphatases [204], thymidine phosphorylase (TP) [198], topoisomerases [205] and aromatase [206].

A series of 2-styrylchromone analogs (Fig. 2.26) were synthesised and examined for their antiproliferative effects on a panel of carcinoma cells, showing the ability to induce cell death through sub-G1 arrest and DNA fragmentation, demonstrating the putative implication on the molecular mechanisms of apoptosis (compound A, Fig. 2.26) [192]. Other studies performed with compound B (Fig. 2.26) proved that its capacity to promote cell death can probably result from the induction of procaspases and other apoptotic enzymes and by a strong decrease of the available ATP [207]. Moreover, inhibitors of poly(ADP-ribose) synthetase and mono(ADP-ribose) transferase with a chromone core were also studied due to their role in cell death [208].

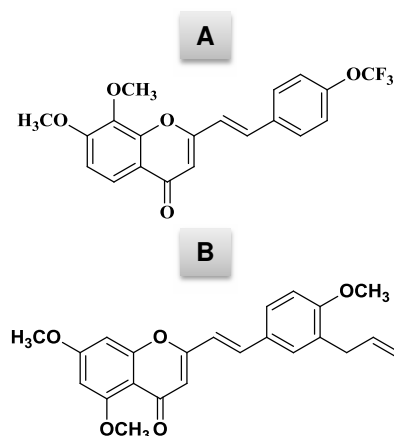


Figure 2.26 2-styrylchromones with antiproliferative activity on a panel of carcinoma cells.

2.5.4.4 Drugs for neurodegenerative diseases

Neurodegenerative diseases such as AD, PD and Huntington's diseases, among others, have in common a neuropathological feature of progressive loss of brain neurons and related functions, with direct consequences on the levels of neurotransmitters. AD and PD are among the two most prevalent neurodegenerative diseases worldwide and their aetiology remains unclear. However, over the last decades it became clear that AD is classically characterized by a loss of basal forebrain cholinergic cells, whereas the most prominent histopathological feature of PD is the loss of dopaminergic neurons and consequent imbalance of ACh and DA neurotransmitters.

Accordingly, increasing the levels in ACh has been regarded as one of the most promising approaches for the symptomatic treatment of AD ^[88]. It was also recently demonstrated that acetylcholinesterase (AChE), an enzyme responsible for the ACh metabolism, could also play a key role in accelerating β -amyloid (A β) plaques deposition, an important factor observed on patients with AD ^[88]. Furthermore and although the mechanism of action is not yet completely understood, as mentioned previously in section 2.2, ACh through its receptors seems to be implied in the regulation of the dopamine in striatum, and by that correlated with the symptomatic treatment in PD. In fact, anticholinergic drugs are among the oldest drugs used to treat PD ^[55, 93]. Other neurotransmitter that can be correlated with both of the diseases is DA. In fact, and despite the important role of DA in PD (previously mentioned in this work), it was recently evidenced that DA might be involved in cognitive dysfunction occurring in AD, mainly due to the strong synaptic interactions with ACh, in different brain areas ^[209, 210].

The application of the chromone backbone, in the discovery and development of new drugs suitable to be applied in patients with neurodegenerative diseases, is still an unexplored field. However, the work performed by Brühlmann *et al.* ^[211] comprised the synthesis and evaluation of chromone derivatives (Fig 2.27 A) as potential AChE and MAO inhibitors. More recently it was shown that several benzyloxy substituted chromones possess high inhibitory activity towards human monoamine oxidase B and some of them showing reversibility ^[212-214]. A small library of (aminoalkoxy) chromones has been prepared and evaluated as DA D₂ receptors agonists. The SAR studies revealed that the type of the substituents at C-2 is an important feature to improve the desired activity and/or selectivity (Fig. 2.27 B) ^[215].

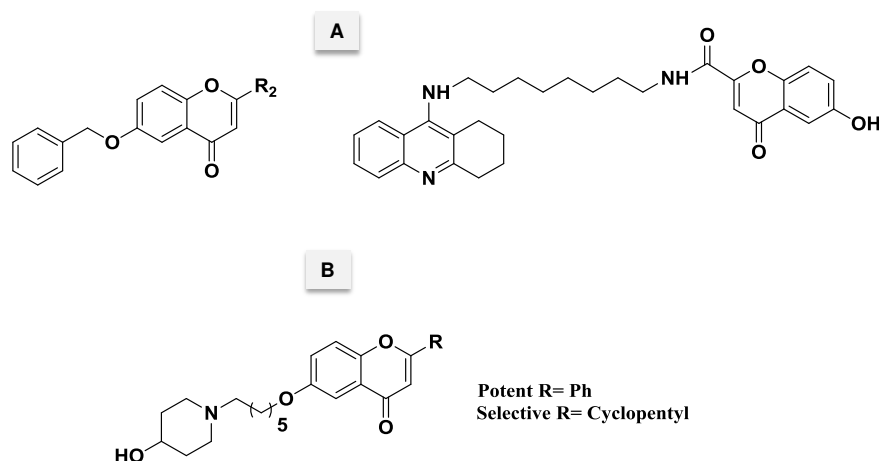


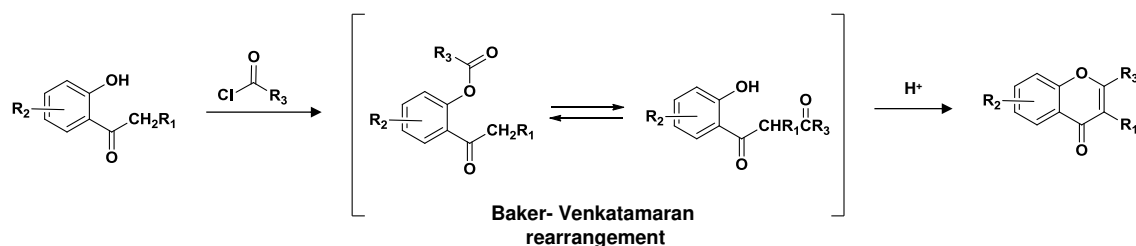
Figure 2.27 Chemical core of chromone derivatives tested as A: AChE and MAO inhibitors and B: Dopamine D₂ agonists.

2.6 Methods of synthesis of simple chromones

Generally, the total synthesis of simple chromones can be attained using starting materials that do not possess a pyran ring in their structure, such as phenols and 2-hydroxyarylalkyl ketones. Despite the advances performed in synthetic strategies they are still the most cited in the literature. Yet, other building blocks, such as 2-hydroxyarylalkynyl ketones and salicylic aldehydes have been recently used. As microwave assisted-synthesis is nowadays a valuable tool in the area of heterocyclic compounds efforts were performed to include this new technique in organic synthesis along the topic.

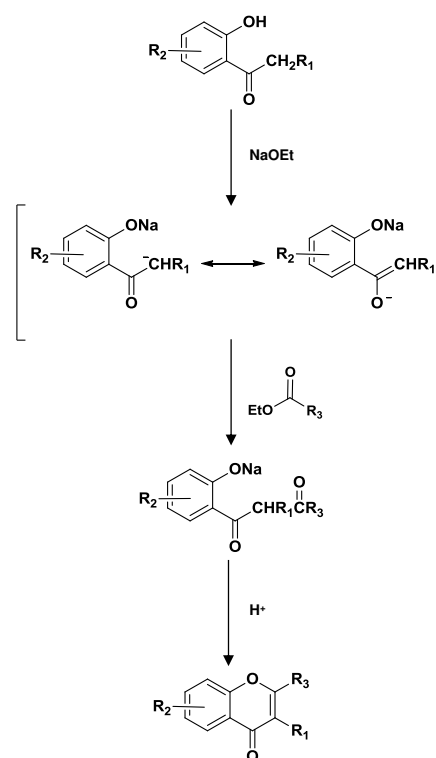
2.6.1 Chromones from 2-hydroxyarylalkyl ketones

The Baker-Venkataratnam rearrangement is perhaps the most charismatic methodology related with the chromone nucleus formation. This rearrangement takes place after the acylation of 2-hydroxyarylalkyl ketones, usually with acyl chlorides. In presence of a base such as potassium carbonate, the acyl intermediate rapidly undergoes a Baker-Venkataratnam rearrangement (scheme 2.1) leading to the formation of 1,3-dioxophenoxy intermediate. Classically, the intermediate compound is isolated and cyclised into the desired chromone under harsh conditions, such as heated concentrated sulphuric or glacial acetic acid. Among the huge diversity of chromone derivatives it is important to remark that a vast number of synthetic 2-styrylchromone derivatives were obtained through this methodology ^[216-220].


 Scheme 2.1 Synthesis of chromones *via* Baker-Venkatamaran rearrangement.

Several modifications have been proposed to this method. One is related with the possibility to perform the cyclisation process *in situ*, surpassing the isolation of the intermediate, using pyridine as a catalyst ^[221,222]. A recent example of this kind of approach is the synthesis of 2,8-disubstituted chromone derivatives and the use of diazabicyclo[5.4.0]undec-7-ene (DBU) and pyridine to promote the cyclization step ^[223]. Another variation of the method involves the acylation step: instead of using the conventional acyl chlorides some authors report the direct application of the carboxylic acids ^[224] or reaction with acid anhydrides as starting materials ^[225]. In addition, the use of other bases rather than potassium carbonate, such as metallic sodium ^[226], sodium alkoxide ^[204, 227-229], sodium hydride ^[204] and potassium or sodium hydroxide ^[230], has also been reported. Dyrager *et al.* ^[230] have synthesised 3-(4-fluorophenyl)-2-(4-pyridyl)chromone derivatives through a microwave-assisted Baker–Venkatamaran rearrangement.

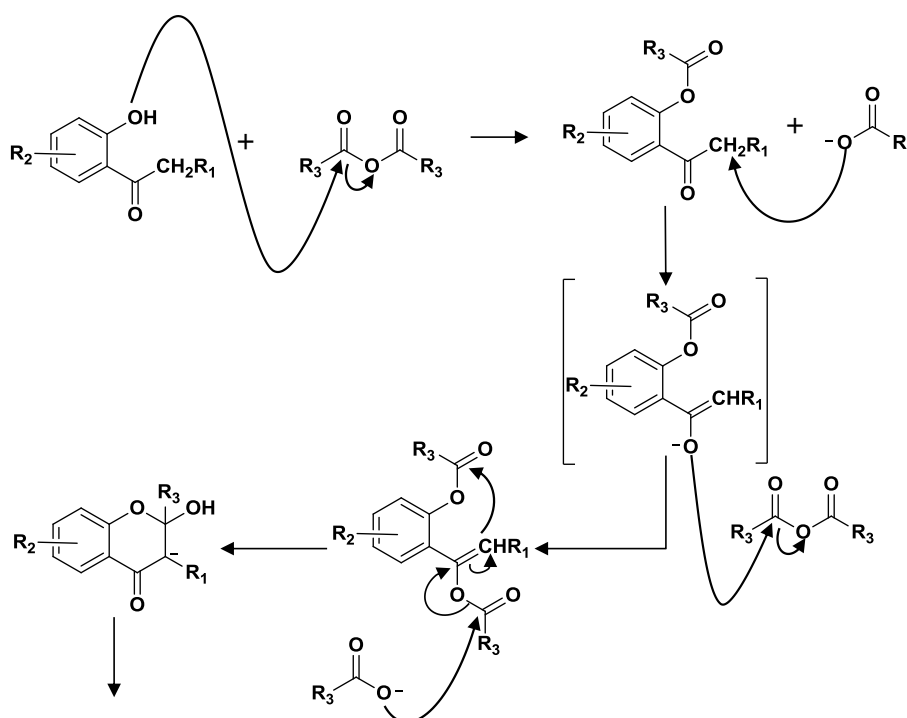
Despite the “popularity” of the Baker-Venkatamaran rearrangement, one of the first methodologies applied to the synthesis of chromones was the Claisen condensation. This well-known methodology was first described to obtain chromones by Kostanecki, Paul and Tambor for the synthesis of 7-ethoxy-4*H*-1-benzopyran-2-carboxylic acid ^[231]. The construction of chromones based on this reaction may be performed in two steps (scheme 2.2). The first involves the reaction of a strong base, traditionally sodium etoxide in ethanol, with a 2-hydroxyarylalkyl ketone and the formation of the corresponding enolate ^[232-234], which reacts with the appropriate carboxylic ester leading to the formation of 1,3-dioxophenoxy salt


 Scheme 2.2 Synthesis of chromones *via* Claisen condensation.

intermediate. The second step, the cyclization of the intermediate, is conventionally performed with heat and under acidic conditions ^[232-234]. An important group of chromone derivatives, the chromone 2-carboxylic acid or esters, may be synthesised by a variation of the Claisen condensation, also known as Kostanecki' reaction ^[235]. Basically this methodology consists in the condensation of the 2-hydroxyacetophenone with diethyl oxalate in the presence of sodium ethoxide in ethanol (EtOH) followed by the oxopropanoate intermediate cyclisation under acidic conditions ^[236-239]. Other modifications to the synthesis of chromones *via* Claisen condensation were also reported ^[237, 240, 241]. Essentially, the reported modifications were focused in finding mild reaction conditions, such as the employment of triethylamine as solvent and base ^[242] although the use of other catalysts like LiH ^[243], NaH in THF ^[195] and NaH in pyridine ^[204, 244, 245] have also been described. Mozingo *et al.* ^[246] reported the use of metallic sodium as catalyst, instead of sodium ethoxide in the synthesis of alkylchromones, such as 2-ethylchromone.

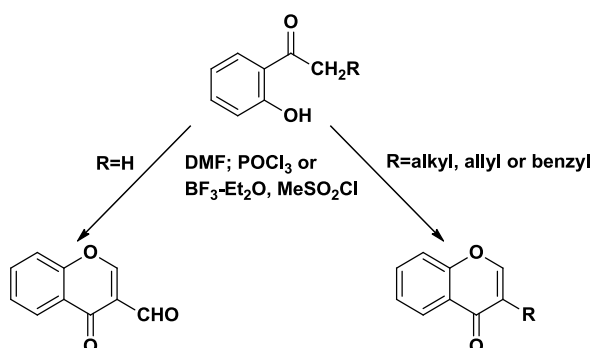
More recently, several chromone derivatives, namely 2,6-dimethylchromone and 2-methyl-6-chlorochromone, were synthesised under microwave irradiation. The synthetic strategy encompassed a Claisen condensation and a two-step procedure comprising the formation of the 1,3-dioxophenoxy intermediate and subsequent cyclisation under acidic conditions ^[247]. The major advantage of this synthesis is that microwave irradiation yields the intermediate within a reduced reaction time.

Kostanecki, Robinson and their co-workers modified the Claisen condensation reaction to obtain diverse chromones, developing what is nowadays known as the Kostanecki-Robinson reaction. In this type of reaction the desired chromone is also obtained using 2-hydroxyarylalkyl ketones as starting materials, by the reaction with aliphatic acid anhydrides in the presence of its corresponding sodium or potassium salts. This procedure obviates the need of the acidification step for ring closure, which is a significant advantage when compared with the classic Claisen reaction. It is noteworthy that the chromone formation does not involve a 1,3-dioxophenoxy intermediate, a requisite in the methods described so far. After the *O*-acylation of the starting material, as emphasized on the proposed reaction mechanism depicted in scheme 2.3, the arylalkyl ketone undergoes enolisation with consequent acylation, affording an enolacetate intermediate, that after aldol intramolecular cyclisation followed by loss of water, delivers the final chromone ^[248].


 Scheme 2.3 Proposal mechanism of Kostanecki- Robinson reaction adapted from ^[248].

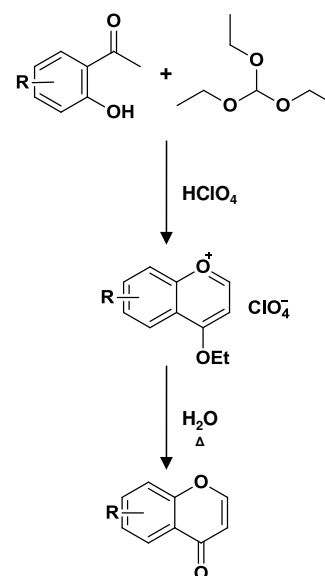
The Kostanecki-Robinson reaction has been applied over the years in the synthesis of a large number of chromones ^[225, 249, 250]. Despite its wide application, this methodology possesses some drawbacks; one of them is related with the possibility of occurrence of the Baker-Venkatamaraman rearrangement and consequent formation of unwanted compounds, namely 3-substituted chromones. This contingency has been explored and adjusted to obtain 3-acylchromones ^[226, 251].

Another important methodology employed in the chromone synthesis is the Vilsmeier-Haack reaction (scheme 2.4). Briefly, this reaction occurs between the appropriate 2-hydroxyalkyl aryl ketone and the (Chloromethylene)dimethylammonium chloride (Vilsmeier reagent). The chloroiminium ion is formed *in situ* from the reaction of a *N,N*-disubstituted formamide, such as dimethylformamide (DMF), with phosphorus oxychloride. In general, the reaction mechanism encompasses the formation of an non-substituted chromone as intermediate which suffers a second attack from the chloroiminium ion, giving rise to 3-substituted chromones ^[252].


 Scheme 2.4 Synthesis of chromones *via*
 Vilsmeier-Haack reaction.

This one pot procedure was applied to the synthesis of chromones for the first time in 1973 and has been widely used since then. Other similar formylating agents, such as DMF-dimethyl acetal, have been used as variants of the Vilsmeier-Haack reagent ^[253]. Recently, the synthesis of 3-formylchromones by the Vilsmeier-Haack reaction was improved using microwave and solid-supported methods ^[254, 255].

The synthesis of non-substituted chromones can be attained *via* benzopyrylium salt intermediates. In this condition, the 2-hydroxyacetophenones used as starting materials react with triethyl *ortho* formate and a strong mineral acid like perchloric acid (scheme 2.5) ^[154, 256-258]. Subsequently, the obtained benzopyrylium salt is converted to the chromone by heating the crude material in water. This method has been extended to the synthesis of 3-substituted chromones, such as 3-hydroxychromones ^[259] and 3-methylchromones ^[260].



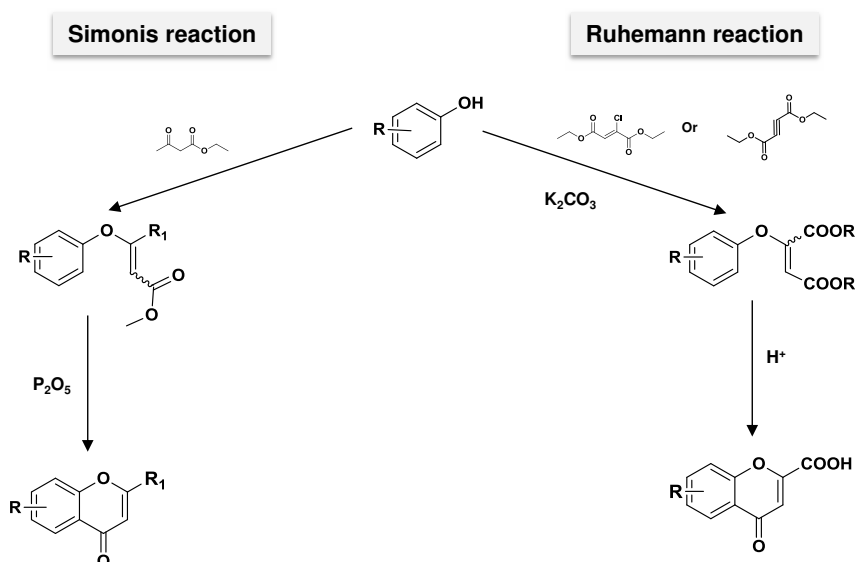
**Scheme 2.5 Synthesis of chromones
via benzopyrylium salt intermediates.**

2.6.2 Synthesis of chromones from phenols

In 1913, Simonis reported a reaction by which different types of phenols were condensed with β -ketoesters (*e.g.* ethyl acetoacetate) in the presence of phosphorus pentoxide (P₂O₅) to obtain chromones, instead of the corresponding coumarins, as a final product. This acid-catalyzed condensation became known as Simonis' reaction (scheme 2.6) ^[244]. The synthesis of chromones by Simonis reaction is usually operative when the phenol used as starting material has electron-withdrawing substituents, such as halogens or nitro groups. It was also found that the presence of alkyl substituents on the α -position of the β -ketoester can favor the formation of the chromone. Classically, phosphorus pentoxide is used as the condensing agent but sulfuric acid ^[143, 144, 261] or polyphosphoric acid ^[262] have also been employed. More recently, Eric Fillion *et al.* ^[263] described a successful synthetic strategy for the synthesis of 2-methylchromones by promoting the condensation of the suitable phenol with 5-(1-methoxyethylidene) Meldrum's acid in the presence of trifluoroacetic acid.

Chromones can be obtained through the reaction of a phenol with acetylenic dicarboxylic acids, esters or with chlorofumaric acid, in basic conditions, such as metallic sodium or K₂CO₃. A particular intermediate is formed (scheme 2.6) which, in presence of sulphuric acid, perchloric acid or hydrogen fluoride cyclises to afford

chromone 2-carboxylic acid. This method, known as Ruhemann reaction, was largely applied to the synthesis of chromone-2-carboxylic acids and derivatives [235]. Ruhemann reaction was also used with slight modifications for the synthesis of flavones and styrylchromones [264]. In 1977, Lee and coworkers proposed a modification of the process using polyphosphoric acid as a catalyst [259].



Scheme 2.6 Synthesis of chromones *via* Simonis and Ruhemann reactions.

2.6.3 Synthesis of chromones from salicylic acids and derivatives

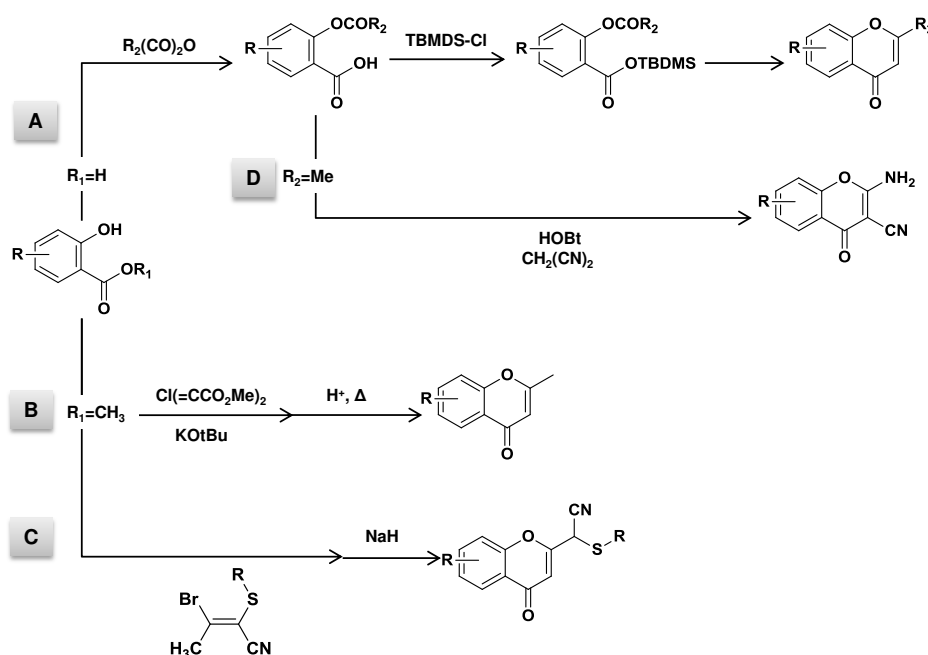
Salicylic acid and its derivatives have been used as starting materials for the obtention of chromones by converting them into *O*-acyl(aryl) derivatives. The subsequent reactions of these derivatives with *tert*-butyldimethylsilyl chloride in the presence of imidazole lead to the formation of the corresponding silyl esters. Chromones were then obtained in moderate to high yields, after reaction with (trimethylsilyl)methylenetriphenylphosphorane. This procedure corresponds to the first report of chromone synthesis *via* intramolecular Wittig ester carbonyl olefination (scheme 2.7A) [265].

Another interesting method comprises the reaction of activated salicylic derivatives with diethyl malonate giving intermediates that undergo subsequent hydrolysis and decarboxylation processes with formation of 2-methylchromones [266]. This type of chromones have also been obtained by the reaction of methyl salicylate with dimethylpenta-2,3-dienedioate, in the presence of $KOtBu/BuOH$ (scheme 2.7B) [267].

Other applications of salicylic acid derivatives as starting materials have been reported in the literature, namely for the synthesis of chromones *via* the condensation

of methyl salicylate with bromocrotononitrile derivatives. The cyclisation of the vinyl ether intermediate was performed in a basic (NaH) medium (scheme 2.7 C)^[268].

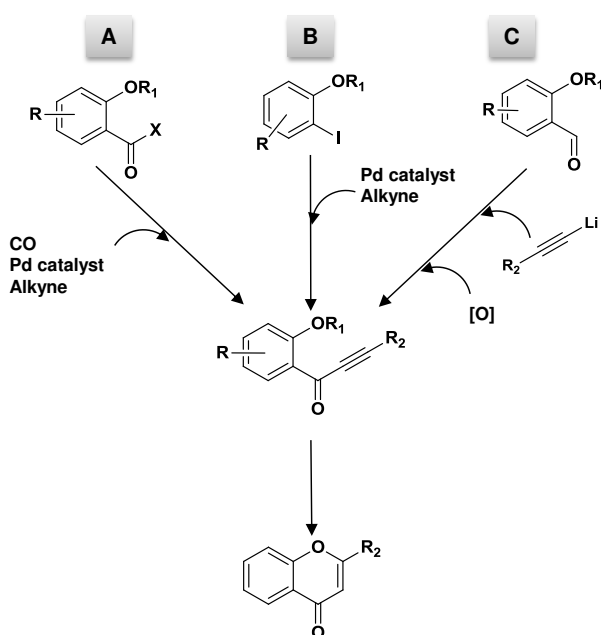
Functionalised 2-amino-3-cyano-4-chromones have also been obtained in a one pot procedure by reacting acetylsalicylic acid derivatives with *N*-hydroxybenzotriazole (HOBt) and malononitrile under basic conditions (NaH). The cyclisation step was attained with acid catalysis (HCl) (scheme 2.7 D)^[269].



Scheme 2.7 Synthesis of chromones from salicylic acids and derivatives.

2.6.4 Synthesis of chromones via C-C cross coupling reactions

Transition metal-catalysed reactions provide nowadays one of the most attractive methodologies for the formation of C–C and C–heteroatom bonds. The application of these reactions has increased tremendously during the past decades and cross-coupling reactions became an important tool for synthetic chemists. Following this tendency, an attractive synthetic method has been developed for the synthesis of chromones involving a

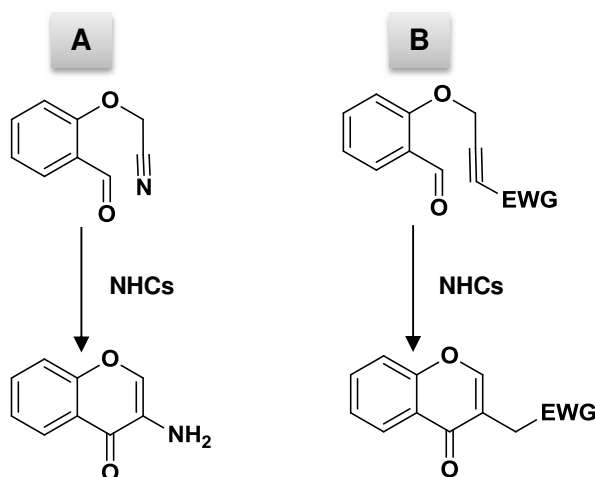


Scheme 2.8 Synthesis of chromones via C-C cross coupling reactions.

one-pot Sonogashira-carbonylation-annulation reaction that involves the reaction of an *ortho*-iodophenol with a terminal acetylene, in the presence of a palladium complex, and the formation of an *ortho*-hydroxyarylalkynylketone intermediate avoiding the harsh reaction conditions (strong bases and acids or high temperature) used in the reactions above mentioned. The obtention of a chromone encompasses a cyclocarbonylation process which occurs *in situ* in the presence of carbon monoxide (Scheme 2.8 A) ^[78]. The reaction proceeds in a short time and with very good yields. The use of microwave irradiation can speed up the process and substantially increasing the yields ^[270]. However, in particular situations a mixture of chromones and aurones can be obtained. This drawback can be minimized by the use of ionic liquids ^[270].

The chromone formation by Sonogashira coupling with palladium catalysis was also performed by reacting an 2-methoxybenzoyl chloride with a terminal acetylene (Scheme 2.8 B) or an 2-methoxybenzaldehyde with a lithium acetylide (Scheme 2.8 C) ^[271]. In all the cases, the intermediate compounds are 2-methoxyarylalkynylketones that after ring closure, performed by iodine monochloride (ICl), afford 3-iodochromones ^[272]. In summary, the obtention of chromones via palladium-mediated catalysis is a simple and high efficient approach.

An interesting alternative to the metal-catalysed C–C cross coupling reactions are the organocatalysed reactions. These reactions are eco-friendly as they are metal free and cost-effective, and are currently one of the most significant green chemistry research areas. In this context, *N*-heterocyclic carbenes (NHCs) have recently gained importance as catalysts of carbon–carbon bond formation. The use of NHCs catalysts was recently proposed for the synthesis of 3-aminochromones and other 3-substituted chromones, (scheme 2.9) ^[273-275]. NHCs catalysts were used with the purpose of promoting the intramolecular cross coupling between the aldehyde and the nitrile function (Scheme 2.9 A) or to enhance the intramolecular reaction of the aldehyde with an activated alkyne (Scheme 2.9 B). This latter reaction is a modification of the known intramolecular Stetter reaction ^[273-275].



Scheme 2.9 Synthesis of chromones catalysed by NHCs.

2.6.5 Synthesis of chromones from chromanones

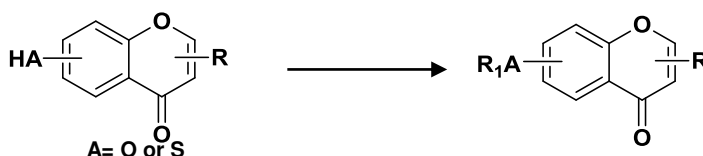
The formation of chromones starting from chromanones is not as common as the methodologies described above, essentially because the starting material is not easily available and the overall yields are often very low ^[259]. In fact, in the last three decades few studies have reported the application of chromanones to obtain chromones and, in most cases, the main approach involves the dehydrogenation or oxidation of the starting material. In order to achieve this goal, several oxidants such as iodide ^[276], vanadium pentoxide ^[277] and 2,3-dichloro-5,6-dicyano-1,4-benzoquinone (DDQ) ^[278] were used. The reaction is often conducted in acidic medium ^[279]. Other catalysts, such as diethoxymethyl acetate ^[280, 281], thallium(III) ^[282] and the Lewis acids AlCl₃ ^[283] and BF₃·Et₂O ^[284] have been also described. Furthermore, chromones can be obtained by dehydration of 2-hydroxychromanones through treatment with HCl in EtOH ^[285]. Dehydrobromination of the starting chromanone is another methodology applied to obtain chromones ^[286, 287]. This reaction is carried out in basic medium and can be performed using microwave irradiation ^[288].

2.6.6 Synthesis of chromones from other chromones

As described before, direct and efficient chemical strategies have been developed for the synthesis of simple chromones. However, in recent years a modification on the strategy of synthesis of simple chromones has been observed, which is related with the need to speed up the drug discovery process, namely for structure-activity-relationships studies, in medicinal chemistry programs. In consequence, several simple functionalised chromones are by now commercially available and used as starting materials. The most common chromones used as starting materials have been found to be 6/7-hydroxy or methoxy, halo, methyl and formylchromones.

The chemical core of chromone possesses three main areas suitable for the introduction of substituents: the aromatic ring and the positions 2- and 3- of the pyrone ring. Furthermore, a proper chemical function (e.g. hydroxy or methoxy) present in the benzopyran core of chromone allows the synthesis of several chromones derivatives with different substituents patterns. For instance, several benzylic, alkyl, and tioalkyl ethers have been obtained

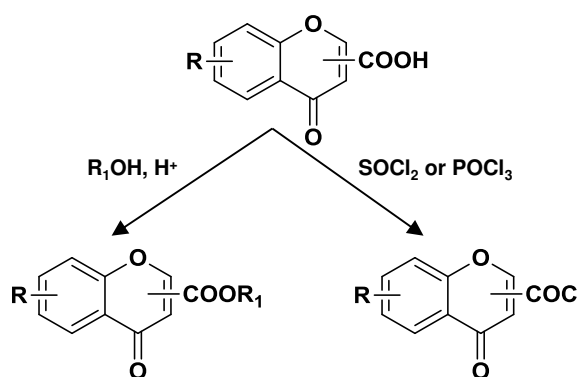
by the conventional methodologies for etherification, using as starting materials hydroxy or thio chromones (scheme 2.10) [195, 214, 289].



Scheme 2.10 Synthesis of chromones from hydroxyl or thiochromones.

Interestingly, although the carboxylic acid is one of the most studied functions to obtain other classes of compounds, the use of the chromone carboxylic acids as starting materials is still very limited.

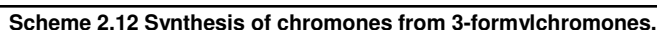
The works performed in this field are mainly related with ester formation (e.g. methyl and ethyl esters) [231] or acyl halides as intermediates for the synthesis of chromone carboxamides [290] (scheme 2.11). Other reported application of the chromone-2-



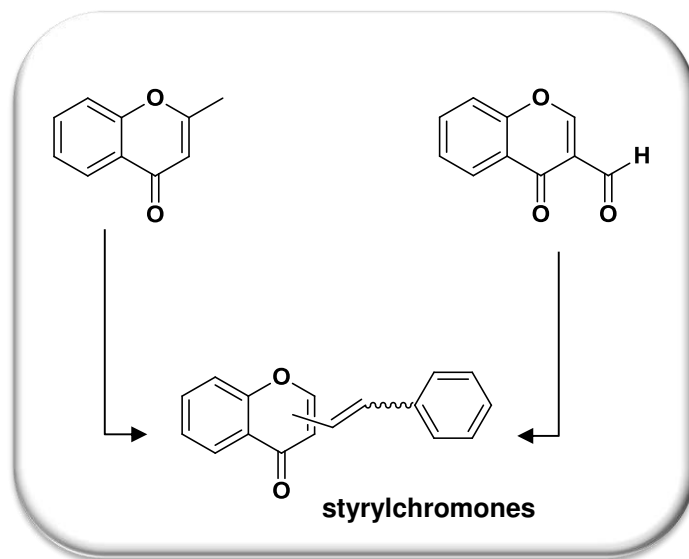
Scheme 2.11 Synthesis of chromones from chromone carboxylic acids.

carboxylic acid is the synthesis of 2-aminoalkyl chromones. The strategy to obtain this compounds comprises the formation of the corresponding methyl esters, reduction with NaBH_4 with the synthesis of the 2-hydroxymethylchromones subsequently transformed, by nucleophilic substitution, to 2-chloromethylchromones, that finally by reaction with several substituted amines will afford the correspondent aminoalkyl chromones. [291].

process can be performed with a suspension of basic alumina in isopropanol^[292] and the oxidation process with sodium chlorite in the presence of aminosulfonic acid^[293]. Interestingly, this last strategy is the most cited to obtain the chromone-3-carboxylic acid while its isomer, chromone 2-carboxylic acid, is usually obtained by a classic methodology from 2-hydroxyarylalkylketones^[293]. The presence of three electron-deficient carbons (C-2, C-4 and CHO) on the 3-formylchromone structure makes this compound an exceptional starting material for several nucleophilic additions, which in turn can lead to a great diversity of derivatives. Taking advantage of these features, several heterocyclic substituted chromones were obtained, namely with aza^[294, 295], diaza^[170, 296], oxa^[297] and dithiazole^[298-302] groups as well as vinyl chromone derivatives^[303, 304] (scheme 2.13).



A particular example of this type of nucleophilic additions is the synthesis of styrylchromones ^[218] by the condensation of a 3-formylchromone with malonic acid in pyridine, either with conventional heating or under microwave irradiation ^[305]. Additionally, styrylchromone derivatives can also be obtained by the condensation of 2-methylchromones (scheme 2.14) with the benzaldehyde derivatives in presence of sodium methoxide or by the reaction of non-substituted chromones (scheme 2.14) with the Grignard reagents or by a C-C cross coupling palladium catalysed reaction ^[218].



Scheme 2.14 Synthesis of styrylchromones from other chromones.

Chapter 3

Results

3.1 Chromone-2- and -3-carboxylic acids inhibit differently monoamine oxidases A and B

Article from Bioorganic & Medicinal Chemistry Letters (2010), 20: 2709–2712.



Contents lists available at ScienceDirect

Bioorganic & Medicinal Chemistry Letters

journal homepage: www.elsevier.com/locate/bmcl



Chromone-2- and -3-carboxylic acids inhibit differently monoamine oxidases A and B

Stefano Alcaro^{a,*}, Alexandra Gaspar^{b,c}, Francesco Ortuso^a, Nuno Milhazes^c, Francisco Orallo^d, Eugenio Uriarte^e, Matilde Yáñez^d, Fernanda Borges^{b,*}

^a Dipartimento di Scienze Farmacobiologiche, Facoltà di Farmacia, Università "Magna Græcia" di Catanzaro, Campus Universitario "S. Venuta", Viale Europa, 88100 Catanzaro, Italy

^b CIQUP/Departamento de Química, Faculdade de Ciências, 4169-007, Universidade do Porto, Porto, Portugal

^c Instituto Superior de Ciências de Saúde-Norte, 4585-116 Gandra PRD, Portugal

^d Departamento de Farmacologia, Facultad de Farmacia, Universidad de Santiago de Compostela, 15782 Santiago de Compostela, Spain

^e Departamento de Química Orgánica, Facultad de Farmacia, Universidad de Santiago de Compostela, 15782 Santiago de Compostela, Spain

ARTICLE INFO

Article history:

Received 24 February 2010

Revised 19 March 2010

Accepted 23 March 2010

Available online 27 March 2010

Keywords:

Chromones

Docking

Monoamine oxidase

Inhibitors

ABSTRACT

Chromone carboxylic acids were evaluated as human monoamine oxidase A and B (hMAO-A and hMAO-B) inhibitors. The biological data indicated that only chromone-3-carboxylic acid is a potent hMAO-B inhibitor, with a high degree of selectivity for hMAO-B compared to hMAO-A. Conversely the chromone-2-carboxylic acid resulted almost inactive against both MAO isoforms. Docking experiments were performed to elucidate the reasons of the different MAO IC₅₀ data and to explain the absence of activity versus selectivity, respectively.

© 2010 Elsevier Ltd. All rights reserved.

Monoamine oxidases (MAOs; EC 1.4.3.4) are widely distributed enzymes that contain a flavin adenine dinucleotide (FAD) covalently bounded to a cysteine residue.¹ Many living organisms possess MAOs and in mammals two isoforms are present, MAO-A and MAO-B, located in the outer membrane of the mitochondria. These two isoforms are involved in the oxidative deamination of exogenous and endogenous amines, including neurotransmitters, thus modulating their concentrations in the brain and peripheral tissues. Physiologically, MAOs oxidize biogenic neurotransmitters such as dopamine, norepinephrine, 5-hydroxytryptamine (5-HT, serotonin) and β-phenethylamine, dietary, and xenobiotic amines such as tyramine and benzylamine (Fig. 1).²

Although MAO-A and MAO-B have an amino acid sequence similarity up to 70% they exhibit different substrate specificity, inhibitor sensitivity, and tissue distribution. MAO-A is located predominantly in catecholaminergic and serotonergic neurons. Consequently, this MAO isoform has a higher affinity for serotonin, epinephrine and norepinephrine and it is more sensitive to inhibition by clorgyline and moclobemide.¹ On the other hand MAO-B is present in dopaminergic neurons and glia and, therefore, has a preferential action on dopamine, β-phenethylamines, benzylam-

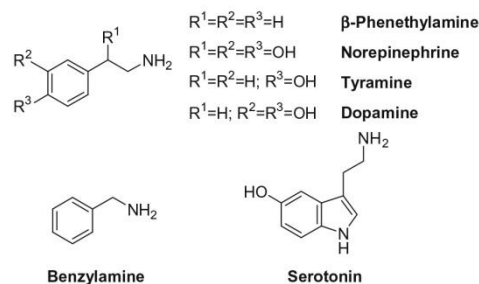


Figure 1. Endogenous, dietary, and xenobiotic amines.

ines and sterically hindered amines. This isoform is selectively inhibited by low concentrations of selegiline (L-deprenyl) and rasagiline.^{1,3}

MAO-A inhibitors are frequently used as antidepressants and anti-anxiety agents while MAO-B inhibitors, alone or combined with L-Dopa, are relevant tools in the therapy of Alzheimer's and Parkinson's diseases.^{1,4} Development of MAO inhibitors is important not only from the standpoint of symptomatic treatment (i.e., by increasing the biological half-life of monoamine neurotransmitters),

* Corresponding authors. Tel.: +39 0961 3694197; fax: +39 0961 391490 (S.A.), tel.: +351 220402560; fax: +351 220402659 (F.B.).

E-mail addresses: alcaro@unicz.it (S. Alcaro), fborges@fc.up.pt (F. Borges).

but also with regard to the neuroprotective effects (i.e., prevention or delay of neurodegeneration itself).

All of these aspects have led to an intensive search for novel MAO inhibitors and this effort has increased considerably in recent years. However, a large number of MAOs inhibitors introduced into clinical practice were abandoned due to adverse effects, such as hepatotoxicity, orthostatic hypotension, and the so-called ‘cheese effect’, which is characterized by hypertensive crises.¹

In spite of the considerable progresses in the understanding of the interactions of MAO isoforms with their specific substrates or inhibitors, there are not any available rules for the rational design of new potent and selective MAO inhibitors. Privileged structures, such as indoles, arylpiperazines, biphenyls, and benzopyranes are considered useful in drug discovery. Different families of nitrogen and oxygen heterocycles, such as xanthenes, coumarins and their precursors (chalcones) have also been extensively used as scaffolds in medicinal chemistry programs searching for novel MAO-B inhibitors.^{4–6}

In order to include other scaffolds in the series of MAO inhibitors the chromone scaffold [(4H)-1-benzopyran-4-one] has been considered, since it is common to a large number of bioactive molecules either of natural or synthetic origin. Until now, numerous biological effects, especially in the popular medicine, have been ascribed to this benzo- γ -pyrone nucleus such as anti-inflammatory, antitumor and antimicrobial activities.⁷ Enzymatic inhibition properties towards different systems, such as oxidoreductases, kinases, tyrosinases, cyclooxygenases have also been recognized.⁸

In this work, we focus our attention on two chromone isomers (Fig. 2) that were screened towards MAO-A and MAO-B (Table 1). Details about the enzymatic evaluations are reported in the Supplementary data.

The results of the enzymatic experiments of the two chromones under study, with respect to the reference compounds, disclose a significant chemical feature related with the location of carboxylic moiety in the γ -pyrone nucleus. In fact, when the acidic substituent is in position 3 of the heterocyclic scaffold the compound **2** acted as MAO-B inhibitor with IC_{50} values in the nanomolar range. Its inhibition effect onto the MAO-A isoform resulted three orders of magnitude lower with a interesting selectivity ratio. Surprisingly the isomer **1**, with the acid moiety in position 2, gave no inhibition

on both MAO isoforms. Compound **2** revealed to bind the hMAO-B exerting a selective inhibition with respect to the A isoform (see Supplementary data).

This curious appraisal attracted our attention and led us to investigate at molecular level the recognition mechanisms of compounds **1** and **2** within both enzymatic clefts by means of molecular modeling experiments. These studies were performed using available hMAO-A and hMAO-B structures deposited into the Protein Data Bank (PDB) as receptor models to understand the enzyme–inhibitor interactions and explain the biological data. Two recently determined MAO crystallographic structures were adopted as targets after a preliminary treatment (see Supplementary data). Ligand flexible docking, followed by fully geometry optimization of the generated complexes, reported the capability of compounds **1** and **2** to fit within both hMAOs catalytic sites, but only the latter compound revealed strong energy favoured binding modes into the hMAO-B (Table 2). Such an observation was in qualitative agreement to the experimental IC_{50} previously discussed.

Then the most stable optimized complexes were graphically inspected and the key enzyme–ligand interacting residues were highlighted (Table 3).

In hMAO-A both compounds **1** and **2** showed a similar orientation (see Supplementary data), with their aromatic and carboxylate moieties respectively directed towards the FAD and the outer side. The latter compound was able to perform a deeper recognition with respect to the former one. Actually, compound **1** did not establish direct contacts to the cofactor with the lack of strong productive interactions into the active site. Moreover, compound **1** recognition was penalized by electrostatic repulsions between its sp^2 oxygen atom and Ile180-Asn181 backbone. These unfavorable interactions, coupled to the lack of the few productive contacts highlighted by compound **2**, could explain the poor complexation energy of **1** within the hMAO-A binding cleft. A similar scenario can be addressed to **2**, but it showed stacking contacts to the Tyr407 and, moderately, to Tyr444 and its ether oxygen, partially negative charged, favorably interacted to FAD C4 that, in the used force field, resulted partially positive charged.

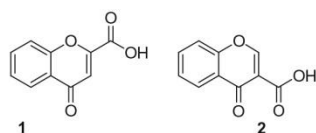


Figure 2. Chemical structures of the chromone isomers **1** and **2**.

Table 1

IC_{50} values for the inhibition of hMAO (in μ M) of chromone carboxylic acids and reference inhibitors

Compounds	hMAO-A	hMAO-B	SI
1	–	–	–
2	–	0.048 \pm 0.0026	>2083 ^b
Clorgyline	0.0052 \pm 0.00092 ^a	63.41 \pm 1.20	0.000082
R-(–)-Deprenyl	68.73 \pm 4.21 ^a	0.017 \pm 0.0019	4043
Iproniazide	6.56 \pm 0.76	7.54 \pm 0.36	0.87
Moclobemide	361.38 \pm 19.37 ^a	–	<0.36 ^b

^a $P < 0.01$ versus the corresponding IC_{50} values obtained against MAO-B.

^b Values obtained under the assumption that the corresponding IC_{50} against MAO-A or MAO-B is the highest concentration tested; SI: hMAO-B selectivity index = IC_{50} (hMAO-A)/ IC_{50} (hMAO-B).

– Inactive at 100 μ M (highest concentration tested).

*** Inactive at 1 mM (highest concentration tested).

Table 2

MM-GBSA interaction energies in kcal/mol of compounds **1** and **2** into the hMAOs

Compounds	hMAO-A	hMAO-B
1	31.11	–1.67
2	–2.86	–22.91

Table 3

Relevant hMAO-A and -B interacting residues with respect to **1** and **2** binding modes

Corresponding residues	Compounds	
	hMAO-A	hMAO-B
	1	2
Tyr69	b	a
Ile180	ab	ab
Asn181	ab	ab
Tyr197	a	ab
Ile207	ab	ab
Phe208	ab	b
Ser209	a	–
Gln215	ab	ab
Ile335	ab	ab*
Leu337	a	ab
Met350	–	a
Phe352	b	ab
Tyr407	ab	ab
Gly443	–	ab
Tyr444	ab	ab
FAD	b	ab

a: hMAO-A interaction; b: hMAO-B interaction; *: hydrogen bond.

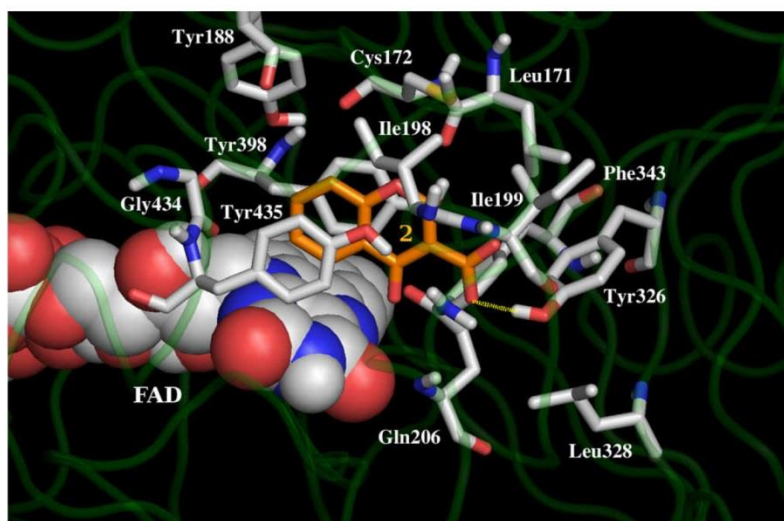


Figure 3. Global minimum energy configuration of compound **2** into the hMAO-B catalytic site. The ligand is reported as orange carbon polytube. The interacting residues are in white carbon polytube and the FAD cofactor is displayed in spacefill rendering. Yellow dotted line indicates the intermolecular hydrogen bond.

Conversely, into the hMAO-B cleft compounds **1** and **2** gave best poses in opposite configurations. The former chromone reported its carboxylate moiety directed toward the FAD electrostatically interacting to the C4 cofactor atom. No stacking contacts were highlighted by the aromatic pyrone ring that hydrophobically interacted to Ile171, Ile199, Tyr326 and Phe343. The sp^2 oxygen atom of **1** electrostatically recognizes the Tyr435 hydroxyl group but, due to a distance larger than 3.0 Å, was not able to establish hydrogen bond (see Supplementary data). Compound **2** showed, into the hMAO-B catalytic site, its aromatic moiety directed toward the inner side and the carboxylate substituent was involved in hydrogen bond to the Tyr326. The pyrone ring perfectly fits between Tyr398 and Tyr435, suggesting a strong stacking interaction, the sp^2 oxygen was located in front of the FAD C4 (Fig. 3).

The compounds **1** and **2** binding modes analysis provided interesting information to rationalize the experimental biological data. The most relevant issue could be addressed to the hydrogen bond established by **2** into the hMAO-B recognition site. Such a productive interaction was allowed by the presence of the Tyr326, substituted, in the hMAO-A, by the Ile335. Taking into account the position of the carboxylate moiety onto the pyrone ring, the hydrogen bond to Tyr326 allowed the perfect fit of **2** aromatic moieties with respect to Tyr398 and Tyr435 and the favorable electrostatic interaction of the sp^2 oxygen to the C4 FAD atom.

Compound **1**, reporting the carboxylate in position 2, was not able to concurrently perform all these productive interactions. In order to verify this observation, we manually built a configuration of **1** starting from the global minimum energy complex of **2** and after fully optimization of the resulting structure we found that the hydrogen bond was conserved, but the stacking to catalytic tyrosines and the electrostatic contact to the C4 FAD was completely lost. Moreover the internal energy of such biased optimized structure was about 13 kcal/mol higher than **1** hMAO-B global minimum configuration, suggesting it as improbable.

In conclusion chromone appears to be an interesting scaffold for the design of selective MAO inhibitors. The easy synthetic accessibility, the potentially low toxicity and especially the versatile binding properties of chromones make them as 'privileged' scaffolds. Our findings pointed out a crucial, undisclosed role of the presence

of a hydrogen donor group in position 3 of the pyrone ring that is able to establish hydrogen bond interactions with active site residues. This discovery opens a new avenue to obtain highly potent and selective MAO-B inhibitors. The docking technique provided new insights on the inhibition mechanism and the rational drug design of this type of inhibitors. The molecular modeling studies highlighted that the most structurally simple chromone derivatives **1** and **2** can fit into the hMAO binding clefts. The hydrogen donor moiety should be located in position 3 of the pyrone ring for obtaining favoured energy and selective recognition of the hMAO-B isoform.

Additional studies are warranted for a systematic lead optimization, modulated by appropriate modifications of length, size, and chemical nature of the substituents, process that can lead to in the future to a drug candidate.

Acknowledgments

The authors dedicate this manuscript to Professor Francisco Orallo Camberio, who left us prematurely, for his outstanding human and professional qualities.

The authors acknowledge for financial support Fundação para a Ciência e a Tecnologia (FCT) (project PTDC/QUI/70359/2006), A.G. doctoral Grant (SFRH/BD/43531/2008) and Ministerio de Sanidad y Consumo (Spain; FISS PI061537 and PI061457)

Supplementary data

Supplementary data (pharmacology, determination of hMAO isoform activity, reversibility and irreversibility experiments, data presentation and statistical analysis, molecular modeling and additional figures) associated with this article can be found, in the online version, at doi:10.1016/j.bmcl.2010.03.081.

References and notes

- (a) Reyes-Parada, M.; Fierro, A.; Iturriaga-Vásquez, A. P.; Cassels, B. K. *Curr. Enzyme Inhib.* **2005**, *1*, 85; (b) Pacher, P.; Kecskeméti, V. *Curr. Med. Chem.* **2004**, *11*, 925.

2. Bertoni, J.; Elmer, L. In *The Role of MAO-B Inhibitors in the Treatment of Parkinson's Disease*; Ebadi, M., Pfeiffer, R. F., Eds.; CRC Press: Florida, 2005; pp 691–704.
3. Lang, A. E.; Lees, A. *Mov. Disord.* **2002**, *17*, 38.
4. (a) Deeb, O.; Alfalah, S.; Clare, B. W. *J. Enzyme Inhib. Med. Chem.* **2007**, *22*, 277; (b) Thull, U.; Kneubühler, S.; Testa, B.; Borges, M. F. M.; Pinto, M. M. *Pharm. Res.* **1993**, *10*, 1187.
5. (a) Santana, L.; González-Díaz, H.; Quezada, E.; Uriarte, E.; Yáñez, M.; Viña, D.; Orallo, F. *J. Med. Chem.* **2008**, *51*, 6740; (b) Binda, C.; Wang, J.; Pisani, L.; Caccia, C.; Carotti, A.; Salvati, P.; Edmondson, D. E.; Mattevi, A. *J. Med. Chem.* **2007**, *50*, 5848; (c) Catto, M.; Nicolotti, O.; Leonetti, F.; Carotti, A.; Favia, A. D.; Soto-Otero, R.; Mendez-Alvarez, E.; Carotti, A. *J. Med. Chem.* **2006**, *49*, 4912; (d) Borges, F.; Roleira, F.; Milhazes, N.; Santana, L.; Uriarte, E. *Curr. Med. Chem.* **2005**, *12*, 887.
6. Chimenti, F.; Fioravanti, R.; Bolasco, A.; Chimenti, P.; Secci, D.; Rossi, F.; Yáñez, M.; Orallo, F.; Ortuso, F.; Alcaro, S. *J. Med. Chem.* **2009**, *52*, 2818.
7. Ellis, G. P., Ed. *The chemistry of heterocyclic compounds, chromenes, chromanones and chromones*; J. Wiley & Sons: New York, 2007; Vol. 31.
8. (a) Ishar, M. P. S.; Singh, G.; Singh, S.; Sreenivasan, K. K.; Singh, G. *Bioorg. Med. Chem. Lett.* **2006**, *16*, 1366; (b) Peixoto, F.; Barros, A. I. R. N. A.; Silva, A. M. S. *J. Biochem. Mol. Toxicol.* **2002**, *16*, 220; (c) Ellis, G. P.; Barker, G. *Prog. Med. Chem.* **1972**, *9*, 65.

3.2 Chromone, a Privileged Scaffold for the Development of Monoamine Oxidase Inhibitors

Article from *Journal Medicinal Chemistry* (2011), 54: 5165–5173

Chromone, a Privileged Scaffold for the Development of Monoamine Oxidase Inhibitors[†]

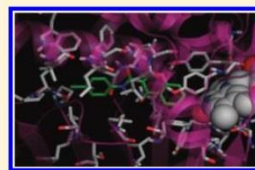
Alexandra Gaspar,^{*,§} Tiago Silva,[‡] Matilde Yáñez,^{||} Dolores Vina,^{||} Francisco Orallo,^{||} Francesco Ortuso,[⊥] Eugenio Uriarte,[§] Stefano Alcaro,^{*,⊥} and Fernanda Borges^{*,‡}

[†]CIQUP/Departamento de Química e Bioquímica, Faculdade de Ciências, Universidade do Porto, 4169-007 Porto, Portugal

[§]Departamento de Química Orgánica and ^{||}Departamento de Farmacología, Facultad de Farmacia, Universidad de Santiago de Compostela, 15782 Santiago de Compostela, Spain

[⊥]Dipartimento di Scienze Farmacobiologiche, Facoltà di Farmacia, Università "Magna Græcia" di Catanzaro, Campus Universitario "S. Venuta", Viale Europa, 88100 Catanzaro, Italy

ABSTRACT: Two series of novel chromone derivatives were synthesized and investigated for their ability to inhibit the activity of monoamine oxidase. The SAR data indicate that chromone derivatives with substituents in position 3 of γ -pyrone nucleus act preferably as MAO-B inhibitors, with IC₅₀ values in the nanomolar to micromolar range. Almost all chromone 3-carboxamides display selectivity toward MAO-B. Identical substitutions on position 2 of γ -pyrone nucleus result in complete loss of activity in both isoforms (chromones 2–12 except 3 and 5). Notably, chromone (19) exhibits an MAO-B IC₅₀ of 63 nM, greater than 1000-fold selectivity over MAO-A, and behaves as a quasi-reversible inhibitor. Docking experiments onto the MAO binding of the most active compound highlight different interaction patterns among the isoforms A and B. The differential analysis of the solvation effects among the chromone isomers gave additional insight about the superior outline of the 3-substituted chromone derivatives.



INTRODUCTION

Monoamine oxidases (MAOs, EC 1.4.3.4) are widely distributed enzymes that contain a flavin adenine dinucleotide (FAD) covalently bounded to a cysteine residue. Several living organisms possess MAOs that are responsible for the major neurotransmitter degrading in the central nervous system (CNS) and peripheral tissues.^{1,2}

In mammals two isoforms of MAOs are present: MAO-A and MAO-B. Both isoforms are involved in the oxidative deamination of exogenous and endogenous amines, including neurotransmitters, thus modulating their concentrations in the brain and peripheral tissues.¹ The MAO-A enzyme is responsible for the deamination of the epinephrine, norepinephrine, and serotonin, whereas the MAO-B enzyme metabolizes β -phenethylamine.^{1,3} The enzyme also plays an important role in the expression of toxicity of the Parkinsonism-producing neurotoxin 1-methyl-4-phenyl-1,2,3,6-tetrahydropyridine by bioactivation into the toxic metabolite, the 1-methyl-4-phenyl-1,2,3,6-tetrahydropyridinium ion.³

The MAO metabolic reaction involves the oxidation of the amine function via oxidative cleavage of the α -CH bond of the substrate with the ensuing generation of an imine intermediate. This pathway is accomplished by the reduction of the flavin cofactor that is reoxidized by molecular oxygen, with simultaneous hydrogen peroxide release. Subsequently, the imine intermediate is hydrolyzed by a nonenzymatic pathway yielding ammonia and the corresponding aldehyde (Scheme 1).²

Expression levels of MAO-B in neuronal tissue are enhanced 4-fold with aging, especially in glial cells, resulting in an increased

level of dopamine metabolism and in the production of higher levels of hydrogen peroxide, which are thought to play a major role in the etiology of neurodegenerative diseases such as Parkinson's and Alzheimer's. MAO-B inhibitors are also currently in clinical trials for the treatment of Alzheimer's disease because an increased level of MAO-B has been detected in the plaque-associated astrocytes of brains from Alzheimer's patients.^{4,5}

Today efforts toward the development of monoamine oxidase inhibitors are focused on selective MAO-A or MAO-B inhibitors. Selective MAO-B inhibitors, alone or combined with L-Dopa, are being examined in the treatment of, for example, schizophrenia, Alzheimer's disease, and Parkinson's disease. The MAO-A inhibitors are effective in the treatment of depression.

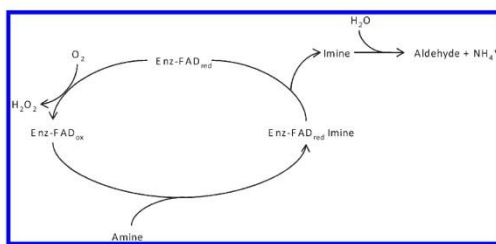
MAO-A is more sensitive to inhibition by clorgyline and moclobemide, and MAO-B is selectively inhibited by low concentrations of selegiline (*R*-(−)-deprenyl) and rasagiline (Scheme 2).^{1,4}

All of these aspects have led to an intensive search for novel MAO inhibitors, and this effort has increased considerably in recent years. However, a large number of MAOs inhibitors introduced into clinical practice were discarded because of adverse effects, such as hepatotoxicity, orthostatic hypotension, and the so-called "cheese effect", which is characterized by hypertensive crises.¹ Currently, the MAO inhibitors of the new generation are usually characterized by their relative specificities for the MAO subtypes and in some cases by the reversibility of their actions.

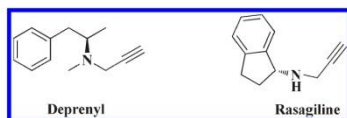
Received: April 10, 2011

Published: June 22, 2011

Scheme 1



Scheme 2



Despite considerable progress in understanding the interactions of the two enzyme forms with their preferred substrates and inhibitors, no general rules are yet available for the rational design of potent and selective inhibitors of MAO possibly because the mechanism of interaction of the new drugs with MAO isoforms has not been fully characterized.

Privileged structures such as indoles, arylpiperazines, biphenyls, and benzopyranes are currently ascribed as supportive approaches in drug discovery. Different families of nitrogen and oxygen heterocycles such as xanthenes, coumarins, and their precursors (chalcones) have also been extensively used as scaffolds in medicinal chemistry programs for searching novel MAO-B inhibitors.^{6–8}

Chromone scaffold [(4*H*)-1-benzopyran-4-one] has been recognized as a pharmacophore of a large number of bioactive molecules of either natural or synthetic origin. Until now, numerous biological effects, especially in popular medicine, have been ascribed to this benzo- γ -pyrone nucleus such as anti-inflammatory, antitumoral, and antimicrobial activities.⁹ Enzymatic inhibition properties toward different systems such as oxidoreductases, kinases, tyrosinases, cyclooxygenases have also been recognized.¹⁰ Recently, our group has reported preliminary studies that point out the relevance of these types of heterocyclic compound as monoamino oxidase inhibitors.^{10,11}

Accordingly, our project has focused on the discovery of new chemical entities (NCEs) for MAO inhibition incorporating privileged structures with benzo- γ -pyrone substructure (Scheme 3). Preliminary studies performed with chromones (**1**) and (**13**) allow disclosure of the importance of the location of a carboxylic moiety in the γ -pyrone nucleus. In fact, when the $-\text{COOH}$ substituent is in position 3 of the heterocyclic scaffold (**13**), it binds the *h*MAO-B, exerting a selective inhibition with respect to the A isoform ($\text{IC}_{50}(\text{hMAO-B}) = 0.048 \pm 0.0026 \text{ nM}$; MAO-B selective index (SI) of >2083).^{10,11} As the inhibition is of irreversible type and in an attempt to develop novel reversible and selective MAO-B inhibitors, the synthesis of 2- and 3-carboxamide chromone derivatives capable of establishing hydrogen interactions with the enzyme was performed. Therefore, functionalized chromone scaffolds suitable to establish structure–activity

relationships were obtained by synthetic strategies and screened toward human MAOs isoforms (*h*MAOs) to evaluate their potency/selectivity ratio. The Protein Data Bank (PDB)¹² availability of experimentally determined cocrystals of *h*MAO-A and -B with different kinds of ligand allows us to also perform structure-based molecular modeling studies with the aim to propose preferred binding modes and to explain the reasons of the isoform selectivity helping in the rational design of new inhibitors.

CHEMISTRY

The functionalization of the chromone nucleus leads to the obtention of two series of novel chromone carboxamides placed at positions C2 and C3 of the γ -pyrone ring. The compounds and the synthetic strategy used for their obtention have been patented¹¹ and are briefly depicted in Scheme 3. Chromone carboxamide derivatives were synthesized straightforwardly, in moderate/high yields, by a one-pot condensation reaction that occurs, in equimolar amounts, between the corresponding chromone carboxylic acid (**1** or **13**) and aniline (phenylamine) or its ring-substituted derivatives. A similar condensation reaction was performed with propylamine and cyclohexylamine. The coupling reagents selected for carboxylic acid activation were organophosphoric compounds, namely, (benzotriazol-1-yloxy)-tris(dimethylamino)phosphonium hexafluorophosphate (BOP) and (benzotriazol-1-yloxy)tripyrrolidinophosphonium hexafluorophosphate (PyBOP).¹³ In all the reactions, *N,N*-diisopropylethylamine (DIPEA) was used instead of the classic triethylamine, since a significant increase of yield was observed due mainly to an improvement in the purification steps.¹¹

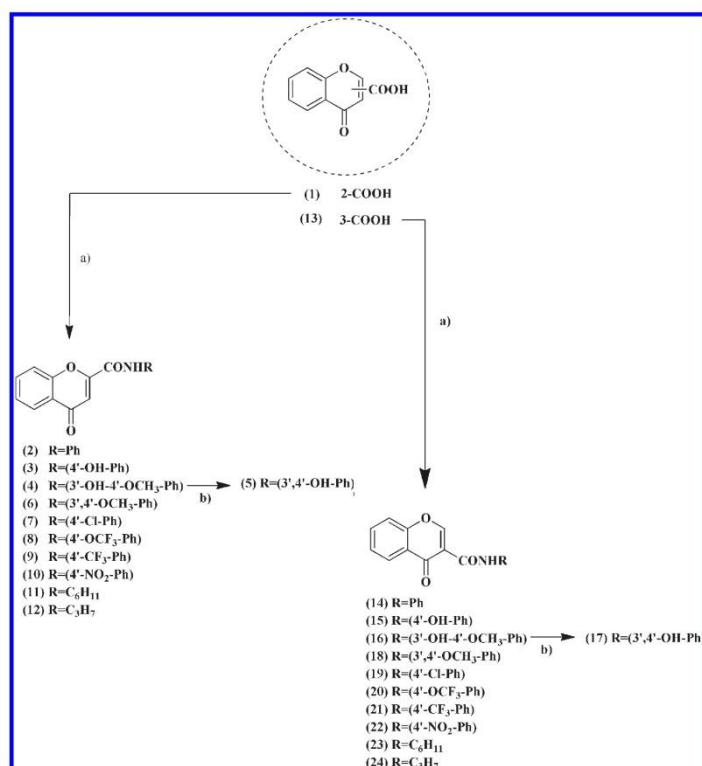
It must be highlighted that the synthetic strategies commonly adopted for the synthesis of these types of amide are usually based on a different approach: first, an acyl halide is obtained through the reaction of a carboxylic acid with thionyl chloride, followed by the reaction with a nucleophilic agent.¹⁴ In fact, the method herein presented is particularly advantageous, since it avoids the step of acyl halide obtention and the drawbacks related with this type of reagent. Furthermore, the use of BOP or PyBOP has several advantages, related with other coupling agents such as dicyclohexylcarbodiimide (DCC), in the purification steps and in the removal of side products. The syntheses of the dihydroxylated compounds **5** and **17** were performed by a demethylation reaction, using boron tribromide (BBr_3), of the monomethoxylated chromones **4** and **16**, respectively. The selected strategy avoids the prior protection of the hydroxyl groups of the starting materials (Scheme 3).

PHARMACOLOGY

The potential effects of the test drugs on *h*MAO activity were investigated by measuring their effects on the production of hydrogen peroxide (H_2O_2) from *p*-tyramine (a common substrate for both *h*MAO-A and *h*MAO-B), using the Amplex Red MAO assay kit (Molecular Probes, Inc., Eugene, OR, U.S.) and microsomal MAO isoforms prepared from insect cells (BTI-TN-SB1-4) infected with recombinant baculovirus containing cDNA inserts for *h*MAO-A or *h*MAO-B (Sigma-Aldrich Química S.A., Alcobendas, Spain).

The production of H_2O_2 catalyzed by MAO isoforms can be detected using 10-acetyl-3,7-dihydroxyphenoxazine (Amplex Red reagent), a nonfluorescent and highly sensitive probe that reacts with H_2O_2 in the presence of horseradish peroxidase to produce a fluorescent product, resorufin.

Scheme 3^a



^a Reagents: (a) RNH₂, BOP or PyBOP, DIPEA in DCM/DMF; (b) BBr₃ in DCM.

In this study, *h*MAO activity was evaluated using the above-mentioned method following the general procedure previously described elsewhere.^{8,15} The drugs (novel compounds and reference inhibitors) were unable to react directly with the Amplex Red reagent, which indicates that they do not interfere with the measurements.

In our experiments and under our experimental conditions, *h*MAO-A displayed a Michaelis constant (K_m) of $457.17 \pm 38.62 \mu\text{M}$ and a maximum reaction velocity (V_{max}) of $185.67 \pm 12.06 \text{ (nmol/min)}/\text{mg}$ protein whereas *h*MAO-B showed a K_m of $220.33 \pm 32.80 \mu\text{M}$ and a V_{max} of $24.32 \pm 1.97 \text{ (nmol/min)}/\text{mg}$ protein ($n = 5$).

The *h*MAO-A and *h*MAO-B inhibition and SI ($[IC_{50}(\text{MAO-A})]/[IC_{50}(\text{MAO-B})]$) data are reported in Table 1.

Reversibility and irreversibility experiments were performed to evaluate the type of the inhibitor, using *R*-(−)deprenyl (irreversible inhibitor) and isatin (reversible inhibitor) as standards.¹⁶

RESULTS AND DISCUSSION

The chemical structures of the examined compounds are depicted in Scheme 3. The results of the *in vitro* evaluation of

inhibitory potencies toward *h*MAO isoforms and selectivity of the chromones under study, and reference compounds, are shown in Table 1. By analyzing such data, one can conclude that chromones bearing substituents in position 3 of γ -pyrone nucleus act preferably as MAO-B inhibitors (iMAO-B) with IC_{50} values in the nanomolar to micromolar range. The same tendency was found with the chromone carboxylic acids.¹⁰ The most promising iMAO-B chromones that are substituted in the para position, with hydroxyl or methoxyl groups or a chloro atom, of the side chain aromatic nucleus (compounds **15**, **16** and **19**, respectively) present IC_{50} values between 63 and 76 nM. The most selective compounds possess electron withdrawing groups (a Cl atom (compound **19**) and a CF₃ group (compound **21**)) in the para position of the exocyclic aromatic nucleus (SI of >1.585 and >909, respectively). The chromone derivative with a hydroxyl group in the para position (compound **15**) is more active and selective as iMAO-B than the compound with two hydroxyl groups located in the para and meta positions (compound **17**). The present results allow us to point out that the inclusion of this type of substituent in the meta position of the 3-aryl substituent could not be beneficial. The derivative **22** with the para position substituted with a strong electron polar and bulky withdrawing group (nitro group) shows a loss of selectivity with an IC_{50}

Table 1. MAO Inhibitory Activities of Chromone Carboxamides and Reference Inhibitors^a

compd	R	IC ₅₀ (hMAO-A) (μM)	IC ₅₀ (hMAO-B) (μM)	SI
2	Ph	c	c	
3	4'-OH-Ph	65.23 ± 5.82	41.90 ± 2.79	1.6
4	3'-OH-4'-OCH ₃ -Ph	c	c	
5	3',4'-OH-Ph	0.19 ± 0.016	2.66 ± 0.13	0.071
6	3',4'-OCH ₃ -Ph	c	c	
7	4'-Cl-Ph	c	c	
8	4'-OCF ₃ -Ph	c	c	
9	4'-CF ₃ -Ph	c	c	
10	4'-NO ₂ -Ph	c	c	
11	C ₆ H ₁₁	c	d	
12	C ₃ H ₇	c	d	
14	Ph	c	0.40 ± 0.022	>250 ^e
15	4'-OH-Ph	4.76 ± 0.39 ^b	0.064 ± 0.0054	74
16	3'-OH-4'-OCH ₃ -Ph	8.34 ± 0.27 ^b	0.076 ± 0.0032	110
17	3',4'-OH-Ph	0.43 ± 0.0035 ^b	0.16 ± 0.013	2.7
18	3',4'-OCH ₃ -Ph	c	2.33 ± 0.07	>43 ^e
19	4'-Cl-Ph	c	0.063 ± 0.0042	>1585 ^e
20	4'-OCF ₃ -Ph	c	1.08 ± 0.072	>93 ^e
21	4'-CF ₃ -Ph	c	0.11 ± 0.0074	>909 ^e
22	4'-NO ₂ -Ph	11.11 ± 0.74	11.78 ± 0.79	0.94
23	C ₆ H ₁₁	c	0.93 ± 0.062	>107 ^e
24	C ₃ H ₇	c	37.69 ± 1.68	>2.7 ^e
R-(−)-deprenyl		68.73 ± 4.21 ^b	0.017 ± 0.0019	4043
iproniazid		6.56 ± 0.76	7.54 ± 0.36	0.87

^a All IC₅₀ values shown in this table are the mean ± SEM from five experiments. SI: hMAO-B selectivity index = IC₅₀(hMAO-A)/IC₅₀(hMAO-B).

^b Level of statistical significance: $P < 0.01$ versus the corresponding IC₅₀ values obtained against MAO-B, as determined by Student's t test. The IC₅₀ values of compounds 2 and 14 were taken from the literature.^{11c} ^c Inactive at 100 μM (highest concentration tested). ^d Inactive at 1 mM (highest concentration tested). ^e Values obtained under the assumption that the corresponding IC₅₀ against MAO-A or MAO-B is the highest concentration tested (100 μM or 1 mM).

of 11 μM for both MAO isoforms. It seems that the electron withdrawing nature, in particular the resonance effect (weak donating), and the spatial volume of the substituents located in the aromatic ring have a particular effect on the potency of the 3-carboxamides.

The chromone carboxamide derivative with an unsubstituted exocyclic aromatic moiety (compound 14) is twice more active than compound 23, a carboxamide with a cyclohexyl instead of the aromatic ring (IC₅₀ of 400 and 930 nM, respectively). The absence of a ring led to a dramatic loss of activity (see linear alkylcarboxamide 24; IC₅₀ of 37 μM). All of the previously mentioned chromone carboxamides, except chromone 22, are inactive toward MAO-A.

Of note is that the chromones bearing the same type of substituents in position 2 of γ-pyrone nucleus (chromones 2–12) present a total loss of MAO inhibition except with compounds 3 and 5. Compound 3, with a hydroxyl group in the para position of the exocyclic aromatic ring, has a comparable inhibitory activity for both isoforms. The introduction of another hydroxyl group in the meta position (compound 5) considerably increases the potency and selectivity toward hMAO-A.

The reversibility studies performed with the chromones 15 and 19 revealed that the carboxamides behave as quasi-reversible MAO-B inhibitors. In fact, the percent of enzymatic inhibition was much lower after repeated washing with respect to R-(−)-deprenyl (irreversible inhibitor) (Table 2).

Table 2. Reversibility and Irreversibility of hMAO Inhibition^a

compd	% hMAO-B inhibition	
	before washing	after repeated washing
R-(−)-deprenyl (25 nM)	53.62 ± 5.15	47.72 ± 6.21
isatin (20 μM)	47.55 ± 5.42	0 ^b
15 (100 nM)	60.31 ± 7.74	23.50 ± 3.71 ^b
19 (100 nM)	59.60 ± 6.96	29.14 ± 4.16

^a Each value is the mean ± SEM from five experiments ($n = 5$). ^b Level of statistical significance: $P < 0.05$ versus the corresponding % hMAO-B inhibition before washing, as determined by Student's t test.

The data so far obtained are in accordance with preliminary results,¹¹ since it supports the assumption that the positive hydrophobicity (+ π) of the substituent, besides inductive and mesomeric effects, located on the phenyl exocyclic moiety markedly influences the potency and selectivity of the chromone carboxamides. The tendency is in perfect agreement with the parameter space of the descriptors defined in the so-called Craig's plot.

In order to highlight the reasons of MAO selectivity, we have carried out a structure-based molecular modeling study using hMAOs cocrystals deposited into the PDB.¹² Similar to our previous work,¹⁷ we have focused our attention onto the most active and

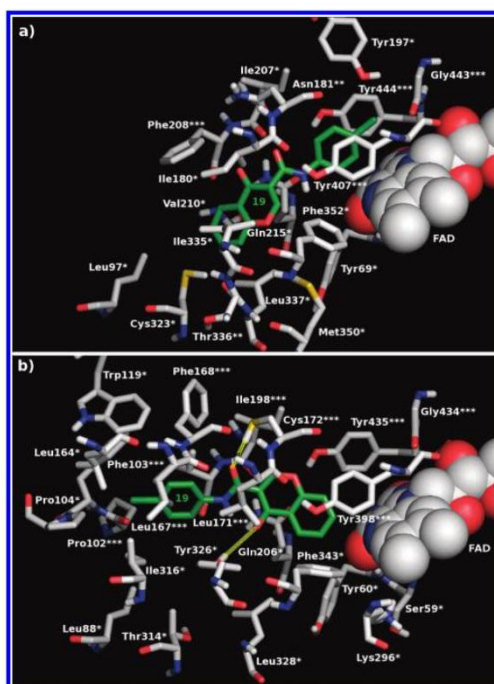


Figure 1. Most stable docking poses of **19** into (a) *h*MAO-A and (b) *h*MAO-B binding sites. Ligand is reported in green carbon sticks. Interacting residues are in gray carbon sticks, and FAD is in space-fill. Yellow dotted lines indicate ligand–enzyme intermolecular hydrogen bonds: *, ligand interaction to side chain; **, ligand interaction to backbone; ***, ligand interaction to both backbone and side chain.

selective compound. So in this series, we have selected **19** as a case study for our theoretical investigation. Also in the present study we have adopted the docking program Glide¹⁸ and the PDB models 2ZSX¹⁹ and 2VSZ²⁰ for mimicking the *h*MAO-A and -B targets, respectively. Details of the molecular modeling procedures are reported in the Experimental Section.

Compound **19** target interaction energies, -7.12 and -207.68 kJ/mol for *h*MAO-A and -B, respectively, were in good agreement with the experimental biological data. The docking proposed configuration indicated a strong difference depending on the target. Actually, the only [*h*MAO-A·**19**] Glide proposed configuration showed the chromone moieties in the entrance gorge while the *p*-chloroanilide side chain recognized the FAD cofactor suggesting a π – π interaction to Tyr407 and Tyr444. Several other residues were involved in such a binding mode but only van der Waals contacts can be designated (Figure 1a).

The interaction of **19** to *h*MAO-B was found to be much more productive with respect to the previous one. First of all, the interaction energy was remarkably lower than in *h*MAO-A and a number of binding modes were proposed by Glide. Moreover, the most stable configuration was in agreement with literature data as concerns the intramolecular hydrogen bond and with the positioning of the chromone ring.¹⁷ Actually, the chromone

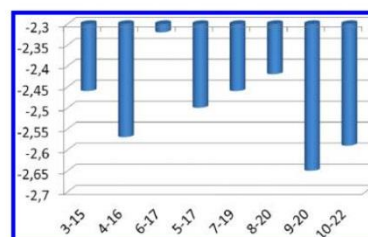


Figure 2. Difference (in kJ/mol) between water solvation energies of 3–10 with respect to their isomers 15–22.

moiety was situated close to the FAD and the *p*-chloroanilide side chain occupied the entrance cavity at the loop formed by residues 99–112. Two intermolecular hydrogen bonds were observed between the carboxamide and the Cys172 and between the chromone sp^2 oxygen and the Tyr326. The hydrophobic side chain of **19** productively interacts with Pro102, Phe103, Leu167, and Ile199.

With the aim to more deeply investigate the reasons for the different recognition of **19** in *h*MAO-A with respect to the *h*MAO-B, the best docking poses, reported in Figure 1b, were superposed using the FAD and the active site backbone residues as geometry references. Such a procedure indicated that *h*MAO-B configuration of **19** in *h*MAO-A loses the hydrogen bond contribution because Cys172 and Tyr326, available into the former enzyme, are replaced by Asn181 and Ile335, respectively. Moreover, in the *h*MAO-A cleft the **19** *p*-chloroanilide moiety bumps against the side chain of Phe208 corresponding to the sterically smaller *h*MAO-B Ile199. The same analysis has been carried out on the **19** *h*MAO-A best pose with respect to *h*MAO-B. In this case we can report clashes between the chromone moiety and the Tyr326 and no hydrogen bond. In order to reduce clashes, both new models have been refined with Glide software, but after the optimization the scenario was not so different: the clashes were reduced, but with respect to the docking best poses, the inhibitor was located more distant from the FAD and no intermolecular hydrogen bonds were established between the ligand and the targets.

After the docking experiments with the most active and selective compound we have repeated the same procedure trying to reproduce by interaction energies the biological trend reported in Table 1, at least for the quantitatively measured values. Since no good correlation was found for the entire set, we have focused our attention onto the conformational and solvation properties of our derivatives. In particular a comparison of the isomers bearing the side chain at the 2- or 3-position onto the chromone ring has been carried out. The conformational properties, investigated by means of Monte Carlo (MC) search, indicated few possible local minimum energy structures in particular for compounds 15–22. Such data could be considered as an entropy benefit of these ligands with respect to their isomers 3–10. The comparative solvation analysis in water revealed a remarkable energy advantage of compounds 3–10 with respect to their isomers 15–22 (Figure 2). Such evidence could contribute to explain the better activity of chromone derivatives reporting the carboxamide side chain at position 3 than at position 2. In fact, the interaction with the target of 3–10 could be penalized into the aqueous environment.

CONCLUSIONS

In the present work evidence was acquired to demonstrate that chromone is a valid scaffold for the design of potent, selective, and reversible MAO inhibitors. Generally chromones bearing substituents in position 3 of γ -pyrone nucleus act as *h*MAO-B selective inhibitors and those bearing substituents in position 2 of the same nucleus selectively inhibit the *h*MAO-A or are inactive. The introduction of a chloro substituent in the para position of the exocyclic aromatic ring of chromone 3-phenyl-carboxamides was crucial for the obtention of a potent and selective iMAO (IC₅₀ = 63 nM; SI > 1585). The easy synthetic accessibility and potentially low toxicity of chromones⁹ make them "privileged" scaffolds. Docking experiments, carried out with the most active and selective compound **19**, indicated the reasons for the better stabilization within the *h*MAO-B isoform versus the -A one. A comparison of **3–10** and **15–22** conformational properties indicated an entropy advantage of the latter in the interaction with both targets. The solvation energies comparison reported a preference of the 2-substituted chromone derivatives for the aqueous solvent. Both results suggested a penalization of **3–10** in target recognition with respect to **15–22**.

Additional studies are warranted for a systematic lead optimization, modulated by appropriate modifications of length, size, and chemical nature of the substituents, a process that can lead to in the future to a drug candidate.

EXPERIMENTAL SECTION

Chemistry. Chromone-2-carboxylic and chromone-3-carboxylic acids, benzotriazol-1-yloxytris(dimethylamino)phosphonium hexafluorophosphate (BOP), benzotriazol-1-yloxytripyrrolidinophosphonium hexafluorophosphate (PyBOP), *N,N*-diisopropylethylamine (DIPEA), dimethylformamide (DMF), boron tribromide (BBr₃), and aniline and its derivatives were purchased from Sigma-Aldrich Química S.A. (Sintra, Portugal). All other reagents and solvents were pro analysis grade and were acquired from Merck (Lisbon, Portugal) and used without additional purification.

Thin-layer chromatography (TLC) was carried out on precoated silica gel 60 F254 (Merck) with layer thickness of 0.2 mm. For analytical control the following systems were used: ethyl acetate/petroleum ether, ethyl acetate/methanol, and chloroform/methanol in several proportions. The spots were visualized under UV detection (254 and 366 nm) and iodine vapor. Normal-phase column chromatography was performed using silica gel 60, 0.2–0.5 or 0.040–0.063 mm (Merck).

Following the workup and after extraction, the organic phases were dried over Na₂SO₄. Solutions were decolorized with activated charcoal when necessary. The recrystallization solvents were ethyl acetate or ethyl ether/*n*-hexane. Solvents were evaporated in a Buchi Rotavapor.

The purity of the final products (>97% purity) was verified by high-performance liquid chromatography (HPLC) equipped with a UV detector. Chromatograms were obtained in an HPLC/DAD system, a Jasco instrument (pump model 880-PU and solvent mixing model 880-30, Tokyo, Japan) equipped with a commercially prepacked Nucleosil RP-18 analytical column (250 mm × 4.6 mm, 5 μ m, Macherey-Nagel, Duren, Germany) and UV detection (Jasco model 875-UV) at the maximum wavelength of 254 nm. The mobile phase consisted of a methanol/water or acetonitrile/water (gradient mode, room temperature) at a flow rate of 1 mL/min. The chromatographic data were processed in a Compaq computer fitted with CSW 1.7 software (DataApex, Czech Republic).

Apparatus. ¹H NMR data were acquired, at room temperature, on a Bruker AMX 300 spectrometer operating at 300.13 MHz. Dimethylsulfoxide-*d*₆ was used as a solvent. Chemical shifts are expressed in δ (ppm) values relative to tetramethylsilane (TMS) as internal reference. Coupling

constants (*J*) are given in Hz. Electron impact mass spectrometry (EI-MS) was carried out on a VG AutoSpec instrument. The data are reported as *m/z* (% of relative intensity of the most important fragments). Melting points were obtained on a Stuart Scientific SMP1 apparatus and are uncorrected.

Synthesis. General Procedure for Amide Obtention. The synthetic procedure corresponds to a one-pot condensation reaction that occurs, in equimolar amounts, between the carboxylic acid and the respective amine according to the following general procedure. 2-Carboxychromone (**1**) or 3-carboxychromone (**13**) (0.50 g, 2.63 mmol) was dissolved in 6 mL of DMF and 0.37 mL of diisopropylethylamine (DIPEA). The solution was then cooled at 0 °C in an ice–water bath, and a BOP (1.16 g, 2.63 mmol) or PyBOP (1.37 g, 2.63 mmol) solution in CH₂Cl₂ (6 mL) was added. The mixture was stirred for 30 min. Afterward, the corresponding amine (phenylamine, 4-hydroxyphenylamine, 3-hydroxy-4-methoxyphenylamine, 3,4-dimethoxyphenylamine, cyclohexylamine, or propylamine) was added in equimolar amount. The temperature was gradually increased to room temperature. The mixture was stirred for additional 4 h.

General Procedure for Demethylation Reactions. The monomethoxylated chromone carboxamide **4** or **16** (0.25 g, 0.80 mmol) was suspended in anhydrous dichloromethane and under argon atmosphere. The resulting suspension was stirred, cooled at –80 °C, and BBr₃ (6 mL of a 1 M solution in dichloromethane) was added dropwise. Once the addition was completed, the reaction mixture was allowed to warm to room temperature with continuous stirring. After BBr₃ destruction with methanol, the purification process was carried out straightforwardly.

The structural elucidation of the other carboxamides was described elsewhere.

***N*-(3,4-Dihydroxyphenyl)-4-oxo-4*H*-1-benzopyran-2-carboxamide (**5**).** Yield: 65%. Mp: 267–271 °C. ¹H NMR: δ = 6.75 (1H, d, *J* = 8.5, H(S')), 6.94 (1H, s, H(3)), 7.04 (1H, dd, *J* = 8.5, 2.4, H(6')), 7.32 (1H, d, *J* = 2.4, H(2')), 7.58 (1H, ddd, *J* = 8.0, 6.8, 1.2, H(6)), 7.85 (1H, d, *J* = 8.0, H(8)), 7.93 (1H, ddd, *J* = 8.5, 7.0, 1.5, H(7')), 8.08 (1H, dd, *J* = 7.6, 1.4, H(S)), 8.94 (1H, s, 3'-OH), 9.17 (1H, s, 4'-OH), 10.49 (1H, s, CONH). EI-MS *m/z*: 298 (10), 297 (M⁺, 52), 296 (19), 146 (100), 124 (92), 105 (57), 97 (16), 89 (74), 77 (15), 69 (19), 68 (15), 63 (16).

***N*-(4-(Chlorophenyl)-4-oxo-4*H*-1-benzopyran-2-carboxamide (**7**).** Yield: 50%. Mp: 268–271 °C. ¹H NMR: δ = 6.97 (1H, s, H(3)), 7.48 (2H, d, *J* = 8.8, H(3'), H(S')), 7.56 (1H, m, H(6')), 7.83–7.96 (4H, m, H(7), H(8), H(2'), H(6')), 8.08 (1H, dd, *J* = 7.9, 1.6, H(S)), 10.87 (1H, s, CONH). EI-MS *m/z*: 301 (34), 300 (33), 299 (M⁺, 100), 298 (50), 282 (15), 270 (24), 173 (14), 145 (28), 101 (18), 90 (10), 89 (89), 69 (16), 63 (14).

***N*-(4-(Trifluoromethoxy)phenyl)-4-oxo-4*H*-1-benzopyran-2-carboxamide (**8**).** Yield: 56%. Mp: 241–244 °C. ¹H NMR: δ = 7.00 (1H, s, H(3)), 7.45 (2H, d, *J* = 8.2, H(3'), H(S')), 7.57 (1H, dd, *J* = 8.2, 7.4, H(6')), 7.90–7.97 (4H, m, H(7), H(8), H(2'), H(6')), 8.08 (1H, d, *J* = 7.6, H(S)), 10.92 (1H, s, CONH). EI-MS *m/z*: 349 (M⁺, 86), 348 (100), 332 (21), 320 (41), 264 (12), 176 (17), 173 (21), 145 (44), 117 (18), 101 (20), 89 (98), 69 (24).

***N*-(4-(Trifluoromethyl)phenyl)-4-oxo-4*H*-1-benzopyran-2-carboxamide (**9**).** Yield: 50%. Mp: 258–261 °C. ¹H NMR: δ = 7.02 (1H, s, H(3)), 7.58 (1H, ddd, *J* = 8.1, 7.0, 1.2, H(6')), 7.81 (2H, d, *J* = 8.8, H(3'), H(S')), 7.86 (1H, dd, *J* = 8.4, 1.0, H(8)), 7.94 (1H, ddd, *J* = 8.6, 7.0, 1.6, H(7')), 8.06 (2H, d, *J* = 8.4, H(2'), H(6')), 8.09 (1H, dd, *J* = 7.6, 1.6, H(S)), 11.04 (1H, s, CONH). EI-MS *m/z*: 333 (M⁺, 35), 332 (100), 303 (16), 173 (15), 145 (32), 117 (12), 101 (11), 89 (58), 69 (15), 57 (12).

***N*-(4-Nitrophenyl)-4-oxo-4*H*-1-benzopyran-2-carboxamide (**10**).** Yield: 15%. Mp: >280 °C. ¹H NMR: δ = 7.04 (1H, s, H(3)), 7.59 (1H, ddd, *J* = 8.2, 7.0, 1.2, H(6')), 7.86 (1H, d, *J* = 7.6, H(8)), 7.96 (1H, ddd, *J* = 8.6, 7.0, 1.6, H(7')), 8.10 (3H, m, H(S), H(2'), H(6')), 8.34 (2H, m, H(3'), H(S')), 11.22 (1H, s, CONH). EI-MS *m/z*: 310 (M⁺, 6), 309

(22), 123 (45), 111 (38), 101 (45), 99 (54), 97 (69), 95 (32), 87 (63), 85 (90), 83 (51), 73 (74), 71 (69), 69 (56), 58 (35), 57 (100), 55 (65).

N-Cyclohexyl-4-oxo-4H-1-benzopyran-2-carboxamide (11). Yield: 60%. Mp: 183–184 °C. ¹H NMR: δ = 1.12–1.86 (10H, m, 2 \times H(2'), 2 \times H(3'), 2 \times H(4'), 2 \times H(5'), 2 \times H(6')), 3.78 (1H, m, H(1')), 6.83 (1H, s, H(3)), 7.54 (1H, dd, J = 7.9, 7.2, H(6)), 7.79 (1H, d, J = 8.4, H(8)), 7.90 (1H, ddd, J = 8.5, 7.0, 1.4, H(7)), 8.05 (1H, d, J = 7.9, H(5)), 8.88 (1H, d, J = 8.1, CONH). EI-MS m/z : 271 (M^{+} , 38), 228 (12), 191 (19), 190 (100), 173 (16), 145 (12), 89 (39).

N-Propyl-4-oxo-4H-1-benzopyran-2-carboxamide (12). Yield: 84%. Mp: 167–171 °C. ¹H NMR (CDCl₃): δ = 1.02 (3H, t, J = 7.4, CH₃), 1.70 (2H, m, CH₂CH₂), 3.47 (2H, m, NHCH₂), 7.02 (1H, bs, CONH), 7.17 (1H, s, H(3)), 7.46 (1H, ddd, J = 8.0, 7.0, 1.0, H(6')), 7.53 (1H, dd, J = 7.9, 1.0, H(8)), 7.74 (1H, ddd, J = 8.6, 7.0, 1.3, H(7')), 8.22 (1H, dd, J = 8.0, 1.6, H(5)). EI-MS m/z : 232 (16), 231 (M^{+} , 100), 216 (26), 203 (12), 202 (22), 190 (10), 189 (30), 174 (19), 173 (93), 159 (20), 146 (12), 145 (43), 101 (15), 89 (83), 69 (17), 63 (11).

N-(3,4-Dihydroxyphenyl)-4-oxo-4H-1-benzopyran-3-carboxamide (17). Yield: 50%. Mp: 266–269 °C. ¹H NMR: δ = 6.82 (1H, d, J = 8.4, H(5')), 6.94 (1H, dd, J = 8.5, 2.4, H(6')), 6.99 (1H, d, J = 2.5, H(2')), 7.33–7.39 (2H, m, H(6), H(8)), 7.69 (1H, dd, J = 8.4, 7.1, H(7)), 7.99 (1H, dd, J = 7.7, 1.3, H(5)), 8.64 (0.7H, s, H(2)), 8.68 (0.7H, s, H(2)), 8.72 (0.3H, s, H(2)), 9.43 (1H, s, OH), 9.46 (1H, s, OH), 11.73 (0.3H, s, CONH), 11.80 (0.3H, s, CONH), 13.42 (0.7H, s, CONH), 13.46 (0.7H, s, CONH). EI-MS m/z : 297 (M^{+} , 7), 281 (11), 208 (13), 207 (73), 173 (100), 149 (24), 121 (72), 97 (20), 95 (27), 83 (27), 81 (33), 77 (21), 73 (36), 71 (26), 69 (40), 55 (57).

N-(4-(Chlorophenyl)-4-oxo-4H-1-benzopyran-3-carboxamide (19). Yield: 47%. Mp: 255–259 °C. ¹H NMR: δ = 7.34 (1H, d, J = 7.8, H(8)), 7.38 (1H, dd, J = 7.6, 1.3, H(6)), 7.54 (2H, d, J = 8.8, H(3'), H(5')), 7.70–7.73 (3H, m, H(2'), H(6'), H(7')), 7.99 (1H, dd, J = 7.8, 1.5, H(5)), 8.85 (0.7H, d, J = 13.8, H(2)), 8.88 (0.3H, d, J = 14.8, H(2)), 8.88 (0.3H, d, J = 14.8, H(2)), 11.84 (0.3H, d, J = 14.8, CONH), 11.84 (0.3H, d, J = 14.8, CONH), 13.39 (0.7H, d, J = 13.8, CONH). EI-MS m/z : 301 (37), 300 (21), 299 (M^{+} , 88), 174 (16), 173 (100), 151 (18), 121 (37), 92 (11), 89 (10).

N-(4-(Trifluoromethoxy)phenyl)-4-oxo-4H-1-benzopyran-3-carboxamide (20). Yield: 55%. Mp: 223–226 °C. ¹H NMR: δ = 7.31–7.38 (2H, m, H(6), H(8)), 7.46 (2H, d, J = 8.7, H(3'), H(5')), 7.71 (1H, ddd, J = 8.5, 7.0, 1.5, H(7')), 7.79 (2H, d, J = 8.7, H(2'), H(6')), 8.00 (1H, dd, J = 7.8, 1.5, H(5)), 8.85 (0.7H, d, J = 13.5, H(2)), 8.89 (0.3H, d, J = 15.3, H(2)), 11.84 (0.3H, d, J = 15.2, CONH), 13.42 (0.7H, d, J = 13.5, CONH). EI-MS m/z : 349 (M^{+} , 31), 201 (13), 174 (12), 173 (100), 121 (30), 92 (10).

N-(4-(Trifluoromethyl)phenyl)-4-oxo-4H-1-benzopyran-3-carboxamide (21). Yield: 55%. Mp: 251–254 °C. ¹H NMR: δ = 7.36 (1H, d, J = 8.0, H(8)), 7.39 (1H, dd, J = 8.0, 1.7, H(6)), 7.73 (1H, ddd, J = 8.3, 7.6, 1.6, H(7')), 7.83–7.92 (4H, m, H(2'), H(3'), H(5'), H(6')), 8.00 (1H, dd, J = 7.8, 1.4, H(5)), 8.95 (0.7H, d, J = 13.7, H(2)), 8.98 (0.3H, d, J = 14.6, H(2)), 11.90 (0.3H, d, J = 14.6, CONH), 13.40 (0.7H, d, J = 13.7, CONH). EI-MS m/z : 333 (M^{+} , 58), 212 (11), 185 (19), 173 (100), 145 (15), 121 (33), 92 (13).

N-(4-Nitrophenyl)-4-oxo-4H-1-benzopyran-3-carboxamide (22). Yield: 35%. Mp: >280 °C. ¹H NMR: δ = 7.35–7.41 (2H, m, H(6), H(8)), 7.74 (1H, ddd, J = 8.2, 7.3, 1.7, H(7')), 7.93–7.96 (2H, m, H(2'), H(6')), 8.00 (1H, dd, J = 7.9, 1.6, H(5)), 8.32 (2H, d, J = 9.2, H(3'), H(5')), 8.97 (0.7H, d, J = 13.5, H(2)), 8.99 (0.3H, d, J = 14.3, H(2)), 11.94 (0.3H, d, J = 14.2, CONH), 13.39 (0.7H, d, J = 13.3, CONH). EI-MS m/z : 310 (M^{+} , 34), 309 (18), 280 (15), 173 (100), 123 (20), 121 (45), 116 (16), 109 (16).

N-Cyclohexyl-4-oxo-4H-1-benzopyran-3-carboxamide (23). Yield: 30%. Mp: 181–184 °C. ¹H NMR: δ = 1.32–1.94 (10H, m, 2 \times H(2'), 2 \times H(3'), 2 \times H(4'), 2 \times H(5'), 2 \times H(6')), 3.70 (1H, m, H(1')), 7.32 (2H, m, H(6), H(8)), 7.66 (1H, dd, J = 8.0, 7.3, H(7')), 8.02

(0.7H, d, J = 7.6, H(5)), 8.11 (0.3H, d, J = 7.6, H(5)), 8.44 (0.7H, d, J = 14.8, H(2)), 8.60 (0.3H, d, J = 14.8, H(2)), 10.31 (0.3H, brs, CONH), 11.85 (0.7H, brs, CONH). EI-MS m/z : 271 (M^{+} , 100), 228 (18), 188 (23), 175 (23), 173 (18), 121 (31), 97 (22), 57 (17).

N-Propyl-4-oxo-4H-1-benzopyran-3-carboxamide (24). Yield: 18%. Mp: 139–142 °C. ¹H NMR: δ = 1.04 (3H, m, CH₃), 1.77 (2H, m, CH₂CH₂), 3.52 (2H, m, NHCH₂), 7.23–7.30 (2H, m, H(6), H(8)), 7.57 (1H, ddd, J = 8.5, 7.0, 1.5, H(7')), 8.03 (0.7H, d, J = 7.6, H(5)), 8.10 (0.3H, d, J = 7.7, H(5)), 8.40 (0.7H, d, J = 15.0, H(2)), 8.55 (0.3H, d, J = 15.0, H(2)), 10.25 (0.3H, brs, CONH), 11.90 (0.7H, brs, CONH). EI-MS m/z : 232 (18), 231 (M^{+} , 100), 215 (56), 203 (17), 202 (19), 189 (10), 188 (20), 175 (50), 173 (10), 122 (19), 121 (16), 92 (15).

Determination of hMAO Isoform Activity. The effects of the test compounds on hMAO isoform enzymatic activity were evaluated by a fluorimetric method following the experimental protocol previously described elsewhere.⁸ Briefly, 0.1 mL of sodium phosphate buffer (0.05 M, pH 7.4) containing various concentrations of the test drugs (new compounds or reference inhibitors) and adequate amounts of recombinant hMAO-A or hMAO-B required and adjusted to obtain in our experimental conditions the same reaction velocity, i.e., to oxidize (in the control group) 165 pmol of *p*-tyramine/min (hMAO-A, 1.1 μ g protein; specific activity, 150 nmol of *p*-tyramine oxidized to (*p*-hydroxyphenylacetaldehyde/min)/mg protein; hMAO-B, 7.5 μ g of protein; specific activity, 22 nmol of (*p*-tyramine transformed/min)/mg protein), was incubated for 15 min at 37 °C in a flat-black-bottom 96-well microtest plate (BD Biosciences, Franklin Lakes, NJ, U.S.) placed in a dark multimode microplate reader chamber. After this incubation period, the reaction was started by adding (final concentrations) 200 μ M Amplex Red reagent, 1 U/mL horseradish peroxidase, and 1 mM *p*-tyramine. The production of H₂O₂ and consequently of resorufin was quantified at 37 °C in a multimode microplate reader (Fluostar Optima, BMG Labtech GmbH, Offenburg, Germany), based on the fluorescence generated (excitation, 545 nm, emission, 590 nm) over a 15 min period, in which the fluorescence increased linearly.

Control experiments were carried out simultaneously by replacing the test drugs (new compounds and reference inhibitors) with appropriate dilutions of the vehicles. In addition, the possible capacity of the above test drugs to modify the fluorescence generated in the reaction mixture due to nonenzymatic inhibition (e.g., for directly reacting with Amplex Red reagent) was determined by adding these drugs to solutions containing only the Amplex Red reagent in a sodium phosphate buffer.

To determine the kinetic parameters of hMAO-A and hMAO-B (K_m and V_{max}), the corresponding enzymatic activity of both isoforms was evaluated (under the experimental conditions described above) in the presence of a number (a wide range) of *p*-tyramine concentrations.

The specific fluorescence emission (used to obtain the final results) was calculated after subtraction of the background activity, which was determined from vials containing all components except the MAO isoforms, which were replaced by a sodium phosphate buffer solution.

Reversibility and Irreversibility Experiments. To evaluate whether compounds 15 and 19 are reversible or irreversible hMAO-B inhibitors, an effective centrifugation–ultrafiltration method (so-called repeated washing) was used.⁸ Briefly, adequate amounts of the recombinant hMAO-B were incubated with a single concentration (see Table 2) of the compounds 15 and 19 or the reference inhibitors *R*-(–)-deprenyl and isatin in a sodium phosphate buffer (0.05 M, pH 7.4) for 15 min at 37 °C. After this incubation period, an aliquot of this incubated mixture was stored at 4 °C and used for subsequent measurement of hMAO-B activity under the experimental conditions indicated above (see the section on determination of MAO activity). The remaining incubated sample (300 μ L) was placed in an Ultrafree-0.5 centrifugal tube (Millipore, Billerica, MA, U.S.) with a 30 kDa Biomax membrane in the middle of the tube and centrifuged (9000g,

20 min, 4 °C) in a centrifuge (J2-MI, Beckman Instruments, Inc., Palo Alto, CA, U.S.). The enzyme retained in the 30 kDa membrane was resuspended in sodium phosphate buffer at 4 °C and centrifuged again (under the same experimental conditions described above) two successive times. After the third centrifugation, the enzyme retained in the membrane was resuspended in sodium phosphate buffer (300 µL) and an aliquot of this suspension was used for subsequent hMAO-B activity determination. Similar studies were carried out on MAO-A activity in the presence of the reference inhibitor moclobemide under the experimental conditions described above.

Control experiments were performed simultaneously (to define 100% hMAO activity) by replacing the test drugs with appropriate dilutions of the vehicles. The corresponding values of percent hMAO inhibition were separately calculated for samples with and without repeated washing.

Statistical Analysis of Data. Data were expressed as the mean (\pm SEM) and were analyzed by ANOVA followed by Dunnett's test. Groups of test data (mean \pm SD) were comparing using the Student's *t* test for paired observations. Values were considered to differ significantly at the level of $p < 0.05$.

Molecular Modeling. The most active and selective compound **19** was built by means of the Maestro²¹ and energy minimized with 2000 steps of Polak–Ribiere conjugated gradient algorithm applied to OPLS-2005 force field²² as implemented in MacroModel.²³ Solvating effects were simulated by means of the GB/SA²⁴ water implicit model as implemented in the same program. Docking simulations were carried out using the ligand flexible algorithm of Glide.¹⁸ The target models of hMAO-A and hMAO-B were obtained from two Protein Data Bank high resolution crystal structures 2Z5X¹⁹ and 2VSZ,²⁰ respectively. After removal of cocrystallized ligands, harmine for 2Z5X and safinamide for 2VSZ, the binding sites were defined by means of a regular box of about 1000 Å³ centered onto the N5 FAD cofactor. Glide XP scoring function was adopted for stability evaluation of the complexes. The quality of our protocols has been evaluated by submitting the X-ray cocrystallized ligands to redocking. In both hMAO-A and -B cases the theoretical complexes were almost identical to the experimental ones, as reported by the root mean square deviation equal to 0.26 and 0.21 Å, respectively.

In order to take into account the solvation effects of the other compounds **3–10** and **15–22**, models of these derivatives were submitted to 1000 iterations of Monte Carlo conformational search as implemented in MacroModel²³ and energy minimized with the same protocol, force field, and implicit model of solvation considered for the most selective compound **19**.

AUTHOR INFORMATION

Corresponding Author

*For S.A.: phone, +39 09613694197; fax, +39 0961391490; e-mail, alcaro@unicz.it. For F.B.: phone, +351 220402560; fax, +351 220402659; e-mail, fborges@fc.up.pt.

ACKNOWLEDGMENT

This work was supported by the Foundation for Science and Technology (FCT), Portugal (Projects PTDC/QUI/70359/2006 and PTDC/QUI-QUI/113687/2009). A.G. (Grant SFRH/BD/43531/2008) and F.B. (Grant SFRH/BSAB/1090/2010) are thankful for the FCT grants. The authors are grateful to Dr. Alfredo Mellace (Department of Chemistry, Nassau Community College NY, USA) for proofreading the revised manuscript.

DEDICATION

[†]This article is dedicated to the memory of Prof. Francisco Orallo, the pharmacologist and friend who believed in us.

ABBREVIATIONS USED

CNS, central nervous system; FAD, flavin adenine dinucleotide; MAO, monoamine oxidase; MAO-A, monoamine oxidase A; MAO-B, monoamine oxidase B; hMAO, human MAO isoform; PDB, Protein Data Bank; SAR, structure–activity relationship

REFERENCES

- (1) (a) Reyes-Parada, M.; Fierro, A.; Iturriaga-Vásquez, A. P.; Cassels, B. K. Monoamine oxidase inhibition in the light of new structural data. *Curr. Enzyme Inhib.* **2005**, *1*, 85–95. (b) Pacher, P.; Kecskeméti, V. Trends in the development of new antidepressants. Is there a light at the end of the tunnel? *Curr. Med. Chem.* **2004**, *11*, 925–943. (c) Edmondson, D. E.; Mattevi, A.; Binda, C.; Li, M.; Hubalek, F. Structure and mechanism of monoamine oxidase. *Curr. Med. Chem.* **2004**, *11*, 1983–1993. (d) Riederer, P.; Lachenmayer, L.; Laux, G. Clinical applications of MAO-inhibitors. *Curr. Med. Chem.* **2004**, *11*, 2033–2043.
- (2) Rigby, S. E.; Basran, J.; Combe, J. P.; Mohsen, A. W.; Toogood, H.; van Thiel, A.; Sutcliffe, M. J.; Leys, D.; Munro, A. W.; Scrutton, N. S. Flavoenzyme catalyzed oxidation of amines: roles for flavin and protein-based radicals. *Biochem. Soc. Trans.* **2005**, *33*, 754–757.
- (3) Bertoni, J.; Elmer, L. The Role of MAO-B Inhibitors in the Treatment of Parkinson's Disease. In *Parkinson's Disease*; Ebadi, M., Pfeiffer, R. F., Eds.; CRC Press: Boca Raton, FL, 2005; pp 691–704.
- (4) Lang, A. E.; Lees, A. MAO-B inhibitors for the treatment of Parkinson's disease. *Mov. Disord.* **2002**, *17*, S38–S44.
- (5) (a) Husain, M.; Shukla, R.; Dikshit, M.; Maheshwari, P. K.; Nag, D.; Srimal, R. C.; Seth, P. K.; Khanna, V. K. Altered platelet monoamine oxidase-B activity in idiopathic Parkinson's disease. *Neurochem. Res.* **2009**, *34*, 1427–1432. (b) Chen, J. J.; Swope, D. M.; Dashtipour, K. Comprehensive review of rasagiline, a second generation monoamine oxidase inhibitor, for the treatment of Parkinson's disease. *Clin. Ther.* **2007**, *29*, 1825–1846.
- (6) (a) Deeb, O.; Alfalah, S.; Clare, B. W. QSAR of aromatic substances: MAO inhibitory activity of xanthone derivatives. *J. Enzyme Inhib. Med. Chem.* **2007**, *22*, 277–286. (b) Thull, U.; Kneubühler, S.; Testa, B.; Borges, M. F.; Pinto, M. M. Substituted xanthenes as selective and reversible monoamine oxidase A (MAO-A) inhibitors. *Pharm. Res.* **1993**, *10*, 1187–1190.
- (7) (a) Santana, L.; González-Díaz, H.; Quezada, E.; Uriarte, E.; Yáñez, M.; Viña, D.; Orallo, F. Quantitative structure–activity relationship and complex network approach to monoamine oxidase A and B inhibitors. *J. Med. Chem.* **2008**, *51*, 6740–6751. (b) Binda, C.; Wang, J.; Pisani, L.; Caccia, C.; Carotti, A.; Salvati, P.; Edmondson, D. E.; Mattevi, A. Structures of human monoamine oxidase B complexes with selective noncovalent inhibitors: safinamide and coumarin analogs. *J. Med. Chem.* **2007**, *50*, 5848–5852. (c) Catto, M.; Nicolotti, O.; Leonetti, F.; Carotti, A.; Favia, A. D.; Soto-Otero, R.; Mendez-Alvarez, E.; Carotti, A. Structural insights into monoamine oxidase inhibitory potency and selectivity of 7-substituted coumarins from ligand- and target-based approaches. *J. Med. Chem.* **2006**, *49*, 4912–4925. (d) Borges, F.; Roleira, F.; Milhazes, N.; Santana, L.; Uriarte, E. Simple coumarins and analogues in medicinal chemistry: occurrence, synthesis and biological activity. *Curr. Med. Chem.* **2005**, *12*, 887–916.
- (8) (a) Chimenti, F.; Secci, D.; Bolasco, A.; Chimenti, P.; Bizzarri, B.; Granese, A.; Carradori, S.; Yáñez, M.; Orallo, F.; Ortuso, F.; Alcaro, S. Synthesis, molecular modeling, and selective inhibitory activity against human monoamine oxidases of 3-carboxamido-7-substituted coumarins. *J. Med. Chem.* **2009**, *52*, 1935–1942. (b) Chimenti, F.; Fioravanti, R.; Bolasco, A.; Chimenti, P.; Secci, D.; Rossi, F.; Yáñez, M.; Orallo, F.; Ortuso, F.; Alcaro, S. Chalcones: a valid scaffold for monoamine oxidase inhibitors. *J. Med. Chem.* **2009**, *52*, 2818–2824. (c) Chimenti, F.; Fioravanti, R.; Bolasco, A.; Chimenti, P.; Secci, D.; Rossi, F.; Yáñez, M.; Orallo, F.; Ortuso, F.; Alcaro, S.; Cirilli, R.; Ferretti, R.; Sanna, M. L. A new series of flavones, thioflavones, and flavanones as selective monoamine oxidase-B inhibitors. *Bioorg. Med. Chem.* **2010**, *18*, 1273–1279.

- (9) Ellis, G. P., Ed. *The Chemistry of Heterocyclic Compounds, Chromenes, Chromanones and Chromones*; J. Wiley & Sons: New York, 2007; Vol. 31.
- (10) (a) Ishar, M. P. S.; Singh, G.; Singh, S.; Sreenivasan, K. K.; Singh, G. Design, synthesis, and evaluation of novel 6-chloro-fluoro-chromone derivatives as potential topoisomerase inhibitor anticancer agents. *Bioorg. Med. Chem. Lett.* **2006**, *16*, 1366–1370. (b) Peixoto, F.; Barros, A. I. R. N. A.; Silva, A. M. S. Interactions of a new 2-styrylchromone with mitochondrial oxidative phosphorylation. *J. Biochem. Mol. Toxicol.* **2002**, *16*, 220–226. (c) Ellis, G. P.; Barker, G. 2. Chromones-2- and -3-carboxylic acids and their derivatives. *Prog. Med. Chem.* **1972**, *9*, 65–116. (d) Alcaro, S.; Gaspar, A.; Ortuso, F.; Milhazes, N.; Orallo, F.; Uriarte, E.; Yáñez, M.; Borges, F. Chromone-2- and -3-carboxylic acids inhibit differently monoamine oxidases A and B. *Bioorg. Med. Chem. Lett.* **2010**, *20*, 2709–2712. (e) Desideri, N.; Bolasco, A.; Fioravanti, R.; Proietti Monaco, L.; Orallo, F.; Yáñez, M.; Ortuso, F.; Alcaro, S. Homoisoflavonoids: natural scaffolds with potent and selective monoamine oxidase-B inhibition properties. *J. Med. Chem.* **2011**, *54*, 2155–2164.
- (11) (a) Borges, M. F. M.; Gaspar, A. M. N.; Garrido, J. M. P. J.; Milhazes, N. J. S. P.; Batoreu, M. C. C. Chromone Derivatives for Use as Antioxidants/Preservatives. WO 2008/104925 A1, 2008; Universidade do Porto, Port, Portugal (*Chem. Abstr.* **2008**, *149*, 332206). (b) Borges, M. F.; Gaspar, A. M. N.; Garrido, J. M. P. J.; Milhazes, N. J. S. P.; Uriarte, E.; Yáñez, M.; Orallo, F. Utilização de Cromonas, Seus Derivados, Seus Sais Farmacêuticos e Seus Pró-Fármacos com Actividade Inibidora da Monoamina Oxidase e Aplicações Terapêuticas Relacionadas. Priority Data PT 104487, 2009; Universidade do Porto, Port, Portugal. (c) Gaspar, A.; Reis, J.; Fonseca, A.; Milhazes, N.; Viña, D.; Uriarte, E.; Borges, M. F. Chromone 3-phenylcarboxamides as potent and selective MAO-B inhibitors. *Bioorg. Med. Chem. Lett.* **2011**, *21*, 707–709.
- (12) Berman, H. M.; Westbrook, J.; Feng, Z.; Gilliland, G.; Bhat, T. N.; Weissig, H.; Shindyalov, I. N.; Bourne, P. E. The Protein Data Bank. *Nucleic Acids Res.* **2000**, *28*, 235–242.
- (13) Dormoy, J. R.; Castro, B. The reaction of hexamethyl phosphoric triamide (HMPT) with phosphoryl chloride: a reexamination. Application to a novel preparation of BOP reagent for peptide coupling. *Tetrahedron Lett.* **1979**, *20*, 3321–3322.
- (14) *Comprehensive Organic Synthesis: Selectivity, Strategy and Efficiency in Modern Organic Chemistry*; Trost, B. M., Fleming, I., Winterfeldt, E., Eds.; Pergamon Press: Oxford, U.K., 1991; Vol. 6.
- (15) Matos, M. J.; Viña, D.; Quezada, E.; Picciau, C.; Delogu, G.; Orallo, F.; Santana, L.; Uriarte, E. A new series of 3-phenylcoumarins as potent and selective MAO-B inhibitors. *Bioorg. Med. Chem. Lett.* **2009**, *19*, 3268–3270.
- (16) Gerlach, M.; Riederer, P.; Youdim, M. B. The molecular pharmacology of L-deprenyl. *Eur. J. Pharmacol.* **1992**, *226*, 97–108.
- (17) Gaspar, A.; Teixeira, F.; Uriarte, E.; Milhazes, N.; Melo, A.; Cordeiro, M. N.; Ortuso, F.; Alcaro, S.; Borges, F. Towards the discovery of a novel class of monoamine oxidase inhibitors: structure–property–activity and docking studies on chromone amides. *ChemMedChem* **2011**, *6*, 628–32.
- (18) (a) *Glide*, version 5.6; Schrodinger, LLC: New York, NY, 2010. (b) Friesner, R. A.; Banks, J. L.; Murphy, R. B.; Halgren, T. A.; Klicic, J. J.; Mainz, D. T.; Repasky, M. P.; Knoll, E. H.; Shaw, D. E.; Shelley, M.; Perry, J. K.; Francis, P.; Shenkin, P. S. Glide: a new approach for rapid, accurate docking and scoring. 1. Method and assessment of docking accuracy. *J. Med. Chem.* **2004**, *47*, 1739–1749. (c) Halgren, T. A.; Murphy, R. B.; Friesner, R. A.; Beard, H. S.; Frye, L. L.; Pollard, W. T.; Banks, J. L. Glide: a new approach for rapid, accurate docking and scoring. 2. Enrichment factors in database screening. *J. Med. Chem.* **2004**, *47*, 1750–1759. (d) Friesner, R. A.; Murphy, R. B.; Repasky, M. P.; Frye, L. L.; Greenwood, J. R.; Halgren, T. A.; Sanschagrin, P. C.; Mainz, D. T. Extra precision glide: docking and scoring incorporating a model of hydrophobic enclosure for protein–ligand complexes. *J. Med. Chem.* **2006**, *49*, 6177–6196. (e) Park, M.; Gao, C.; Stern, H. A. Estimating binding affinities by docking/scoring methods using variable protonation states. *Proteins* **2010**, *79*, 304–314.
- (19) Son, S. Y.; Ma, J.; Kondou, Y.; Yoshimura, M.; Yamashita, E.; Tsukihara, T. Structure of human monoamine oxidase A at 2.2 Å resolution: the control of opening the entry for substrates/inhibitors. *Proc. Natl. Acad. Sci. U.S.A.* **2008**, *105*, 5739–5744; data deposition at www.pdb.org (PDB code 2Z5X).
- (20) Binda, C.; Wang, J.; Pisani, L.; Caccia, C.; Carotti, A.; Salvati, P.; Edmondson, D. E.; Mattevi, A. Structures of human monoamine oxidase B complexes with selective noncovalent inhibitors: safinamide and coumarin analogs. *J. Med. Chem.* **2007**, *50*, 5848–5852; data deposition at www.pdb.org (PDB code 2V5Z).
- (21) *Maestro*, version 9.1; Schrodinger, LLC: New York, NY, 2010.
- (22) Kaminski, G.; Friesner, R. A.; Tirado-Rives, J.; Jorgensen, W. L. Evaluation and reparametrization of the OPLS-AA force field for proteins via comparison with accurate quantum chemical calculations on peptides. *J. Phys. Chem. B* **2001**, *105*, 6474–6487.
- (23) (a) *MacroModel*, version 9.8; Schrodinger, LLC, New York, NY, 2010. (b) Mohamadi, F.; Richards, N. G. J.; Guida, W. C.; Liskamp, R.; Lipton, M.; Caufield, C.; Chang, G.; Hendrickson, T.; Still, W. C. MacroModel—an integrated software system for modeling organic and bioorganic molecules using molecular mechanics. *J. Comput. Chem.* **1990**, *11*, 440–467.
- (24) Hasel, W.; Hendrickson, T. F.; Still, W. C. A rapid approximation to the solvent accessible surface areas of atoms. *Tetrahedron Comput. Methodol.* **1988**, *1*, 103–116.

3.3 Towards the Discovery of a Novel Class of Monoamine Oxidase Inhibitors: Structure–Property–Activity and Docking Studies on Chromone Amides.

Article from *ChemMedChem* (2011), 6: 628–632.

DOI: 10.1002/cmdc.201000452

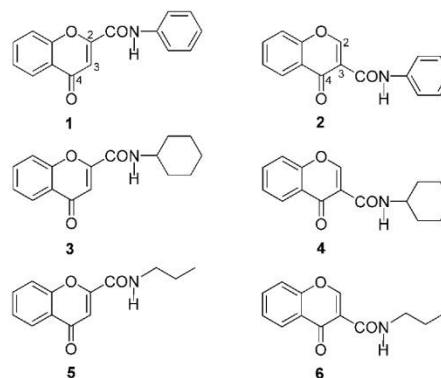
Towards the Discovery of a Novel Class of Monoamine Oxidase Inhibitors: Structure–Property–Activity and Docking Studies on Chromone Amides

Alexandra Gaspar,^[a] Filipe Teixeira,^[c] Eugenio Uriarte,^[d] Nuno Milhazes,^[a, e] André Melo,^[c] M. Natália D. S. Cordeiro,^[c] Francesco Ortuso,^[b] Stefano Alcaro,^{*,[b]} and Fernanda Borges^{*,[a]}

Monoamine oxidase (MAO) is a mammalian enzyme present in two isoforms (MAO-A and MAO-B) that is localized on the outer mitochondrial membrane and is involved in the oxidative deamination of exogenous and endogenous amines. Due to their central role in neurotransmitter metabolism, these isoforms represent attractive drug targets. In fact, MAO-A inhibitors are frequently used as antidepressants and anxiolytic agents, while MAO-B inhibitors are relevant tools in the therapy of Alzheimer's and Parkinson's diseases.^[1]

The chromone scaffold (4*H*)-1-benzopyran-4-one has been recognized as a putative pharmacophore for several targets.^[2] It has been recently studied as a valid scaffold for the design of selective MAO-B inhibitors.^[3] Furthermore, the simplicity of its synthesis make chromone carboxamide derivatives attractive to medicinal chemists.^[3] Recent data obtained by our group has shown that the presence of the same type of substituents on the 2- or 3-position of the pyrone ring discloses different pharmacological profiles—a circumstance that can be illustrated with the following chromone isomers: *N*-phenyl-4-oxo-4*H*-chromone-2-carboxamide (**1**) and *N*-phenyl-4-oxo-4*H*-chromone-3-carboxamide (**2**); the former is inactive, while the latter is a selective and potent MAO-B inhibitor: IC₅₀ (*h*MAO-B) = 0.40 ± 0.022 μM, selectivity index (SI) > 250.

To gain insight into the physicochemical properties that determine the activity of these types of benzopyran derivatives (**1** and **2**), it was decided to further explore the regioselectivity of the carboxamide function by acquiring relevant theoretical and spectroscopic data.



From the conformational analysis of chromones **1** and **2**, it can be concluded that the diagram of the relative potential energy of the two isomers shows that they have different profiles (Figure 1). The energetic difference between the minima detected suggests the presence of an added stabilizing driving force, for example, an intramolecular hydrogen bond in chromone **2** (Figure 2). Conformational analysis also shows that, because of the presumed hydrogen bond, the structure of chromone **2** is much more rigid than that of **1** (Figure 2). Therefore, a subsequent study evaluating the thermodynamic stability of the most relevant prototropic tautomers/rotomers of compound **2** in the gas phase, while taking solvent effects into account, was performed. Accordingly, the presumed existence of the two species stabilized by intramolecular hydrogen bonds (amide **2a**/iminol **2c** tautomers) was included.^[4–6] The data clearly indicates that, in the gas phase, tautomers **2b** and **2c** are thermodynamically unstable when compared to tautomer **2a**. The significance of the hydrogen bond as a stabilizing force on the structure of **2** can be explained by the relatively large enthalpies (see Table 1). Since preliminary calculations showed that the iminol tautomer (**2c**) was approximately 15 kcal mol^{−1} higher in energy, it was deemed energetically unfavorable and consequently omitted from subsequent studies.

In order to provide experimental evidence for the presence of the hydrogen bond, NMR spectra (acquired in CDCl₃ and DMSO) were collected and analyzed.¹ The data obtained so far corroborates the presence, in solution, of a strong intramolecular hydrogen bond in compound **2** (Table 2).^[5, 6] The strong hy-

[a] A. Gaspar, Prof. N. Milhazes, Prof. F. Borges
CIQUP, Departamento de Química e Bioquímica
Faculdade de Ciências, Universidade do Porto
Rua Campo Alegre 687, 4169-007 Porto (Portugal)
Fax: (+351) 220 402 009
E-mail: fborges@fc.up.pt

[b] Dr. F. Ortuso, Prof. S. Alcaro
Dipartimento di Scienze Farmacobiologiche
Università "Magna Graecia" di Catanzaro
Complesso "Nini Barbieri", 88021, Roccella di Borgia, Catanzaro (Italy)
Fax: (+39) 0961 391 490
E-mail: alcaro@unicz.it

[c] F. Teixeira, Prof. A. Melo, Prof. M. N. D. S. Cordeiro
REQUIMTE, Departamento de Química e Bioquímica
Faculdade de Ciências, Universidade do Porto, Porto (Portugal)

[d] Prof. E. Uriarte
Departamento de Química Orgánica, Facultad de Farmacia
Universidad de Santiago de Compostela
Avda. das Ciencias, 15782 Santiago de Compostela (Spain)

[e] Prof. N. Milhazes
Instituto Superior de Ciências de Saúde-Norte
R. Central de Gandra, 1317 Gandra PRD (Portugal)

Supporting information for this article is available on the WWW under <http://dx.doi.org/10.1002/cmdc.201000452>.

¹ Note: the polar aprotic solvent characteristics of DMSO are excellent for hydrogen bond acceptance that to some extent can disrupt the hydrogen bond that is being sought out via NMR by forming intermolecular hydrogen bonds between itself and the system under study.

COMMUNICATIONS

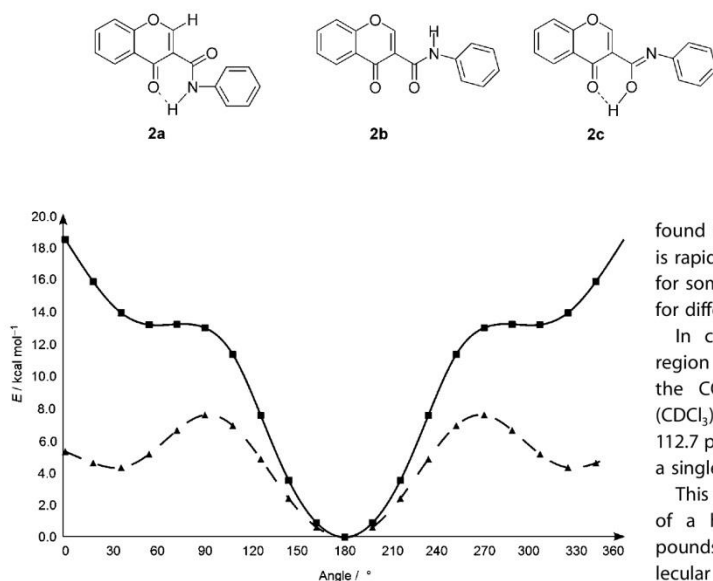


Figure 1. Potential energy profile for the relaxed scan of the amide group dihedral angle (τ) with respect to the plane of the benzopyran ring at the B3LYP/6-31G(d,p) level theory for compounds **1** (\blacktriangle) and **2** (\blacksquare). The energy profiles traced for compounds **3** and **5** closely resemble that of compound **1**. Similarly, compounds **4** and **6** mimic the behavior of compound **2**.

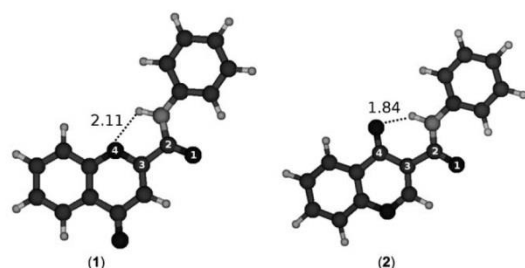


Figure 2. Molecular structures of compounds **1** and **2** in their most stable conformations [conformational analysis of the 1-2-3-4 torsion angle (τ)]. Similar arrangements and results were achieved for compounds **3–6**. Representative interatomic lengths are given in angstroms.

drogen bond established between amide N–H and the carbonyl group of the γ -pyrone ring causes a downfield shift from the usual positions normally observed for typical hydrogen and carbon nuclei (δ = 13.71/11.94 ppm (CDCl_3) and δ = 13.48/11.87 ppm (DMSO); δ = 166.2/164.5 ppm (CDCl_3) and δ = 163.8/162.3 ppm (DMSO), respectively). After addition of D_2O , the ^1H signals disappeared in the spectra confirming the presence of exchangeable protons. The H2 and C2 chemical shifts (δ = 9.05/8.91 ppm (CDCl_3) and δ = 8.93/8.90 ppm (DMSO); δ = 155.9/154.4 ppm (CDCl_3) and δ = 155.5/154.2 ppm (DMSO), respectively) and the existence of two C=O signals in the ^{13}C spectra [δ = 182.8/179.6 ppm (CDCl_3) and δ = 180.3/178.6 ppm

(DMSO)] are also evidence for the existence of tautomers. In solution the tautomers are not present in the same ratio (60:40 in CDCl_3 and 70:30 in DMSO).² The presence of other tautomeric forms in solution under these experimental conditions was

found to be negligible. Since tautomeric conversion is rapid on the NMR time scale, we observed splitting for some signals. Similar findings have been reported for different types of systems.^[7,8]

In contrast, compound **1** present in the same region has only two signals: one corresponding to the CONH function [δ = 8.56 ppm; δ = 155.2 ppm (CDCl_3)] and the other to H3/C3 [δ = 7.28 ppm; δ = 112.7 ppm (CDCl_3)], thus confirming the presence of a single structure in solution.

This preliminary study points out that the presence of a hydrogen-bond network in chromone compounds is crucial for MAO-B selectivity. The intramolecular resonance-assisted hydrogen bond (RAHB) present in chromone-3-carboxamide (**2**) allows the stabilization of a folded state with the formation of a six-membered, hydrogen-bonded pseudocycle that appears to be important for biological activity.^[9,10] Accordingly, it can be anticipated that the type and position of the substituents on the aromatic nucleus of the chromone carboxamide side chain can influence the strength of the hydrogen bond consequently affecting the potency of this type of MAO-B inhibitor. Therefore, structure–property–activity relationships (SPAR) studies were performed to attain this goal.

With the aim to reinforce the data thus far obtained, other chromone derivatives were synthesized and their biological activities evaluated. Compounds **3** and **5** have their side chains in the 2-position, while their corresponding isomers **4** and **6** have the side chain in the 3-position. These molecules represent pairs of isomers related to the position of their substituents onto the γ -pyrone ring and having different substituents (saturated cyclic and linear alkanes) located on the carboxamide side chain. Chromones **3** and **5** are inactive towards both MAO isoforms, as was the case for compound **1**. Isomeric compounds **4** and **6** are less active (**4**: IC_{50} (hMAO-B) = $0.93 \pm 0.062 \mu\text{M}$; $\text{SI} > 107$; **6**: IC_{50} (hMAO-B) = $37.69 \pm 1.68 \mu\text{M}$; $\text{SI} > 2.7$), and less selective than compound **2** (IC_{50} (hMAO-B) = $0.40 \pm 0.022 \mu\text{M}$; $\text{SI} > 250$).

Similar theoretical calculations and spectroscopic studies were also performed for these compounds to gain further insight about the structure, chemical behavior, and chromone biological activity. Spectroscopic data obtained for chromones **3–6** (Table 2) are in accordance with previous results; the intramolecular hydrogen bond is present in all the chromone-3-carboxamides. As observed earlier in this paper, the energy profile

² Note: the chemical shifts of CONH and H2 of compound **2** remain nearly unchanged in DMSO, thus supporting the proposed stability of the tautomers.

CHEMMEDCHEM

Table 1. Energies, relative energies (ΔE), relative enthalpies (ΔH) and Gibbs energies (ΔG) of the putative tautomers of **2** in the gas phase and in solution.^[a]

Compd	$\tau^{[b]}$ [°]	Energy + ZPVE [Ha]	Gas phase			Energy + ZPVE [Ha]	CHCl ₃		
			ΔE	ΔH	ΔG [kcal mol ⁻¹]		ΔE	ΔH	ΔG [kcal mol ⁻¹]
2a	180.0	−896.56345	0.00	0.00	0.00	−896.56605	0.00	0.00	0.00
2b	0.0	−896.53548	17.55	17.42	17.62	−896.54471	13.40	13.27	13.47
2c	0.0	−896.54141	13.83	13.83	13.45	−896.54315	14.37	14.38	14.00

[a] All the energies are relative to the most stable conformer of **2** and include the zero-point vibrational energy (ZPVE) corrections. Enthalpies and Gibbs energies also include the thermal translational, rotational and vibrational contributions at 298 K. [b] 1-2-3-4 Dihedral angle (τ).

Table 2. Experimental ¹H and ¹³C NMR chemical shifts (δ), in CDCl₃ and DMSO, relevant for the hydrogen-bond assessment in chromones.

Compd	CDCl ₃		[D ₆]DMSO		Δδ ¹ H ^[b] [ppm]
	¹ H NMR δ [ppm]	¹³ C NMR δ [ppm]	¹ H NMR δ [ppm]	¹³ C NMR δ [ppm]	
<i>Inactive</i>					
1	8.56 (CONH)	178.0 (C4)	10.77 (CONH)	177.4 (C4)	2.21 (CONH)
	7.28 (H3)	155.2 (CONH)	6.99 (H3)	155.8 (CONH)	−0.29 (H3)
		112.7 (C3)		111.1 (C3)	
3	6.79/6.78 (CONH)	179.1 (C4)	8.85/8.83 (CONH)	178.7 (C4)	2.06/2.05 (CONH)
	7.16 (H3)	159.1 (CONH)	6.83 (H3)	159.4 (CONH)	−0.33 (H3)
		112.9 (C3)		111.9 (C3)	
5	7.04 (CONH)	179.1 (C4)	9.13 (CONH)	178.7 (C4)	2.09 (CONH)
	7.16 (H3)	160.1 (CONH)	6.83 (H3)	160.3 (CONH)	−0.33 (H3)
		112.9 (C3)		111.7 (C3)	
<i>Active</i>					
2	13.71/11.94 (CONH) ^[a]	182.8/179.6 (C4)	13.48/11.87 (CONH) ^[a]	180.3/178.6 (C4)	−0.23/−0.07 (CONH)
	9.05/8.91 (H2)	166.2/164.5 (CONH)	8.93/8.90 (H2)	163.8/162.3 (CONH)	−0.12/−0.01 (H2)
		155.9/154.4 (C2)		155.5/154.2 (C2)	
4	11.85/10.30 (CONH)	181.3 (C4)	11.84/10.31 (CONH)	179.6 (C4)	−0.01/0.01 (CONH)
	8.62/8.51 (H2)	164.1 (CONH)	8.61/8.50 (H2)	162.6 (CONH)	−0.01/−0.01 (H2)
		160.2 (C2)		162.3 (C2)	
6	11.94/10.28 (CONH)	181.5 (C4)	11.70/10.36 (CONH)	179.3 (C4)	−0.24/0.08 (CONH)
	8.57/8.41 (H2)	164.0 (CONH)	8.60/8.47 (H2)	162.7 (CONH)	0.03/0.06 (H2)
		162.4 (C2)		162.2 (C2)	

[a] Exchange with D₂O. [b] $\Delta\delta$ ¹H = (δ DMSO − δ CDCl₃).

for compounds **3** and **5**, with respect to the torsion angle between the γ -pyrone ring and the side chain located at the 2-position, showed an energy barrier of approximately 7 kcal mol⁻¹ (Figure 1). On the other hand, the energy profiles of compounds **4** and **6** show an energy barrier of approximately 12 kcal mol⁻¹ for the most stable conformer and a shallow region where another conformer was found (Figure 1). These results agree with those previously obtained for chromones **1** and **2**. Such energy profiles were obtained irrespective of the type of substituent attached at the N-position of the carboxamide side chain. Remarkably, the more energetic conformer of compounds **2**, **4** and **6** can return to the less energetic form virtually without any significant energy barrier. Vibrational analysis further confirmed the aforementioned conformers as true minima in the potential energy surface (PES) and allowed certain inferences to be made for thermodynamic considerations. Variations in energy in the equilibrium between the two conformers are presented in Table 1 for both vacuum and solution (DMSO) phase. In general, the most stable conformation is fa-

vored by ~3.5 kcal mol⁻¹ in compounds **1**, **3** and **5**, and by almost 11 kcal mol⁻¹ if the side chain is connected to the 3-position of the pyrone ring. The solvent seems to have a significant effect in this equilibrium, as it stabilizes the more energetic conformer—relative to the more stable one—thus decreasing ΔH . This effect is particularly relevant in compounds **1**, **3** and **5**. Both energetic profiling and thermodynamics support the following evidence: chromones with a side chain in the 2-position of the pyrone ring may exist freely as a mixture of two conformers around the amide bond, whereas the side chain at the 3-position locks the chromones into a fixed conformation.

Furthermore, a Monte Carlo (MC) conformational search revealed that the geometry of the carboxamide substituents was driven by an intermolecular hydrogen bond between the amide (donor) and oxygen atoms (acceptors) located in the γ -pyrone ring. This observation highlighted a remarkable constraint for the degrees of freedom of all compounds (Figure 1). In order to evaluate the possible role of the intramolecular hy-

COMMUNICATIONS

drogen bond with respect to MAO inhibition, the Boltzmann-weighted solvation energies (Supporting Information) was computed for the six chromones. Unsurprisingly, inactive compounds **1**, **3** and **5** were revealed to have higher stability in an aqueous environment than active compounds **2**, **4** and **6** (Table 3 and the Supporting Information). The weaker intramo-

Table 3. Boltzmann-weighted solvation energies for chromones 1–6.

Inactive Compd	E_{solv} [kcal mol ⁻¹]	Active Compd	E_{solv} [kcal mol ⁻¹]	ΔE_{solv}
1	-10.55	2	-8.27	2.28
3	-8.11	4	-6.09	2.02
5	-8.55	6	-6.49	2.06

lecular hydrogen bonds of **1**, **3** and **5**, when compared to those of **2**, **4** and **6**, allow for improved water interaction of the inactive compounds relative to the active ones. We have attributed the lack of MAO activity for compounds **1**, **3** and **5** to this observation. To this end, these molecules appear to have a preference for an aqueous environment surrounding the enzymes preventing their recognition both by the hMAO-A and hMAO-B active sites.

Taking into account the assumption above, we focused exclusively on compounds **2**, **4** and **6**. The recognition of the hMAO-A and hMAO-B catalytic clefts by compounds **2**, **4** and **6** was investigated by means of Glide flexible docking simulations.^[11] Two new, high-resolution, crystallographic models, deposited into the Protein Data Bank (PDB),^[12] codes 2Z5Y^[13] and 2V5Z,^[14] have been considered as hMAO-A and hMAO-B receptor models, respectively (Supporting Information). The ability of the Glide flexible method to reproduce the crystallographic poses of the ligands included in the 2Z5Y and 2V5Z PDB models has been tested by redocking the complexes. The best poses obtained using Glide, when compared with the original PDB geometries, were within root mean square (RMS) deviations of 0.266 Å and 0.210 Å, respectively (see the Supporting Information).

In good qualitative agreement with the experimental IC₅₀ values, docking results indicated productive binding modes to only the hMAO-B target for all compounds (Table 4). Theoretical binding modes were visually inspected, highlighting a similar type of interaction for all the compounds (Figure 3). Remarkably, the proposed binding modes of our chromone inhibitors showed the carboxamide side chain located toward the

FAD cofactor and the γ -pyrone ring located towards the pocket entrance interacting with hydrophobic residues Leu 171 and Ile 199. The position of the chromones in the hMAO-B binding cleft could be mainly driven by electrostatic interactions. Actually, in all cases, the γ -sp² oxygen was directed towards the Cys172 thiol group and its influence, computed by the docking program, discriminated amongst the **2**, **4** and **6** chromone carboxamides. Moreover, all compounds accepted one hydrogen bond from the Tyr386 side chain. This last interaction involved the carbonyl oxygen of the carboxamide of the most active compounds **2** and **4** and the chromone ether oxygen of **6**. Therefore, this hydrogen bond contributes to the different hMAO-B affinity profiles of our inhibitors. Both of the mentioned electrostatic interactions can be used to rationalize the isoform selectivity of our molecules; in fact, hMAO-B Cys172 and Tyr386 are replaced by Asn181 and Ile335 in hMAO-A.

Finally, the type of carboxamide substituent (phenyl-, cyclohexyl- and propyl- for **2**, **4** and **6**, respectively) represented another relevant contributor to the chromone-hMAO-B interactions. Such a moiety was predicted to be located in approximately the same area, surrounded by Leu 171, Ile 198, Gln 206, Tyr398 and Phe343. The small propyl group of compound **6** can participate in a limited number of interactions compared with the phenyl group of **2** and the cyclohexyl moiety of **4**. On the other hand, the cyclohexyl group of **4** shows a hydrophobic interaction, while the phenyl of the most potent compound (**2**) also established hydrogen- π interactions with the Tyr398 and Gln206 side chains. For a complete list of the most relevant interacting residues see table S1 in the Supporting Information.

In conclusion, a combined theoretical and experimental study carried out on chromone carboxamides indicated that 3-substituted derivatives are superior inhibitors for the MAO-B isoform. These type of chromone derivatives are able to establish a crucial intramolecular hydrogen bond essential to exert: a) the stabilization of the free ligands in a linear conformation with a high level of co-planarity between the chromone and the benzamidic substituent—as demonstrated by *ab initio* calculations; b) a better fit into the MAO-B enzymatic cleft—supported in the docking calculations mainly by solvating and electrostatic contributions; c) selective inhibition of the isoform B—as demonstrated by the enzymatic experiments. These results will be useful for the rational design of highly potent and/or selective MAO inhibitors based on the chromone scaffold.

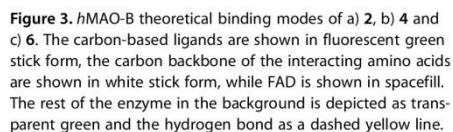
Acknowledgements

The authors acknowledge the Portuguese Fundação para a Ciência e a Tecnologia (FCT) for financial support (project: PTDC/QUI/70359/2006), and doctoral grants to A.G. and F.T. (SFRH/BD/43531/2008 and SFRH/BD/64314/2009). The authors are grateful to Dr. Alfredo Mellace (Department of Chemistry, Nassau Community College NY, USA) for proofreading the revised manuscript.

Table 4. Glide XP ranking for compounds **2**, **4** and **6**, with respect to hMAO-A and hMAO-B receptor models.

Compd	hMAO-A ^[a]	hMAO-B
2	–	–7.14
4	–	–5.80
6	–	–5.29

[a] No docking solutions were found within the hMAO-A binding site.



- [1] a) D. E. Edmondson, A. Mattevi, C. Binda, M. Li, F. Hubálek, *Curr. Med. Chem.* **2004**, *11*, 1983–1993; b) P. Riederer, L. Lachenmayer, G. Laux, *Curr. Med. Chem.* **2004**, *11*, 2033–2043.
- [2] *The Chemistry of Heterocyclic Compounds, Chromenes, Chromanones and Chromones*, Vol. 31, (Ed.: G. P. Ellis), John Wiley & Sons, Inc., Hoboken, **1977**.
- [3] a) M. F. Martins Borges, A. M. Neves Gaspar, J. M. Pinto de Jesus Garrido, N. J. Da Silva Pereira Milhazes, (Universidade do Porto; Port, Portugal), PT 103665, WO 2008/104925 A1, **2008** [*Chem. Abstr.* **2008**, *149*, 332206]; b) M. F. Martins Borges, A. M. Neves Gaspar, J. M. Pinto de Jesus Garrido, N. J. Da Silva Pereira Milhazes, (Universidade do Porto; Port, Portugal), PT 104487, **2009**.
- [4] M. Malecka, *J. Mol. Struct.* **2007**, *831*, 135–143.
- [5] E. D. Raczynska, W. Kosinska, B. Osmialowski, R. Gawinecki, *Chem. Rev.* **2005**, *105*, 3561–3612.
- [6] J. E. van Muijlwijk-Koezen, H. Timmerman, R. Link, H. van der Goot, A. P. Ijzerman, *J. Med. Chem.* **1998**, *41*, 3994–4000.
- [7] N. Binbuga, T. P. Schultz, W. P. Henry, *Tetrahedron Lett.* **2008**, *49*, 5762–5765.
- [8] G. A. Jeffrey, *An Introduction to Hydrogen Bonding*, Oxford University Press, Oxford, **1997**.
- [9] P. Gilli, V. Bertolasi, L. Pretto, A. Lycka, G. Gilli, *J. Am. Chem. Soc.* **2002**, *124*, 13554–13567; P. Gilli, V. Bertolasi, L. Pretto, L. Antonov, G. Gilli, *J. Am. Chem. Soc.* **2005**, *127*, 4943–4953.
- [10] B. Kuhn, P. Mohr, M. Stahl, *J. Med. Chem.* **2010**, *53*, 2601–2611.
- [11] a) M. D. Eldridge, C. W. Murray, T. R. Auton, G. V. Paolini, R. P. Mee, *J. Comput.-Aided Mol. Des.* **1997**, *11*, 425–445; b) T. A. Halgren, R. B. Murphy, R. A. Friesner, H. S. Beard, L. L. Frye, W. T. Pollard, J. L. Banks, *J. Med. Chem.* **2004**, *47*, 1750–1759; c) R. A. Friesner, J. L. Banks, R. B. Murphy, T. A. Halgren, J. J. Klicic, D. T. Mainz, M. P. Repasky, E. H. Knoll, D. E. Shaw, M. Shelley, J. K. Perry, P. Francis, P. S. Shenkin, *J. Med. Chem.* **2004**, *47*, 1739–1749.
- [12] H. M. Berman, J. Westbrook, Z. Feng, G. Gilliland, T. N. Bhat, H. Weissig, I. N. Shindyalov, P. E. Bourne, *Nucleic Acids Res.* **2000**, *28*, 235–242.
- [13] S. Y. Son, J. Ma, Y. Kondou, M. Yoshimura, E. Yamashita, T. Tsukihara, *Proc. Natl. Acad. Sci. USA* **2008**, *105*, 5739–5744.
- [14] C. Binda, J. Wang, L. Pisani, C. Caccia, A. Carotti, P. Salvati, D. E. Edmondson, A. Mattevi, *J. Med. Chem.* **2007**, *50*, 5848–5852.

Received: October 16, 2010
Revised: December 23, 2010
Published online on January 25, 2011

3.4 Chromone 3-phenylcarboxamides as potent and selective MAO-B inhibitors

Article reprinted from Bioorganic & Medicinal Chemistry Letters (2011), 21: 707–709.



Contents lists available at ScienceDirect

Bioorganic & Medicinal Chemistry Letters

journal homepage: www.elsevier.com/locate/bmcl

Chromone 3-phenylcarboxamides as potent and selective MAO-B inhibitors

Alexandra Gaspar^a, Joana Reis^a, André Fonseca^a, Nuno Milhazes^{a,b}, Dolores Viña^{c,d}, Eugenio Uriarte^{c,d},
Fernanda Borges^{a,*}^a CIQ/Departamento de Química e Bioquímica, Faculdade de Ciências, Universidade do Porto, 4169-007 Porto, Portugal^b Instituto Superior de Ciências da Saúde, Norte, Rua Central de Gandra, 1317, 4585-116 Gandra PRD, Portugal^c Departamento de Farmacología, Facultad de Farmacia, Universidad de Santiago de Compostela, 15782 Santiago de Compostela, Spain^d Departamento de Química Orgánica, Facultad de Farmacia, Universidad de Santiago de Compostela, 15782 Santiago de Compostela, Spain

ARTICLE INFO

Article history:

Received 8 November 2010

Revised 26 November 2010

Accepted 30 November 2010

Available online 5 December 2010

Keywords:

Chromone

hMAO-B

Neurodegenerative diseases

ABSTRACT

Monoamine oxidase (MAO) is an enzyme, present in mammals in two isoforms MAO-A and MAO-B. These isoforms have a crucial role in neurotransmitters metabolism, representing an attractive drug target in the therapy of neurodegenerative diseases (MAO-B) and depression (MAO-A). In this context, our work has been focused on the discovery of new chemical entities (NCEs) for MAO inhibition, based on the development of chromone carboxamides. Chromone derivatives with a carboxamide function located in position 2- and 3- of the benzo- γ -pyrone core, (compounds **2–6** and **8–12**) were synthesized, with moderate/good yields, by a one-pot condensation reaction using phosphonium salts as coupling reagents. The synthetic compounds were screened towards human MAO isoforms (hMAO) to evaluate their potency and selectivity. The chromone-3-carboxamides show high selectivity to hMAO-B, with compounds **9** and **12** displaying IC₅₀ values at nanomolar range.

© 2010 Published by Elsevier Ltd.

Parkinson's disease (PD) is a neurodegenerative disorder characterized by a myriad of symptoms that gradually decreases the quality of life of the patient. The first line of treatment is a dopamine replacement therapy with Levodopa.¹ Among other therapeutic strategies monoamine oxidase B (MAO-B) inhibitors have also been extensively used in PD. In fact, selective MAO-B inhibitors (i.e., deprenyl and rasagiline) are currently used, alone or in combination with Levodopa, in the symptomatic treatment of Parkinson's disease. The side effects associated with the use of deprenyl and, to a lesser extent, rasagiline, likely due to their irreversible mechanism of inhibition, and the potential application of MAO-B inhibitors as anti-Alzheimer's agents are at the moment the driving forces for the discovery of novel potent and selective MAO-B inhibitors.^{2,3}

Privileged structures, such as benzopyranes, are currently ascribed as supportive approaches in drug discovery. In fact, different families of natural nitrogen and oxygen heterocycles, such as xanthenes and coumarins, have also been used as scaffolds in medicinal chemistry programs for searching novel MAO-B inhibitors.^{4,5}

Chromones (benzopyran-4-one) are one of the most abundant groups of naturally occurring heterocyclic compounds.⁴ Because of their structural features they occupy an important place in the realm of natural products and synthetic organic chemistry. In addition, remarkable antioxidant, anticancer and enzymatic inhibition properties have been ascribed to these systems.⁵

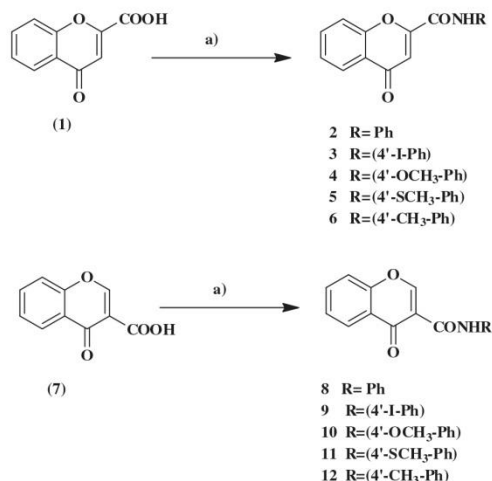
Noteworthy evidences have been already acquired to reinforce the interest of simple coumarins (benzopyran-2-one) as potent and selective monoamine oxidase inhibitors (hMAO) and that their affinity and selectivity can be efficiently modulated by appropriate substitution patterns in the heterocyclic moiety.⁶ However, in which concerns the benzopyran-4-one scaffold, only few works were found in the literature about their putative potential as hMAO.⁷

Accordingly, our project has been focused on the discovery of new chemical entities for MAO inhibition with benzopyran-4-one substructure (Scheme 1). Preliminary studies performed with chromones (**1**) and (**7**) allow disclosing a significant chemical feature: the importance of the location of a carboxylic moiety in the γ -pyrone nucleus. In fact, when the –COOH substituent is in position 3 of the heterocyclic scaffold (**7**) binds to hMAO-B, exerting a selective inhibition with respect to A isoform (IC₅₀ hMAO-B 0.048 \pm 0.0026 nM; SI >2083). The inhibition is of irreversible type (data not shown). Its isomer (**1**), with the carboxylic function in position 2, doesn't present activity for both MAO isoforms.⁸ Molecular modeling studies performed with the chromone carboxylic acids reveal a crucial, undisclosed role of the presence of an hydrogen donor group in position 3 of the pyrone ring that could be able to establish hydrogen bond interactions with active site residues.⁸

In this context, and in an attempt to develop novel reversible and selective MAO-B inhibitors, the synthesis of 2- and 3-carboxamide chromone derivatives capable of establishing hydrogen interactions with the enzyme was performed. In this work, several 2- and 3-phenylcarboxamide chromones with or without different

* Corresponding author.

E-mail address: fborges@fc.up.pt (F. Borges).



Scheme 1. Structure of the chromones under study. Reagents and conditions: (a) BOP or PyBOP, R-C₆H₄-NH₂, CH₂Cl₂, DMF, DIPEA.

type of substituents in *para*-position of the exocyclic aromatic nucleus (Scheme 1) were obtained by an expedite synthetic strategy and screened towards human MAO isoforms (hMAO) to evaluate their potency/selectivity ratio.

The chromone derivatives **2–6** and **8–12** were efficiently synthesized according to the synthetic protocol outlined in Scheme 1.⁹ Chromone carboxamide derivatives were synthesized straightforward by a one-pot condensation reaction that occurs, in equimolar amounts, between the corresponding chromone carboxylic acid (compound **1** or **7**) and aniline or its ring-substituted derivatives. The reaction was clean and the compounds were obtained with moderate/high yields (50%–80%). After the reaction, the crude products were purified by flash column chromatography and crystallization.

The MAO inhibitory activity of compounds **2–6** and **8–12** was evaluated *in vitro* by the measurement of the enzymatic activity of human recombinant MAO isoforms in BTI insect cells infected with baculovirus.¹⁰ Then, the IC₅₀ values and MAO-B selectivity ratios (SI) [IC₅₀ (MAO-A)]/[IC₅₀ (MAO-B)] for inhibitory effects of both new compounds and reference compounds (R(–)-deprenyl and iproniazide) were calculated.

The results of the inhibitory potencies and selectivities of the chromones under study towards MAO isoforms, and reference compounds, are depicted in Table 1. From the data one can conclude that 'chromones bearing carboxamide substituents in position 3 of the γ -pyrone nucleus' act preferably as MAO-B inhibitors (IMAO-B) with IC₅₀ values in micro to nanomolar range (**8–12**). The same tendency was found with the chromone carboxylic acids.⁸ In addition, one can conclude that the type of substituents in the *para*-position of the exocyclic aromatic ring can modulate the affinity and selectivity of the chromones-3-carboxamides as IMAO-B. The introduction of a methoxyl group (**10**) seems to have no effect in IMAO-B potency when compared with the activity found for compound (**8**). Nevertheless it is important to point out that the introduction of a thiomethyl group (**11**), a bioisostere of the methoxyl function, has improved the potency of the compound 3–4-fold relatively to the compounds **8** and **10**. The most promissory compounds as IMAO-B, with an IC₅₀ <75 nM and a SI of >1440, are the compounds **9** and **12**, which are substituted in *para*-position by iodo and methyl groups, respectively, representing an improvement of potency of six fold relatively

Table 1
hMAO-A and hMAO-B inhibitory activity results for compounds **2–6**, **8–12** and reference compounds

Compound	hMAO-A IC ₅₀ (μ M)	hMAO-B IC ₅₀ (μ M)	SI
2 R = Ph	a	a	—
3 R = (4'-I-Ph)	a	a	—
4 R = (4'-OCH ₃ -Ph)	a	a	—
5 R = (4'-SCH ₃ -Ph)	a	a	—
6 R = (4'-CH ₃ -Ph)	a	a	—
8 R = Ph	a	0.40 \pm 0.022	>250 ^c
9 R = (4'-I-Ph)	a	0.069 \pm 0.003	>1449 ^c
10 R = (4'-OCH ₃ -Ph)	a	0.45 \pm 0.029	>222 ^c
11 R = (4'-SCH ₃ -Ph)	a	0.12 \pm 0.0080	>833 ^c
12 R = (4'-CH ₃ -Ph)	a	0.068 \pm 0.003	>1471 ^c
Deprenyl	68.73 \pm 4.21 ^b	0.017 \pm 0.002	4043
Iproniazide	6.56 \pm 0.76	7.54 \pm 0.36	0.87

^a Inactive at 100 μ M (highest concentration tested). At higher concentrations the compounds precipitate.

^b *P* <0.01 versus the corresponding IC₅₀ values obtained against hMAO-B, as determined by ANOVA/Dunnett's.

^c Values obtained under the assumption that the corresponding IC₅₀ against hMAO-A is the highest concentration tested (100 μ M).

to compounds **8** and **10**. From the overall data it was concluded that the positive hydrophobicity (+ π) of the substituent, besides inductive and mesomeric effects, located on the phenyl exocyclic moiety markedly influence the potency and selectivity of the chromone carboxamides.

Noteworthy to mark out that the chromones bearing the same type of substituents in position 2 of γ -pyrone nucleus (chromones **2–6**) present a total loss of MAO activity.

Preliminary studies on the type of hMAO inhibition were performed revealing that chromone 3-phenylcarboxamides behave as quasi-reversible MAO-B inhibitors (data not shown).

In the present Letter, the effect of the introduction of a methyl or iodo substituent in *para*-position of the exocyclic aromatic ring of chromone 3-phenylcarboxamides was outlined. In fact, the introduction of this type of groups improves the pharmacologic potential of chromone 3-phenylcarboxamides confirming that this lead could be effectively optimized in a candidate for the treatment of neurodegenerative diseases. These findings have encouraged us to continue the efforts towards the optimization of the lead compound.

In conclusion chromone appears to be an interesting scaffold for the design of selective IMAO. The easy synthetic accessibility and especially the versatile binding properties of chromones make them as 'privileged' scaffolds. These discoveries open a new avenue to obtain highly potent and selective MAO-B inhibitors structurally based on chromone scaffold.

Acknowledgements

The authors acknowledge Portuguese Fundação para a Ciência e a Tecnologia (FCT) for financial support (project PTDC/QUI/70359/2006) and AG doctoral grant (SFRH/BD/43531/2008).

References and notes

- Foley, P.; Gerlach, M.; Youdim, M. B. H.; Riederer, P. *Parkinsonism Relat. Disord.* **2000**, *6*, 25.
- Rezak, M. *Dis. Mon.* **2007**, *53*, 214.
- Riederer, P.; Lachenmayer, L.; Laux, G. *Curr. Med. Chem.* **2004**, *11*, 2033.
- The Chemistry of Heterocyclic Compounds, Chromenes, Chromanones and Chromones*; Ellis, G. P., Ed.; J. Wiley and Sons: New York, 2007; Vol. 31.
- Shaw, A. Y.; Chang, C. Y.; Liao, H. H.; Lu, P. J.; Chen, H. L.; Yang, C. N.; Li, H. Y. *Eur. J. Med. Chem.* **2009**, *44*, 2552.
- (a) Borges, F.; Roleira, F.; Milhazes, N.; Santana, L.; Uriarte, E. *Curr. Med. Chem.* **2005**, *12*, 887; (b) Matos, M. J.; Viña, D.; Janeiro, P.; Borges, F.; Santana, L.; Uriarte, E. *Bioorg. Med. Chem. Lett.* **2010**, *20*, 5157.
- Brühlmann, C.; Ooms, F.; Carrupt, P. A.; Testa, B.; Catto, M.; Leonetti, F.; Altomare, C.; Carotti, A. *J. Med. Chem.* **2001**, *44*, 3195.

8. Alcaro, S.; Gaspar, A.; Ortuso, F.; Milhazes, N.; Orallo, F.; Uriarte, E.; Yáñez, M.; Borges, F. *Bioorg. Med. Chem. Lett.* **2010**, *20*, 2709.
9. (a) Borges, M. F. M.; Gaspar, A. M. N.; Garrido, J. M. P. J.; Milhazes, N. J. S. P.; Batoreu, M. C. C. WO2008104925A1 and PT103665. (b) Borges, M. F. M.; Gaspar, A. M. N.; Garrido, J. M. P. J.; Milhazes, N. J. S. P.; Uriarte, E.; Yáñez, M.; Orallo, F. PT104487.
General procedure for amide obtention. 2-Carboxychromone (**1**) or 3-carboxychromone (**7**) (2.63 mmol) was dissolved in 6 mL of DMF and 0.37 mL of diisopropylethylamine (DIPEA). The solution was then cooled to 0 °C and a BOP (2.63 mmol) or PyBOP (2.63 mmol) solution in CH₂Cl₂ (6 mL) was added and the mixture was stirred for 30 min. After, the corresponding amine was added in equimolar amount and the temperature was let to gradually increase to room temperature. The reaction was stirred for additional 4–6 h.
10. *Evaluation of human monoamine oxidase (hMAO) isoform activity.* The effects of the tested compounds on hMAO isoform enzymatic activity were evaluated by a fluorimetric method following the experimental protocol previously described (Santana, L.; Uriarte, E.; González-Díaz, H.; Quezada, E.; Uriarte, E.; Yáñez, M.; Viña, D.; Orallo, F. *J. Med. Chem.* **2008**, *51*, 75). Briefly, 0.1 mL of sodium phosphate buffer (0.05 M, pH 7.4) containing the test drugs in various concentrations and adequate amounts of recombinant hMAO-A or hMAO-B required and adjusted to obtain in our experimental conditions the same reaction velocity. The reaction was started by adding (final concentrations) 200 µM Amplex[®] Red reagent, 1 U/mL horseradish peroxidase and 1 mM *p*-tyramine. The production of H₂O₂ and, consequently, of resorufin was quantified at 37 °C in a microplate fluorescence reader (excitation: 545 nm, emission: 590 nm) over a 15 min period, in which the fluorescence increased linearly. Control experiments were carried out simultaneously. The control activity of hMAO-A and hMAO-B (using *p*-tyramine as a common substrate for both isoforms) was 165 ± 2 pmol of *p*-tyramine oxidized to *p*-hydroxyphenylacetaldehyde/min (*n* = 20). All IC₅₀ values shown in the table are expressed as means ± SEM from five experiments.

3.5 In search for new chemical entities as adenosine receptor ligands: Development of agents based on benzo- γ -pyrone skeleton.

Article reprinted from European Journal of Medicinal Chemistry (2012), 54, 914-918



Contents lists available at SciVerse ScienceDirect

European Journal of Medicinal Chemistry

journal homepage: <http://www.elsevier.com/locate/ejmech>



Short communication

In search for new chemical entities as adenosine receptor ligands: Development of agents based on benzo- γ -pyrone skeleton

Alexandra Gaspar^{a,b}, Joana Reis^a, Maria João Matos^{a,b}, Eugenio Uriarte^b, Fernanda Borges^{a,*}

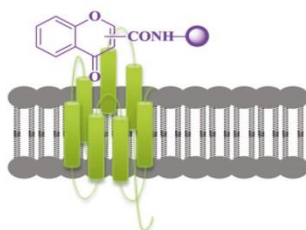
^a CIQUP/Departamento de Química e Bioquímica, Faculdade de Ciências, Universidade do Porto, Porto, Portugal

^b Departamento de Química Orgânica, Facultad de Farmacia, Universidad de Santiago de Compostela, Spain

HIGHLIGHTS

- Search for New Chemical Entities as adenosine receptor ligands.
- Benzo- γ -pyrone scaffold.
- N-phenylchromone-3-carboxamide as a promising scaffold for the development of selective A_{2B} AR antagonists.

GRAPHICAL ABSTRACT



ARTICLE INFO

Article history:

Received 1 March 2012

Received in revised form

18 May 2012

Accepted 23 May 2012

Available online 1 June 2012

Keywords:

Chromone carboxamides
Adenosine receptor ligands
SAR
ADME

ABSTRACT

A selected series of chromone carboxamides synthesized in our laboratory were evaluated by radioligand binding studies towards adenosine receptors. All the chromone-3-carboxamides (compounds **8–12**) exhibit A_{2B} receptor displacement percentage superior to 50%. The best results were obtained with phenolic substituents (compounds **9** and **12**) in the position 3 of pyrone ring with a K_i value of 2890 and 1350 nM. In addition, the predicted ADME properties for the chromone carboxamides under study are in accordance with the general requirements for the drug discovery and development process and in turn they have potential to emerge as a drug candidate.

In summary, N-phenylchromone-3-carboxamide may be proposed as a promising scaffold that can undergo optimization as a selective A_{2B} AR antagonist given its lower affinity for A_1 AR and A_{2A} AR. Accordingly, one can propose this new chromone class as a promising scaffold for tackling adenosine receptors, namely of A_{2B} subtype.

© 2012 Elsevier Masson SAS. All rights reserved.

1. Introduction

Adenosine is an endogenous extracellular purine nucleoside that modulates multiple vital physiological and pathophysiological processes, mainly through the interaction with four subtypes of cell-surface G-protein coupled adenosine receptors (ARs), named

A_1 , A_{2A} , A_{2B} and A_3 receptors [1,2]. A variety of physiological actions can be ascribed to adenosine including effects on heart rate and atrial contractility, vascular smooth muscle tone, release of neurotransmitters, lipolysis, renal, platelet and white blood cell functions [1,2]. Hence, selective AR modulators may hold therapeutic value in cardiovascular, neoplastic, chronic inflammatory and neurodegenerative disorders [1–4]. In fact, the importance of designing selective AR antagonists is boosted by recent findings of adenosine involvement in cancer and various CNS dysfunctions [5,6]. The medicinal chemistry, pharmacology and potential therapeutic applications of each subtype selective AR ligands have been extensively reviewed in recent years [7,8]. After more than three

* Corresponding author. Departamento de Química e Bioquímica, Faculdade de Ciências, Universidade do Porto, Rua Campo Alegre 687, 4169 007 Porto, Portugal. Tel.: +351 220 402 560; fax: +351 220 402 009.
E-mail address: fborges@fc.up.pt (F. Borges).

decades of research, a considerable number of selective agonists and antagonists of adenosine receptors have been discovered and clinically evaluated, despite that only few (e.g. Regadenoson) has been approved by FDA [7,9]. Main failure problems are related to side effects due to the ubiquity of the receptors or to low absorption, short half-life of compounds and toxicity of the ligands [7]. Among AR antagonists, several different types of xanthine-derived and nonxanthine-based heterocyclic structures have been identified although some phase I studies were stopped due to the high lipophilicity and because of absorption, distribution, metabolism, excretion limitations (ADME) [7].

Drug discovery process has changed dramatically over the past decade as there is an increasing demand to obtain more drug candidates and decrease attrition during drug development. Traditionally, drug discovery programs were driven solely by potency, regardless of the properties. As a result, the development of non-drug-like molecules was costly, had high risk and low success rate. Recent attention has focused on early detection of ADME properties allowing medicinal chemists to consider these properties at the same time as they are optimising potency [10–12]. Concurrently, despite the steady increase in R&D expenditures within the pharmaceutical industry, the number of new chemical entities (NCEs) reaching the market has actually decreased dramatically [13,14]. Therefore, privileged structures, such as indoles, arylpiperazines, biphenyls and benzopyranes (e.g. coumarins and chromones), are currently ascribed as supportive approaches in drug discovery that have been used successfully in medicinal chemistry programs to identify NCEs [15].

Benzopyrone has been recognized as a privileged structure and a fruitful approach to the discovery of novel biologically active molecules. Until now, numerous biological activities have been ascribed to this scaffold, namely anti-inflammatory or antitumoral and several CNS-targeted effects [16–20].

Therefore, a project focused on the discovery of NCEs that incorporate a simple benzo- γ -pyrone (chromen-4-one) substructure as AR ligands has been developed. Based on knowledge acquired so far no information on the development of putative adenosine receptor ligands based on this type of scaffold have been reported, except for the flavonoid family [21,22]. However, it must be pointed out that flavonoids are natural secondary metabolites that possess mandatorily a C6–C3–C6 skeleton, which include in the central part a chromone or chromane unit. The present chromone series possess some structural similarities with flavones, according to the biosynthetic classification, namely the presence of A and C rings, but the B ring directly linked to C ring is absent (Fig. 1).

Therefore, the aim of the present study is to identify novel adenosine receptor ligands based on chromone scaffold (Scheme 1). Drug efficacy and selectivity of the chromones towards A_1 , A_{2A} , A_{2B} and A_3 ARs and assessment of their drug-like properties were the guidelines in the present drug discovery process.

2. Results and discussion

2.1. Synthesis

Chromone carboxamides were obtained by functionalization of the chromone nucleus at positions C2 and C3 of the γ -pyrone ring and are briefly depicted in Scheme 1. The synthetic strategy has been patented [23,24]. Chromone carboxamide derivatives were synthesized straightforward, in moderate/high yields, by a one-pot condensation reaction, using BOP ((Benzotriazol-1-yloxy)tripyrrolidinophosphonium hexafluorophosphate) as a coupling reagent, that occurs between the corresponding chromone carboxylic acid (compounds **1** or **7**) and aniline (phenylamine) or its ring-substituted derivatives [25,26]. Dihydroxylated chromones **6** and **12** were obtained by a demethylation reaction with boron tribromide (BBr_3) of the monomethoxylated chromones **4** and **10**, respectively [27].

2.2. Binding assays and structure–affinity relationships

All chromone derivatives were tested to evaluate their affinity at hA_1 , hA_{2A} , hA_{2B} and hA_3 adenosine receptors. The displacement percentage values of the chromones derivatives at cloned adenosine receptors expressed in CHO (hA_1), HeLa cells (hA_{2A} and hA_3) and HEK-293 cells (hA_{2B}), are depicted in Fig. 2. The radioligands [3H]DPCPX, [3H]ZM241385 and [3H]NECA were used for A_1 and A_{2B} , A_{2A} , and A_3 receptors, respectively [28]. Assays were carried out by co-incubation of compounds, in at least six different concentrations, with the appropriate radioactive ligand. The affinity values of the compounds that did not fully displace specific radioligand binding at 10 μ M are given only in terms of displacement percentage (Fig. 2). For the compounds that exhibit displacement percentage values greater than 50% the inhibition constants (K_i) were calculated (see Table 1). The affinity of the reference ligands for each receptor was also performed under the same experimental conditions.

Despite the low or moderate affinity of the majority of the chromones under study to the adenosine receptors (Fig. 2) the SAR results obtained on this type of benzopyran scaffold suggest particular trends according to the type and position of the substituents positioned in the pyran nucleus. Chromone derivatives

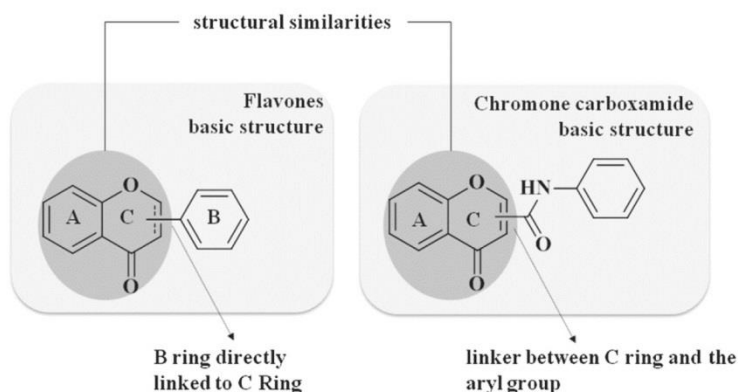
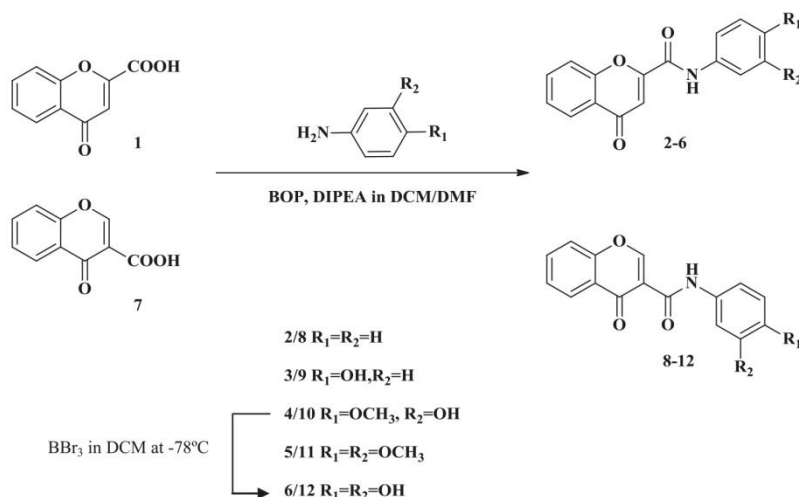


Fig. 1. Flavone and chromone carboxamide scaffolds.



Scheme 1. Synthetic strategy used for the obtention of chromone carboxamides. Abbreviations: BOP: (Benzotriazol-1-yloxy)tripyrrolidinophosphonium hexafluorophosphate); BBr₃: Boron tribromide solution (1.0 M in dichloromethane); DCM: dichloromethane; DIPEA: *N,N*-Diisopropylethylamine; DMF: *N,N*-Dimethylformamide.

with substituents in position 2 (compounds **1–6**) present higher affinity for A₁ and A₃ receptors, while derivatives with the same type of substituents in position 3 of the chromone scaffold present superior affinity to A_{2B} receptors (Fig. 2). The presence of a phenylcarboxamide substituent in the position 2 of the pyrone ring (compounds **2–6**), as a replacement for the carboxylic acid function (compound **1**), enhance the chromone affinity for all the receptors subtypes (Fig. 2). The presence of a hydroxyl group in *meta* position of the aromatic ring of the carboxamide side chain (compound **4**) seems to be significant for the affinity for A₁ and A₃AR. The presence of two methoxyl (compound **5**) or two hydroxyl groups (compound **6**) reduce the affinity for AR (Fig. 2). Compound **4** can be anticipated as promising hit compound for A₃AR. The activity of chromone-3-carboxamides is noticeably influenced by the aromatic pattern of the *N*-phenyl carboxamide substituent. All chromone-3-carboxamides (compounds **8–12**) display affinity, and selectivity, for A_{2B}AR, with a receptor displacement percentage greater than 50%. Compound **8** is approximately two times less

effective on A₃AR presenting about 3% affinity for A₁ and A_{2A}AR (see Fig. 2). From the data obtained it can be also concluded that the A_{2B}AR affinity binding can be modulated by introduction of substituents in the aromatic ring of the side chain (compounds **9–12**). Chromones with a hydroxyl in *para* position of the aryl exocyclic ring (compounds **9** and **12**) present the best affinity for A_{2B}AR with *K_i* values of 2890 and 1350 nM, respectively (Table 1).

The overall results suggest that chromone isomerism and that the type and position of the substituents in the phenyl side chain can be the starting point in the development of new and more selective adenosine ligands.

2.3. Theoretical evaluation of ADME properties

To better correlate the overall properties of the chromone compounds the lipophilicity, expressed as the octanol–water partition coefficient and herein called log*P*, was calculated using the Molinspiration property calculation program (see Table 2) [29].

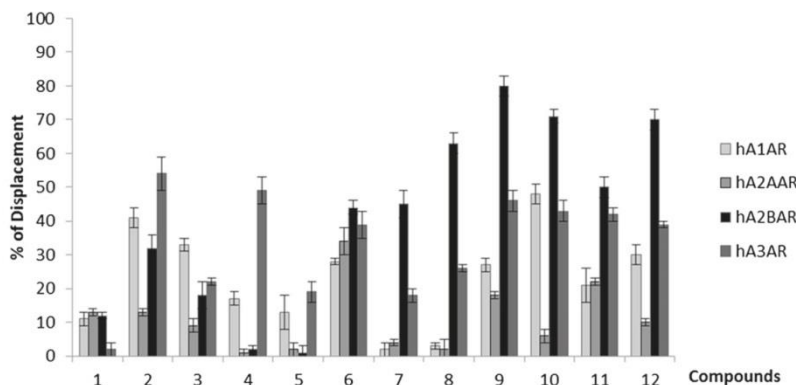
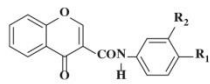


Fig. 2. Affinities of chromones carboxamides at adenosine A₁, A_{2A}, A_{2B} and A₃ receptors expressed as percentage displacement of specific binding at a concentration of 10 μM (A₁AR and A_{2B}AR: [³H]DPCPX; A_{2A}AR: [³H]ZM241385; A₃AR: [³H]NECA).

Table 1

Affinity binding data for chromone-3-carboxamides and control compound at $hA_{2B}AR$.



Compound	R ₁	R ₂	K _i (nM)
8	H	H	8510 ± 1420
9	OH	H	2890 ± 1210
10	OCH ₃	OH	5820 ± 2220
11	OCH ₃	OCH ₃	6390 ± 2160
12	OH	OH	1350 ± 320
MRS 1754			10.39

Table 2

Structural properties of the chromone derivatives^a.

Chromone compounds	logP	Molecular weight	TPSA	n-OH acceptors	n-OHNH donors	Volume
2/8	2.95/2.64	265.27	59.31	4	1	231.38
3/9	2.47/2.16	281.27	79.54	5	2	239.39
4/10	2.29/1.98	311.29	88.77	6	2	264.94
5/11	2.59/2.28	325.32	77.78	6	1	282.47
6/12	1.98/1.67	297.27	99.76	6	3	247.42

^a TPSA, topological polar surface area; n-OH, number of hydrogen acceptors; n-OHNH, number of hydrogen bond donors. The data was determined with Molinspiration calculation software.

From the data obtained, one can notice that all the chromone derivatives possess logP values compatible with those required to cross membranes.

In addition the theoretical prediction of ADME properties of all compounds was carried out (see Table 2). From the data obtained it can be observed that no violations of Lipinski's rule (molecular weight, logP, number of hydrogen donors and acceptors) were found making the chromone derivatives promising agents [30]. Topological polar surface area (TPSA), described to be a predictive indicator of membrane penetration, is also found to be positive for these potential drugs [31].

3. Conclusions

In summary, herein we report the discovery of a novel class of adenosine receptor ligands structurally based on chromone scaffold. On the basis of the obtained structure–affinity relationships chromone-3-carboxamides represent a novel class of AR ligands endowed with likeable affinities toward the $hA_{2B}AR$ subtype. These small molecules possess advantages against xanthine derivatives, classic model for the development of A_{2B} antagonists, since they do not present the metabolic drawbacks of this type of heterocyclic compounds. Till to date no A_{2B} antagonist ligand approved drug was discovered although the search for potent and selective ligands for the $A_{2B}AR$ subtype is still a hot topic. It has been demonstrated that this AR subtype regulates a number of biological functions (e.g., vascular tone, cytokine release, and angiogenesis).

Structure–affinity and ADME relationships evidenced that N-phenyl-4-oxo-4H-chromone-3-carboxamide as a promising lead structure that can undergo optimization as a selective $A_{2B}AR$ antagonist. In fact, the chromone carboxamides predicted ADME properties are in accordance with the general requirements of the drug discovery and development process. After lead optimization, in accordance with the drug discovery and development process on

the field of adenosine receptor ligands, the functional behavior of the most promising ligand will be determined.

Acknowledgements

This work was supported by the Foundation for Science and Technology (FCT), Portugal (projects PTDC/QUI/70359/2006 and PTDC/QUI–QUI/113687/2009). A. Gaspar (SFRH/BD/43531/2008), M.J. Matos (SFRH/BD/61262/2009) and F. Borges (SFRH/BSAB/1090/2010) thank FCT grants.

References

- B.B. Fredholm, A.P. Ijzerman, K.A. Jacobson, J. Linden, C.E. Müller, International union of basic and clinical pharmacology. LXXXI. Nomenclature and classification of adenosine receptors—an update, *Pharmacol. Rev.* 63 (2011) 1–34.
- C.E. Müller, K.A. Jacobson, Recent developments in adenosine receptor ligands and their potential as novel drugs, *Biochim. Biophys. Acta* 1808 (2011) 1290–1308.
- K.A. Jacobson, Introduction to adenosine receptors as therapeutic targets, in: C.N. Wilson, S.J. Mustafa (Eds.), *Adenosine Receptors in Health and Disease*, Springer Berlin Heidelberg, 2009, pp. 1–24.
- P.G. Baraldi, B. Cacciari, R. Romagnoli, S. Merighi, K. Varani, P.A. Borea, G. Spalluto, A3 adenosine receptor ligands: history and perspectives, *Med. Res. Rev.* 20 (2000) 103–128.
- S. Gessi, S. Merighi, V. Sacchetti, C. Simioni, P.A. Borea, Adenosine receptors and cancer, *Biochim. Biophys. Acta* 1808 (2011) 1400–1412.
- K. Varani, F. Vincenzi, A. Tosi, S. Gessi, I. Casetta, G. Granieri, P. Fazio, E. Leung, S. MacLennan, E. Granieri, P.A. Borea, A2A adenosine receptor overexpression and functionality, as well as TNF- α levels, correlate with motor symptoms in Parkinson's disease, *FASEB J.* 24 (2010) 587–598.
- P.G. Baraldi, M.A. Tabrizi, S. Gessi, P.A. Borea, Adenosine receptor antagonists: translating medicinal chemistry and pharmacology into clinical utility, *Chem. Rev.* 108 (2008) 238–263.
- T.W. Stone, S. Ceruti, M.P. Abbraccio, Adenosine receptors and neurological disease: neuroprotection and neurodegeneration, in: C.N. Wilson, S.J. Mustafa (Eds.), *Adenosine Receptors in Health and Disease*, Springer Berlin Heidelberg, 2009, pp. 535–587.
- P. Fishman, S. Bar-Yehuda, M. Synowitz, J.D. Powell, K.N. Klotz, S. Gessi, P.A. Borea, in: C.N. Wilson, S.J. Mustafa (Eds.), *Adenosine Receptors and Cancer*, Springer Berlin Heidelberg, 2009, pp. 399–441.
- G.W. Caldwell, Z. Yan, W. Tang, M. Dasgupta, B. Hasting, ADME optimization and toxicity assessment in early- and late-phase drug discovery, *Curr. Top. Med. Chem.* 9 (2009) 965–980.
- H. Zhao, Z. Guo, Medicinal chemistry strategies in follow-on drug discovery, *Drug Discov. Today* 14 (2009) 516–522.
- J. Wang, S. Skolnik, Recent advances in physicochemical and ADMET profiling in drug discovery, *Chem. Biodiv.* 6 (2009) 1887–1899.
- P.G. Wyatt, The emerging academic drug-discovery sector, *Future Med. Chem.* 1 (2009) 1013–1017.
- L.F. Raveglia, G.A. Giardina, Accelerating the drug-discovery process: new tools and technologies available to medicinal chemists, *Future Med. Chem.* 1 (2009) 1019–1023.
- L.J.S. Knutsen, Drug discovery management, small is still beautiful: why a number of companies get it wrong, *Drug Discov. Today* 16 (2011) 476–484.
- A. Gaspar, J. Reis, A. Fonseca, N. Milhazes, D. Vina, E. Uriarte, F. Borges, Chromone 3-phenylcarboxamides as potent and selective MAO-B inhibitors, *Bioorg. Med. Chem. Lett.* 21 (2011) 707–709.
- G.P. Ellis, Chromenes, chromanones, and chromones—Introduction, in: *Chemistry of Heterocyclic Compounds*, John Wiley & Sons, Inc., 2008, pp. 1–10.
- M.P. Ishar, G. Singh, S. Singh, K.K. Sreenivasan, Design, synthesis, and evaluation of novel 6-chloro-/fluorochromone derivatives as potential topoisomerase inhibitor anticancer agents, *Bioorg. Med. Chem. Lett.* 16 (2006) 1366–1370.
- F. Chimenti, R. Fioravanti, A. Bolasco, P. Chimenti, D. Secci, F. Rossi, M. Yanez, F. Orallo, F. Ortuso, S. Alcaro, R. Cirilli, R. Ferretti, M.L. Sanna, A new series of flavones, thioflavones, and flavanones as selective monoamine oxidase-B inhibitors, *Bioorg. Med. Chem.* 18 (2010) 1273–1279.
- F. Chimenti, D. Secci, A. Bolasco, P. Chimenti, B. Bizzarri, A. Granese, S. Carradori, M. Yanez, F. Orallo, F. Ortuso, S. Alcaro, Synthesis, molecular modeling, and selective inhibitory activity against human monoamine oxidases of 3-carboxamido-7-substituted coumarins, *J. Med. Chem.* 52 (2009) 1935–1942.
- Y. Karton, J.L. Jiang, X.D. Ji, N. Melman, M.E. Olah, G.L. Stiles, K.A. Jacobson, Synthesis and biological activities of flavonoid derivatives as A3 adenosine receptor antagonists, *J. Med. Chem.* 39 (1996) 2293–2301.
- X.D. Ji, N. Melman, K.A. Jacobson, Interactions of flavonoids and other phytochemicals with adenosine receptors, *J. Med. Chem.* 39 (1996) 781–788.

- [23] M.F.M. Borges, A.M.N. Gaspar, J.M.P.J. Garrido, N.J.S.P. Milhazes, M.C.C. Batoreu, WO2008104925A1 and PT103665.
- [24] M.F.M. Borges, A.M.N. Gaspar, J.M.P.J. Garrido, N.J.S.P. Milhazes, E. Uriarte, M. Yáñez, F. Orallo, PT104487, 2009.
- [25] A. Gaspar, F. Teixeira, E. Uriarte, N. Milhazes, A. Melo, M.N. Cordeiro, F. Ortuso, S. Alcaro, F. Borges, Towards the discovery of a novel class of monoamine oxidase inhibitors: structure-property-activity and docking studies on chromone amides, *ChemMedChem* 6 (2011) 628–632.
- [26] The 2-carboxychromone (1) or 3-carboxychromone (7) (2.63 mmol; 0.50 g) was dissolved in DMF (6 mL) and DIPEA (0.37 mL). The solution was cooled at 0 °C (ice water bath) and a solution of BOP (2.63 mmol; 1.16 g) in CH₂Cl₂ (6 mL) was added. The mixture is stirred at the mentioned temperature during 30 min. After then the corresponding amine was added (phenylamine, 4-hydroxyphenylamine, 3-hydroxy-4-methoxyphenylamine or 3,4-dimethoxyphenylamine). The temperature was gradually increased to room temperature being the reaction kept, with stirring, for 4 h. The crude material was then purified by flash chromatography, using the most suitable elution system for each compound (normally acetyl acetate or acetyl acetate/dichloromethane 5:5). The appropriate fractions were combined and the solvent evaporated under reduced pressure. Then, if found necessary, mixed solvent recrystallization was used to purify the product. *N*-(4-Hydroxyphenyl)-4-oxo-4H-1-benzopyran-2-carboxamide (3): Yield: 51%; MP: 277–281 °C; ¹H NMR: δ = 6.80 (2H, *d*, *J* = 8.9 H(3'), H(5')), 6.95 (1H, *s*, H(3')), 7.57 (1H, *ddd*, *J* = 7.9; 7.0; 1.1 H(6')), 7.58 (2H, *d*, *J* = 8.8 H(2'), H(6')), 7.84 (1H, *d*, *J* = 8.0 H(8')), 7.94 (1H, *ddd*, *J* = 8.5; 7.0; 1.6 H(7')), 8.09 (1H, *dd*, *J* = 7.9; 1.4 H(5')), 10.60 (1H, *s*, NH), MS/El *m/z* (%): 282 (18), 281 (M+•, 100), 280 (23), 146 (51), 108 (25), 105 (17), 89 (22). *N*-(3-Hydroxy-4-methoxyphenyl)-4-oxo-4H-1-benzopyran-2-carboxamide (4): Yield: 57%; MP: 266–267 °C; ¹H NMR: δ = 3.78 (3H, *s*, OCH₃), 6.95 (1H, *s*, H(3')), 6.96 (1H, *d*, *J* = 8.8 H(5')), 7.18 (1H, *dd*, *J* = 8.8; 2.5 H(6')), 7.36 (1H, *d*, *J* = 2.5 H(2')), 7.57 (1H, *ddd*, *J* = 8.0; 6.8; 1.2 H(6')), 7.85 (1H, *d*, *J* = 7.5 H(8')), 7.94 (1H, *ddd*, *J* = 8.5; 7.0; 1.6 H(7')), 8.09 (1H, *dd*, *J* = 7.9; 1.6 H(5')), 9.23 (1H, *s*, 3'-OH), 10.55 (1H, *s*, NH), MS/El *m/z* (%): 312 (18), 311 (M+•, 100), 310 (54), 268 (36), 207 (26), 145 (15), 89 (31). *N*-(3,4-Dimethoxyphenyl)-4-oxo-4H-1-benzopyran-2-carboxamide (5): Yield: 45%; MP: 196–198 °C; ¹H NMR: δ = 3.77, 3.79 (6H, 2s, 2 × OCH₃), 6.97 (1H, *s*, H(3')), 7.01 (1H, *d*, *J* = 8.7 H(5')), 7.40 (1H, *dd*, *J* = 8.7; 2.4 H(6')), 7.48 (1H, *d*, *J* = 2.4 H(2')), 7.58 (1H, *ddd*, *J* = 8.0; 6.8; 1.2 H(6')), 7.86 (1H, *d*, *J* = 7.7 H(8')), 7.95 (1H, *ddd*, *J* = 8.5; 7.0; 1.6 H(7')), 8.10 (1H, *dd*, *J* = 8.0; 1.5 H(5')), 10.66 (1H, *s*, NH), MS/El *m/z* (%): 326 (20), 325 (M+•, 100), 310 (21), 308 (15), 173 (24), 145 (22), 89 (37). *N*-(4-Hydroxyphenyl)-4-oxo-4H-1-benzopyran-3-carboxamide (9): Yield: 55%; MP: 290–293 °C; ¹H NMR: δ = 6.96 (2H, *m*, H(3'), H(5')), 7.38–7.32 (2H, *m*, H(6'), H(8')), 7.50 (2H, *d*, *J* = 8.6 H(2'), H(6')), 7.98 (1H, *d*, *J* = 7.3 H(5')), 7.73–7.68 (1H, *m*, H(7')), 9.87/9.83 (1H, *s*, OH), 8.71/8.76 (1H, *s*, H(2')), 11.85/13.53 (1H, *s*, NH), MS/El *m/z* (%): 282 (19), 281 (M+•, 100), 207 (29), 121 (15), 58 (21). *N*-(3-Hydroxy-4-methoxyphenyl)-4-oxo-4H-1-benzopyran-3-carboxamide (10): Yield: 45%; MP: 255–257 °C; ¹H NMR: δ = 3.81 (3H, *s*, OCH₃), 7.08–6.99 (3H, *m*, H(2'), H(5') H(6')), 7.38–7.32 (2H, *m*, H(6'), H(8')), 7.99 (1H, *d*, *J* = 7.7 H(5')), 7.73–7.68 (1H, *m*, H(7')), 8.72/8.68 (1H, *s*, H(2')), 9.55 (1H, *s*, OH), 11.78/13.42 (1H, *s*, NH), MS/El *m/z* (%): 312 (19), 311 (M+•, 100), 296 (31), 207 (15), 176 (15), 121 (38). *N*-(3,4-Dimethoxyphenyl)-4-oxo-4H-1-benzopyran-3-carboxamide (11): Yield: 50%; MP: 248–254 °C; ¹H NMR: δ = 3.77 (3H, *s*, 3'-OCH₃), 3.85 (3H, *s*, 4'-OCH₃), 7.01 (1H, *d*, *J* = 8.6 H(5'), H(6')), 7.14 (1H, *dd*, *J* = 8.6; 1.6 H(5')), 7.37–7.30 (3H, *m*, H(6'), H(8'), H(2')), 7.73–7.68 (1H, *m*, H(7')), 7.96 (1H, *d*, *J* = 7.7 H(5')), 8.86/8.83 (1H, *s*, H(2')), 11.82/13.58 (1H, *s*, NH), MS/El *m/z* (%): 326 (21), 325 (M+•, 100), 311 (10), 310 (63), 207 (60), 173 (62), 121 (17), 93 (20), 79 (15), 77 (15).
- [27] A. Gaspar, T. Silva, M. Yáñez, D. Vina, F. Orallo, F. Ortuso, E. Uriarte, S. Alcaro, F. Borges, Chromone, a privileged scaffold for the development of monoamine oxidase inhibitors, *J. Med. Chem.* 54 (2011) 5165–5173.
- [28] Biological assay procedures: (i) A₁ receptor assay: a radioligand binding assay was performed in membranes from CHO transfected cells with human A₁AR, using [³H]DPCPX as specific radioligand for this type of receptors; (ii) A_{2B} receptor assay: a radioligand binding assay was performed in membranes from HEK 293 transfected cells with human A_{2B} receptor, using [³H]DPCPX as a specific radioligand for this type of receptors; (iii) A_{2A} receptor assay: a radioligand binding assay was performed in membranes from HeLa transfected cells with human A_{2A} receptor, using [³H]ZM241385 as a specific radioligand for this type of receptors; (iv) A₃ receptor assay: a radioligand binding assay was performed in membranes from HeLa transfected cells with human A₃ receptor, using [³H]NECA as a specific radioligand for this type of receptors. For details see V. Yaziji, D. Rodríguez, H. Gutiérrez-de-Terán, A. Coelho, O. Caamaño, X. García-Mera, J. Brea, M.I. Loza, M.I. Cadavid, E. Sotelo, Pyrimidine derivatives as potent and selective A₃ adenosine receptor antagonists, *J. Med. Chem.* 54 (2011) 457–471.
- [29] M cheminformatics, Bratislava, Slovak Republic, <http://www.molinspiration.com/services/properties.html> (2009).
- [30] C.A. Lipinski, F. Lombardo, B.W. Dominy, P.J. Feeney, Experimental and computational approaches to estimate solubility and permeability in drug discovery and development settings, *Adv. Drug Deliv. Rev.* 23 (1997) 3–25.
- [31] P. Ertl, B. Rohde, P. Selzer, Fast calculation of molecular polar surface area as a sum of fragment-based contributions and its application to the prediction of drug transport properties, *J. Med. Chem.* 43 (2000) 3714–3717.

3.6 Discovery of novel A3 adenosine receptor ligands based on chromone scaffold

Article reprinted from Biochemical Pharmacology (2012), 84: 21–29.



Contents lists available at SciVerse ScienceDirect

Biochemical Pharmacology

journal homepage: www.elsevier.com/locate/biochempharm



Discovery of novel A₃ adenosine receptor ligands based on chromone scaffold

Alexandra Gaspar^a, Joana Reis^a, Sonja Kachler^c, Silvia Paoletta^d, Eugenio Uriarte^{a,b,c,d}, Karl-Norbert Klotz^c, Stefano Moro^d, Fernanda Borges^{a,*}

^a CIQUP/Departamento de Química e Bioquímica, Faculdade de Ciências, Universidade do Porto, 4169-007 Porto, Portugal

^b Departamento de Química Orgánica, Facultad de Farmacia, Universidad de Santiago de Compostela, 15782 Santiago de Compostela, Spain

^c Institut für Pharmakologie und Toxikologie, Universität Würzburg, 97078 Würzburg, Germany

^d Molecular Modeling Section (MMS), Dipartimento di Scienze Farmaceutiche, Università di Padova, via Marzolo 5, I-35131 Padova, Italy

ARTICLE INFO

Article history:

Received 27 January 2012

Accepted 9 March 2012

Available online 17 March 2012

Keywords:

Drug discovery

Adenosine receptor ligand

Chromone scaffold

ABSTRACT

A project focused on the discovery of new chemical entities (NCEs) as AR ligands that incorporate a benzo- γ -pyrone [(4H)-1-benzopyran-4-one] substructure has been developed. Accordingly, two series of novel chromone carboxamides placed at positions C2 (compounds **2–13**) and C3 (compounds **15–26**) of the γ -pyrone ring were synthesized using chromone carboxylic acids (compounds **1** or **14**) as starting materials. From this study and on the basis of the obtained structure–activity relationships it was concluded that the chromone carboxamide scaffold represent a novel class of AR ligands. The most remarkable chromones were compounds **21** and **26** that present a better affinity for A₃AR (K_i = 3680 nM and K_i = 3750 nM, respectively). Receptor-driven molecular modeling studies provide information on the binding/selectivity data of the chromone. The data so far acquired are instrumental for future optimization of chromone carboxamide as a selective A₃AR antagonist.

© 2012 Elsevier Inc. All rights reserved.

1. Introduction

Cancer is a very complex disease, linked with different initiating causes, cofactors and promoters, and several types of cellular damage. Advancing knowledge on the cellular and molecular biology of the processes that regulate cell proliferation, cell differentiation and cellular responses to external signals provide a wealth of information about the biochemistry and biology of the

cancer cell and how it differs from a normal one [1]. Accordingly, a number of potential targets as well as the development of a new generation of anticancer agents must be exploited, based on the differences between normal and cancer cells [2].

During the last decade different approaches to treating cancer have been developed based mainly on specific targets that are mostly expressed in tumor but not in normal cells [2]. Interestingly, it was already shown that adenosine receptor (AR) levels in various tumor cells are up regulated, a finding which may suggest that a specific AR may serve as a biological marker and as a target for specific ligands leading to cell growth inhibition [3]. In particular, the human A₃ AR, which is the most recently identified adenosine receptor, is involved in a variety of important physiological processes that include inflammation, cell growth and immunosuppression [4–7].

There have been many attempts to design and develop A₃ AR agonists and antagonists, and over the past decade, the search for ligands that show selectivity toward individual receptor subtypes has intensified as their role in many therapeutic areas expands [4,8,9]. Despite the intense discovery efforts the overall process has failed to deliver selective (agonists or antagonists) drug candidates, with exception of CF102 (1-[2-chloro-6-[[[3-(iodophenyl)methyl]amino]-9H-purin-9-yl]-1-deoxy-N-methyl- β -D-ribofuran uronamide, Cl-IB-MECA) that is in clinical trials [4,10,11]. Main problems include side effects due to the ubiquity of the receptors or to low absorption, short half-life and toxicity of the ligands [10]. These facts prompted an intensive research effort

Abbreviations: [³H]CCPA, [³H](2R,3R,4S,5R)-2-[2-chloro-6-(cyclopentylamino)-purin-9-yl]-5-(hydroxymethyl)oxolane-3,4-diol; [³H]HEMADO, [³H] 2-(1-Hexynyl)-N⁶-methyladenosine; [³H]NECA, [³H]adenosine-5'-(N-ethylcarboxamide); AR, Adenosine receptor; Arg, arginine; Asn, asparagine; Asp, aspartic acid; BBr₃, boron tribromide; BOP, (benzotriazol-1-yloxy)tris(dimethylamino)phosphonium hexafluorophosphate; CHO, Chinese hamster ovary cells; Cys, cysteine; DAD, diode-array detector; DIPEA, N,N-diisopropylethylamine; DMF, dimethylformamide; EI-MS, electron impact mass spectra; Glu, glutamic acid; HPLC, high performance liquid chromatography; Ile, isoleucine; K_i, inhibition constant; Leu, leucine; MOE, molecular operating environment; MOPAC, molecular orbital PACKage; NCE, new chemical entity; NMR, nuclear magnetic resonance; PLANTS, protein-Ligand ANT System; Phe, phenylalanine; Pro, proline; PyBOP, benzotriazol-1-yloxytripyrrolidinophosphonium hexafluorophosphate; R-PIA, N-R-N⁶-(1-methyl-2-phenylethyl)adenosine; SAR, structure–affinity relationship; TLC, thin layer chromatography; TMS, tetramethylsilane; Trp, tryptophan; Tyr, tyrosine; UV, ultraviolet; ZM241385, 4-(2-[7-Amino-2-(2-furyl)]1,2,4-triazolo[2,3-a][1,3,5]triazin-5-ylamino)ethylphenol.

* Corresponding author at: CIQUP/Department of Chemistry and Biochemistry, Faculty of Sciences, University of Porto, Porto 4169-007, Portugal.

Tel.: +351 220402560.

E-mail address: fborges@fc.up.pt (F. Borges).

toward the development of novel, selective and potent AR receptor ligands suitable for chemotherapeutic purposes.

Concurrently, despite the steady increase in R&D expenditures within the pharmaceutical industry, the number of new chemical entities (NCEs) reaching the market has actually decreased dramatically. Therefore, privileged structures, such as indoles, arylpiperazines, biphenyls and benzopyranes (e.g. coumarins and chromones), are currently considered as potentially successful approaches in drug discovery and have been used successfully before in medicinal chemistry programs to identify NCEs [12].

Accordingly, a project focused on the discovery of NCEs as AR ligands that incorporate a benzo- γ -pyrone [(4*H*)-1-benzopyran-4-one] substructure has been developed. Based on knowledge acquired so far no information on the development of putative adenosine ligands based on this type of scaffold have been reported, concerning the flavonoid family. However, flavonoids are natural secondary metabolites that possess a C6–C3–C6 skeleton. The present chromone series possess some structural similarities with flavones, namely the presence of A and C rings, but the B ring is absent.

Therefore, the aim of the present study is the design and synthesis of a library of novel adenosine receptor ligands based on the chromone scaffold that was obtained through the application of innovative synthetic strategies (Scheme 1) [13]. Lead discovery of new AR ligands based on a chromone scaffold guided by structure–affinity–relationships (SAR) and molecular modeling is the aim of the present work.

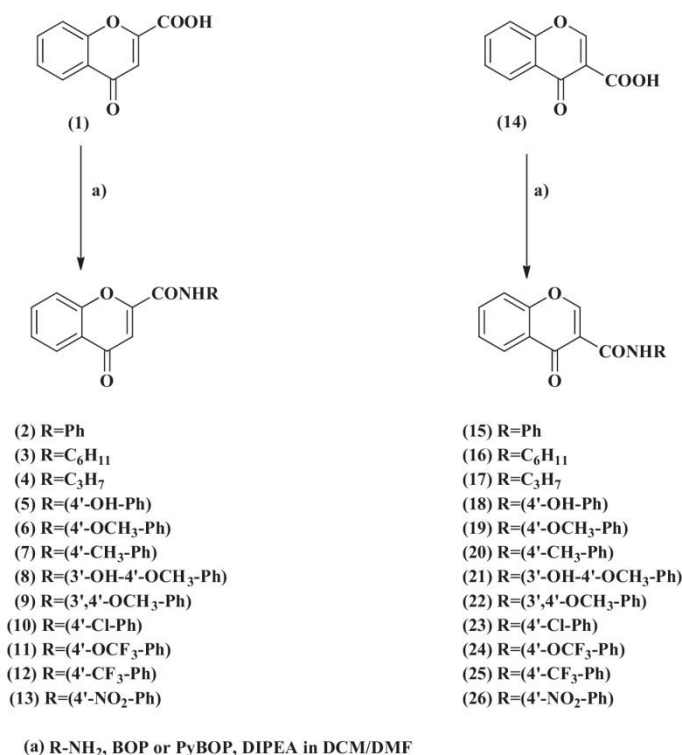
2. Materials and methods

2.1. Materials

Chromone-2-carboxylic acid and chromone-3-carboxylic acid, (benzotriazol-1-yloxy)tris(dimethylamino)phosphonium hexafluorophosphate (BOP), benzotriazol-1-yloxytripyrrolidinophosphonium hexafluorophosphate (PyBOP), *N,N*-diisopropylethylamine (DIPEA), dimethylformamide (DMF), boron tribromide (BBr₃), aniline and its derivatives were purchased from Sigma–Aldrich Química S.A. (Sintra, Portugal). All other reagents and solvents were *pro analysis* grade and were acquired from Merck (Lisbon, Portugal) and used without additional purification.

Thin-layer chromatography (TLC) was carried out on pre-coated silica gel 60 F254 (Merck, Lisbon, Portugal) with layer thickness of 0.2 mm. For analytical control the following systems were used: ethyl acetate/petroleum ether, ethyl acetate/methanol, chloroform/methanol in several proportions. The spots were visualized under UV detection (254 and 366 nm) and iodine vapor. Normal-phase column chromatography was performed using silica gel 60 0.2–0.5 or 0.040–0.063 mm (Merck, Lisbon, Portugal).

The purity of the final products (>97% purity) was verified by high-performance liquid chromatography (HPLC) equipped with a UV detector. Chromatograms were obtained in an HPLC/DAD system, a Jasco instrument (pumps model 880-PU and solvent mixing model 880-30, Tokyo, Japan), equipped with a commercially prepacked Nucleosil RP-18 analytical column (250 mm × 4.6 mm, 5 μ m, Macherey–Nagel, Duren, Germany), and UV detection (Jasco



Scheme 1. Structure of the chromone carboxamides under study.

model 875-UV) at the maximum wavelength of 254 nm. The mobile phase consisted of a methanol/water or acetonitrile/water (gradient mode, room temperature) at a flow rate of 1 mL/min. The chromatographic data was processed in a Compaq computer, fitted with CSW 1.7 software (DataApex, Czech Republic). ^1H NMR data were acquired, at room temperature, on a Bruker AMX 300 spectrometer operating at 300.13 MHz, respectively. Dimethylsulfoxide- d_6 was used as a solvent; chemical shifts are expressed in δ (ppm) values relative to tetramethylsilane (TMS) as internal reference; coupling constants (J) are given in Hz. Electron impact mass spectra (EI-MS) were carried out on a VG AutoSpec instrument; the data are reported as m/z (% of relative intensity of the most important fragments). Melting points were obtained on a Stuart Scientific SMP1 apparatus and are uncorrected.

2.2. Synthesis of chromone carboxamide derivatives

General procedure: 2-Carboxychromone (**1**) or 3-carboxychromone (**14**) (0.50 g; 2.63 mmol) was dissolved in DMF (6 mL) and of DIPEA (0.37 mL). The solution was then cooled at 0 °C in an ice-water bath, and a BOP (1.16 g; 2.63 mmol) or PyBOP (1.37 g; 2.63 mmol) solution in CH_2Cl_2 (6 mL) was added. The mixture was stirred during 30 min. After, the phenylamine derivative was added in equimolar amount. The temperature was gradually increased to room temperature. The reaction was stirred for additional 4 h. Following the workup and after extraction, the organic phases were dried over Na_2SO_4 . Solutions were decolorized with activated charcoal, when necessary. The recrystallization solvents were ethyl acetate or ethyl ether/n-hexane.

2.2.1. *N*-(4-Methoxyphenyl)-4-oxo-4H-1-benzopyran-2-carboxamide (**6**)

Yield: 85%; MP: 214–223 °C; ^1H NMR (CDCl_3): 3.83 (3H, s, OCH_3), 6.94 (2H, d, $J = 9.2$, H(3'), H(5')), 7.27 (1H, s, H(3)), 7.49 (1H, ddd, $J = 8.0$; 7.2; 1.0, H(6)), 7.59–7.64 (3H, m, H(8), H(2'), H(6')), 7.78 (1H, ddd, $J = 8.5$; 7.1; 1.6, H(7)), 8.25 (1H, dd, $J = 8.0$, 1.6, H(5)), 8.53 (1H, s, NH). MS/EI m/z (int.rel.): 296 (14), 295 (M^+ , 100), 294 (30), 266 (15), 173 (13), 145 (10), 122 (68), 95 (17), 89 (22), 71 (10), 69 (11), 57 (15).

2.2.2. *N*-(4-Methylphenyl)-4-oxo-4H-1-benzopyran-2-carboxamide (**7**)

Yield: 56%; MP: 233–237 °C; ^1H NMR [$(\text{CD}_3)_2\text{SO}$]: 2.30 (3H, s, CH_3), 6.97 (1H, s, H(3)), 7.23 (2H, d, $J = 8.2$, H(3'), H(5')), 7.57 (1H, ddd, $J = 7.9$, 7.0, 1.0, H(6)), 7.69 (2H, d, $J = 8.3$, H(2'), H(6')), 7.85 (1H, dd, $J = 8.5$, 1.0, H(8)), 7.93 (1H, ddd, $J = 8.5$, 7.0, 1.5, H(7)), 8.08 (1H, dd, $J = 8.0$, 1.4, H(5)), 10.68 (1H, s, NH); MS/EI m/z (int.rel.): 280 (32), 279 (M^+ , 100), 278 (94), 264 (10), 262 (29), 251 (11), 250 (46), 233 (14), 158 (17), 107 (10), 106 (35), 89 (53), 79 (14), 77 (20).

2.2.3. *N*-(3,4-Dimethoxyphenyl)-4-oxo-4H-1-benzopyran-2-carboxamide (**9**)

Yield: 45%; MP: 196–198 °C; ^1H NMR [$(\text{CD}_3)_2\text{SO}$]: 3.77/3.79 (6H, 2 s, 2 \times OCH_3), 6.97 (1H, s, H(3)), 7.01 (1H, d, $J = 8.7$, H(5')), 7.40 (1H, dd, $J = 8.7$; 2.4, H(6')), 7.48 (1H, d, $J = 2.4$, H(2')), 7.58 (1H, ddd, $J = 8.0$, 6.8, 1.2, H(6)), 7.86 (1H, d, $J = 7.7$, H(8)), 7.95 (1H, ddd, $J = 8.5$, 7.0, 1.6, H(7)), 8.10 (1H, dd, $J = 8.0$, 1.5, H(5)), 10.66 (1H, s, NH); MS/EI m/z (int.rel.): 326 (20), 325 (M^+ , 100), 310 (21), 308 (15), 173 (24), 145 (22), 89 (37).

2.2.4. *N*-(4-Methoxyphenyl)-4-oxo-4H-1-benzopyran-3-carboxamide (**19**)

Yield: 55%; MP: 173–177 °C; ^1H NMR (CDCl_3): 3.84 (3H, s, OCH_3), 6.98 (2H, d, $J = 9.0$, H(3'), H(5')), 7.25–7.32 (4H, m, H(6), H(8), H(2'), H(6')), 7.59 (1H, ddd, $J = 8.6$, 6.9, 1.7, H(7)), 8.06/8.14 (1H, dd, $J = 7.8$, 1.6, H(5)), 8.80/8.94 (1H, s, H(2)), 11.95/13.76 (1H, s,

NH), 13.76 (0.7H, s, NH); MS/EI m/z (int.rel.): 296 (55), 295 (M^+ , 100), 280 (27), 252 (21), 174 (22), 173 (94), 147 (18), 132 (14), 121 (37), 92 (14), 77 (12).

2.2.5. *N*-(4-Methylphenyl)-4-oxo-4H-1-benzopyran-3-carboxamide (**20**)

Yield: 44%; MP: 179–182 °C; ^1H NMR (CDCl_3): 2.39 (3H, s, CH_3), 7.23–7.32 (6H, m, H(6), H(8), H(2'), H(3'), H(5'), H(6')), 7.60 (1H, ddd, $J = 8.6$, 7.0, 1.6, H(7)), 8.07/8.14 (1H, dd, $J = 7.8$, 1.6, H(5)), 8.86/8.99 (1H, s, H(2)), 11.92/13.69 (1H, s, NH); MS/EI m/z (int.rel.): 280 (57), 279 (M^+ , 99), 278 (21), 250 (10), 174 (24), 173 (100), 159 (16), 158 (23), 131 (37), 130 (44), 121 (44), 92 (11), 91 (24), 77 (12), 65 (20).

2.2.6. *N*-(3,4-Dimethoxyphenyl)-4-oxo-4H-1-benzopyran-3-carboxamide (**22**)

Yield: 50%; MP: 248–254 °C; ^1H NMR (CDCl_3): 3.77 (3H, s, 3'- OCH_3), 3.85 (3H, s, 4'- OCH_3), 7.01 (1H, d, $J = 8.6$, H(6')), 7.14 (1H, dd, $J = 8.6$, 1.6, H(5')), 7.37–7.30 (3H, m, H(6), H(8), H(2')), 7.73–7.68 (1H, m, H(7)), 7.96 (1H, d, $J = 7.7$, H(5)), 8.86/8.83 (1H, s, H(2)), 11.82/13.58 (1H, s, NH), 13.58 (0.7 H, s, NH); MS/EI m/z (int.rel.): 326 (21), 325 (M^+ , 100), 311 (10), 310 (63), 207 (60), 173 (62), 121 (17), 93 (20), 79 (15), 77 (15).

The structural elucidation of the other carboxamides was described elsewhere [14,15].

2.3. Radioligand binding assays

2.3.1. CHO membrane preparation

All the pharmacological methods including in membrane preparation for radioligand binding experiments followed the procedures as described earlier [16].

Membranes for radioligand binding were prepared from cells stably transfected with the human adenosine receptor subtypes (A_1 , A_{2A} , and A_3 expressed on CHO cells) in a two-step procedure. In the first low-speed step ($1000 \times g$ for 4 min), the cell fragments and nuclei were removed. After that, the crude membrane fraction was sedimented from the supernatant at $100,000 \times g$ for 30 min. The membrane pellet was then resuspended in the specific buffer used for the respective binding experiments, frozen in liquid nitrogen, and stored at -80°C . For the measurement of the adenylyl cyclase activity in A_{2B} receptor expressed on CHO cells, only one step of centrifugation was used in which the homogenate was sedimented for 30 min at $54,000 \times g$. The resulting crude membrane pellet was resuspended in 50 mM Tris-HCl, pH 7.4 and immediately used for the adenylyl cyclase assay.

2.3.2. Human cloned A_1 , A_{2A} , A_3 adenosine receptor binding assay

Binding of [^3H]CCPA (2-chloro- N^6 -cyclopentyladenosine, GE Healthcare, Freiburg, Germany) to CHO cells transfected with the human recombinant A_1 adenosine receptor was performed as previously described [16]. Competition experiments were performed for 3 h at 25 °C in 200 μL of buffer containing 1 nM [^3H]CCPA, 0.2 U/mL adenosine deaminase, 20 μg of membrane protein in 50 mM Tris/HCl, pH 7.4 and tested compound in different concentrations. Nonspecific binding was determined in the presence of 1 mM theophylline and amounted to <5% of total binding [16].

Binding of [^3H]NECA (*N*-ethylcarboxamidoadenosine, GE Healthcare, Freiburg, Germany) to CHO cells transfected with the human recombinant A_{2A} adenosine receptors was performed following the conditions as described for the A_1 receptor binding [16]. In the competition experiments, samples containing a protein amount of 50 μg , 30 nM [^3H]NECA and tested compound in different concentrations were incubated for 3 h at 25 °C. Nonspecific binding was determined in the presence of 100 μM R-PIA (R-N 6 -phenylisopropyladenosine) and represented about 50% of total binding [16].

Binding of [³H]HEMADO (2-(1-hexynyl)-N-methyladenosine, Tocris, Bristol, UK) to CHO cells transfected with the human recombinant A₃ adenosine receptors was carried out as previously described [16,17].

The competition experiments were performed for 3 h at 25 °C in buffer solution containing 1 nM [³H]HEMADO, 20 µg membrane protein in 50 mM Tris–HCl, 1 mM EDTA (ethylenediaminetetraacetate), 10 mM MgCl₂, pH 8.25 and tested compound in different concentrations. Nonspecific binding was determined in the presence of 100 µM R-PIA and was below 2% of total binding [17].

All incubations were done in 96 well microplates with filter bottoms allowing for separation of bound and free ligand by filtration. Membranes with bound ligand were washed with icecold buffer to remove unbound ligand [16,17]. K_i values from competition experiments were calculated with the program SCTFIT [19] and are reported as geometric means of at least three independent experiments with 95% confidence limits [16,17].

2.3.3. Adenylyl cyclase activity

Because of the lack of a suitable radioligand for hA_{2B} receptor in binding assay, the potency of antagonists at A_{2B} receptor (expressed on CHO cells) was determined in adenylyl cyclase experiments instead. The procedure was carried out as described previously with minor modifications [16]. Membranes were incubated with about 150,000 cpm of [α-³²P]ATP (Hartmann-Analytic, Braunschweig, Germany) for 20 min in the incubation mixture as described [16] without EGTA and NaCl. For agonists, the EC₅₀ values for the stimulation of adenylyl cyclase were calculated with the Hill equation. Hill coefficients in all experiments were near unity. IC₅₀ values for concentration-dependent inhibition of NECA-stimulated adenylyl cyclase caused by antagonists were calculated accordingly. Dissociation constants (K_i) for antagonist were then calculated from the Cheng and Prusoff equation [18].

2.4. Molecular modeling

All modeling studies were carried out on a 20 CPU (Intel Core2 Quad CPU 2.40 GHz) Linux cluster. Homology modeling, energy calculation, and analyses of docking poses were performed using the Molecular Operating Environment (MOE, version 2008.10) suite [20]. The software package MOPAC (version 7) [21], implemented in MOE suite, was utilized for all quantum mechanical calculations. Docking simulation was performed using GOLD suite [21].

2.4.1. Homology models of hA₃ AR

Based on the assumption that GPCRs share similar TM boundaries and overall topology, a homology model of the hA₃ adenosine receptor was constructed, as previously reported [22,23], based on a template of the recently published crystal structure of hA_{2A} receptor (PDB code: 3EML) [24].

The numbering of the amino acids follows the arbitrary scheme by Ballesteros and Weinstein. According to this scheme, each amino acid identifier starts with the helix number, followed by the position relative to a reference residue among the most conserved amino acid in that helix. The number 50 is arbitrarily assigned to the reference residue [25].

Firstly, the amino acid sequences of TM helices of the hA₃ receptor were aligned with those of the template, guided by the highly conserved amino acid residues, including the DRY motif (Asp3.49, Arg3.50, and Tyr3.51) and three proline residues (Pro4.60, Pro6.50, and Pro7.50) in the TM segments of GPCRs. The same boundaries were applied for the TM helices of hA₃ receptor as they were identified from the 3D structure for the corresponding sequences of the template, the coordinates of which were used to construct the seven TM helices for hA₃ receptor. Then,

the loop domains were constructed by the loop search method implemented in MOE on the basis of the structure of compatible fragments found in the Protein Data Bank. In particular, loops were modeled first in random order. For each loop, a contact energy function analyzed the list of candidates collected in the segment searching stage, taking into account all atoms already modeled and any atoms specified by the user as belonging to the model environment. These energies were then used to make a Boltzmann-weighted choice from the candidates, the coordinates of which were then copied to the model. Subsequently, the side chains were modeled using a library of rotamers generated by systematic clustering of the Protein Data Bank data, using the same procedure. Side chains belonging to residues whose backbone coordinates were copied from a template and were modeled first, followed by side chains of modeled loops. Outgaps and their side chains were modeled last. Special caution has to be given to EL2 because amino acids of this loop could be involved in direct interactions with the ligands. A driving force to the peculiar fold of the EL2 loop might be the presence of a disulfide bridge between cysteines in TM3 and EL2. Since this covalent link is conserved in both hA_{2A} and hA₃ receptors, the EL2 loop was modeled using a constrained geometry around the EL2-TM3 disulfide bridge. The constraints were applied before the construction of the homology model, in particular during the sequence alignment, selecting the cysteine residues involved in the disulfide bridge in hA_{2A} to be constrained with the corresponding cysteine residues in hA₃ sequence. In particular, Cys166 (EL2) and Cys77 (3.25) of the hA_{2A} receptor were constrained, respectively, with Cys166 (EL2) and Cys83 (3.25) of the hA₃ receptor. During the alignment, MOE-Align attempted to minimize the number of constraint violations. Then, after running the homology modeling, the presence of the conserved disulfide bridge in the model was manually checked. After the heavy atoms were modeled, all hydrogen atoms were added using the Protonate 3D methodology part of the MOE suite. This application assigned a protonation state for each chemical groups that minimized the total free energy of the system (taking titration into account) [26].

Protein stereochemistry evaluation was then performed by several tools (Ramachandran plot; backbone bond lengths, angles and dihedral plots; clash contacts report; rotamers strain energy report) implemented in MOE suite [20].

2.4.2. Molecular docking of adenosine receptors antagonists

Ligand structures were built using MOE-builder tool, part of the MOE suite [20], and were subjected to MMFF94x energy minimization until the rms of conjugate gradient was <0.05 kcal/mol Å⁻¹. Partial charges for the ligands were calculated using PM3/ESP methodology.

Four different programs have been used to calibrate our docking protocols: MOE-Dock [20], GOLD [27], Glide [28], and PLANTS [29]. In particular, ZM-241385 was re-docked into the crystal structure of the hA_{2A} adenosine receptor (PDB code: 3EML) with different docking algorithms and scoring functions, as already described [22]. Then, RMSD values between predicted and crystallographic positions of ZM-241385 were calculated for each of the docking algorithms. The results showed that docking simulations performed with GOLD gave the lowest RMSD value, the lowest mean RMSD value and the highest number of poses with RMSD value <2.5 Å.

On the basis of the best docking performance, all antagonist structures were docked into the hypothetical TM binding site of the hA₃ AR model and that of the hA_{2A} AR crystal structure, by using the docking tool of the GOLD suite [27]. Searching was conducted within a user-specified docking sphere, using the Genetic Algorithm protocol and the GoldScore scoring function. GOLD

performs a user-specified number of independent docking runs (25 in our specific case) and writes the resulting conformations and their energies in a molecular database file. The resulting docked complexes were subjected to MMFF94x energy minimization until the rms of conjugate gradient was <0.1 kcal/mol Å⁻¹. Charges for the ligands were imported from the MOPAC output files using PM3/ESP methodology.

Prediction of antagonist–receptor complex stability (in terms of corresponding pK_i value) and the quantitative analysis for non-bonded intermolecular interactions (H-bonds, transition metal, water bridges, hydrophobic, electrostatic) were calculated and visualized using several tools implemented in MOE suite [20].

Electrostatic and hydrophobic contributions to the binding energy of individual amino acids have been calculated as implemented in MOE suite [20]. In order to estimate the electrostatic contributions, atomic charges for the ligands were calculated using PM3/ESP methodology. Partial charges for protein amino acids were calculated on the basis of the AMBER99 force field.

3. Results and discussion

3.1. Chemistry

Two series of novel chromone carboxamides placed at positions C2 (compounds **2–13**) and C3 (compounds **15–26**) of the γ-pyrone ring were synthesized using chromone carboxylic acids (compounds **1** or **14**) as starting materials (Scheme 1).

Carboxylic acids may be converted into carboxamides by treating them with amines. However, the direct reaction does not occur spontaneously at ambient temperature, with the necessary elimination of water only taking place at high temperatures [30,31]. In order to activate carboxylic acids, one can use so-called coupling reagents that act as stand-alone reagents to generate compounds such as acid chlorides, (mixed) anhydrides, carbonic anhydrides or active esters [31].

The synthetic strategy used in this work is depicted in Scheme 1. Briefly the synthesis of the chromone carboxamide derivatives was based on a one-pot condensation with the activation *in situ* of the carboxylic acid function using a coupling reagent under mild reaction conditions. The coupling reagents selected for carboxylic

acid activation were organophosphoric compounds, namely (benzotriazol-1-yloxy)tris(dimethylamino) phosphonium hexafluorophosphate (BOP) and (benzotriazol-1-yloxy) tripyrrolidino-phosphonium hexafluorophosphate (PyBOP) [31]. In all the reactions, *N,N*-diisopropylethylamine (DIPEA) was used instead of the classic triethylamine since a significant yield increase was observed due mainly to an improvement in the purification steps [13].

The synthetic procedure has an advantage over the Schotten–Baumann reaction since it avoids the step of generation of an acyl halide with reagents such as thionyl chloride or phosphorus pentachloride, circumventing some of the drawbacks related to the use of this type of reagents, namely the ring-opening of the benzopyran nucleus [32]. Furthermore, phosphonium salts (BOP or PyBOP) were selected as coupling reagents since some of the side reactions described with the employment of carbodiimides are avoided facilitating product purification with improvement of the yield of the reaction [31].

3.2. Pharmacology

3.2.1. Binding affinity at human A₁, A_{2A}, and A₃ adenosine receptors

The affinity of the new potential antagonists for the human adenosine receptor subtypes hA₁, hA_{2A}, hA₃ (expressed in Chinese hamster ovary (CHO) cells) was determined in radioligand competition experiments [16–19]. In this assay, we measured the displacement of: (i) specific [³H]CCPA binding at hA₁ receptors, (ii) specific [³H]NECA binding at hA_{2A} and [³H]HEMADO binding at hA₃ receptors. The data were expressed as K_i (dissociation constant), which was calculated with the program SCTFIT [19], and given as geometric means of at least three experiments, including 95% confidence intervals. The receptor binding affinities of the synthesized compounds (**2–13** and **15–26**) are reported in Tables 1 and 2, respectively.

3.2.2. Adenylyl cyclase activity

Because of the lack of a suitable radioligand for hA_{2B} receptor in binding assay, the potency of antagonists at hA_{2B} receptor (expressed on CHO cells) was determined in adenylyl cyclase experiments instead. The procedure was carried out as described previously in Klotz et al. with minor modifications [16]. In this

Table 1
Affinity (K_i, nM) of chromones **1–13** in radioligand binding assays at human A₁, A_{2A} and A₃ adenosine receptors.

Compound	R	hA ₁	hA _{2A}	hA ₃	Selectivity	
		K _i (nM)	K _i (nM)	K _i (nM)	hA ₁ /hA ₃	hA _{2A} /hA ₃
1	OH	>100,000	>100,000	>100,000	–	–
2	NH–Ph	>100,000	>100,000	14,200 (11,800–17,100)	>7.0	>7.0
3	NH–C ₆ H ₁₁	>100,000	>100,000	38,700 (27,400–54,700)	>2.6	>2.6
4	NH–C ₃ H ₇	>100,000	>100,000	>100,000	–	–
5	NH–(4′–OH–Ph)	>100,000	28,300 (19,600–40,700)	46,300 (38,100–56,300)	>2.2	0.61
6	NH–(4′–OCH ₃ –Ph)	>100,000	>100,000	9580 (7600–12,100)	>10	>10
7	NH–(4′–CH ₃ –Ph)	>100,000	>100,000	15,800 (12,200–20,400)	>6.3	>6.3
8	NH–(3′–OH–4′–OCH ₃ –Ph)	>100,000	35,700 (32,700–39,100)	15,400 (10,100–23,400)	>6.5	2.3
9	NH–(3′–OCH ₃ –4′–OCH ₃ –Ph)	>100,000	>100,000	27,900 (18,300–42,700)	>3.6	>3.6
10	NH–(4′–Cl–Ph)	>100,000	>100,000	>100,000	–	–
11	NH–(4′–OCF ₃ –Ph)	>100,000	>100,000	>100,000	–	–
12	NH–(4′–CF ₃ –Ph)	>100,000	>100,000	>100,000	–	–
13	NH–(4′–NO ₂ –Ph)	>100,000	>100,000	>100,000	–	–

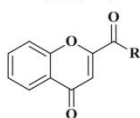
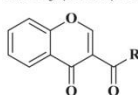


Table 2

Affinity (K_i , nM) of chromones **14–26** in radioligand binding assays at human A_1 , A_{2A} and A_3 adenosine receptors.



Compound	R	hA_1	hA_{2A}	hA_3	Selectivity	
		K_i (nM)	K_i (nM)	K_i (nM)	hA_1/hA_3	hA_{2A}/hA_3
14	OH	>100,000	>100,000	>100,000	–	–
15	NH–Ph	>100,000	>100,000	>100,000	–	–
16	NH–C ₆ H ₁₁	18,400 (16,600–20,400)	26,900 (18,300–39,600)	71,300 (66,000–77,100)	0.26	0.38
17	NH–C ₃ H ₇	19,300 (18,400–20,200)	41,600 (32,400–53,500)	40,800 (37,000–44,900)	0.47	1.0
18	NH–(4′–OH–Ph)	10,400 (8870–12,300)	22,100 (20,100–24,400)	8,860 (7460–10,500)	1.2	2.5
19	NH–(4′–OCH ₃ –Ph)	18,600 (14,500–23,800)	10,100 (8660–11,900)	6070 (4710–7830)	3.1	1.7
20	NH–(4′–CH ₃ –Ph)	>100,000	>100,000	16,600 (15,600–17,600)	>6.0	>6.0
21	NH–(3′–OH–4′–OCH ₃ –Ph)	8590 (7240–10,200)	6850 (6220–7550)	3680 (2770–4900)	2.3	1.9
22	NH–(3′–OCH ₃ –4′–OCH ₃ –Ph)	11,700 (10,300–13,300)	12,400 (10,200–15,000)	6690 (5610–7980)	1.8	1.9
23	NH–(4′–Cl–Ph)	25,600 (10,400–32,200)	17,400 (13,700–22,200)	16,400 (15,700–17,100)	1.6	1.1
24	NH–(4′–OCF ₃ –Ph)	>100,000	>100,000	>100,000	–	–
25	NH–(4′–CF ₃ –Ph)	>100,000	>100,000	>100,000	–	–
26	NH–(4′–NO ₂ –Ph)	>100,000	14,300 (10,500–19,500)	3750 (3530–3980)	>26	3.8

assay, the NECA-stimulated adenylyl cyclase activity was inhibited with increasing concentrations of antagonist. As a result, cAMP (cyclic adenosine monophosphate) production was inhibited in a concentration-dependent fashion, and IC_{50} and K_i values, respectively, were determined.

3.3. Molecular modeling

The recently published crystal structure of the human A_{2A} adenosine receptor, in complex with the antagonist ZM241385 (PDB code: 3EML) [24] provides a new template to perform homology modeling of other GPCRs and in particular of adenosine receptors. Therefore we built up a homology model of the hA_3 receptor based on the crystal structure of the hA_{2A} receptor (methodological details were summarized in Section 2.4.1) [22,23].

In the process of selecting a reliable docking protocol to be employed in the following docking studies of these new derivatives, we have evaluated the ability of different docking softwares in reproducing the crystallographic pose of ZM241385 inside the binding cavity of human A_{2A} receptor. As reported in Section 2.4.2, among the four different types of programs used to calibrate our docking protocol, the Gold programs was finally chosen since it showed the best performance with regard to the calculated RMSD values relative to the crystallographic pose of ZM241385 [22].

Consequently, based on the selected docking protocol, we performed docking simulations to identify the hypothetical binding mode of the newly synthesized derivatives inside the human A_{2A} and A_3 adenosine receptors.

3.4. Structure–affinity relationship studies

Chromone carboxamide derivatives (**2–13** and **15–26**) of the chromone carboxylic acids (compounds **1** and **14**) were obtained in a one pot reaction and with good yields (45–85%) (Scheme 1). Their affinity to bind to human A_1 , A_{2A} and A_3 adenosine receptors (AR) expressed in CHO cells (compounds **2–13** in Table 1 and compounds **15–26** in Table 2) was determined. Due to the lack of a useful radioligand for hA_{2B} AR, the inhibition of NECA-stimulated adenylyl cyclase activity by chromone carboxylic acids and carboxamides was determined. For all the tested compounds no measurable activity ($K_i > 100,000$ nM) was detected.

The binding assays data clearly show that chromone carboxylic acids (compounds **1** and **14**) are devoid of activity and the corresponding carboxamides derivatives are compounds with diverse affinity and selectivity toward human A_1 , A_{2A} and A_3 AR (Tables 1 and 2).

A more cautious look on the data allows to conclude that the affinity and/or selectivity of chromone carboxamides is influenced by the relative position of the carbonyl function of the carboxamide group on the benzopyran nucleus and by the type of amine (aromatic, cyclic and aliphatic) that is located in the nitrogen atom. In general, it can be also inferred that the presence of electron donors or withdrawing groups on the phenyl substituent of the carboxamide also modulate the affinity and selectivity of chromone carboxamides for the subtypes of ARs.

From the data the following specific conclusions can be drawn:

- For carboxamides located in position 2 of the pyran nucleus (compounds **2–13**): the presence of a phenyl (compound **2**) or a cyclohexyl substituent (compound **3**) is tolerated and a fair affinity for A_3 AR is observed. However, no binding was detected with a linear alkyl substituent (compound **4**). These observations allow to infer that probably in this type of systems the spatial volume of the substituent is an important feature. The presence of electron withdrawing substituents in the phenyl ring located in the nitrogen atom, such as chlorine (compound **10**), trifluoromethoxy (compound **11**), trifluoromethyl (compound **12**) or nitro (compound **13**) groups in *para* position give rise to a lack of affinity for all the adenosine receptors subtypes.
- On other hand the presence of electron donors in the phenyl ring located in the nitrogen atom, in *para* position, (compounds **5–9**) result in the display of a noticeable affinity/selectivity for the A_3 AR.
- For carboxamides located in position 3 of the pyran nucleus (compounds **15–26**): in this chromone carboxamide isomeric series the conclusions were not as straightforward as in the series with a 2-substituted pyran. However, for this type of benzopyran derivatives the results show that similar to the 2-substituted isomers the presence of electron donating groups in the phenyl substituent increase the affinity and selectivity for the human A_3 AR (compounds **18–22**). It is to note that compounds **18** and **19** exhibit micromolar affinity for all the studied receptors but without a significant selectivity. With

exception of compound **26** with a nitro function in *para* position, that have high A_3 AR affinity, the chromone derivatives with electron withdrawing groups have no measurable affinity for adenosine receptors (compound **24** and **25**). Moreover, it is important to highlight that compounds **21** and **26** present the best affinity for A_3 receptor with a $K_i = 3684$ nM and $K_i = 3750$ nM, respectively.

A molecular modeling investigation was performed for all the newly synthesized analogues, in order to identify their hypothetical binding modes at both the crystallographic structure of hA_{2A} AR and the hA_3 AR model. The analysis was extended to docking simulations and *per residue* electrostatic and hydrophobic contributions.

The first important consideration is that almost all the new analogues showed different possible binding poses at both the hA_{2A} AR and the hA_3 AR. In fact, even if all ligands made contacts mainly with residues belonging to TM2, TM3, TM6, TM7, and EL2, they can accommodate different orientations inside the binding pockets.

Fig. 1 shows the selected binding modes of compound **21**, a chromone with the carboxamide located in position 3 of the pyran nucleus, obtained after docking simulations at the hA_{2A} AR and the hA_3 AR. Among all the herein reported derivatives, compound **21**

possesses the highest affinity at both receptors (K_i $hA_{2A} = 6850$ nM, K_i $hA_3 = 3684$ nM). At both receptor subtypes ligand-recognition occurred in the upper region of the TM bundle, and the chromone nucleus was surrounded by TMs 3, 5, 6, 7.

The hypothetical binding pose of compound **21** at the hA_{2A} AR (Fig. 1, panel A) showed an H-bonding interaction with Asn253 (6.55) and a stabilizing interaction with Phe168 (EL2). Interestingly, the important role in ligand binding of these two residues was previously revealed by site-directed mutagenesis studies [33,34] and by the crystallographic binding pose of ZM241385 inside the hA_{2A} AR binding pocket [24].

Moreover, the hydroxyl group on the phenyl ring of compound **21** interacted with Tyr271 (7.36), forming a weak H-bond. Finally, the ligand also formed hydrophobic interactions with some residues of the binding site, including Leu85 (3.33), Trp246 (6.48), Leu249 (6.51), Tyr271 (7.36) and Ile274 (7.39).

On the other hand, the docking pose of compound **21** at the hA_3 AR was located in the same region of the TM bundle as at the hA_{2A} AR, but the orientation of the ligand was different (Fig. 1, Panel B). In this case, the ligand formed two H-bonds with Asn250 (6.55) and a stabilizing interaction with Phe168 (EL2). Moreover, the complex is stabilized by hydrophobic interactions occurring between the ligand and some residues of the binding site, such as Leu91 (3.33), Trp243 (6.48), Leu246 (6.51) and Leu264 (7.35).

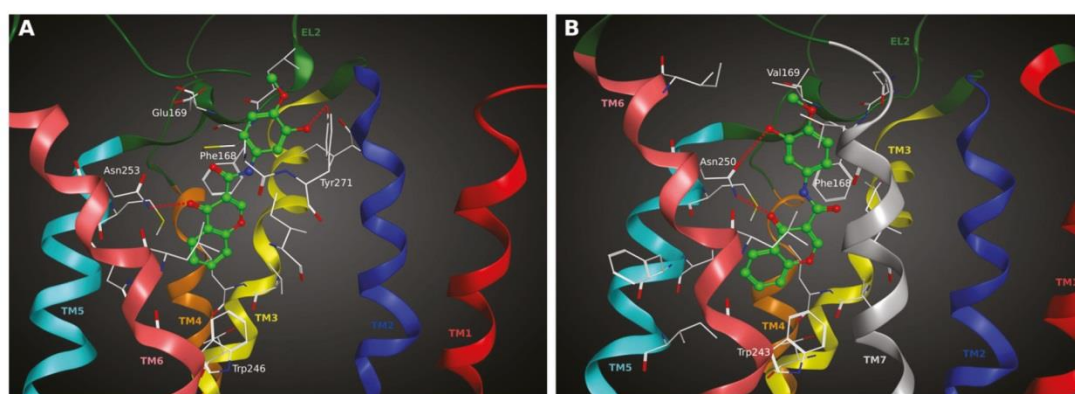


Fig. 1. Hypothetical binding modes of compound **21** obtained after docking simulations: (A) inside the hA_{2A} AR binding site; (B) inside the hA_3 AR binding site. Poses are viewed from the membrane side facing TM6, TM7, and TM1. In panel A, the view of TM7 is omitted. Side chains of some amino acids important for ligand recognition and H-bonding interactions are highlighted. Hydrogen atoms are not displayed.

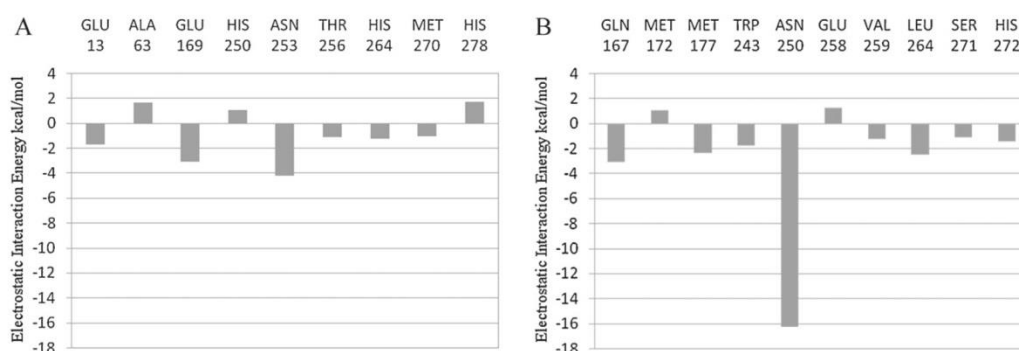


Fig. 2. Calculated electrostatic interaction energy (in kcal/mol) between the ligand and each single amino acid involved in ligand recognition observed from the hypothetical binding modes of compound **21** inside (A) hA_{2A} AR and (B) hA_3 AR binding sites.

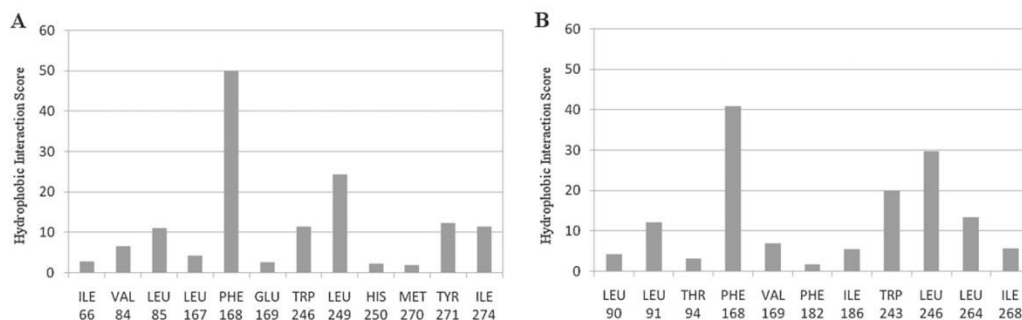


Fig. 3. Calculated hydrophobic interaction scores (in arbitrary hydrophobic units) between the ligand and each single amino acid involved in ligand recognition observed from the hypothetical binding modes of compound **21** inside (A) *hA_{2A}* AR and (B) *hA₃* AR binding sites.

Another antagonist of this series with affinity at the *hA₃* AR comparable to compound **21** is compound **26** (K_i *hA₃* = 3750 nM). The binding orientation, obtained after docking simulation, of this ligand at this receptor is very similar to the one observed for compound **21** (data not shown). In this case, compound **26** formed one H-bonding interaction with Asn250 (6.55) and a stabilizing interaction with Phe168 (EL2).

Analyzing the calculated electrostatic contribution *per residue* to the whole interaction energy for both the complexes between compound **21** and these two adenosine receptor subtypes (Fig. 2), the main stabilizing factor was found to be related to Asn 6.55 (Asn253 in *hA_{2A}* AR and Asn250 in *hA₃* AR), due to the H-bonding interactions with the ligand above described. However, the calculated electrostatic contribution of this Asn residue is much more stabilizing for the *hA₃* AR complex (−16 kcal/mol for *hA₃* AR complex compared to −4 kcal/mol for *hA_{2A}* AR complex).

As shown in Fig. 3, the hydrophobic interaction scores patterns showed the strongest stabilizing contribution corresponding to the interactions of the ligand with Phe168 (EL2) at both receptors.

In conclusion, at the *hA_{2A}* AR compound **21** was able to interact with Asn253 (6.55) and Phe168 (EL2), important residues in ligand recognition, but it did not form strong interaction with Glu169 (EL2), another residue with an important role in ligand binding as revealed by the crystallographic binding pose of ZM241385 inside the *hA_{2A}* AR binding pocket [24]. At the *hA₃* AR compound **21** formed stronger, but still not optimal, interactions with the residues of the binding site, and in particular with Asn250 (6.55). This difference could be the reason for the higher affinity of this compound for this adenosine receptor subtype compared to the *hA_{2A}* subtype.

On the whole, the proposed binding modes reflect the ability of compound **21** to bind both *hA_{2A}* and *hA₃* adenosine receptor subtypes with K_i in the low micromolar range and without a very good selectivity profile.

4. Conclusions

Evidence was acquired to demonstrate that chromone is a valid scaffold for the design of novel adenosine receptor ligands. The easy synthetic accessibility and the decoration capability of chromones make them “privileged” scaffolds.

From this study and on the basis of the obtained structure–activity relationships it was concluded that chromone carboxamides represent a novel class of AR ligands. The most remarkable chromones were compounds **21** and **26** that present a better affinity for *A₃* AR (K_i = 3680 nM and K_i = 3750 nM, respectively). The results obtained so far pointed out a crucial and undisclosed role of the presence of an amide substituent of the pyrone ring and

that the type of substituent on the aromatic ring of the chromone amide side chain is crucial for the optimization of affinity and selectivity. Receptor-driven molecular modeling studies provide information on the binding/selectivity data of the chromone. The data so far acquired are instrumental for future optimization of chromone carboxamide lead as a selective *A₃*AR antagonist.

Acknowledgments

This work was supported by the Foundation for Science and Technology (FCT), Portugal (project PTDC/QUI/70359/2006 and PTDC/QUI-QUI/113687/2009).

A. Gaspar (SFRH/BD/43531/2008) and FB (SFRH/BSAB/1090/2010) thanks FCT grants. The work coordinated by S.M. was carried out with financial support from the University of Padova, Italy, and the Italian Ministry for University and Research (MIUR), Rome, Italy. S.M. is very grateful to Chemical Computing Group Inc. (Montreal, Quebec, Canada) for the scientific and technical partnership.

References

- [1] Erik S. Mechanisms of cancer cell invasion. *Curr Opin Genetics Dev* 2005;15: 87–96.
- [2] Aggarwal BB, Sethi G, Baladandayuthapani V, Krishnan S, Shishodia S. Targeting cell signaling pathways for drug discovery: an old lock needs a new key. *J Cell Biochem* 2007;102:580–92.
- [3] Gessi S, Merighi S, Sacchetto V, Simioni C, Borea PA. Adenosine receptors and cancer. *BBA – Biomembr* 2011;1808:1400–12.
- [4] Fishman P, Bar-Yehuda S, Varani K, Gessi S, Merighi S, Borea PA. Agonists and antagonists: molecular mechanisms and therapeutic applications. In: Borea PE, editor. *A3 adenosine receptors from cell biology to pharmacology and therapeutics*. Dordrecht Heidelberg London New York: Springer; 2010.
- [5] Gessi S, Merighi S, Varani K, Leung E, Mac Lennan S, Borea PA. The *A₃* adenosine receptor: an enigmatic player in cell biology. *Pharmacol Ther* 2008;117:123–40.
- [6] Fishman P, Jacobson KA, Ochaion A, Cohen S, Bar-Yehuda S. The anti-cancer effect of *A₃* adenosine receptor agonists: a novel, targeted therapy. *Immunol Endocr Metabol Agents Med Chem* 2007;7:298–303.
- [7] Hasko G, Linden J, Cronstein B, Pacher P. Adenosine receptors: therapeutic aspects for inflammatory and immune diseases. *Nat Rev Drug Discov* 2008;7: 759–70.
- [8] Baraldi PG, Romagnoli R, Saponaro G, Baraldi S, Tabrizi MADP. *A3* adenosine receptor antagonists: history and future perspectives. In: Borea PA, editor. *A3 adenosine receptors from cell biology to pharmacology and therapeutics*. Dordrecht Heidelberg London New York: Springer; 2010.
- [9] DeNinno MP, Masamune H, Chenard LK, DiRico KJ, Eller C, Etienne JB, et al. The synthesis of highly potent, selective, and water-soluble agonists at the human adenosine *A₃* receptor. *Bioorg Med Chem Lett* 2006;16:2525–7.
- [10] Baraldi PG, Tabrizi MA, Gessi S, Borea PA. Adenosine receptor antagonists: translating medicinal chemistry and pharmacology into clinical utility. *Chem Rev* 2008;108:238–63.
- [11] Jacobson KA. Introduction to adenosine receptors as therapeutic targets. In: Wilson CN, Mustafa SJ, editors. *Adenosine receptors in health and disease*. Berlin Heidelberg: Springer-Verlag; 2009.

- [12] Lars JSK. Drug discovery management, small is still beautiful: why a number of companies get it wrong. *Drug Discov Today* 2011;16:476–84.
- [13] Borges F, Gaspar A, Garrido J, Milhazes N, Batoreu MC. Chromone derivatives for use as antioxidants/preservatives. PT 103665, WO 2008/104925.
- [14] Gaspar A, Silva T, Yáñez M, Vina D, Orallo F, Ortuso F, et al. Chromone, a privileged scaffold for the development of monoamine oxidase inhibitors. *J Med Chem* 2011;54:5165–73.
- [15] Gaspar A, Teixeira F, Uriarte E, Milhazes N, Melo A, Cordeiro MNDS, et al. Towards the discovery of a novel class of monoamine oxidase inhibitors: structure–property–activity and docking studies on chromone amides. *Chem-MedChem* 2011;6:628–32.
- [16] Klotz KN, Hessling J, Hegler J, Owman C, Kull B, Fredholm BB, et al. Comparative pharmacology of human adenosine receptor subtypes—characterization of stably transfected receptors in CHO cells. *N-S Arch Pharmacol* 1997;357: 1–9.
- [17] Klotz KN, Falgner N, Kachler S, Lambertucci C, Vittori S, Volpini R, et al. [³H]HEMADO—a novel tritiated agonist selective for the human adenosine A₃ receptor. *Eur J Pharmacol* 2007;556(1–3):14–8.
- [18] Cheng Y-C, Prusoff WH. Relationship between the inhibition constant (K_i) and the concentration of inhibitor which causes 50 per cent inhibition (IC₅₀) of an enzymatic reaction. *Biochem Pharmacol* 1973;22:3099–108.
- [19] De Lean A, Hancock AA, Lefkowitz RJ. Validation, statistical analysis of a computer modeling method for quantitative analysis of radioligand binding data for mixtures of pharmacological receptor subtypes. *J Mol Pharmacol* 1982;21:5–16.
- [20] MOE. (Molecular Operating Environment), version 2008.10; software available from Chemical Computing Group Inc. (1010 Sherbrooke Street West, Suite 910, Montreal, Quebec, Canada H3A 2R7); <http://www.chemcomp.com>.
- [21] Stewart JJP. MOPAC Version 7. Tokyo, Japan: Fujitsu Limited; 1993.
- [22] Lenzi O, Colotta V, Catarzi D, Varano F, Poli D, Filacchioni G, et al. 2-Phenylpyrazolo[4,3-d]pyrimidin-7-one as a new scaffold to obtain potent and selective human A₃ adenosine receptor antagonists: new insights into the receptor-antagonist recognition. *J Med Chem* 2009;52:7640–52.
- [23] Morizzo E, Federico S, Spalluto G, Human Moro S. A₃ adenosine receptor as versatile G protein-coupled receptor example to validate the receptor homology modeling technology. *Curr Pharm Des* 2009;15:4069–84.
- [24] Jaakola V-P, Griffith MT, Hanson MA, Cherezov V, Chien EYT, Lane JR, et al. The 2.6 Ångstrom crystal structure of a human A_{2A} adenosine receptor bound to an antagonist. *Science* 2008;322:1211–7.
- [25] Ballesteros JA, Weinstein H. Integrated methods for the construction of three-dimensional models and computational probing of structure-function relations in G protein-coupled receptors. In: Stuart CS, editor. *Methods in neurosciences*. Academic Press; 1995. p. 366–428.
- [26] Labute P. Protonate 3D: assignment of ionization states and hydrogen coordinates to macromolecular structures. *Proteins Struct Funct Bioinf* 2009;75:187–205.
- [27] GOLD suite, version 4.0.1; software available from Cambridge Crystallographic Data Centre Cambridge Crystallographic Data Centre (12 Union Road Cambridge CB2 1EZ UK); <http://www.ccdc.cam.ac.uk>.
- [28] Friesner RA, Banks JL, Murphy RB, Halgren TA, Klicic JJ, Mainz DT, et al. Glide: A new approach for rapid, accurate docking and scoring. 1. Method and assessment of docking accuracy. *J Med Chem* 2004;47:1739–49.
- [29] Korb O, Stutzle T, Exner TE. Empirical scoring functions for advanced protein-ligand docking with PLANTS. *J Chem Inf Model* 2009;49:84–96.
- [30] Allen CL, Williams MJ. Metal-catalysed approaches to amide bond formation. *Chem Soc Rev* 2011;40:3405–15.
- [31] Han S-Y, Kim Y-A. Recent development of peptide coupling reagents in organic synthesis. *Tetrahedron* 2004;60:2447–67.
- [32] Ellis GP. General methods of preparing chromones. In: *Chemistry of heterocyclic compounds*. John Wiley & Sons, Inc.; 2008. pp. 495–555.
- [33] Kim J, Wess J, van Rhee AM, Schöneberg T, Jacobson KA. Site-directed mutagenesis identifies residues involved in ligand recognition in the human A adenosine receptor. *J Biol Chem* 1995;270:13987–97.
- [34] Jaakola V-P, Lane JR, Lin JY, Katritch V, Ijzerman AP, Stevens RC. Ligand binding and subtype selectivity of the human A_{2A} adenosine receptor. *J Biol Chem* 2010;285:13032–44.

3.7 Combining QSAR classification models for predictive modeling of human monoamine oxidase inhibitors.

Article from European Journal of Medicinal Chemistry (2013), 59: 75-90.



Contents lists available at SciVerse ScienceDirect

European Journal of Medicinal Chemistry

journal homepage: <http://www.elsevier.com/locate/ejmech>



Original article

Combining QSAR classification models for predictive modeling of human monoamine oxidase inhibitors

Aliuska Morales Helguera^{a,b,c,*}, Alfonso Pérez-Garrido^{d,e}, Alexandra Gaspar^a, Joana Reis^a, Fernando Cagide^a, Dolores Vina^f, M.Natália D.S. Cordeiro^g, Fernanda Borges^{a,*}

^a CIQ, Departamento de Química e Bioquímica, Faculdade de Ciências, Universidade do Porto, Porto 4169-007, Portugal

^b CBQ, Universidad Central Marta Abreu de Las Villas, Santa Clara, 54830 Villa Clara, Cuba

^c Departamento de Química, Universidad Central Marta Abreu de Las Villas, Santa Clara, 54830 Villa Clara, Cuba

^d Cátedra de Ingeniería y Toxicología Ambiental, Universidad Católica San Antonio, Guadalupe, Murcia, Spain

^e Departamento de Tecnología de la Alimentación y de la Nutrición, Universidad Católica San Antonio, Guadalupe, Murcia, Spain

^f Departamento de Farmacología, Facultad de Farmacia, Universidad de Santiago de Compostela, 15782 Santiago de Compostela, Spain

^g REQUIMTE, Departamento de Química e Bioquímica, Faculdade de Ciências, Universidade do Porto, Porto 4169-007, Portugal

ARTICLE INFO

Article history:

Received 26 June 2012

Received in revised form

16 October 2012

Accepted 18 October 2012

Available online 1 November 2012

Keywords:

Monoamine oxidase inhibitor

Selectivity

hMAO-A

hMAO-B

QSAR

Consensus

ABSTRACT

Due to their role in the metabolism of monoamine neurotransmitters, MAO-A and MAO-B present a significant pharmacological interest. For instance the inhibitors of human MAO-B are considered useful tools for the treatment of Parkinson Disease. Therefore, the rational design and synthesis of new MAOs inhibitors is considered of great importance for the development of new and more effective treatments of Parkinson Disease. In this work, Quantitative Structure Activity Relationships (QSAR) has been developed to predict the human MAO inhibitory activity and selectivity. The first step was the selection of a suitable dataset of heterocyclic compounds that include chromones, coumarins, chalcones, thiazolylhydrazones, etc. These compounds were previously synthesized in one of our laboratories, or elsewhere, and their activities measured by the same assays and for the same laboratory staff. Applying linear discriminant analysis to data derived from a variety of molecular representations and feature selection algorithms, reliable QSAR models were built which could be used to predict for test compounds the inhibitory activity and selectivity toward human MAO. This work also showed how several QSAR models can be combined to make better predictions. The final models exhibit significant statistics, interpretability, as well as displaying predictive power on an external validation set made up of chromone derivatives with unknown activity (that are being reported here for first time) synthesized by our group, and coumarins recently reported in the literature.

© 2012 Elsevier Masson SAS. All rights reserved.

1. Introduction

The monoamine oxidase (EC 1.4.3.4; MAO) is a flavoprotein localized in the outer mitochondrial membrane and present in practically all mammalian tissues. The primary role of MAO lies in the metabolism of amines and in the regulation of neurotransmitter levels and intracellular amine stores [1].

All mammals contain two MAO isoforms, MAO-A and MAO-B. They can be distinguished by their respective substrate

preferences, by their sensitivities to the acetylenic inhibitors clorgyline and L-deprenyl (selegiline), and by their tissue distribution [1–3]. MAO-A, predominant isoform in the gastrointestinal tract [2], is primarily responsible for the oxidation of tyramine. Its peripheral inhibition has been associated with the risk for an acute hypertensive syndrome known as the “cheese reaction” [4]. Whereas the MAO-B is the predominant subtype in the human brain, where it acts in the breakdown of the dopamine (DA), as well as in the deamination of β -phenylethylamine, an endogenous amine that stimulates the release of DA and inhibits its neuronal reuptake [5]. Expression levels of MAO-B in neuronal tissue enhance 4-fold with aging, especially in glial cells, resulting in an increased level of DA metabolism and in the production of higher levels of dopanil and hydrogen peroxide (H_2O_2). Increased levels of cellular H_2O_2 promote apoptotic signaling events resulting in

* Corresponding authors. CIQ, Departamento de Química e Bioquímica, Faculdade de Ciências, Universidade do Porto, Porto 4169-007, Portugal. Tel.: +351 220402560; fax: +351 220402659.

E-mail addresses: aliuskamhelguera@yahoo.es (A.M. Helguera), fborges@fc.up.pt (F. Borges).

a decreased level of DA-producing cells [6], which are thought to play a major role in the etiology of neurodegenerative diseases such as Parkinson's and Alzheimer's [6,7].

Due to their role in the metabolism of monoamine neurotransmitters, MAO inhibitors can be useful in treatment of psychiatric and neurological diseases. Actually, MAO-A selective inhibitors act as antidepressant and anxiolytic agents while selective MAO-B inhibitors are an attractive therapeutic intervention for patients with Parkinson's disease [1,8–10].

The recognition of the importance of MAO as a drug target has produced a growing interest in the development of MAO inhibitors. Privileged structures, such as indoles, arylpiperazines, biphenyls and benzopyranes are currently ascribed as supportive approaches in drug discovery. Different families of heterocycles, such as oxadiazolones, tetrazoles, oxadiazinones, indenopyridazines, pyrazoles, xanthenes, coumarins and their precursors (chalcones) have also been extensively used as scaffolds in medicinal chemistry programs, namely for the search of novel MAO inhibitors [11–19].

Recently, a discovery and development of new chemical entities as human MAO (hMAO) inhibitors belonging to chromone (benzo- γ -pyrone) nucleus [20–23] validating the scaffold for the design of potent, selective and reversible MAO inhibitors. In general, chromones substituted in position-3 of γ -pyrone nucleus act as hMAO-B selective inhibitors and those substituted in position-2 of the pyrone nucleus inhibit the hMAO-A or are inactive. The –COOH substituent in position 3- of this heterocyclic scaffold as well as the introduction of a chloro substituent in *para* position of the exocyclic aromatic ring of chromone 3-phenylcarboxamides improve the potency and selectivity of hMAO-B inhibitors (see Fig. 1).

In spite of the considerable advancements in the studies on the interactions of MAO isoforms with their specific substrates or inhibitors [24], there are not any available rules for the rational design of new potent and selective MAO inhibitors. Although several medicinal chemistry approaches can be used for the identification of hits, generation of leads, and optimization of leads into drug candidates, no rational guidelines have been available yet. Quantitative structure–activity relationships (QSAR) are important strategies that can be applied for the successful design of potent and selective MAO inhibitors [25].

QSAR methodology consists of a representation of the chemical structure using molecular descriptors and a multivariate analysis that relates the biological activity of one compound to its chemical structure. Several methodologies have established QSAR to predict

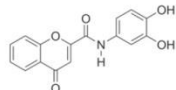
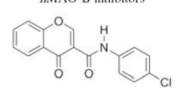
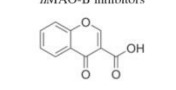
the inhibition on MAOs. The most of them are based on specific kind of compound (congeneric series), e.g. coumarin, pirindole, xanthone, etc. [11,26,27] or use chemicals assayed by different experimental protocols [28].

One of the first QSAR studies to predict inhibitory MAO activity is developed in 1974 by Martin et al. [29]. The study involved a relatively small dataset (20 chemicals) of aminotetralins and aminoindans with antidepressant activity reported. Linear discriminant analysis was used as multivariate analysis technique and only two molecular descriptors: Taft steric parameter and an indicator variable were statistically significant. Also field-based 3D-QSAR like comparative molecular field analysis (CoMFA) is among the computational methods that have been extensively used to this end [24,26,27,30–33]. This popular 3D QSAR approach makes suggestion regarding steric or electronic modifications of the training set compounds that are likely to increase their activity. Some examples on the use of CoMFA to understand MAO-selectivity include the work of Gnerre et al. to unveil structural requirement for selective binding of 7-X-benzyloxy meta-substituted 3,4-dimethylcoumarin derivatives to the MAO [27]. The chemical interpretation of the resulting CoMFA model suggests lipophilicity as the property that should influence MAO-B versus MAO-A selectivity, while the presence of an electron-withdrawing substituent should favor the MAO-A inhibition. However in CoMFA, the alignment of the molecules is a main issue because the relative interaction energies strongly depend on the relative molecular position [34]. This problem is considered [35] a leading cause to incorrect QSAR models, specifically those created with CoMFA.

An alternative to the CoMFA model of MAO inhibitors is the use of the receptor based alignment, recently proposed by Chimenti et al [24]. This computational approach is possible because the crystallographic structure of human MAO-B and MAO-A have been recently published [36,37]. Combining docking with CoMFA/QSAR may enhance the probability of finding potent inhibitors. However the current methodology has limitations like as: the high time-consuming of molecular geometry optimization and its application only to homogeneous series of compounds due to the requirement for structural alignment.

Other QSAR model to predict MAO-A inhibitory activity was developed by Núñez et al. [11] using a dataset of 42 xanthenes derivatives and E-state index, molecular connectivity and shape descriptors. After the exclusion of 7 outliers the model had a determination coefficient of 0.847. The only validation methods of the model were, leave one out and jackknife technique. There was no division of the dataset into training and test sets. Consequently, the model external predictivity power was not evaluated. In light of recent studies is important to make the external validation [38], this omission compromises the application of this model to predict accurately the MAO inhibition of compounds that were not used for the model development. Some other authors validate their MAO–QSAR model using one or two compounds that were not used in the model development [39], and still claim their models are predictive.

On the other hand, the information on the inhibitory MAO activity of many molecules reported in the literature is limited and directed to behavioral tests and assays on bovine or rat mitochondrial MAOs [24]. Therefore, many of the QSAR studies to predict inhibitory MAO activity were based on databases assayed in non-human MAO tests [11,24,26,27,30]. However the access to purified recombinant human MAO-A [40] and MAO-B [41] as well as conditions for the crystallization of MAO-B complexes with several inhibitors [36,42], has resulted in explosive growth of amount of human MAO inhibition data [13,14,17,28,32,43–55]. This progress has provided new opportunities for the design and fast computer-assisted development of drugs involved in the human

Structure	Exp. inhibitory activity	References
<i>h</i> MAO-A inhibitors		
	pIC_{50} (<i>h</i> MAO-A) = 6.72 pIC_{50} (<i>h</i> MAO-B) = 5.58 pSI^a = -1.15	[24]
<i>h</i> MAO-B inhibitors		
	pIC_{50} (<i>h</i> MAO-A) < 4.00 pIC_{50} (<i>h</i> MAO-B) = 7.20 pSI^a > 3.20	[24]
<i>h</i> MAO-B inhibitors		
	pIC_{50} (<i>h</i> MAO-A) < 4.00 pIC_{50} (<i>h</i> MAO-B) = 7.32 pSI^a > 3.32	[21]

^a pSI is the selectivity to *h*MAO-B and it is calculated as follows: $pSI = pIC_{50}(hMAO-B) - pIC_{50}(hMAO-A)$.

^a pSI is the selectivity to hMAO-B and it is calculated as follow: $pSI = pIC_{50}(hMAO-B) - pIC_{50}(hMAO-A)$.

Fig. 1. Examples of potent and selective hMAO inhibitors based on the chromone scaffold.

MAO metabolic pathway, since accumulating evidence has shown that inhibition data from rat MAO test often strongly differ from data collected with similar methods from human enzymes [56].

In the present paper, we assemble a set of over 450 different nitrogen and oxygen heterocycles as well as other synthetic analogs obtained in our laboratories [20,21,23] or elsewhere [13,14,17,28,32,43–55] that were evaluated toward human MAO in a single and consistent inhibition assay [57]. Herein, 0D, 1D and 2D and molecular descriptors along with linear discriminant analysis and feature selection algorithms were used to build reliable predictive QSAR models from the available data. The final models were reliable displaying significant statistics and were predictive on an external validation set comprising chromone derivatives of unknown activity and coumarins recently reported in the literature [58]. Our work also highlights that different combinations of the QSAR models increase our chance for success, whereas a conventional QSAR approach using only one model and one type of descriptors has a higher chance to fail.

2. Materials and methods

2.1. Dataset

Different types of heterocyclic such as chromones, homoiso-flavonoids, coumarins and their precursors (chalcones) and a 2-hydrazinylthiazoles and pyrazoles have been included in our database. They were experimentally assayed for their inhibitory effects (IC_{50}) on the hMAO-A and hMAO-B isoforms. The experiments were all conducted at the Department of Pharmacology of Faculty of Pharmacy of University of Santiago de Compostela in Spain, following the same *in vitro* assay protocols that were previously described [57]. To note that the biological data used along the work has been measured by a single protocol at the same laboratory.

The compounds were first classified into four groups according to their IC_{50} values and the selectivity indexes (SI). The first group, designated as inhibitors, include all chemicals with $IC_{50} < 20 \mu M$ ($pIC_{50} > 4.70$). The second one, named as non-inhibitors, include those compounds with $IC_{50} > 20 \mu M$ ($pIC_{50} < 4.70$). The third group, named as hMAO-B selective ligands, contains those substances with $pSI > 1.70$ while fourth one, named as hMAO-B non-selective ligand comprises those compounds with $pSI < 1.70$. pSI is the selectivity to hMAO-B and it is calculated as follow: $pSI = pIC_{50}(hMAO-B) - pIC_{50}(hMAO-A)$. In this dataset, there are stereoisomers, which cannot be distinguished by the present 2D descriptors but had nevertheless similar IC_{50} values; in such cases, one of the isomers was discarded. Consequently, our dataset is formed by 449 organic compounds. Table S1 of the Supplementary material displays a complete listing of the compounds and the reported experimental data.

The present large dataset was divided into training and test sets to obtain validated QSAR models. In this work, the *k*-Means Cluster Analysis (*k*-MCA) technique was applied to setup both sets representative of the entire experimental universe.

2.2. *k*-Means cluster analysis

The Joining Tree Clustering (JTC) technique was applied to the whole date set of compounds to set the appropriate number of clusters and the Ward's method was used as a criterion of linking. JTC is implemented in the STATISTICA software (version 8.0) [59]. The distances between clusters are determined by the greatest distance between any two objects in the different clusters (this is known as "furthest neighbors"), while the distances between cases are computed by Euclidean or City-block (Manhattan) distances.

An appropriate number of clusters for each class; inhibitors and non-inhibitors from three dataset (both isoforms and selectivity)

were selected (Figure S1 of the Supplementary material). For a better visualization, the optimal number of clusters was highlighted with a red line cutting the branches. Once the number of clusters to be developed was estimated, the *k*-MCA was applied to design the training and prediction sets. By using this technique, it is possible to obtain exactly *k* different clusters of greatest possible distinction that can be assessed by comparing the means of the resulting *k*-clusters. Another indicator of the good performance of this technique is the magnitude of the Fisher ratio values from the analysis of variance developed on each dimension (Table S3 of the Supplementary material). For this aim, the STATISTICA software (version 8.0) [59] was used.

After the partition of the whole data into different statistically representative cluster of compounds, the training and test sets were selected from the members of these clusters.

Choosing the suitable variables to be used in the cluster strategy can be a problem in this case due to the availability of a large number of molecular descriptors to undergo subsequent variable selection while developing QSAR predictive models. However, this problem can be solved by using a linear dimensionality reduction technique. In that way useful structural information can be kept as much as possible to be used in the clustering technique without rejecting any descriptor in advance. Principal Component Analysis (PCA) has been used to identify orthogonal directions of maximum variance in the original data projecting it into a lower-dimensionality space formed by a sub-set of the highest-variance components. As a result, the most significant factors produced by the PCA can be the input of the clustering analysis.

2.3. Molecular descriptors

Different sets of 0D, 1D, 2D and molecular descriptors available in the DRAGON (version 5.4) [60], MOE (version 2008.10) [61] and MODESLAB (version 1.5) [62] software has been used in the present work. All them have had a long history in structure-activity and structure-property correlation [25,63–65]. They include, for instance, pure topological descriptors, walk and path counts, connectivity indices, information indices, or 2D-autocorrelations. Taking into account the structural diversity of the compounds an initial subset of descriptors was computed for each molecule from the SMILES (Simplified Molecular Input Line Entry Specification) inputting of chemical structures. By disregarding descriptors with constant or near constant values inside each class, three final subset of 360, 174 and 226 molecular descriptors were generated by using DRAGON, MOE and MODESLAB, respectively.

2.4. Modeling technique

Linear Discriminant Analysis (LDA), specifically the LDA technique implemented in the STATISTICA software (version 8.0) [59], was used to find the classification models (Eq. (1)), that best describe the inhibitory activity *P*, as a linear combination of the predictor *X*-variables (descriptors) weighted by the a_n coefficients:

$$P = a_0 + a_1X_1 + a_2X_2 + \dots + a_nX_n \quad (1)$$

LDA is based on finding the linear combinations with large ratios of between-group to within-group sums of squares [66]. This technique constructs a separating hyperplane between the two groups: e.g. inhibitors and non-inhibitors. The hyperplane is described by the linear discriminant function (Eq. (1)), which is defined by the geometric means between the centroids (i.e. the centers of gravity) of the both groups.

In developing the models, *P* values of 1 and −1 were assigned to inhibitor (or selective) and non-inhibitor (non-selective) group,

respectively. However, posteriori probabilities were used instead to assert the models classification of compounds.

2.5. Feature selection

The Replacement Method (RM) [67] was used as the variable selection procedure, which was implemented in the STATISTICA Visual Basic [59]. Following this method, we observed the variation in the performance of the selected model by minimizing the ROC (Receiver Operating Characteristic) graph Euclidean Distance (ROCED) corrected with FIT (λ) (named here as ROCFIT). The mathematical definition of the ROCFIT parameter has been previously described [68], so we will limit ourselves to a brief outline highlighting only its most important aspects.

By analogy with the FIT Kubinyi function [69,70] used in regression analysis, a similar function has been defined, named FIT (λ), which can be used in the discriminant analysis. FIT (λ) is defined as follows:

$$\text{FIT}(\lambda) = \frac{(1 - \lambda)(n - l - 1)}{(n + l^2)\lambda} \quad (2)$$

where n is the number of cases, l is the number of parameters of our model and λ is the Wilk's lambda. Therefore, a higher value for this parameter means improving the usefulness of our model.

Other parameter, ROCED, has been recently introduced [68]. ROCED is based on the ROC graph, and is useful for organizing classifiers. In a ROC graph, true positives (TP or sensitivity) are plotted on the Y-axis and false positives (FP or 1 – specificity) are plotted on the X-axis. The point (1, 1) represents perfect classification and the line $Y = X$ represents random classification. One point in ROC graph is better than another if it is to the northwest (TP is higher, FP is lower, or both) [71]. Thus, the most finely tuned classifiers are those whose points fall in the left upper triangle as close as possible to the corner.

Fig. 2 shows the plot of the sensitivity vs. 1 – specificity to one classifier and the two points on ROC graph denote the classifications for both training and test sets. The distances d_1 and d_2 are expressed as Euclidean distances and their values represent the distance between the real classifier and the perfect classifier, i.e. point (1, 1). Therefore it is necessary that these two distances are as small as possible. Thus, ROCED, a parameter relating them is defined as follows:

$$\text{ROCED} = (d_1 - d_2 + 1)(d_1 + d_2)(d_2 + 1) \quad (3)$$

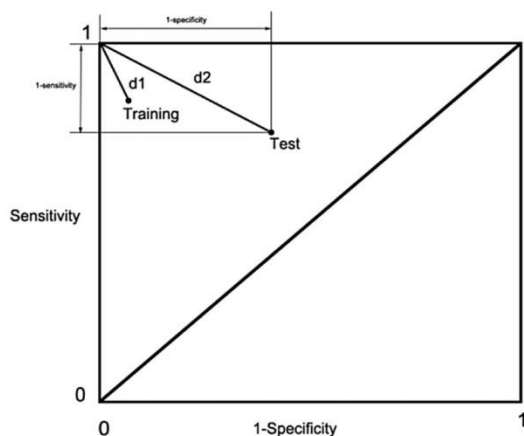


Fig. 2. Distances in a ROC graph for the selection of classification models.

A small ROCED value means improving the performance of our classifier. It was found that the ROCED parameter gets a better balance between sensitivity and specificity for both training and test sets than other indices, like the Wilk's lambda [68]. However when the ROCED parameter was used, some linear discriminant models showed the lower statistical significance [68].

To solve this problem, another parameter (ROCFIT) has been defined (see Eq. (4)). It maintains the ROCED capabilities while improving the significance of the models due to the inclusion of FIT (λ).

$$\text{ROCFIT} = \frac{\text{ROCED}}{\text{FIT}(\lambda)} \quad (4)$$

According with Eq. (4), the best classifiers are those with lower values for both ROCED and ROCFIT and high value for FIT (λ).

In all cases, the calculations were performed for a number of variables between 3 and 12. For the evaluation of the model performance several indexes were calculated for each model (Wilk's lambda, sensibility (Se), specificity (Sp), accuracy (Ac), precision (Pr), enrichment factor (EF) [72], Matthews correlation coefficient (MCC) [73], Robust Initial Enhancement (RIE) [74] and Boltzmann-Enhanced Discrimination of ROC (BEDROC) [75]) based on a prior probability of 0.5 and the area under the ROC curve for both the training and test sets. Most of these indexes are based on the confusion matrix (Table 1), e.g. $\text{Se} = \text{TP}/(\text{TP} + \text{FN})$; $\text{Sp} = \text{TN}/(\text{TN} + \text{FP})$; $\text{Ac} = (\text{TP} + \text{TN})/N$, where $N = \text{TP} + \text{FP} + \text{TN} + \text{FN}$ is the total of compounds in the analyzed set. All calculations were performed with the STATISTICA software [59].

The predictivity of our final models was also evaluated by using an external set of compounds that was not used in the model setup. Validation of the final model with compounds, which are not part of the training set, is a necessary step to ensure generalization, and also of great relevance to future QSAR studies.

2.6. Y-randomization test

To ensure the robustness of a QSAR model we carried out a Y-randomization test [76]. In this test, the Y-vector (response-variable) is randomly swapped and new models are generated. This process is repeated several times (iterations: 300) and the average of the parameters: sensitivity, specificity, accuracy, Wilk's lambda, etc. for each model is reported. It is expected that the resulting classifiers should have lower statistical parameters for training and test sets than the classifiers developed using the real Y-response. If the opposite happens then an acceptable QSAR model cannot be obtained for the specific modeling methods and data, e.g. independent variables of the model are randomly associated to the response variable.

2.7. Applicability domain

There are several methods for assessing the applicability domain (AD) of QSAR models [77–79] but the most common one encompasses determining the leverage values for each compound [80]. Leverage (h) values are calculated for both training and test sets and are computed by Eq. (5).

$$h_{ii} = x_i^T (X^T X)^{-1} x_i \quad (5)$$

where x_i is the descriptor row-vector of the query chemical.

Table 1
Confusion matrix in two cases problem.

		Predicted class	
		Positive	Negative
True class	Positive	TP: true positive	FN: false negative
	Negative	FP: false positive	TN: true negative

These values represent the distance from the chemical to the centroid of the modeled space. A Williams plot, i.e. the plot of standardized residuals versus leverage values (h), was then used for an immediate and simple graphical detection of both the response outliers and structurally-influential chemicals in the model. From this plot, the ADs were established inside a squared area within $\pm x$ standard deviations and a leverage threshold h^* (h^* was generally fixed at $3p'/n$, where n is the number of training compounds and p' the number of model parameters, whereas $x = 2$ or 3), lying outside this area (vertical lines) the outliers and (horizontal lines) the influential chemicals. For predictions, only the predicted activity for chemicals belonging to the chemical domain of the training set should be proposed and used.

2.8. Analysis of the final models

Once the optimization of the models by using RM was concluded, the best and different models were submitted to a consensus process. To this end, we firstly select the models with the best performance and sort them according with the minimization of parameter ROCFIT. Finally, a distance measure between these models was adopted to check the similarity/diversity among the final models [69].

2.9. Consensus

In order to improve the predictions, a series of combinations of the best and diverse QSAR models was carried out. We combined the individual models in each of three ways as follows [81]:

Majority Vote (Unanimity, Simple Majority and Plurality): Considering two classes, that is to say, inhibitors/non-inhibitors or MAO-B selective/MAO-B non-selective, this consensus pattern gives an accurate class label if all classifier are in agreement (Unanimity), at least 50 percent of the classifiers have +1 values (Simple Majority) or most of the classifiers (Plurality) give correct answers [81].

Weighted Majority Vote: If the classifiers in the ensemble do not display identical accuracy, then this consensus pattern gives to the more competent classifiers more power in making the final decision [81].

Naive Bayes: A Bayesian network consists of a structural model and a set of conditional probabilities. Assume that all attributes (molecular descriptors) are fully independent given the class, and then the resulting Bayesian network classifiers are called naive Bayesian classifiers (simply NB). NB uses the following equation to estimate the probability of a test instance x belonging to class c :

$$P(c|x)_{NB} = P(c) \prod_{j=1}^m P(a_j|c) \quad (6)$$

where m is the number of attributes, a_j is the j th attribute value of x , the prior probability $P(c)$ and the conditional probability $P(a_j|c)$. To construct naive Bayes classifiers, we only need to estimate the probability values of $P(c)$ and $P(a_j|c)$, $j = 1, 2, \dots, m$, from the training data [81].

2.10. Chemistry

For the external validation of our strategy, we synthesized 10 new chromone derivatives decorated at 2, 3 positions of the exocyclic aromatic moiety of the carboxamide substituent and 6 position of the chromone nucleus (**450–459**) and inspected their hMAO inhibitory activities and selectivity. The structures, pharmacological profiles of all new synthesized chromones are reported in Table 2, while the general synthetic strategy to get the majority of the chromones is depicted in Scheme 1.

Recently Matos et al. [58] reported the hMAO inhibitory activity of 15 new 3-arylchromone derivatives substituted at 2, 3, 4 and 5 position of the exocyclic aromatic ring and in the C6 of the coumarin scaffold (**460–475**). These compounds were also included into our external validation set. Table 2 reports the structures and hMAO inhibitory activities of these coumarins.

2.11. General

All chemicals used during this research were purchased from Sigma–Aldrich and were *pro analysis* grade.

^1H , and ^{13}C NMR were obtained on a Bruker AMX 300 spectrometer, operating at 300.13 and 75.47 MHz, respectively, at room temperature. Chemical shifts are expressed as δ (ppm) values relative to tetramethylsilane (TMS) as an internal reference; coupling constants (J) are given in Hz. The mass spectra (MS) were obtained using a VG AutoSpec electron impact spectrophotometer and recorded in m/z . Thin-layer-chromatography was carried out on precoated silica gel 60 F254 plates with a layer thickness of 0.2 mm. The spots were visualized under UV detection (254 nm). Normal or flash column chromatography was performed using silica gel 60 0.2–0.5 or 0.040–0.063 mm, respectively. Solvents were partially evaporated using a Büchi Rotavapor.

The synthesis of the *N*-methyl-4-oxo-*N*-phenyl-4*H*-chromene-2-carboxamide (**450**) was performed according the procedure previously described by Borges et al. [22,24]. The structural data was in accordance to that described elsewhere [82,83].

2.12. Synthesis of chromones **451**, **452** and **457**

The Fischer esterification reaction was performed following the procedure by Borges and coworkers [84]. Accordingly, a solution of the chromone carboxylic acid (5 mmol) in 75 ml of the alcohol, containing 2 ml of H_2SO_4 conc., was refluxed for approximately 24 h. After cooling the solvent was partially evaporated and the solution neutralized using NaHCO_3 (5%). After extraction with diethyl ether, the organic phases were combined and washed with water. The solution was dried over Na_2SO_4 anhydrous and the solvent evaporated. The crude product was purified by flash column chromatography.

2.12.1. Propyl-4-oxo-4*H*-benzopyran-2-carboxylate (**451**)

Column chromatographic conditions: silica gel 60 0.040–0.063 and chloroform.

Yield: 52%; ^1H NMR (CDCl_3): 1.05 (3H, t, $J = 7.4$ Hz, $\text{CH}_2\text{CH}_2\text{CH}_3$), 1.76–1.90 (2H, m, $\text{CH}_2\text{CH}_2\text{CH}_3$), 4.37 (2H, t, $J = 6.6$, $\text{CH}_2\text{CH}_2\text{CH}_3$), 7.13 (1H, s, H(3)), 7.46 (1H, ddd, $J = 7.0, 7.7, 1.0$ Hz, (H6)), 7.62 (1H, d, $J = 8.4$ Hz, H(8)), 7.75 (1H, ddd, $J = 8.4, 7.0, 1.6$ Hz, H(7)), 8.21 (1H, dd, $J = 7.7, 1.6$ Hz, (H5)); ^{13}C NMR(CDCl_3): 10.8 ($\text{CH}_2\text{CH}_2\text{CH}_3$), 22.3 ($\text{CH}_2\text{CH}_2\text{CH}_3$), 68.9 ($\text{CH}_2\text{CH}_2\text{CH}_3$), 115.2 C(3), 119.3 C(8), 124.9 C(4a), 126.2 C(5), 126.4 C(6), 135.2 C(7), 152.7 C(8a), 154.2 C(2), 160.2 (COO $\text{CH}_2\text{CH}_2\text{CH}_3$), 179.0 C(4). EM/IE : 232 (M^{+*}).

2.12.2. Propyl-4-oxo-4*H*-benzopyran-3-carboxylate (**452**)

Column chromatographic conditions: silica gel 60 0.040–0.063 and ethyl acetate/dichloromethane (1:9).

Yield: 60%; ^1H NMR (CDCl_3): 1.04 (3H, t, $J = 7.4$ Hz, $\text{CH}_2\text{CH}_2\text{CH}_3$), 1.75–1.84 (2H, m, $\text{CH}_2\text{CH}_2\text{CH}_3$), 4.30 (2H, t, $J = 6.8$ Hz, $\text{CH}_2\text{CH}_2\text{CH}_3$), 7.39–7.47 (2H, m, H(6), H(8)), 7.68 (1H, ddd, $J = 8.4, 7.0, 1.6$ Hz, H(7)), 8.27–8.30 (1H, m, H(5)), 8.66 (1H, s, H(2)); ^{13}C NMR: 10.3 ($\text{CH}_2\text{CH}_2\text{CH}_3$), 21.8 ($\text{CH}_2\text{CH}_2\text{CH}_3$), 68.4 ($\text{CH}_2\text{CH}_2\text{CH}_3$), 114.7 C(3), 118.7 C(8), 124.4 C(4a), 125.6 C(5), 125.8 C(6), 134.7 C(7), 152.2 C(8a), 155.9 C(2), 160.5 (COOPr), 178.4 C(4). EM/IE : 232 (M^{+*}).

Table 2

Chromones and coumarins used as the external validation set along with the observed and predicted inhibitory activity on hMAO-A and hMAO-B and selectivity.

ID	R ₁	R ₂	R ₃	hMAO-A			hMAO-B			hMAO-B selectivity										
				Obs.		Pred. ^c	Obs.		Pred. ^c	Obs.		Pred. ^c	Obs.		Pred. ^c	Obs.				
				pIC ₅₀	C ^a		pIC ₅₀	C ^a		pSI ^d	C ^b		pSI ^d	C ^b		17	18	19	20	21
450	CONCH ₃ Ph	H	H	<4.00	-1	-1	<4.00	-1	-1	-1	-1	-1	0	-1	-1	-1	-1	-1	-1	-1
451	COO(CH ₂) ₂ CH ₃	H	H	<4.00	-1	-1	4.45	-1	-1	-1	-1	-1	>0.45	-1	-1	-1	-1	-1	-1	-1
452	H	COO(CH ₂) ₂ CH ₃	H	<4.00	-1	-1	5.25	1	1	1	1	1	>1.25	-1	-1	1	1	1	1	1
453	COOH	H	Cl	<4.00	-1	-1	<3.00	-1	-1	-1	-1	-1	<-1.00	-1	-1	-1	-1	-1	-1	-1
454	H	COOH	Cl	<4.00	-1	-1	<3.00	-1	1	1	1	1	<-1.00	-1	1	1	1	1	1	1
455	COOCH ₂ CH ₃	H	Cl	<4.00	-1	-1	4.41	-1	-1	-1	-1	-1	>0.41	-1	-1	-1	-1	-1	-1	-1
456	COOCH ₂ CH ₃	H	H	<4.00	-1	-1	<4.00	-1	-1	-1	-1	-1	0	-1	-1	-1	-1	-1	-1	-1
457	H	COOCH ₂ CH ₃	H	<4.00	-1	-1	5.72	1	1	1	1	1	>1.72	1	1	1	1	1	1	1
458	CH ₂ OH	H	H	<4.00	-1	-1	<4.00	-1	-1	-1	-1	-1	0	-1	-1	-1	-1	-1	-1	-1
459	H	CH ₂ OH	H	<4.00	-1	-1	4.42	-1	1	1	1	1	>0.42	-1	-1	1	1	1	1	-1

ID	R	R ₂	R ₃	R ₄	R ₅	hMAO-A											hMAO-B											hMAO-B selectivity										
						Obs.		Pred. ^c	Obs.										Pred. ^c	Obs.		Pred. ^c	Obs.					Pred. ^c	Obs.									
						pIC ₅₀	C ^a		1	2	3	4	5	6	7	8	9	10		11	pIC ₅₀		C ^a	12	13	14	15		16	pSI ^d	C ^b	17	18	19	20	21		
460	OCH ₃	H	CH ₃	H	H	<4.00	-1	-1	-1	-1	-1	-1	1	-1	1	-1	-1	7.77	1	1	1	1	-1	-1	>3.77	1	1	1	1	-1	-1							
461	OCH ₃	H	H	CH ₃	H	<4.00	-1	-1	-1	-1	-1	-1	1	-1	1	-1	-1	8.82	1	1	1	1	1	1	>4.82	1	1	1	1	-1	-1							
462	OH	H	H	CH ₃	H	<4.00	-1	-1	-1	-1	-1	-1	1	1	1	-1	-1	7.17	1	1	-1	1	-1	-1	>2.57	1	1	1	1	-1	-1							
463	C ₃ H ₅ O ₂	H	H	CH ₃	H	<4.00	-1	1	-1	1	1	-1	1	1	1	-1	-1	5.26	1	1	1	1	1	-1	>1.26	-1	-1	-1	-1	-1	-1							
464	C ₅ H ₉ O	H	H	CH ₃	H	<4.00	-1	-1	-1	-1	-1	-1	1	1	1	-1	-1	4.84	1	1	1	1	1	-1	>0.84	-1	-1	-1	-1	-1	-1							
465	CH ₃	H	H	CH ₃	H	<4.00	-1	-1	-1	1	-1	1	1	1	-1	-1	-1	9.51	1	1	1	1	1	-1	>5.51	1	-1	-1	1	-1	-1							
466	CH ₃	H	CH ₃	H	H	<4.00	-1	-1	-1	1	-1	1	1	1	1	-1	-1	7.82	1	1	1	1	-1	-1	>3.82	1	-1	-1	1	-1	-1							
467	CH ₃	H	OCH ₃	OCH ₃	H	<4.00	-1	-1	-1	-1	-1	-1	1	-1	1	-1	-1	8.56	1	1	1	1	-1	-1	>3.96	1	1	1	1	-1	-1							
468	CH ₃	H	Br	OCH ₃	H	<4.00	-1	-1	-1	-1	-1	-1	1	1	1	-1	-1	9.13	1	-1	-1	1	-1	-1	>5.13	1	1	1	1	-1	-1							
469	CH ₃	H	OCH ₃	Br	H	<4.00	-1	-1	-1	-1	-1	-1	1	1	1	-1	-1	8.49	1	1	1	1	1	1	>4.49	1	1	1	1	-1	-1							
470	CH ₃	Br	OCH ₃	H	OCH ₃	<4.00	-1	-1	-1	-1	-1	-1	1	1	1	-1	-1	4.27	-1	-1	-1	-1	-1	-1	>0.27	-1	1	1	1	-1	-1							
471	CH ₃	Br	OCH ₃	OCH ₃	OCH ₃	<4.00	-1	-1	-1	-1	-1	-1	1	1	1	1	<4.00	-1	1	1	1	-1	-1	0	-1	1	-1	1	1	-1	-1							
472	CH ₃	H	OH	H	H	<4.00	-1	-1	-1	-1	-1	-1	1	1	1	-1	-1	6.19	1	-1	1	1	-1	-1	>1.73	1	1	1	1	-1	-1							
473	CH ₃	OH	H	H	H	<4.00	-1	-1	-1	-1	-1	-1	1	1	1	-1	-1	6.92	1	1	-1	-1	-1	-1	>2.25	1	1	1	1	-1	-1							
474	CH ₃	H	C ₃ H ₅ O ₂	H	H	<4.00	-1	1	-1	1	1	1	1	1	-1	-1	-1	6.74	1	-1	1	1	1	1	>2.74	1	-1	-1	-1	-1	-1							

All pIC₅₀ (–log IC₅₀) values shown in this table are negative log-transformation of IC₅₀ values. pIC₅₀ < 4.00 and pIC₅₀ < 3.00 indicate inactive compound at 100 μM (highest concentration tested) and 1 mM (highest concentration tested), respectively. pSI: selectivity to hMAO-B = pIC₅₀ (hMAO-B) – pIC₅₀ (hMAO-A).

^a C: 1 if pIC₅₀ > 4.70 and –1 if pIC₅₀ < 4.70.

^b C: 1 if pSI > 1.70 and –1 if pSI < 1.70.

^c It is referred to the prediction of the ligand class by each model (the models are identified by their numbers in Tables 4–6). The classification represented in bold means unreliable prediction due to it is outside of the AD of the model.

^d pSI is the selectivity to hMAO-B and it is calculated as follow: pSI = pIC₅₀(hMAO-B) – pIC₅₀(hMAO-A).

2.12.3. Ethyl-4-oxo-4H-benzopyran-3-carboxylate (457)

Column chromatographic conditions: silica gel 60 0.040–0.063 and petroleum ether/ethyl acetate (5:5).

Yield: 60%; ¹H NMR (CDCl₃): 1.40 (3H, t, J = 7.1 Hz, CH₂CH₃), 4.36–4.44 (2H, m, CH₂CH₃), 7.30–7.51 (2H, m, H(6), H(8)), 7.71 (1H, ddd, J = 8.4, 7.0, 1.6 Hz, H(7)), 8.26–8.30 (1H, m, H(5)), 8.67 (1H, s, H(2)); ¹³C NMR (CDCl₃): 14.7 (CH₂CH₃), 61.8 (CH₂CH₃), 113.4 C(3), 116.7 C(4a), 118.6 C(8), 125.6 C(5), 126.7 C(6), 134.6 C(7), 152.7 C(8a), 162.2 C(2), 163.7 COOH, 179.5 C(4). EM/IE: 218 (M⁺).

2.13. Synthesis of 6-chloro-4-oxo-4H-benzopyran-2-carboxylic acid (453)

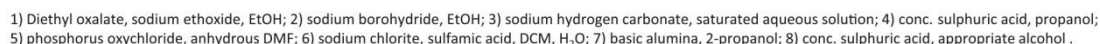
The reaction procedure was adapted from Hadjeri et al. [85]. Accordingly, ethyl-(6-chloro-4-oxo-4H-benzopyran)-2-carboxylate (1.98 mmol) was added to a saturated solution of NaHCO₃

(10 ml) and the reaction was kept at 80 °C for 3 h. After cooling the solution was acidified with HCl conc., diluted into water and extracted with ethyl acetate and dried with Na₂SO₄ anhydrous. After evaporation of the organic phase the crude material was purified by recrystallization from ethyl acetate.

Yield (η): 60%. ¹H NMR (MeOH): 7.15 (1H, s, H(2)), 7.57 (1H, d, J = 8.9 Hz, H(8)), 7.87 (1H, dd, J = 8.9, 2.5 Hz, H(7)), 8.30 (1H, d, J = 2.5 Hz, H(5)). ¹³C NMR (MeOH): 112.9 C(3), 119.4 C(8), 124.1 C(4a), 125.1 C(5), 126.2 C(6), 137.2 C(7), 155.9 C(8a), 163.8 C(2), 179.0 C(4). EM/IE: 226 (M⁺ + 1).

2.14. Synthesis of 6-chloro-4-oxo-4H-benzopyran-3-carboxylic acid (454)

A solution of NaClO₂ 80%, (17 mmol) in water (400 ml) was added dropwise to a mixture of 6-chloro-3-formyl-4-oxo-4H-



Scheme 1. General procedure for preparation of some of the chromones used as external set.

Yield: 48%. ^1H NMR (CDCl_3): 10.37 (1H, s, COOH), 9.02 (1H, s, H(2)), 8.30 (1H, d, $J = 2.6$ Hz, H(5)), 7.81 (1H, dd, $J = 8.97, 2.6$ Hz, H(7)), 7.63 (1H, d, $J = 8.97$ Hz, H(8)). ^{13}C NMR (CDCl_3): 113.3 (C(3), 120.4 (C(8), 124.2 (C(4a), 125.8 (C(5), 126.6 (C(6), 136.5 (C(7), 155.5 (C(8a), 163.7 (C(2), 164.2 COOH, 178.5 (C(4). *EM/IE*: 226 ($\text{M}^+ + 1$).

2.15. Synthesis of chromones **455** and **456**

Yield: 70%; ^1H NMR (CDCl_3): 1.44 (3H, t, $J = 7.1$ Hz, CH_2CH_3), 4.47 (2H, m, CH_2CH_3), 7.12 (1H, s, H(3)), 7.58 (1H, d, $J = 9.0$ Hz, H(8)), 7.68 (1H, dd, $J = 9.0$, 2.5 Hz, H(7)), 8.15 (1H, d, $J = 2.5$ Hz, H(5)) ^{13}C NMR (CDCl_3): 14.1 (CH_2CH_3), 63.1 (CH_2CH_3), 114.6 C(3), 120.5 C(8), 125.1 C(4a), 125.3 C(5), 132.0 C(6), 134.9 C(7), 152.4 C(8a), 154.2 C(2), 160.2 (COOEt), 177.2 C(4). *EM/IE*: 254 ($\text{M} +$) 2, 252 (M^{+}).

Yield: 75%. ^1H NMR (CDCl_3): 1.44 (3H, t, J = 7.1 Hz, $\text{COOCH}_2\text{CH}_3$), 4.48 (2H, m, $\text{COOCH}_2\text{CH}_3$), 7.14 (1H, s, H(3)), 7.46 (1H, dd, J = 8.0, 7.1, 1.0 Hz, H(6)), 7.63 (1H, dd, J = 8.3, 1.0 Hz, H(8)), 7.76 (1H, dd, J = 8.6, 7.0, 1.6 Hz, H(7)), 8.21 (1H, dd, J = 8.5, 1.6 Hz, H(5)). ^{13}C NMR (CDCl_3): 14.1 (CH_2CH_3), 63.0 ($\text{COOCH}_2\text{CH}_3$), 114.8 C(3), 119.0 C(8), 125.2 C(4a), 125.7 C(5), 125.9 C(6), 134.8 C(7), 152.0 C(8a), 155.5 C(2), 162.5 (COOEt), 178.5 C(4). *EM/IE*: 218 (M^{+}).

To a suspension of ethyl-4-oxo-4*H*-benzopyran-2-carboxylate in methanol (40 ml) an equimolar amount of NaBH₄ was added dropwise. The reaction was kept with stirring for 24 h. The solvent was evaporated and the residue was extracted with ethyl ether. The combined organic extracts were washed with water, HCl (1 M) and NaHCO₃ 5% and dried over Na₂SO₄ anhydrous. After evaporation the residue was purified by flash column chromatography (ethyl

acetate/petroleum ether (5:5)), giving rise to the desire product. The reaction procedure was adapted from Payard et al. [88].

Yield: 43%. MP: 167–172 °C. ¹H NMR: 2.95 (1H, t, *J* = 6.7 Hz, CH₂OH), 4.62 (2H, d, *J* = 6.3 Hz, CH₂OH), 6.50 (1H, s, H(3)), 7.40 (1H, ddd, *J* = 7.9, 7.0, 1.0 Hz, H(6)), 7.42 (1H, d, *J* = 8.6 Hz, H(8)), 7.66 (1H, ddd, *J* = 8.6, 7.0, 1.6 Hz, H(7)), 8.18 (1H, dd, *J* = 8.5, 1.6 Hz, H(5)). ¹³C NMR: 61.534 (CH₂OH), 108.4 C(3), 117.9 C(8), 123.9 C(4a), 125.2 C(6), 125.8 C(5), 133.8 C(7), 167.8 C(2), 156.2 C(8a), 178.5 C(4). EM/IE: 176 (M⁺).

2.17. Synthesis of 6-chloro-3-formyl-4-oxo-4H-benzopyran (c)

A solution of 2-hydroxy-5-chloroacetophenone (40 mmol) in anhydrous *N,N*-dimethylformamide (80 ml) was stirred at –10 °C for 30 min. Then POCl₃ (80 mmol) was added dropwise at –10 °C during 1 h. The mixture was stirred at room temperature for 12 h and poured into water (200 ml). After it was extracted with dichloromethane and dried over Na₂SO₄ anhydrous. After evaporation of the filtrate a yellow solid was obtained which was recrystallized from *n*-hexane. The reaction procedure was adapted from Zhao et al. [89].

Yield: 75%. ¹H NMR (CDCl₃): 7.52 (1H, d, *J* = 8.9 Hz, H(8)), 7.71 (1H, dd, *J* = 8.9, 2.6 Hz, H(7)), 8.26 (1H, d, *J* = 2.6 Hz, H(5)), 8.55 (1H, s, H(2)), 10.37 (1H, s, CHO); ¹³C NMR: 120.7 C(4a), 120.8 C(8), 126.1 C(5), 126.7 C(3), 133.3 C(6), 135.5 C(7), 154.9 C(8a), 161.2 C(2), 175.3 C(4), 188.6 (CHO). EM/IE *m/z*: 208 (M⁺ + 1).

2.18. Synthesis of 3-hydroxymethyl-4-oxo-4H-benzopyran (459)

A suspension of formylchromone (5.6 mmol) and basic Al₂O₃ (20 g) in 2-propanol (200 ml) was kept, with stirring, at 75 °C for 4 h. The mixture was filtered by celite and the solvent evaporated. The crude material was purified by flash chromatography (ethyl acetate/petroleum ether (5:5) with gradient elution) and recrystallized from ethanol. The reaction procedure was adapted from Araya-Maturana et al. [90].

Yield: 48%. ¹H NMR (CDCl₃): 3.09 (1H, t, *J* = 6.2 Hz, CH₂OH), 4.60 (2H, d, *J* = 5.6 Hz, CH₂OH), 7.96 (1H, s, H(2)), 7.44 (1H, ddd, *J* = 7.9, 7.6, 0.9 Hz, H(6)), 7.48 (1H, d, *J* = 8.4 Hz, H(8)), 7.70 (1H, ddd, *J* = 8.5, 7.0, 1.6 Hz, H(7)), 8.23 (1H, dd, *J* = 8.0, 1.6 Hz, H(5)). ¹³C NMR (CDCl₃): 58.7 (CH₂OH), 118.3 C(8), 123.1 C(4a), 123.8 C(3), 125.3 C(6), 125.6 C(5), 134.0 C(7), 152.7 C(2), 156.6 C(8a), 178.6 C(4). EM/IE: 176 (M⁺).

2.19. Determination of human MAO isoform activity and selectivity

The evaluations of the MAO inhibitory activity and calculation of the selectivity profile were performed using the experimental

protocol previously described [57]. These assays were developed at Department of Pharmacology of the Faculty of Pharmacy of University of Santiago de Compostela in Spain.

3. Results and discussion

The starting group of molecular descriptors stemming from the Dragon software for the further development of the QSAR study encompassed a total of 450 descriptors. To reduce the number of dimensions to take into account for the cluster analysis without losing much structural information, a PCA, implemented into DRAGON software [60], was carried out.

In doing so, 73 principal components (PC) were calculated in the PCA. However, judging from the magnitude (and significance *p*-levels) of the *F* values, the first principal components of constitutional descriptors (PC01–01), topological descriptors (PC02–01), walk and path counts (PC03–01), connectivity indices (PC04–01), information indices (PC05–01), 2D-autocorrelation (PC-06–01), Burden eigenvalues (PC08–01), eigenvalue-based indices (PC10–01) are the major criteria for assigning cases to clusters (see Table S2 of the Supplementary material). Setting-up these conditions, the *k*-MCA and JTC techniques yielded different clusters for each subset (Table S2 of the Supplementary material). For the hMAO-A inhibition data, the *k*-MCA splits the inhibitor compounds in five clusters comprising 90, 37, 38, 2 and 7 members and the non-inhibitory compounds in six clusters including 78, 98, 35, 37, 27 members. For hMAO-B inhibition data, the *k*-MCA splits the inhibitor compounds in six clusters with 48, 121, 15, 75, 34 and 5 members each other, while the non-inhibitory compounds in four clusters including 59, 34, 38 and 20 members. Finally for the selectivity data the *k*-MCA splits the hMAO-B selective compounds in four clusters each one with 38, 47, 13 and 11 members and the non-selective compounds in five clusters with 65, 23, 151, 84 and 17 members.

The selection of each test set was carried out by leaving out 20% of compounds (specifically one chemical every four chemicals) in each cluster after the cluster was sorted by the Euclidean distance criterion. Table 3 reports the distribution data indicating the number of inhibitors/non-inhibitors and selective/non-selective compounds in training and test sets, whereas Fig. 3 reflects that it is possible to obtain chemically balanced training and test sets. From a structural perspective, the compounds inside all six datasets (three training set and three test set) are highly diverse (Fig. 4). For example, the chemical structures of the inhibitors in the hMAO-B training set fall into at least seven classes, such as chalcones, coumarins, chromones, thiazoles, pyrazoles, homoisoflavonoids and flavonoid derivatives. Therefore, considering the limited chemical diversity in the training set of previous MAO inhibition QSAR models [11,19,27], this work provides a unique, large and

Table 3

Data distribution indicating the number clusters for each subset and the number of compounds for each cluster. In addition Table 3 illustrates the number of inhibitors, non-inhibitors and hMAO-B selective/non-selective compounds in the training and test sets.

Subsets		No. of clusters	Members ^a	Training set	Test set	Total per row
hMAO-A	Non-inhibitors	6	78, 98, 35, 37, 27	220	55	275
	Inhibitors	5	90, 37, 38, 2, 7	140	34	174
	Total per column			360	89	449
hMAO-B	Non-inhibitors	4	59, 34, 38, 20	121	30	151
	Inhibitors	6	48, 121, 15, 75, 34, 5	239	59	298
	Total per column			360	89	449
Selectivity ^b	Non-selective	5	65, 23, 151, 84, 17	272	68	340
	Selective ^c	4	38, 47, 13, 11	88	21	109
	Total per column			360	89	449

^a Number of compounds in each cluster.

^b It referred to selectivity to hMAO-B.

^c It referred to the number of compounds that have IC₅₀(hMAO-A)/IC₅₀(hMAO-B) > 50.

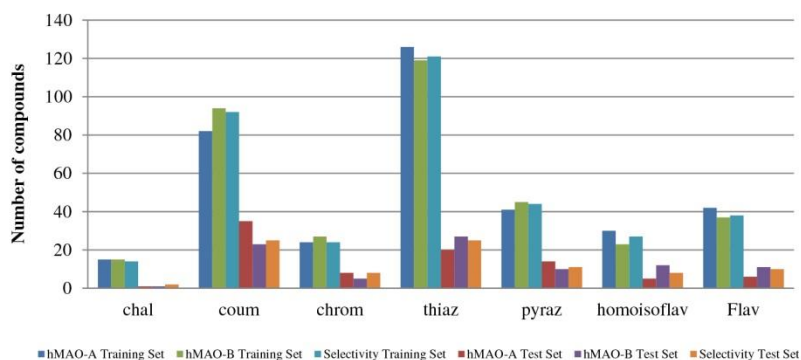


Fig. 3. Distribution representation of the number of compounds by chemical classes in training and test sets. The chemical classes were chalcones (chal), coumarins (coum), chromones (chrom), hydrazone-thiazole derivatives (thiaz), pyrazoles (pyraz), homoisoflavonoids (homoisoflav) and flavonoids (flav).

diverse dataset for modeling *h*MAO inhibitory activity. All these data were measured in one laboratory under strict experimental control [57] and thus represent a valuable source for making QSAR models with a broad applicability, which could be used prospectively to predict possible inhibitory activity for diverse organic compounds.

The first step to obtain the best predictive models derived from the training sets, by combining LDA and RM along with the DRAGON, MOE and TOPS–MODE structural representations, was to select the most significant variables. Toward that end, the RM was carried out as described in the Materials and Methods section. In general, LDA models with Wilk's lambda (λ) and ROCFIT values for the training sets lesser of 0.74 and 3.20 respectively, were accepted. As a consequence, several models were available for each target response. To compare them, we calculated Model distances for pairs of models based in their molecular descriptors [69,91]. These distances take into account the correlation of the molecular descriptors within and between models and allow us to cluster similar models, catching the most diverse models in such a way as to preserve maximum information and diversity. Due to the large amount of statistical information of this procedure, here we only

show the best and different models derived from each molecular descriptor set and for the three target response; *h*MAO-A inhibition, *h*MAO-B inhibition and selectivity to *h*MAO-B (SI) (Table 4 and Table S4 of the Supplementary material). The meaning of each descriptor included in such models is shown in Table S3 of the Supplementary material.

According with the results shown in Table 4 several aspects can be summarized.

The *h*MAO-A models (Model 1–11) produce the best statistical models. Indices like as; Matthews's correlation coefficient (0.71–0.81 for the training set), accuracy (91.11%–85.83% for the training set and 77.53%–88.64% for the test set) sensibility (83.57%–90.00% for the training set and 73.53%–88.24% for the test set) specificity (86.36%–93.18% for the training set and 83.64%–90.91% for the test set) and precision (0.9 and 0.8 for training and test sets, respectively) have the most high values while the ROCFIT (0.34–0.90) parameters and Wilk's lambdas (0.31–0.48) present the most low values. The correlation matrix (Table S5 of the Supplementary material) for each QSAR model also indicates low correlation coefficients between the descriptors, which is desirable in the development of QSAR models based on LDA.

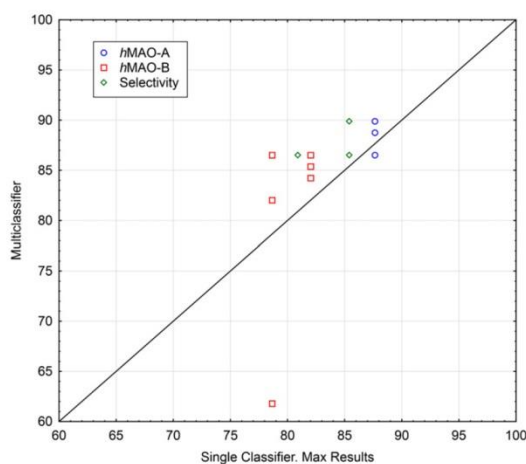


Fig. 4. Comparison of the results from 3 database using the multiclassifiers vs independent classifiers.

Table 4
The final best population of models for hMAO-A, hMAO-B and selectivity datasets.

ID	Subsets	MD	Size	ROCFIT	Training set										Test set										p-Level			
					λ	AUC	MCC	Se	Sp	Ac	EF	Pr	RIE	BEDROC	AUC	MCC	Se	Sp	Ac	Se ^a	Sp ^a	Ac ^a	E	EF		Pr	RIE	BEDROC
1	hMAO-A	Dragon	12	0.34	0.37	0.95	0.77	89.29	88.18	88.61	2.13	0.89	2.53	0.98	0.86	0.74	88.24	87.27	87.64	90.91	87.27	88.64	1	2.12	0.81	2.34	0.89	<0.0001
2		Dragon	10	0.38	0.37	0.95	0.80	90.00	90.91	90.56	2.22	0.90	2.54	0.99	0.88	0.71	79.41	90.91	86.52	79.41	90.91	86.52	0	2.21	0.84	2.46	0.94	<0.0001
3		Dragon	7	0.46	0.45	0.92	0.74	89.29	85.91	87.22	2.06	0.89	2.36	0.92	0.82	0.70	85.29	85.45	85.39	85.29	85.45	85.39	0	2.05	0.78	2.34	0.90	<0.0001
4		Dragon	9	0.48	0.35	0.96	0.81	87.86	93.18	91.11	2.29	0.88	2.45	0.96	0.88	0.62	73.53	87.27	82.02	72.73	88.89	82.76	2	2.05	0.78	2.36	0.90	<0.0001
5	hMAO-B	Dragon	6	0.54	0.43	0.94	0.75	86.43	88.64	87.78	2.13	0.86	2.48	0.96	0.86	0.65	79.41	85.45	83.15	78.79	85.45	82.95	1	2.02	0.77	2.38	0.91	<0.0001
6		Dragon	11	0.60	0.31	0.97	0.81	89.29	91.82	90.83	2.25	0.89	2.56	1.00	0.84	0.52	67.65	83.64	77.53	66.67	83.33	77.01	2	1.88	0.72	2.26	0.86	<0.0001
7		MOE	11	0.46	0.32	0.96	0.81	89.29	91.82	90.83	2.25	0.89	2.55	0.99	0.84	0.57	73.53	83.64	79.78	73.53	83.64	79.78	0	1.92	0.74	2.30	0.88	<0.0001
8		MOE	12	0.46	0.41	0.95	0.78	87.14	91.36	89.72	2.22	0.87	2.55	0.99	0.89	0.70	85.29	85.45	85.39	85.29	85.45	85.39	0	2.05	0.78	2.48	0.95	<0.0001
9	Selectivity	MOE	7	0.52	0.43	0.93	0.74	87.14	87.27	87.22	2.09	0.87	2.47	0.96	0.86	0.72	85.29	87.27	86.52	85.29	87.27	86.52	0	2.11	0.81	2.22	0.85	<0.0001
10		TOPS-MODE	9	0.70	0.48	0.93	0.71	85.00	86.36	85.83	2.05	0.85	2.53	0.99	0.83	0.69	76.47	90.91	85.39	76.47	90.91	85.39	0	2.20	0.76	2.23	0.85	<0.0001
11		TOPS-MODE	8	0.90	0.41	0.93	0.78	83.57	93.18	89.44	2.28	0.84	2.56	1.00	0.78	0.51	58.82	89.09	77.53	58.82	89.09	77.53	0	2.01	0.77	2.23	0.85	<0.0001
12		Dragon	12	1.50	0.54	0.90	0.57	84.10	73.55	80.56	1.30	0.84	1.50	1.00	0.78	0.60	86.44	73.33	82.02	87.93	72.41	82.76	2	1.30	0.86	1.10	0.73	<0.0001
13	hMAO-B	Dragon	11	2.31	0.65	0.86	0.54	78.66	76.86	78.06	1.31	0.79	1.46	0.97	0.78	0.53	77.97	76.67	77.53	79.31	75.86	78.16	2	1.31	0.87	0.79	0.52	<0.0001
14		Dragon	7	2.75	0.63	0.86	0.53	81.17	73.55	78.61	1.29	0.81	1.50	0.99	0.75	0.50	89.83	56.67	78.65	91.38	55.17	79.31	2	1.21	0.80	1.35	0.89	<0.0001
15		MOE	10	2.06	0.62	0.87	0.60	80.75	80.99	80.83	1.35	0.81	1.46	0.97	0.77	0.55	84.75	70.00	79.78	86.21	68.97	80.46	2	1.28	0.85	1.08	0.72	<0.0001
16		MOE	11	2.42	0.69	0.84	0.56	78.66	79.34	78.89	1.33	0.79	1.49	0.99	0.83	0.57	79.66	80.00	79.78	79.31	82.76	80.46	2	1.34	0.89	1.38	0.91	<0.0001
17	Selectivity	Dragon	12	2.03	0.67	0.88	0.55	82.95	79.04	80.00	2.30	0.83	3.43	0.84	0.88	0.63	85.71	83.82	84.27	85.00	84.85	84.88	3	2.63	0.62	2.58	0.61	<0.0001
18		Dragon	11	2.11	0.69	0.88	0.55	81.82	79.04	79.72	2.28	0.82	3.40	0.84	0.84	0.56	80.95	80.88	80.90	80.95	80.88	80.90	0	2.40	0.57	2.82	0.67	<0.0001
19		Dragon	10	2.27	0.72	0.85	0.50	80.68	76.10	77.22	2.14	0.81	3.21	0.79	0.90	0.67	90.48	83.82	85.39	90.48	83.58	85.23	1	2.68	0.63	3.57	0.85	<0.0001
20		MOE	12	2.84	0.74	0.86	0.52	81.82	76.84	78.06	2.18	0.82	2.63	0.65	0.89	0.63	90.48	80.88	83.15	90.48	80.30	82.76	2	2.52	0.59	2.37	0.57	<0.0001
21	MOE																											
22		MOE	12	3.13	0.72	0.86	0.45	78.41	72.43	73.89	1.96	0.78	3.25	0.80	0.87	0.54	85.71	76.47	78.65	85.71	76.47	78.65	0	2.24	0.53	3.27	0.78	<0.0001

MD: the program used to calculate the Molecular Descriptors, ROCHT: Receiver Operating Characteristic graph Euclidean Distance corrected with FIT (λ), λ : Wilk's lambda, AUC: area under the ROC curve, MCC: Matthews correlation coefficient, Se: sensitivity (true positive rate), Sp: specificity (true negative rate), Ac: accuracy, EF: enrichment factor, Pr: precision, RIE: robust initial enhancement, BEDROC: Boltzmann-enhanced discrimination of ROC descriptor.

^a It referred the statistics but considering the applicability domain of the model.

A comparison of the number of models generated to *h*MAO-A, *h*MAO-B inhibitory activities and *h*MAO-B selectivity showed that, the final model population for *h*MAO-A training set (11 models) is higher than the *h*MAO-B (6 models) and selectivity (6 models) datasets.

Among three descriptor sets used in combination with the LDA classification method, DRAGON and MOE descriptors afforded models with higher predictive power than those using TOPS–MODE approach. The TOPS–MODE approach only gave models with higher accuracy for the study of the *h*MAO-A inhibition dataset.

Results of the Y-randomization test (Table S6 in Supplementary material) suggest that all classification models using actual data represent robust quantitative structure–activity correlations. Indeed, none of the models built with randomized activities of the training set had $Ac > 60.00\%$ and $\lambda < 0.97$. Therefore, randomization of values of the inhibitory activity and the selectivity produced no significant models.

3.1. External validation for the QSAR models

In the optimization step of drug discovery the principal application of the present developed QSAR models is the prediction of the *h*MAO inhibitory activity and *h*MAO-B isoform selectivity of ligands that were not used in the model development. To evaluate the prediction capability of our approach, we have considered an additional test set (*external* test set). This is formed by two chemical classes, chromones and coumarins. The first one consists of 10 novel chromone derivatives decorated at 2, 3 of the exocyclic aromatic moiety of the carboxamide substituent and 6 position of the chromone nucleus (**450**–**459**), which have been synthesized and biologically evaluated here for first time (Table 2). The second one involves 15 new experimentally tested coumarins on *h*MAO inhibition, which were published after these QSAR models were developed [58].

The *h*MAO-A and *h*MAO-B inhibition data is reported in Table 2 together with the selectivity index ($SI = IC_{50}hMAO-A/IC_{50}hMAO-B$). The Dragon, MOE and TOPS–MODE molecular descriptors of these new 10 chromones and 15 coumarins have been used as input matrix for the previously generated classifiers (1–21, Table 4). In

most cases, our QSAR models are able to assign the correct class for the external set with at least 70% of accuracy (Table 5), being considered as predictive models. No predictive models were also obtained, for instance Model 16. These results confirm that the validation of the QSAR model using an external test set is an important part of the QSAR analysis [38]. Table 5 also shows that in some models the predictive ability improves when the AD is considered (e.g. model 15, 20, 21). The definition of the AD is useful in the identification of chemicals that fall outside of it and for which the model does less accurate predictions [77].

The best prediction performance is achieved by the *h*MAO-A models. For example, models 2 excellently classify to the 100% of the external set as *h*MAO-A non-inhibitors. By analyzing the statistical class-base parameters, good values of accuracy have been obtained for the *h*MAO-B classifiers ($Ac > 76\%$), with the exception of Model 16. The selectivity models give adequate accuracy results. One out of five selectivity models only gives an accuracy of 76%, the remaining ones only about 70%.

The 10 new chromones derivatives that were included in the external validation set are an outcome of a diverse decoration of chromone scaffold in three different positions. From the data, one can conclude that some chromone derivatives show inhibitory activity toward *h*MAO-B in the micromolar range. The most active chromone **457** and **452** ($IC_{50}(hMAO-B) = 1.89 \pm 0.08 \mu M$ and $5.65 \pm 0.38 \mu M$, respectively) have a carboxylic acid function in the 3 position of γ -pyrone. Compound **457** also shows the highest *h*MAO-B selectivity from the external set ($SI > 52.91$). All chromones in the external set are inactive toward *h*MAO-A. From this chromone data, and in accordance with recent published data of our group [20,21,23], we can conclude that the same type of substitutions on the position-2 of γ -pyrone nucleus causes a total loss of *h*MAO-B inhibitory activity (e.g. **451** vs. **452**, **456** vs. **457**, **458** vs. **459**).

Our selectivity models are able to predict the selectivity toward *h*MAO-B of the compound **457**. But erroneously, most of them also recognize the chromones **452** (models: 18–21), **454** (models: 17–21) and **459** (models: 17–19) as *h*MAO-B selective inhibitors (Table 2), increasing the false positive rate of these single classifiers. A possible explanation to this model fail could be the similar structure of the false positive ligands and other selective ones, e.g.

Table 5

The statistic extracted from the previous QSAR models, using the external set.

ID	Subsets	MD	Se	Sp	Ac	Se ^a	Sp ^a	Ac ^a	Excluded chemicals
1	<i>h</i> MAO-A	Dragon	—	92.00	92.00	—	92.00	92.00	0
2		Dragon	—	100.00	100.00	—	100.00	100.00	0
3		Dragon	—	84.00	84.00	—	84.00	84.00	0
4		Dragon	—	92.00	92.00	—	92.00	92.00	0
5		Dragon	—	88.00	88.00	—	88.00	88.00	0
6		Dragon	—	92.00	92.00	—	92.00	92.00	0
7		MOE	—	40.00	40.00	—	100.00	100.00	15
8		MOE	—	56.00	56.00	—	100.00	100.00	15
9		MOE	—	40.00	40.00	—	76.92	76.92	12
10		TOPS–MODE	—	96.00	96.00	—	96.00	96.00	0
11		TOPS–MODE	—	92.00	92.00	—	92.00	92.00	0
12	<i>h</i> MAO-B	Dragon	86.67	70.00	80.00	86.67	70.00	80.00	0
13		Dragon	86.67	70.00	80.00	86.67	75.00	82.61	2
14		Dragon	80.00	80.00	80.00	80.00	77.778	79.17	1
15		MOE	53.33	90.00	68.00	63.64	90.00	76.19	4
16		MOE	20.00	60.00	36.00	25.00	60.00	40.91	3
17	Selectivity	Dragon	75.00	69.23	72.00	75.00	69.23	72.00	0
18		Dragon	66.67	69.23	68.00	66.67	69.23	68.00	0
19		Dragon	91.67	61.54	76.00	91.67	61.54	76.00	0
20		MOE	8.33	76.92	44.00	100.00	66.67	70.00	15
21		MOE	8.33	76.92	44.00	100.00	66.67	70.00	15

MD: the program used to calculate the Molecular Descriptors. Se: sensitivity (true positive rate), Sp: specificity (true negative rate), Ac: accuracy.

^a It referred the statistics but considering the applicability domain of the model determined by the William's plot.

457 vs. **452** (Table 2). It is interesting to note, that **452** is not selective to hMAO-B, however it is considered by our selectivity models as hMAO-B inhibitor (models: 18–21 in Table 2).

The other 15 chemicals in the external set are the result of several substitutions in 5 different positions, explored to improve their selectivity [58]. Many of them display high hMAO-B inhibitory activity and selectivity with IC₅₀ values in nanomolar range. It confirms that the coumarin nucleus is an attractive scaffold in the MAO inhibitor development, which has been extensively explored to this end [33].

The analysis of the experimental and predicted data of the external set containing coumarins by the above mentioned models supports that the AD definition is essential. For instance, all the compounds excluded from the AD of models 7, 8, 9, 20 and 21 (Tables 2 and 6) are coumarin derivatives and most of them were bad predicted by these classifiers. Then considering the AD of the models, it is noteworthy how most of the selective coumarins in the external set are correctly classified. Some exceptions, regarding the quality of the potency and selectivity predictions are represented for coumarins **468** and **473**. Surprisingly, the majority of the models wrongly predicted them as hMAO-B non-inhibitors (e.g. coumarin: **468** and models: 12, 13 and 15, 16) and then they were perfectly predicted as selective against hMAO-B.

In conclusion, it is indispensable to consider AD of the model in order to make reliable predictions. The comparison of all experimental data with the predicted pharmacological activities by hMAO-A, hMAO-B and selectivity models on the external set demonstrated in general, the good prediction performance of our individual models. However a logical combination of these individual models could improve the theoretical predictions.

3.2. Structural interpretation of the hMAO-B selectivity

The structural interpretation of all models involved in the modeling of three endpoints is a very hard task. So, we only analyzed descriptors with high frequency found in validated hMAO-B selectivity models to elucidate the chemical features that may be responsible for hMAO-B selectivity. The selectivity calculations were performed based on reliable experimental data (see Section Materials and methods). Table 6 lists the top 11 most frequent descriptors found in three validated and different Dragon and two MOE models with both accuracies of training and test sets greater than 74%.

In fact, it is expected that the descriptors selected by the most validated and different models should be critical chemical determinants of the respective biological activity. Among all descriptors families, the contributions of shape descriptors were found to be significant, suggesting a high importance of steric factors in the enzyme selectivity [92].

Thus, the shape-related Dragon/MOE most frequent descriptors in Table 6 are associated with van der Waals volumes or areas, such as MATS3v, PEOE_VSA + 1 and Q_VSA_FNEG and one is related with self-returning walk count of order 5 (SRW05). The latter is closely related with the presence of five member rings in the chemical structure and it was found that the presence of these rings occurs predominantly in non-selective ligands. This finding is in agreement with the previous SAR results obtained with a series of N1-thiocarbamoyl-3,5-di(hetero)aryl-4,5-dihydro-(1H)-pyrazole derivatives [52] where the simultaneous presence of heteroaromatic substituents in 3- and 5-position of the pyrazoline ring (e.g. compounds **379**, **380**, **384** and **385**, Table S1 of the Supplementary material) leads to a decrease in the potency and selectivity for the hMAO-B activity.

Consistently, three of the most frequent descriptors are based on the counting of atom-centered fragments, C-019 and of chemical functional groups, nArCO and nCrS, and bonds (b_1rotN). The first one (C-019) describes the =CRX fragment (Table 7), where R represents any group linked through carbon; X represents any electronegative atom (O, N, S, P, Se, halogens) and = represents a double bond. This fragment is included mainly in non-selective ligands (Table 7) and it is in correspondence with experimental evidences. For instance, Borges et al. found that chromones with substituents at the position 2 of γ -pyrone nucleus (e.g. chromone **76**, Table 7) in general gives rise to a total loss of activity while the same type of substitutions at the position 3 of γ -pyrone nucleus act preferably as hMAO-B inhibitors and are hMAO-B selective [20,23]. In addition, Santana et al. also found that coumarins with electronegative groups substituted at the position 3 of γ -pyrone nucleus (e.g. coumarin **102**, Table 7) decrease the hMAO-B selectivity [28]. In contrast to previous referred descriptor, the chemical group that represents to aromatic ketones (nArCO) can be mapped onto selective and non-selective molecules. However, it can be found predominantly in selective ligands, especially in compounds **260–294** (Table S1 of the Supplementary material). These 35 chemicals belong to the homoisoflavonoid family, of which 19 are

Table 6
Symbols and definitions of more frequent variables in selectivity models.

Symbols	Means	Frequency			Total
		hMAO-A	hMAO-B	Selectivity	
<i>Dragon</i>					
nCrS	Number of ring secondary C(sp ³)	0	0	3	3
AMW	Average molecular weight	0	0	2	2
C-019	=CRX, where R represents any group linked through carbon; X represents any electronegative atom (O, N, S, P, Se, halogens) and = represents a double bond.	0	3	2	5
GATS3p	Geary autocorrelation – lag 3/weighted by atomic polarizabilities	0	0	2	2
MATS3v	Moran autocorrelation – lag 3/weighted by atomic van der Waals volumes	1	0	2	3
nArCO	Number of ketones (aromatic)	0	0	2	2
SRW05	Self-returning walk count of order 05	0	0	2	2
<i>MOE</i>					
b_1rotN	Number of rotatable single bonds. Conjugated single bonds are not included (e.g., ester and peptide bonds)	0	1	2	3
GCUT_PEOE_2	The GCUT descriptors are calculated from the eigenvalues of a modified graph distance adjacency matrix. Each <i>ij</i> entry of the adjacency matrix takes the value 1/sqr(<i>dij</i>) where <i>dij</i> is the (modified) graph distance between atoms <i>i</i> and <i>j</i> . The diagonal takes the value of the PEOE partial charges. The resulting eigenvalues are sorted and the smallest, 1/3 ile, 2/3-ile and largest eigenvalues are reported.	0	0	2	2
PEOE_VSA + 1	Sum of <i>v_i</i> where <i>q_i</i> is in the range [0.05,0.10].	0	0	2	2
Q_VSA_FNEG	Fractional negative van der Waals surface area. This is the sum of the <i>v_i</i> such that <i>q_i</i> is negative divided by the total surface area. The <i>v_i</i> values are calculated using a connection table approximation.	0	0	2	2

In bold is marked the variable frequencies. Frequency is the number of times each descriptor occurred in the 5 validated and different selectivity models (Table 5).

Table 7
Structural representation of counting of atom-centered fragments and of chemical functional groups.

Descriptors	Structural representation of the descriptors	Example of compounds
C-019: =CRX		Chemicals 76 , 102 and 402 (C-019 = 1). Non-selective ligands (76) chromone (102) coumarin (402) flavonoid
nArCO: number of ketones (aromatic)	 Y = Al or Ar	Chemicals 270 (nArCO = 1). Selective ligand (270) homoisoflavonoid
nCrS: number of ring secondary C(sp ³)	 Y: H or any heteroatom	Chemical 343 (nCrS = 4). Selective ligand (343) hydrazine

R: any group linked through carbon; Al: aliphatic chain linked through carbon unless otherwise stated; Ar: aromatic ring linked through carbon unless otherwise stated; X: O, N, S, P, Se, halogens.

selective ligands and 16 are non-selective. It is interesting to note that exactly the similar behavior presents nCrS and b₁rotN descriptors, which represent number of ring secondary C(sp³) and rotatable single bonds, respectively. They can be found in selective and non-selective ligands.

Another molecular descriptor that was frequently present was the average of molecular weight (AMW), Geary autocorrelation – lag 3/ weighted by atomic polarizabilities (GAT3p) and descriptors calculated from the eigenvalues of a modified graph distance adjacency matrix, weighted with partial charges (GCUT_PEOE_2).

The results of more frequent descriptors analysis reinforce our knowledge of the subtype selectivity and may potentially provide important hints useful in the design of hMAO-B selective inhibitors. In addition to that, these molecular descriptors were derived from molecular structure using low computational resources, making them very attractive and widely used in Medicinal Chemistry [25].

3.3. Consensus predictions of inhibition activity (pIC₅₀) and hMAO-B selectivity for compounds used as test sets and external validation set for the hMAO ligand datasets

Even though the predictive ability of individual models was, in general, good, we have applied the model consensus in an attempt to improve the accuracy on the predictions. By this method, the best classifiers (Table 4) were combined to create more useful multi-classifiers. The multi-classifier accuracy achieved by using different subsets of individual classifiers and different output combination (majority vote, weighted majority vote and Naive Bayes) is shown in Table 8. To evaluate the prediction capability of these combinatorial QSAR approaches, the test set and an additional test set (*external set*, Table 2), consisting of 10 novel chromone derivatives (**450–459**) and 15 coumarins (**460–475**) were considered.

hMAO-A inhibition. Two single classifier combinations resulted to this set, identified in Table 8 as (1 + 2 + 5 + 8 + 9 + 10) and

Table 8
Multiclassifier accuracy results using different subsets of single classifiers and different output combination.

Biological activity	Sets	Single classifier combinations ^a	Single classifier results Max result ^b	Multiclassifier results				
				Majority vote			Weighted majority vote	Naïve Bayes
				Unanimity	Simple	Plurality		
<i>h</i> MAO-A	Test set	1 + 2 + 5 + 8 + 9 + 11	87.64 (88.64)	89.89	89.89	89.89	86.52	88.76
		1 + 2 + 5 + 8 + 9 + 10	87.64 (88.64)	88.76	88.76	88.76	89.89	89.89
	External set	1 + 2 + 5 + 8 + 9 + 11	100	76.00 (100.00)	80.00 (95.24)	96.00	96.00	96.00
		1 + 2 + 5 + 8 + 9 + 10	100	76.00 (100.00)	80.00 (100.00)	96.00	96.00	96.00
<i>h</i> MAO-B	Test set	13 + 14	78.65 (79.31)	86.52	86.52	86.52	61.80 (91.67)	82.02
		12 + 13 + 14 + 16	82.02 (82.76)	84.23 (86.21)	85.39	84.23 (86.21)	57.30 (86.44)	86.52
	External set	13 + 14	80 (82.61)	72.00 (85.71)	68.00 (89.47)	72.00 (85.71)	80.00	88.00
		12 + 13 + 14 + 16	80 (82.61)	20.00 (83.33)	68.00 (89.47)	84.00 (87.50)	84.00	88.00
<i>h</i> MAO-B selectivity	Test set	18 + 19	85.39 (85.23)	89.89	89.89	89.89	41.57 (97.37)	86.52
		18 + 21	80.90	86.52	86.52	86.52	86.52 (87.50)	86.52
		17 + 18 + 19 + 21	85.39 (85.23)	88.76	88.76	88.76	26.97 (92.31)	89.89
	External set	18 + 19	76.00	64.00 (76.19)	64.00 (76.19)	64.00 (76.19)	68.00	68.00
		18 + 21	68.00 (70.00)	64.00 (69.56)	24.00 (75.00)	64.00 (69.56)	68.00	72.00
		17 + 18 + 19 + 21	76.00	60.00 (83.33)	64.00 (76.19)	68.00	68.00	68.00

In brackets are the accuracies, taking into account the application domain of the single classifiers.

^a It only showed the best single classifier combinations. The numbers of this column mean the identification code of the classifier (ID) showed in Table 5.

^b It is the best accuracy obtained from the single classifiers that combined to form the multiclassifier.

(1 + 2 + 5 + 8 + 9 + 11). Both combinations of the individual models have a max accuracy of 89.89% for the test set and 100%, considering the AD, for the external validation set. In the test set case our multiclassifiers achieved higher accuracy than individual classifiers (87.64%), while in the external set case, the accuracy of the multiclassifiers was only the same to the single classifier when the AD was taken into account.

*h*MAO-B inhibition. Like to *h*MAO-A inhibition, two best combination of single models were obtained to the *h*MAO-B dataset (13 + 14) and (12 + 13 + 14 + 16). The best classifications of individual models and their combinations are given in Table 8 for test and external sets. To the test set, our multi-classifiers got better accuracy than single classifiers (i.e. (13 + 14) combination: from 78.65% to 86.52% and (12 + 13 + 14 + 16) combination: from 82.02% to 86.52%). If the AD of the single models is taken into account, then it greatly increased (from 79.31% to 91.67%). To the external set the accuracy of multi-classifiers was higher than single classifiers if the AD is considered. However, when the Naïve Bayes consensus pattern was used as combination of individual models (without consider the AD), the accuracy of both multi-classifiers increased to 88.00%.

*h*MAO-B selectivity. To this dataset, three combinations of individual models (18 + 19; 18 + 21; 17 + 18 + 19 + 21) were considered as the best ones. Generally to the test set the multi-classifiers have higher accuracy than the individual models (Table 8). In contrast, the combinations perform poorly for the external set, but this scenario changes when the AD is considered. Particularly, when the unanimity consensus pattern is used as combination of individual models and the AD of single models is also taken into account, the accuracy of one multi-classifier (17 + 18 + 19 + 21) increased from 60.00% to 83.33%. In the unanimity consensus pattern a prediction is given if all models are in agreement.

To summarize, Fig. 4 shows the comparisons between the proposed QSAR models combinations and the best results of the single classifiers, considering the test set predictions. Each dot represents a comparison: if the point lies above the line means that our multi-classifiers achieved higher accuracy than individual classifiers. Thus, in general combinations of multiple classifiers have been found to be consistently more accurate than a single classifier, increasing our chance for success. In addition it important

to consider the AD definition for the single classifiers, due it improves the predictions of them and their combinations. These results confirm the importance of employing the combinatorial QSAR approach to reach the goal of finding the most predictive QSAR method/descriptor combination for each specific dataset.

4. Conclusions

This work provided a unique, large and diverse dataset for modeling *h*MAO inhibitory activity. All these data were measured in one laboratory under strict experimental control, so they represent a valuable source for making QSAR models with a broad applicability. On this database, a novel classifier combining 0D, 1D and 2D molecular descriptors along with Linear Discriminant Analysis and the Replacement Method as the variable selection method was presented as a powerful tool for the prediction of *h*MAO-A and *h*MAO-B inhibitory activities and to infer about the selectivity toward *h*MAO-B of new chromones derivatives. Twenty one statistically meaningful and structurally diverse models have been generated from the same training set by using different endpoints: *h*MAO-A inhibition, *h*MAO-B inhibition and selectivity toward *h*MAO-B, and positive results were achieved in the validation procedure. The interpretation of the models allowed derivate some chemical features, which can be considered important in the *h*MAO-B selectivity. For instance, the presence of five member rings or the =CRX fragment (R: any group linked through carbon; X: electronegative atom and =: double bond) in the chemical structure decreases the selectivity. The predictive ability of individual model was acceptable, but the combinatorial QSAR approach improved our predictive results. Thus the application of individual models and especially, their combinations were able to assign with acceptable accuracy the *h*MAO inhibitory activity and selectivity of an external set, conformed by 10 new chromones derivatives described here for first time and 15 coumarins, recently reported in the literature.

The QSAR methodology presented in this paper reflects recent progress made in our groups toward successful QSAR modeling of human MAO inhibition. All models and their combinations used in our study are available on request of the Medicinal Chemistry Community.

Acknowledgments

Foundation for Science and Technology (FCT), European Social Fund and the Programme for human potential (POPH), Portugal, COMPETE/QREN/EU and AECID (projects PTDC/QUI/70359/2006, PTDC/QUI-QUI/113687/2009 and D/024153/09) are acknowledged for financial support. The authors acknowledge FCT grants (SFRH/BPD/63946/2009; SFRH/BD/43531/2008 and SFRH/BPD/74491/2010).

Appendix A. Supplementary material

Supplementary data related to this article can be found at <http://dx.doi.org/10.1016/j.ejmech.2012.10.035>.

References

- [1] L.W. Elmer, J.M. Bertoni, The increasing role of monoamine oxidase type B inhibitors in Parkinson's disease therapy, *Expert Opin. Pharmacother.* 9 (2008) 2759–2772.
- [2] J.J. Chen, D.M. Swope, K. Dashtipour, Comprehensive review of rasagiline, a second-generation monoamine oxidase inhibitor, for the treatment of Parkinson's disease, *Clin. Ther.* 29 (2007) 1825–1849.
- [3] M.B. Youdim, D. Edmondson, K.F. Tipton, The therapeutic potential of monoamine oxidase inhibitors, *Nat. Rev. Neurosci.* 7 (2006) 295–309.
- [4] D.S. Knudsen Gerber, Selegiline and rasagiline: twins or distant cousins? guidelines, *Consult Pharm.* 26 (2011) 48–51.
- [5] J.J. Chen, D.M. Swope, Pharmacotherapy for Parkinson's disease, *Pharmacotherapy* 27 (2007) 1615–1735.
- [6] J.K. Mallajosyula, D. Kaur, S.J. Chinta, S. Rajagopalan, A. Rane, D.G. Nicholls, D.A. Di Monte, H. MacArthur, J.K. Andersen, MAO B elevation in mouse brain astrocytes results in Parkinson's pathology, *PLoS One* 3 (2008) e1616.
- [7] J.S. Fowler, J. Logan, N.D. Volkow, G.J. Wang, R.R. MacGregor, Y.S. Ding, Monoamine oxidase: radiotracer development and human studies, *Methods* 27 (2002) 263–277.
- [8] C.M. Vandenberg, MAOIs and transdermal delivery, *J. Clin. Psychiatry* 73 (2012) e28.
- [9] A.A. Patkar, C.U. Pae, P.S. Masand, Transdermal selegiline: the new generation of monoamine oxidase inhibitors, *CNS Spectrum* 11 (2006) 363–375.
- [10] O. Weinreb, T. Amit, O. Bar-Am, M. Yegor-Falach, M.B. Youdim, The neuroprotective mechanism of action of the multimodal drug lisdostigil, *Front. Biosci. J. Virtual Libr.* 13 (2008) 5131–5137.
- [11] M.B. Núñez, F.P. Maguna, N.B. Okulika, E.A. Castro, QSAR modeling of the MAO inhibitory activity of xanthenes derivatives, *Bioorg. Med. Chem. Lett.* 14 (2004) 5611–5617.
- [12] L. Pisani, G. Muncipinto, T. Miscioscia, I.O. Nicolotti, F. Leonetti, M. Catto, C. Caccia, P. Salvati, R. Soto-Otero, E. Mendez-Alvarez, C. Passeleu, A. Carotti, Discovery of a novel class of potent coumarin monoamine oxidase B inhibitors: development and biopharmacological profiling of 7-[(3-chlorobenzyl)oxy]-4-[(methylamino)methyl]-2H-chromen-2-one methanesulfonate (NW-1772) as a highly potent, selective, reversible, and orally active monoamine oxidase B inhibitor, *J. Med. Chem.* 52 (21) (2009) 6685–6706.
- [13] M.J. Matos, D. Vina, C. Picciau, F. Orallo, L. Santana, E. Uriarte, Synthesis and evaluation of 6-methyl-3-phenylcoumarins as potent and selective MAO-B inhibitors, *Bioorg. Med. Chem. Lett.* 19 (2009) 5053–5055.
- [14] M.J. Matos, D. Vina, E. Quezada, C. Picciau, G. Delogu, F. Orallo, L. Santana, E. Uriarte, A new series of 3-phenylcoumarins as potent and selective MAO-B inhibitors, *Bioorg. Med. Chem. Lett.* 19 (2009) 3268–3270.
- [15] N. Gökhan-Kelekçi, O. Simsek, A. Ercan, K. Yelekçi, Z. Sahin, S. İşik, G. Uçar, A. Bilgin, Synthesis and molecular modeling of some novel hexahydroindazole derivatives as potent monoamine oxidase inhibitors, *Bioorg. Med. Chem.* 17 (18) (2009) 6761–6772.
- [16] L.H. Prins, J.P. Petzer, S.F. Malan, Inhibition of monoamine oxidase by indole and benzofuran derivatives, *Eur. J. Med. Chem.* 45 (2010) 4458–4466.
- [17] R. Fioravanti, A. Bolasco, F. Manna, F. Rossi, F. Orallo, M. Yáñez, A. Vitali, F. Ortuso, S. Alcaro, Synthesis and molecular modelling studies of prenylated pyrazolines as MAO-B inhibitors, *Bioorg. Med. Chem. Lett.* 20 (2010) 6479–6482.
- [18] J. Wouters, F. Ooms, S. Jegham, J.J. Koenig, P. George, F. Durant, Reversible inhibition of type B monoamine oxidase. Theoretical study of model diazo heterocyclic compounds, *Eur. J. Med. Chem.* 32 (1997) 721–730.
- [19] S. Kneubühler, U. Thull, C. Altomare, V. Carta, P. Gaillard, P.A. Carrupt, A. Carotti, B. Testa, Inhibition of monoamine oxidase-b by 5H-Indeno[1,2c]pyridazines: biological activities, quantitative structure-activity relationships (QSARs) and 3D-QSARs, *J. Med. Chem.* (1995) 3874–3883.
- [20] S. Alcaro, A. Gaspar, F. Ortuso, N. Milhazes, F. Orallo, E. Uriarte, M. Yáñez, F. Borges, Chromone-2- and -3-carboxylic acids inhibit differently monoamine oxidases A and B, *Bioorg. Med. Chem. Lett.* 20 (2010) 2709–2712.
- [21] A. Gaspar, J. Reis, A. Fonseca, N. Milhazes, D. Vina, E. Uriarte, F. Borges, Chromone 3-phenylcarboxamides as potent and selective MAO-B inhibitors, *Bioorg. Med. Chem. Lett.* 21 (2011) 707–709.
- [22] A. Gaspar, F. Teixeira, E. Uriarte, N. Milhazes, A. Melo, N.D.S. Cordeiro, F. Ortuso, S. Alcaro, F. Borges, Towards the discovery of a novel class of monoamine oxidase inhibitors: structure–property–activity and docking studies on chromone amides, *ChemMedChem* 6 (2011) 628–632.
- [23] A. Gaspar, T. Silva, M. Yáñez, D. Vina, F. Orallo, F. Ortuso, E. Uriarte, S. Alcaro, F. Borges, Chromone a privileged scaffold for the development of monoamine oxidase inhibitors, *J. Med. Chem.* 54 (2011) 5165–5173.
- [24] F. Chimenti, A. Bolasco, F. Manna, D. Secci, P. Chimenti, A. Granese, O. Befani, P. Turini, R. Cirilli, F. La Torre, S. Alcaro, F. Ortuso, T. Langer, Synthesis, biological evaluation and 3D-QSAR of 1,3,5-Trisubstituted-4,5-Dihydro-(1H)-pyrazole derivatives as potent and highly selective monoamine oxidase A inhibitors, *Curr. Med. Chem.* 13 (2006) 1411–1428.
- [25] A. Helguera, R. Combes, M. González, N. Cordeiro, Applications of 2D descriptors in drug design: a DRAGON tale, *Curr. Top. Med. Chem.* 8 (2008) 1628–1655.
- [26] A.E. Medvedev, A.V. Veselovsky, V.I. Shvedov, O.V. Tikhonova, T.A. Moskvitina, O.A. Fedotova, L.N. Azenova, N.S. Kamyshanskaya, A.Z. Kirek, A.S. Ivanov, Inhibition of monoamine oxidase by pirlindole analogues: 3D-QSAR and CoMFA analysis, *J. Chem. Inf. Comput. Sci.* 38 (1998) 1137–1144.
- [27] C. Gnerre, M. Catto, F. Leonetti, P. Weber, P.A. Carrupt, C. Altomare, A. Carotti, B. Testa, Inhibition of monoamine oxidases by functionalized coumarin derivatives: biological activities, QSARs, and 3D-QSARs, *J. Med. Chem.* 43 (2000) 4747–4758.
- [28] L. Santana, H. González-Díaz, E. Quezada, E. Uriarte, M. Yáñez, D. Viña, F. Orallo, Quantitative structure-activity relationship and complex network approach to monoamine oxidase A and B inhibitors, *J. Med. Chem.* 51 (2008) 6740–6751.
- [29] Y.C. Martin, J.B. Holland, C.H. Jarboe, N. Plotnikoff, Discriminant analysis of the relationship between physical properties and the inhibition of monoamine oxidase by aminotetralins and aminoindans, *J. Med. Chem.* 17 (1974) 409–413.
- [30] A. Gallardo-Godoy, A. Fierro, T.H. McLean, M. Castillo, B.K. Cassels, M. Reyes-Parada, D.E. Nichols, Sulfur-substituted *n*-alkyl phenethylamines as selective and reversible MAO-A inhibitors: biological activities, CoMFA analysis, and active site modeling, *J. Med. Chem.* 48 (2005) 2407–2419.
- [31] W.T. Harkcom, D.R. Bevan, Molecular docking of inhibitors into monoamine oxidase B, *Biochem. Biophys. Res. Commun.* 360 (2007) 401–406.
- [32] F. Chimenti, D. Secci, A. Bolasco, P. Chimenti, A. Granese, S. Carradori, E. Maccioni, M.C. Cardia, M. Yáñez, F. Orallo, S. Alcaro, F. Ortuso, R. Cirilli, R. Ferretti, S. Distinto, J. Kirchmair, T. Langer, Synthesis, semipreparative HPLC separation, biological evaluation, and 3D-QSAR of hydrazothiazole derivatives as human monoamine oxidase Binhibitors, *Bioorg. Med. Chem.* 18 (2010) 5063–5070.
- [33] M. Reyes-Parada, A. Fierro, P. Iturriaga-Vásquez, B.K. Cassels, Monoamine oxidase inhibition in the light of new structural data, *Curr. Enzym. Inhib.* 1 (2005) 85–95.
- [34] J. Bajorath, Methods in molecular biology, in: J.M. Walker (Ed.), *Chemo-informatics: Concepts, Methods, and Tools for Drug Discovery*, Humana Press Inc., Totowa, New Jersey, 2004.
- [35] C. Lemmen, T. Lengauer, Computational methods for the structural alignment of molecules, *J. Comput. Aided Mol. Des.* 14 (2000) 215–232.
- [36] C. Binda, M. Li, F. Hubalek, N. Restelli, D.E. Edmondson, A. Mattevi, Insights into the mode of inhibition of human mitochondrial monoamine oxidase B from high-resolution crystal structures, *Proc. Natl. Acad. Sci. U. S. A.* 100 (2003) 9750–9755.
- [37] S.Y. Son, J. Ma, Y. Kondou, M. Yoshimura, E. Yamashita, T. Tsukihara, Structure of human monoamine oxidase A at 2.2-Å resolution: the control of opening the entry for substrates/inhibitors, *Proc. Natl. Acad. Sci. U. S. A.* 105 (2008) 5739–5744.
- [38] A. Tropsha, P. Gramatica, V.K. Gombar, The importance of being earnest: validation is the absolute essential for successful application and interpretation of QSPR models, *QSAR Comb. Sci.* 22 (2003) 69–77.
- [39] J.A. Moron, M. Campillo, V. Pérez, M. Unzeta, L.J. Pardo, Molecular determinants of MAO selectivity in a series of indolylmethylamine derivatives: biological activities, 3D-QSAR/CoMFA analysis, and computational simulation of ligand recognition, *J. Med. Chem.* 43 (2000) 1684–1691.
- [40] M. Li, F. Hubalek, P. Newton-Vinson, D.E. Edmondson, High-level expression of human liver monoamine oxidase A in *Pichia pastoris*: comparison with the enzyme expressed in *Saccharomyces cerevisiae*, *Protein Expr. Purif.* 24 (2002) 152–162.
- [41] P. Newton-Vinson, F. Hubalek, D.E. Edmondson, High-level expression of human liver monoamine oxidase B in *Pichia pastoris*, *Protein Expr. Purif.* 20 (2000) 334–345.
- [42] C. Binda, F. Hubalek, M. Li, Y. Herzog, J. Sterling, D.E. Edmondson, A. Mattevi, Crystal structures of MAO B in complex with four inhibitors of the N-propargylaminoindan class, *J. Med. Chem.* 47 (2004) 1767–1774.
- [43] F. Chimenti, R. Fioravanti, A. Bolasco, P. Chimenti, D. Secci, F. Rossi, M. Yáñez, F. Orallo, F. Ortuso, S. Alcaro, Chalcones: a valid scaffold for monoamine oxidases inhibitors, *J. Med. Chem.* 52 (2009) 2818–2824.
- [44] F. Chimenti, D. Secci, A. Bolasco, P. Chimenti, B. Bizzarri, A. Granese, S. Carradori, M. Yáñez, F. Orallo, F. Ortuso, S. Alcaro, Synthesis, molecular modeling, and selective inhibitory activity against human monoamine oxidases of 3-carboxamido-7-substituted coumarins, *J. Med. Chem.* 52 (2009) 1935–1942.
- [45] F. Chimenti, S. Carradori, D. Secci, A. Bolasco, P. Chimenti, A. Granese, B. Bizzarri, Synthesis and biological evaluation of novel conjugated coumarin-thiazole systems, *J. Heterocycl. Chem.* 46 (2009) 575–578.

- [46] F. Chimentì, D. Secci, A. Bolasco, P. Chimentì, A. Granese, S. Carradori, M. Yáñez, F. Orallo, M.L. Sanna, B. Gallinella, R. Cirilli, Synthesis, stereochemical separation, and biological evaluation of selective inhibitors of human MAO-B: 1-(4-arylthiazol-2-yl)-2-(3-methylcyclohexylidene)hydrazines, *J. Med. Chem.* 53 (2010) 6516–6520.
- [47] F. Chimentì, D. Secci, A. Bolasco, P. Chimentì, A. Granese, S. Carradori, M. D'Ascenzio, M. Yáñez, F. Orallo, Synthesis and selective inhibition of human monoamine oxidases of a large scaffold of (4,5-substituted-thiazol-2-yl) hydrazones, *Med. Chem. Commun.* 1 (2010) 61–72.
- [48] N. Desideri, A. Bolasco, R. Fioravanti, L.P. Monaco, F. Orallo, M. Yáñez, F. Ortuso, S. Alcaro, Homoisoflavonoids: natural scaffolds with potent and selective monoamine oxidase-B inhibition properties, *J. Med. Chem.* 54 (2011) 2155–2164.
- [49] E. Maccioni, S. Alcaro, F. Orallo, M.C. Cardia, S. Distinto, G. Costa, M. Yáñez, M.L. Sanna, S. Vigo, R. Meleddu, D. Secci, Synthesis of new 3-aryl-4,5-dihydropyrazole-1-carbothioamide derivatives. An investigation on their ability to inhibit monoamine oxidase, *Eur. J. Med. Chem.* 45 (2010) 4490–4498.
- [50] M.J. Matos, D. Vina, P. Janeiro, F. Borges, L. Santana, E. Uriarte, New halogenated 3-phenylcoumarins as potent and selective MAO-B inhibitors, *Bioorg. Med. Chem. Lett.* 20 (2010) 5157–5160.
- [51] F. Chimentì, A. Bolasco, D. Secci, P. Chimentì, A. Granese, S. Carradori, M. Yáñez, F. Orallo, F. Ortuso, S. Alcaro, Investigations on the 2-thiazolylhydrazine scaffold: synthesis and molecular modeling of selective human monoamine oxidase inhibitors, *Bioorg. Med. Chem.* 18 (2010) 5715–5723.
- [52] F. Chimentì, S. Carradori, D. Secci, A. Bolasco, B. Bizzarri, P. Chimentì, A. Granese, M. Yáñez, F. Orallo, Synthesis and inhibitory activity against human monoamine oxidase of N1-thiocarbamoyl-3,5-di(hetero)aryl-4,5-dihydro-(1H)-pyrazole derivatives, *Eur. J. Med. Chem.* 45 (2010) 800–804.
- [53] F. Chimentì, R. Fioravanti, A. Bolasco, P. Chimentì, D. Secci, F. Rossi, M. Yáñez, F. Orallo, F. Ortuso, S. Alcaro, R. Cirilli, R. Ferretti, M.L. Sanna, A new series of flavones, thioflavones, and flavanones as selective monoamine oxidase-B inhibitors, *Bioorg. Med. Chem.* 18 (2010) 1273–1279.
- [54] N.E. Vergel, J.L. Lopez, F. Orallo, D. Vina, D.M. Buitrago, E. del Olmo, J.A. Mico, M.F. Guerrero, Antidepressant-like profile and MAO-A inhibitory activity of 4-propyl-2H-benz[*h*]-chromen-2-one, *Life Sci.* 86 (2010) 819–824.
- [55] G. Delogu, C. Piccau, G. Ferino, E. Quezada, G. Podda, E. Uriarte, D. Vina, Synthesis, human monoamine oxidase inhibitory activity and molecular docking studies of 3-heteroarylcoumarin derivatives, *Eur. J. Med. Chem.* 46 (2011) 1147–1152.
- [56] L. Novaroli, A. Daina, E. Favre, J. Bravo, A. Carotti, F. Leonetti, M. Catto, P.A. Carrupt, M. Reist, Impact of species-dependent differences on screening, design, and development of MAO B inhibitors, *J. Med. Chem.* 49 (2006) 6264–6272.
- [57] M. Yáñez, N. Fraiz, E. Cano, F. Orallo, Inhibitory effects of cis- and trans-resveratrol on noradrenaline and 5-hydroxytryptamine uptake and on monoamine oxidase activity, *Biochem. Biophys. Res. Commun.* 344 (2006) 688–695.
- [58] M.J. Matos, C. Teran, Y. Perez-Castillo, E. Uriarte, L. Santana, D. Vina, Synthesis and study of a series of 3-arylcoumarins as potent and selective monoamine oxidase B inhibitors, *J. Med. Chem.* 54 (2011) 7127–7137.
- [59] I. StatSoft, STATISTICA (Data Analysis Software System), Version 8.0 (2007), USA, www.statsoft.com.
- [60] S. Talet, Dragon for Windows (Software for Molecular Descriptors Calculation), version 5.4-2006 (2006), Milano, Italy, www.talet.mi.it.
- [61] Molecular Operating Environment (MOE), Chemical Computing Group, Inc., Montreal, QC, Canada, 2008.
- [62] Y. Gutierrez, E. Estrada, MODESLAB 1.0 (Molecular DEScriptors LABoratory) for Windows (2002).
- [63] B.K. Sharma, P. Pilania, K. Sarbhai, P. Singh, Y.S. Prabhakar, Chemometric descriptors in modeling the carbonic anhydrase inhibition activity of sulfonamide and sulfamate derivatives, *Mol. Divers.* 14 (2010) 371–384.
- [64] M.Y. Shen, B.H. Su, E.X. Esposito, A.J. Hopfinger, Y.J. Tseng, A comprehensive support vector machine binary HERG classification model based on extensive but biased end point HERG data sets, *Chem. Res. Toxicol.* 24 (2011) 934–949.
- [65] E. Estrada, How the parts organize in the whole? A top-down view of molecular descriptors and properties for QSAR and drug design, *Mini Rev. Med. Chem.* 8 (2008) 213–221.
- [66] R.A. Fisher, The use of multiple measurements in taxonomic problems, *Ann. Eugen.* 7 (1936) 179–188.
- [67] A.M. Helguera, P.R. Duchowicz, M.Á.C. Pérez, E.A. Castro, M.N.D.S. Cordeiro, M.P. González, Application of the replacement method as a novel variable selection strategy in QSAR. 1. Carcinogenic potential, *Chemom. Intell. Lab. Syst.* 81 (2006) 180.
- [68] A. Perez-Garrido, A.M. Helguera, F. Borges, M.N. Cordeiro, V. Rivero, A.G. Escudero, Two new parameters based on distances in a receiver operating characteristic chart for the selection of classification models, *J. Chem. Inf. Model.* 51 (2011) 2746–2759.
- [69] R. Leardi, Nature-inspired Methods in Chemometrics: Genetic Algorithms and Artificial Neural Networks, Elsevier, Genova, Italy, 2003.
- [70] H. Kubinyi, Variable selection in QSAR studies. I. An evolutionary algorithm, *Quant. Struct. Activity Relatsh.* 13 (1994) 285–294.
- [71] F. Provost, T. Fawcett, Analysis and Visualization of Classifier Performance: Comparison under Imprecise Class and Cost Distributions, AAAI Press, 1997, Huntington Beach, CA, Menlo Park.
- [72] D.A. Pearlman, P.S. Charifson, Improved scoring of ligand–protein interactions using OWFEG free energy grids, *J. Med. Chem.* 44 (2001) 502–511.
- [73] B.W. Matthews, Comparison of the predicted and observed secondary structure of T4 phage lysozyme, *Biochim. Biophys. Acta* 405 (1975) 442–451.
- [74] R.P. Sheridan, S.B. Singh, E.M. Fluder, S.K. Kearsley, Protocols for bridging the peptide to nonpeptide gap in topological similarity searches, *J. Chem. Inf. Comput. Sci.* 41 (2001) 1395–1406.
- [75] J.F. Truchon, C.I. Bayly, Evaluating virtual screening methods: good and bad metrics for the “early recognition” problem, *J. Chem. Inf. Model.* 47 (2007) 488–508.
- [76] S. Wold, L. Eriksson, Statistical validation of QSAR results, in: H. van de Waterbeemd (Ed.), *Chemometrics Methods in Molecular Design*, VCH, New York, 1995, pp. 309–318.
- [77] T.I. Netzeva, A.P. Worth, T. Aldenberg, R. Benigni, M.T.D. Cronin, P. Gramatica, J.S. Jaworska, S. Kahn, G. Klopman, C.A. Marchant, G. Myatt, N. Nikolova-Jeliazkova, G.Y. Patlewicz, R. Perkins, D.W. Roberts, T.W. Schultz, D.T. Stanton, J.J.M. van de Sandt, W. Tong, G. Veith, C. Yang, Current status of methods for defining the applicability domain of (quantitative) structure–activity relationships. The report and recommendations of ECVAM workshop 52, *Altern. Lab. Anim.* 33 (2005) 155–173.
- [78] S. Zhang, A. Golbraikh, S. Oloff, H. Kohn, A. Tropsha, A novel automated lazy learning QSAR (ALL-QSAR) approach: method development, applications, and virtual screening of chemical databases using validated ALL-QSAR models, *J. Chem. Inf. Model.* 46 (2006) 1984–1995.
- [79] G. Melagraki, A. Afantitis, H. Sarimveis, P.A. Koutentis, G. Kollas, I. Igglessi-Markopoulou, Predictive QSAR workflow for the in silico identification and screening of novel HDAC inhibitors, *Mol. Divers.* 13 (2009) 301–311.
- [80] L. Eriksson, J. Jaworska, A.P. Worth, M.T.D. Cronin, R.M. McDowell, P. Gramatica, Methods for reliability and uncertainty assessment and for applicability evaluations of classification- and regression-based QSARs, *Environ. Health Perspect.* 111 (2003) 1361–1375.
- [81] L.I. Kuncheva, Combining Pattern Classifiers. Methods and Algorithms, John Wiley & Sons, Inc., Hoboken, New Jersey, 2004.
- [82] G.P. Ellis, G.J. Becket, D. Shaw, H.K. Wilson, C.J. Vardey, I.F. Skidmore, Benzopyrones. 14. Synthesis and antiallergic properties of some N-tetrazo-lylcarboxamides and related compounds, *J. Med. Chem.* 21 (1978) 1120–1126.
- [83] D.N. Davidson, P.T. Kaye, Chromone studies. Part 3. NMR analysis of rotational isomerism in 4-oxo-4H-chromene-2-carboxamides, *J. Chem. Soc. Perkin Trans. 2* (1991) 927–930.
- [84] A. Gaspar, E.M. Garrido, M. Esteves, E. Quezada, N. Milhazes, J. Garrido, F. Borges, New insights into the antioxidant activity of hydroxycinnamic acids: synthesis and physicochemical characterization of novel halogenated derivatives, *Eur. J. Med. Chem.* 44 (2009) 2092–2099.
- [85] M. Hadjeri, M. Barbier, X. Ronot, A.M. Mariotte, A. Boumendjel, J. Boutonnet, Modulation of P-glycoprotein-mediated multidrug resistance by flavonoid derivatives and analogues, *J. Med. Chem.* 46 (2003) 2125–2131.
- [86] N. Ishizuka, K. Matsumura, K. Sakai, M. Fujimoto, S. Mihara, T. Yamamori, Structure-activity relationships of a novel class of endothelin-A receptor antagonists and discovery of potent and selective receptor antagonist, 2-(benzo[1,3]dioxol-5-yl)-6-isopropoxy-4-(4-methoxyphenyl)-2H-chromene-3-carboxylic acid (S-1255). 1. Study on structure-activity relationships and basic structure crucial for ET(A) antagonism, *J. Med. Chem.* 45 (2002) 2041–2055.
- [87] T. Walenzyk, C. Carola, H. Buchholz, B. König, Chromone derivatives which bind to human hair, *Tetrahedron* 61 (2005) 7366–7377.
- [88] M. Payard, M. Geneviève, P. Tronche, P. Bastide, J. Bastide, Recherche de composés antiallergiques dérivés de l'hydroxyméthyl-2 chromone et analogues structuraux, *Eur. J. Med. Chem.* 20 (1985) 117–120.
- [89] P.-L. Zhao, J. Li, G.-F. Yang, Synthesis and insecticidal activity of chromanone and chromone analogues of diacylhydrazines, *Bioorg. Med. Chem.* 15 (2007) 1888–1895.
- [90] R. Araya-Maturana, J. Heredia-Moya, H. Pessoa-Mahana, B. Weiss-López, Improved selective reduction of 3-formylchromones using basic alumina and 2-propanol, *Synth. Commun.* 33 (2003) 3225–3231.
- [91] R. Todeschini, V. Consonni, M. Pavan, A distance measure between models: a tool for similarity/diversity analysis of model populations, *Chemom. Intell. Lab. Syst.* 70 (2004) 55–61.
- [92] A.K. Upadhyay, D.E. E., Development of spin-labeled pargyline analogues as specific inhibitors of human monoamine oxidases A and B, *Biochemistry* 48 (2009) 3928–3935.

3.8 Synthesis and NMR studies of novel chromone-2-carboxamide derivatives.

Article from Magnetic Resonance in Chemistry (2013), 51: 251–254.

Synthesis and NMR studies of novel chromone-2-carboxamide derivatives

Alexandra Gaspar,^{a,b} Fernando Cagide,^a Elias Quezada,^a Joana Reis,^a Eugenio Uriarte^b and Fernanda Borges^{a,*}

Chromones are heterocyclic compounds of natural or synthetic origin that possess relevant pharmacological activities. Versatile functionalization of the chromone nucleus allows attaining of a chemical diversity suitable to perform structure–activity relationships in drug discovery and development programs. Accordingly, the synthesis and identification of novel chromone carboxamide derivatives with electron-donating and electron-withdrawing substituents in different positions of the exocyclic ring are reported in this work. Their complete structural characterization was performed using one-dimensional and two-dimensional resonance techniques. The data acquired are useful for a prompt analysis of related compounds that encompass our integrated medicinal chemistry sketch. Copyright © 2013 John Wiley & Sons, Ltd.

Keywords: synthesis; chromone carboxamides; ¹H NMR; ¹³C NMR; HMQC; HMBC

Introduction

Chromones are benzannulated oxygen-containing heterocyclic compounds widely distributed in nature that have a γ-pyrone ring. In fact, the chemical core of chromone has an important place in the realm of natural products, in synthetic organic chemistry, and in drug discovery programs because of its particular structural features and diverse pharmacological properties. The importance of the chromone nucleus is well recognized not only by the development of new and improved synthetic methods^[1,2] but also by their application in medicinal chemistry programs.^[3]

The chromone scaffold has emerged as a privileged structure for drug discovery because of the versatile pharmacological profile and good drug-like properties.^[3,4] Besides anti-asthmatic, anti-inflammatory, anticoagulant, anticancer, and antimicrobial activities, their application for neurodegenerative diseases, such as Parkinson, was recently highlighted.^[3–5] In fact, the versatile functionalization of chromone allows attaining chemical diversity suitable in either improving the pharmacological profile or discovering new biological applications. Therefore, in a continuation of our previous studies in the development of novel small-molecule agents to address the therapeutic needs of neurodegenerative diseases,^[6] the synthesis of novel chromone carboxamide derivatives with electron-donating and electron-withdrawing substituents in different positions of the exocyclic ring (Fig. 1) was performed. The selected compounds were appropriate for a complete identification by 1D and 2D NMR techniques and for data extrapolation for other chromone derivatives of our library, speeding up the structure–activity studies of the medicinal chemistry program.

Experimental

Synthesis

The chromone derivatives were synthesized by two synthetic approaches, previously developed by our group.^[5,6]

Method A

To a solution of chromone-2-carboxylic acid (1.1 mmol) in dimethylformamide (1.5 ml), phosphoryl chloride (POCl₃; 1 mmol) was added. The mixture was stirred at room temperature for 30 min with the *in situ* formation of the corresponding acyl chloride. Then, the aromatic amine with the pretended aromatic pattern was added. The system was heated to 160 °C for 5 min in a microwave apparatus, and the mixture was poured into a beaker, and water was added. The formed solid was filtered and purified by recrystallization (CH₂Cl₂/*n*-hexane).

N-(2-Methoxyphenyl)-4-oxo-4H-benzopyran-2-carboxamide (**1**): Yield 90%; EIMS (*m/z*): 295 (*M*⁺, 100), 266 (20), 191 (41), 89 (35) 57 (3).

N-(3-Methoxyphenyl)-4-oxo-4H-benzopyran-2-carboxamide (**2**): Yield 65%; EIMS (*m/z*): 295 (*M*⁺, 15), 294 (100), 266 (13), 89 (2), 57 (8).

N-(2-Bromophenyl)-4-oxo-4H-benzopyran-2-carboxamide (**4**): Yield 45%; EIMS (*m/z*): 345 (*M* + 2, 8), 344 (6), 343 (*M*⁺, 8), 342 (4), 264 (100), 121 (8), 89 (40), 63 (8).

N-(3-Bromophenyl)-4-oxo-4H-benzopyran-2-carboxamide (**5**): Yield 60%; EIMS (*m/z*): 345 (*M* + 2, 22), 344 (100), 343 (*M*⁺, 22), 342 (100), 316 (14), 314 (15), 89 (32), 63 (6).

Method B

To a solution of the chromone-2-carboxylic acid (1 mmol) in dimethylformamide (2.5 ml) at 4 °C was added a solution of benzotriazol-1-yl-oxytriethylphosphonium hexafluorophosphate

* Correspondence to: Fernanda Borges, Departamento de Química e Bioquímica, Faculdade de Ciências, Universidade do Porto, Rua Campo Alegre 687, 4169-007 Porto, Portugal. E-mail: fborges@fcup.pt

a CIQUP/Departamento de Química e Bioquímica Faculdade de Ciências, Universidade do Porto, Porto, 4169-007, Portugal

b Departamento de Química Orgánica, Facultad de Farmacia, Universidad de Santiago de Compostela, 15782, Santiago de Compostela, Spain

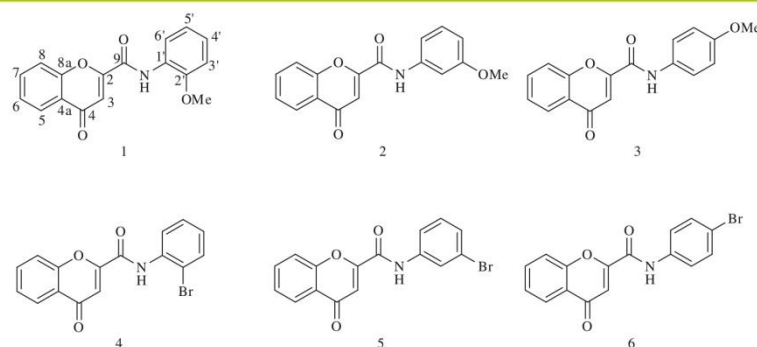


Figure 1. Structure of the chromone carboxamide derivatives.

(1 mmol) in CH_2Cl_2 (2.5 ml). The mixture was kept in an ice bath and stirred for 30 min. Then, the substituted aromatic amine was added, and the mixture was allowed to warm up to room temperature. The reaction was kept with stirring for 4 h. Work-up of the crude material was performed by a liquid–liquid extraction (CH_2Cl_2), followed by flash chromatography ($\text{CH}_2\text{Cl}_2/\text{MeOH}$) and final purification by recrystallization (ethyl acetate/*n*-hexane).

N-(4-Methoxyphenyl)-4-oxo-4H-benzopyran-2-carboxamide (**3**)

Yield 85%; EIMS (m/z): 296 (14), 295 (M^+ , 100), 294 (30), 266 (15), 173 (13), 145 (10), 122 (68), 95 (17), 89 (22), 71 (10), 69 (11), 57 (15).

N-(4-Bromophenyl)-4-oxo-4H-benzopyran-2-carboxamide (**6**)

Yield 70%; EIMS (m/z): 345 ($M + 2$, 48), 344 (38), 343 (M^+ , 49), 342 (28), 145 (20), 89 (100), 63 (21).

NMR spectroscopy

^1H and ^{13}C NMR spectra of the samples, approximately 10% solutions in deuterated dimethyl sulfoxide, were recorded at room temperature in 5-mm-outer-diameter tubes. TMS was used as internal standard, and chemical shifts are expressed in parts per million (δ) and J in hertz. 1D ^{13}C NMR was recorded on a Bruker AMX 500 (Billerica, MA) NMR spectrometer operating at 125.77 MHz, typically with a 30° pulse flip angle, a pulse repetition time of 4.8 s, and a spectral width of 31.250 Hz with 32K data points. For the DEPT sequence, the width of the 90° pulse for ^{13}C was 4 μs , and that of the 90° pulse for ^1H was 9.5 μs ; the delay $2J_{\text{CH}}$ was set to 3.5 ms. One-bond HMQC spectra were recorded on a Bruker AMX 500 spectrometer using a pulse sequence that allowed gradient selection (Bruker programs INV4GS and INVGSLPLRND). The spectra were collected in the t_1 domain in 256 experiments with 2K data points and spectral widths of 5.050 and 27.669 Hz in the F_2 (^1H) and F_1 (^{13}C) dimensions, respectively. The relaxation delay D_1 was set to 2 s. The data were processed using sine-bell weighting functions in both dimensions.

EIMS were carried out on a VG AutoSpec (Fison, Ipswich, United Kingdom) instrument; the data are reported as m/z (percentage of relative intensity of the most important fragments).

Microwave-assisted synthesis was executed in a Biotage® Initiator Microwave Synthesizer (Uppsala, Sweden).

Results and Discussion

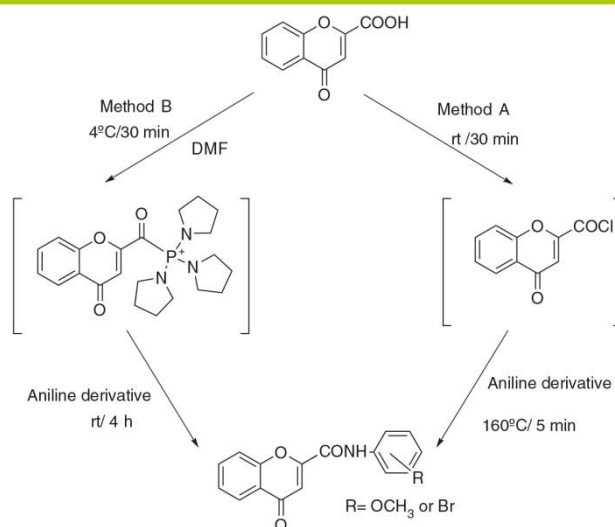
The chromone carboxamides were obtained following the synthetic strategies outlined in Scheme 1. Briefly, method A includes

an attempt to accelerate the synthetic process by the application of a microwave-assisted process via acyl chloride. In this methodology, the formation of the acyl chloride intermediate was attained by the reaction of the chromone-2-carboxylic acid, with phosphorus oxychloride. The chromone carboxamide was synthesized by taking advantage of a microwave reactor involving a condensation reaction between the previously mentioned intermediate and the aniline derivative. On the other hand, method B is based on the activation of the carboxylic acid function under mild reaction conditions using the coupling reagent benzotriazol-1-yl-oxytripyrrolidinophosphonium hexafluorophosphate. The *in situ* generated intermediate reacts with the appropriate aniline derivative, giving rise to the target chromone. It is noteworthy that the microwave-assisted reaction of the products was finished in a short time with a low-price reagent and easier work-up.

The complete structural characterization of the six synthesized compounds was achieved by the combined use of 1D and 2D NMR techniques, such as HMQC and HMBC. The ^1H and ^{13}C chemical shifts (δ) and coupling constants, obtained for **1–6** (Fig. 1) as well as the HMBC ^{13}C – ^1H correlations, allowing unambiguous assignments of all carbons and hydrogen atoms, are depicted in Tables 1 and 2.

The structure of **1** (Fig. 1) was assigned through a detailed analysis of 2D NMR experiments. The signals of the protons at carbons 3 and 5–8 were easily assigned by their chemical shift (δ), multiplicities, and direct correlation (HMQC) between the protons and their direct attached carbons. H-5 disclosed a long-range correlation (HMBC) with C-7 and with two quaternary carbons at $\delta = 155.48$ and 177.73 ppm. These signals were attributed to carbons 8a and 4, respectively, because of their distinct chemical environment. H-8 displayed a direct correlation with C-6, C-8a, and a quaternary carbon at $\delta = 124.11$ ppm that was assigned to C-4a. From the HMBC experiments, it was verified that the H-3 signal shows a long-range correlation with those of C-4, C-4a, and also two carbons, one at $\delta = 155.86$ ppm, assigned to C-9, and the other at $\delta = 157.82$ ppm, assigned to C-2. The data were confirmed by a long-range correlation between the N–H proton and a tertiary carbon at $\delta = 124.27$ ppm, assigned to C-6', and a quaternary carbon at $\delta = 151.75$ ppm, assigned to C-2' and with C-2. Furthermore, the C-2' chemical shift assignment was also confirmed by a long-range interaction with the methoxyl protons. H-6' exhibits a correlation with the quaternary carbon C-2', a tertiary carbon at $\delta = 127.21$ ppm, assigned to C-4', and a quaternary carbon $\delta = 125.73$ ppm, assigned to C-1'. Finally, the ^{13}C

Structural elucidation of chromone-2-carboxamides



Scheme 1. Synthetic strategies used for the obtention of chromone carboxamide derivatives.

NMR signal carbons at $\delta = 112.04$ and 120.90 were assigned to C-3' and C-5', respectively. This was performed on the basis of HMBC data that indicate a long-range correlation of the H-5 with C-1' and C-3'. Moreover, for H-3', a long-range correlation between the tertiary carbon C-5' and the quaternary carbons C-1' and C-2' was observed.

The structure of **2** (Fig. 1), particularly the carbons of the chromone carboxamide structure (**2**, **3**, **4**, **4a**, **5**, **6**, **7**, **8**, **8a**, and

9), was assigned by the same approach as described for **1**. The methyl protons exhibit a long-range interaction with a carbon at $\delta = 159.93$ ppm, which was assigned to C-3'. The ¹³C NMR signal detected at $\delta = 107.20$ ppm was readily attributed to C-2' by the HMQC experiments. By analysis of the HMBC results, it was observed that H-2' correlates with the quaternary carbon C-3' and a quaternary carbon with $\delta = 139.17$ ppm, assigned to C1'. In addition, a correlation was detected for the H-2' with

Table 1. ¹H and ¹³C chemical shifts and HMBC correlations for **1–3**

	1			2			3		
	¹ H ^a	¹³ C	HMBC ^b	¹ H ^a	¹³ C	HMBC ^b	¹ H ^a	¹³ C	HMBC ^b
2	—	157.82	—	—	158.17	—	—	157.75	—
3	6.92 (s)	111.41	C2, C4, C4a, C9	6.96 (s)	111.54	C2, C4, C4a, C9	6.94 (s)	111.35	C2, C4, C4a, C9
4	—	177.73	—	—	177.76	—	—	177.77	—
4a	—	124.11	—	—	124.15	—	—	124.14	—
5	8.07 (d, 7.8)	125.43	C4, C7, C8a	8.06 (d, 7.8)	125.39	C4, C7, C8a	8.06 (d, 8.8)	125.39	C4, C7, C8a
6	7.55 (m)	126.62	C4a, C8	7.55 (m)	126.59	C4a, C8	7.54 (m)	126.55	C4a, C8
7	7.90 (m)	135.53	C5, C8a	7.91 (m)	135.50	C5, C8a	7.91 (m)	135.47	C5, C8a
8	7.82 (m)	119.42	C4a, C6, C8a	7.84 (d, 7.8)	119.49	C4a, C6, C8a	7.82 (d, 8.8)	119.45	C4a, C6, C8a
8a	—	155.48	—	—	155.60	—	—	155.62	—
9	—	155.86	—	—	156.08	—	—	156.31	—
1'	—	125.73	—	—	139.17	—	—	130.94	—
2'	—	151.75	—	7.45 (s)	107.20	C1', C3', C4', C6'	7.70 (d, 8.8)	123.15	C1', C4', C6'
3'	7.14 (d, 7.8)	112.04	C1', C2', C5'	—	159.93	—	6.97 (d, 8.8)	114.40	C1', C4', C5'
4'	7.24 (m)	127.21	C2', C6'	6.77 (d, 8.8)	110.93	C2', C3', C6'	—	156.87	—
5'	7.00 (m)	120.90	C1', C3'	7.31 (m)	130.10	C1', C3'	6.97 (d, 8.8)	114.40	C1', C3', C4'
6'	7.82 (m)	124.27	C1', C2', C4'	7.39 (d, 8.8)	113.68	C1', C2', C4'	7.70 (d, 8.8)	123.15	C1', C2', C4'
CH ₃ O	3.88 (s)	56.34	C2'	3.76 (s)	55.58	C3'	3.75 (s)	55.68	C4'
NH	10.01 (br)	—	C2, C2', C6'	10.68 (br)	—	C2, C2', C6'	10.64 (br)	—	C2, C2', C6'

^aChemical shifts δ in parts per million (multiplicity, *J* in hertz); solvent: dimethyl sulfoxide.

^bCarbons coupled to the corresponding H atom.

Table 2. ^1H and ^{13}C chemical shifts and HMBC correlations for 4–6

	4			5			6		
	$^1\text{H}^a$	^{13}C	HMBC ^b	$^1\text{H}^a$	^{13}C	HMBC ^b	$^1\text{H}^a$	^{13}C	HMBC ^b
2	—	158.47	—	—	158.43	—	—	158.32	—
3	6.95 (s)	111.69	C2, C4, C4a, C9	6.97 (s)	111.73	C2, C4, C4a, C9	6.97 (s)	111.66	C2, C4, C4a, C9
4	—	177.68	—	—	177.72	—	—	177.73	—
4a	—	124.14	—	—	124.15	—	—	124.15	—
5	8.08 (d, 8.8)	125.47	C4, C7, C8a	8.07 (m)	125.43	C4, C7, C8a	8.07 (d, 7.8)	125.41	C4, C7, C8a
6	7.56 (m)	126.69	C4a, C8	7.55 (m)	126.65	C4a, C8	7.55 (m)	126.62	C4a, C8
7	7.91 (m)	135.66	C5, C8a	7.92 (m)	135.59	C5, C8a	7.92 (m)	135.56	C5, C8a
8	7.80 (d, 8.8)	119.38	C4a, C6, C8a	7.81 (m)	119.44	C4a, C6, C8a	7.83 (d, 7.8)	119.47	C4a, C6, C8a
8a	—	155.54	—	—	155.57	—	—	155.60	—
9	—	155.59	—	—	155.73	—	—	155.91	—
1'	—	135.49	—	—	139.62	—	—	137.43	—
2'	—	120.61	—	8.07 (m)	123.83	C1', C3', C4', C6'	7.78 (d, 8.8)	123.43	C1', C4', C6'
3'	7.64 (d, 8.8)	128.78	C1', C2', C5'	—	121.93	—	7.60 (d, 8.8)	132.16	C1', C4', C5'
4'	7.29 (m)	129.20	C2', C6'	7.38 (m)	128.01	C2', C3', C6'	—	117.30	—
5'	7.47 (m)	128.88	C1', C3'	7.38 (m)	131.32	C1', C3'	7.60 (d, 8.8)	132.16	C1', C3', C4'
6'	7.76 (d, 8.8)	133.35	C1', C2', C4'	7.81 (m)	120.26	C1', C2', C4'	7.78 (d, 8.8)	123.43	C1', C2', C4'
NH	10.66 (br)	—	C2, C2', C6'	10.83 (br)	—	C2, C2', C6'	10.84 (br)	—	C2, C2', C6'

^aChemical shifts δ in parts per million (multiplicity, J in hertz); solvent: dimethyl sulfoxide.

^bCarbons coupled to the corresponding H atom.

two tertiary carbons with $\delta = 110.93$ ppm and $\delta = 113.68$ ppm that were easily assigned to C-4' and C-6', respectively. This was based on the chemical shifts and multiplicities of the protons directly linked to these carbons and the direct HMQC correlation with those carbons atoms. Finally, the signal observed at $\delta = 130.10$ ppm was assigned to C5' according to their directly attached proton.

The structural similarity of **3** (Fig. 1) compared with **1** and **2** allows an unambiguous interpretation of the NMR data. However, the presence of the methoxyl group in the *para*-position at the exocyclic aromatic ring causes chemical shift changes, due to inductive and resonance effects, confirmed by 2D NMR experiments. The protons of the methoxyl group display a long-range correlation with a quaternary carbon at $\delta = 156.87$ ppm that was assigned to C-4'. So, the ^1H NMR signal at $\delta = 6.97$ ppm was assigned to H-3'/H-5', two chemically equivalent protons, as it has a long-range correlation with C-4'. Likewise, the chemically equivalent protons H-2'/H-6' are located at $\delta = 7.70$ in the NMR spectra.

The signal assignments of **4**, **5**, and **6** (Fig. 1) were performed by analogy with **1**, **2**, and **3**. However, as expected, the bromide substituent has a different effect on the chemical shift of the carbons directly attached: for **4**, the signal of C-2' appears at $\delta = 120.61$ ppm; for **5**, the signal for C-3' appears at $\delta = 121.93$ ppm; and, finally, for **6**, with the bromide group in *para*-position, the C-4' chemical shift is $\delta = 117.30$ ppm.

Conclusions

Novel chromone carboxamide derivatives with electron-donating and electron-withdrawing substituents in different positions of the exocyclic ring were obtained in moderate to high yields by either classic or microwave reactions. However, in the microwave-assisted

reaction, the target compounds were obtained in a shorter time with a low-price reagent and easier work-up. The compounds were further characterized by 1D and 2D NMR techniques that allowed full NMR signal assignments. The acquired data constitute a valuable database for the unambiguous identification of the chromone library developed with the aim of our medicinal chemistry program.

Acknowledgements

The authors thank the Foundation for Science and Technology (FCT), Portugal (PTDC/QUI-QUI/113687/2009), for support through FCT grants to A. Gaspar (SFRH/BD/43531/2008), F. Cagide (SFRH/BPD/74491/2010), and E. Quezada (SFRH/BPD/74596/2010).

References

- [1] N. G. Li, Z. H. Shi, Y. P. Tang, H. Y. Ma, J. P. Yang, B. Q. Li, Z. J. Wang, S. L. Song, J. A. Duana, *J. Heterocycl. Chem.* **2010**, *47*, 785–799.
- [2] (a) M. Lacova, H. El-Shaer, D. Loos, M. Matulova, J. Chovancova, M. Furdik, *Molecules* **1998**, *3*, 120–131; (b) S. Vedachalam, Q.-L. Wong, B. Maji, J. Zeng, J. Ma, X.-W. Liu, *Adv. Synth. Catal.* **2011**, *353*, 219–225.
- [3] (a) T. Höglberg, M. Vora, S. D. Drake, L. A. Mitscher, D. T. W. Chu, *Acta Chem Scand* **1984**, *38b*, 359–366; (b) M. Mazzei, A. Balbi, G. Roma, M. D. Braccio, G. Leoncini, E. Buzzi, M. Maresca, *Eur J Med Chem* **1988**, *23*, 237–242; (c) T. Inaba, K. Tanaka, R. Takeno, H. Nagaki, C. Yoshida, S. Takano, *Chem Pharm Bull* **2000**, *48*, 131–139; (d) K. S. Lee, S. H. Seo, Y. H. Lee, H. D. Kim, M. H. Son, B. Y. Chung, J. Y. Lee, C. Jin, Y. S. Lee, *Bioorg Med Chem Lett* **2005**, *15*, 2857–2860; (e) S. K. Sharma, S. Kumar, K. Chand, A. Kathuria, A. Gupta, R. Jain, *Curr Med Chem* **2011**, *18*, 3825–3852.
- [4] A. M. Edwards, J. B. L. Howell, *Clin Exp Allergy* **2000**, *30*, 756–774.
- [5] (a) A. Gaspar, T. Silva, M. Yáñez, D. Vina, F. Orallo, F. Ortuso, E. Uriarte, S. Alcaro, F. Borges, *J. Med. Chem.* **2011**, *54*, 5165–5173; (b) A. Gaspar, F. Teixeira, E. Uriarte, N. Milhazes, A. Melo, M. N. D. S. Cordeiro, F. Ortuso, S. Alcaro, F. Borges, *Chem. Med. Chem.* **2011**, *6*, 628–632.
- [6] F. Cagide, J. Reis, A. Gaspar, F. Borges, *Tetrahedron Lett* **2011**, *52*, 6446–6449.

Chapter 4

Integrated Overview of the performed Studies

As previously described in chapter 2 simple chromones can be a valid scaffold for medicinal chemistry drug discovery programs. However, and despite the pharmacological properties so far described for simple chromones, their application in the field of neurodegenerative diseases is still an open issue. The emergent need and pressing need for new therapeutic entities (NTEs), e.g. repurposed drugs, or new chemical entities (NCEs) for this type of diseases encouraged the design and development of the drug discovery project performed in this thesis. The project is mainly focused in the synthesis, development and biological evaluation of small, concise and diverse chromone libraries, comprising mainly functionalised chromones in 2- and 3- positions, as new NCEs for neurodegenerative diseases, particularly PD. In the following sections will be address the synthetic work executed and the biological evaluation of the synthesised libraries.

4.1 Design, synthesis and structural characterisation of the diverse functionalized chromone libraries

The generation of new lead compounds in drug discovery is nowadays a process mainly focused in the development of suitable chemical libraries providing reliable SARs. Chemical libraries are collections of different molecules sharing a common chemical core, which can be achieved by a diversity of approaches, for instance by combinatorial chemistry. This concept is a common practice in Pharma industry and it is often used to create a large variety of structurally related molecules in a short time, which are subsequently screened against a variety of targets by high throughput screening (HTS).

Accordingly the conception of the chromone chemical libraries herein described were inspired in combinatorial chemistry and parallel synthesis, methodological concepts useful for the development of smaller and more specialized libraries based on a particular skeleton. Furthermore, the synthetic methodologies developed along this work were selected taking in account the possibility of the scale-up of the processes, using whenever possible available and cost-effective starting materials, straightforward one-pot synthetic and environment-friendly procedures, and choosing, if possible, simple and effective work-ups for product isolation and purification.

The design of the chemical libraries based on the chromone scaffold encompasses the synthesis of several functionalised chromone derivatives, mainly located in the positions 2- or 3- of the pyrone ring but also in position 6/7- of the aromatic ring, such as alkyl esters, alcohols, carboxylic acids and amides. The synthesised chromones are depicted in the tables 4.1, 4.2 and 4.3.

Table 4.1. Chromone library I: ester, carboxylic acid, hydroxymethyl and formylchromone derivatives.

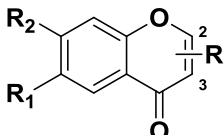
2-Substituted chromones					3-Substituted chromones	
Compound	Yield	R	R ₁	R ₂	Compound	Yield
1	81%	COOC ₂ H ₅	H	H	2	60%
3	52%	COOC ₃ H ₇	H	H	4	60%
5	60%	COOC ₂ H ₅	Cl	H	-	-
6	72%	COOC ₂ H ₅	H	OCH ₃	-	-
7	62%	COOH	H	OCH ₃	-	-
8	60%	COOH	Cl	H	9	48%
-	-	CHO	Cl	H	10	75%
11	65%	COOC ₂ H ₅	Br	H	-	-
-	-	CHO	Br	H	12	85%
13	43%	CH ₂ OH	H	H	14	48%
15	55%	COOC ₂ H ₅	C ₆ H ₅	H	-	-
17	30%	COOH	C ₆ H ₅	H	-	-
-	-	CHO	C ₆ H ₅	H	18	30%

Table 4.2 Chromone library II: phenylcarboxamide chromone derivatives.

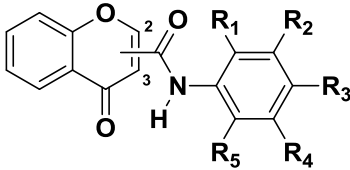
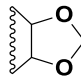
2-Substituted chromones							3-Substituted chromones	
Compound	Yield	R1	R2	R3	R4	R5	Compound	Yield
19	81%	H	H	H	H	H	20	60%
21	56%	H	H	CH ₃	H	H	22	45%
23	40%	CH ₃	H	H	H	H	24	52%
25	77%	H	CH ₃	H	H	H	26	54%
27	75%	CH ₃	CH ₃	H	H	H	28	63%
29	67%	H	H	C ₂ H ₅	H	H	30	56%
31	69%	H	H	C ₄ H ₉	H	H	32	49%
33	85%	H	H	OCH ₃	H	H	34	30%
35	90%	OCH ₃	H	H	H	H	36	72%
37	65%	H	OCH ₃	H	H	H	38	42%
39	50%	H	OCH ₃	OCH ₃	H	H	40	45%
41	62%	H	H			H	42	40%
43	51%	H	H	OH	H	H	44	55%
45	57%	H	OH	OCH ₃	H	H	46	45%
47	65%	H	OH	OH	H	H	48	50%
49	30%	H	H	NO ₂	H	H	50	37%
51	82%	H	H	COOC ₂ H ₅	H	H	52	89%
53	65%	H	H	COOH	H	H	54	63%
55	70%	H	H	SCH ₃	H	H	56	60%
57	45%	H	H	SO ₂ CH ₃	H	H	-	-
58	26%	H	H	NH ₂	H	H	-	-
59	50%	H	H	CF ₃	H	H	60	55%
61	56%	H	H	OCF ₃	H	H	62	55%
63	72%	H	H	F	H	H	64	50%
65	50%	H	H	Cl	H	H	66	47%
67	23%	Cl	H	H	H	H	68	23%
69	33%	H	Cl	H	H	H	70	49%
71	70%	H	H	Br	H	H	72	64%

Table 4.2 (cont.): Chromone library II: phenylchromone carboxamide derivatives.

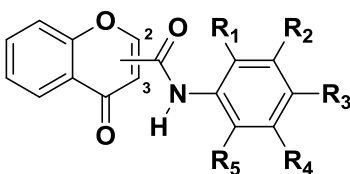
2-Substituted chromones							3-Substituted chromones	
Compound	Yield	R1	R2	R3	R4	R5	Compound	Yield
73	45%	Br	H	H	H	H	74	25%
75	60%	H	Br	H	H	H	76	42%
77	95%	H	H	I	H	H	78	50%
79	71%	H	H	CN	H	H	80	50%

Table 4.3: Chromone library III: alkyl, phenyl and heterocyclic chromone carboxamide derivatives.

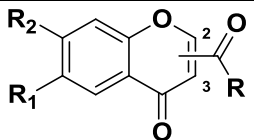
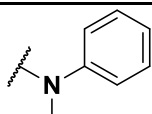
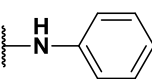
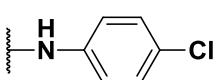
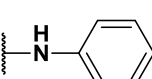
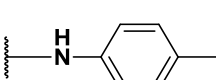
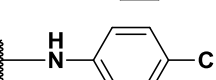
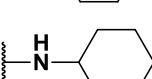
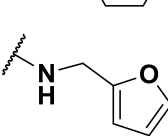
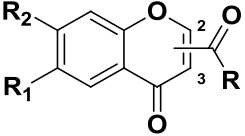
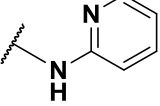
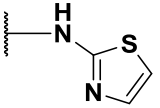
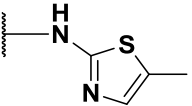
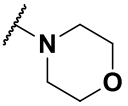
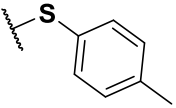
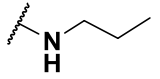
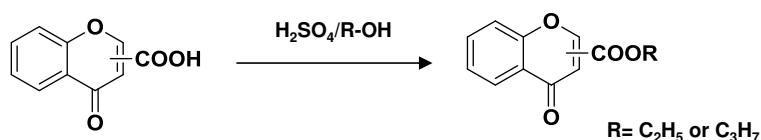
2-Substituted chromones					3-Substituted chromones	
Compound	Yield	R	R ₁	R ₂	Compound	Yield
81	35%		H	H	82	30%
83	60%		Cl	H	84	45%
85	67%		Cl	H	86	48%
87	72%		OCH ₃	H	-	-
88	85%		OCH ₃	H	-	-
89	65%		OCH ₃	H	-	-
90	60%		H	H	91	30%
92	35%		H	H	93	48%

Table 4.3 (cont.): Chromone library III: alkyl, phenyl and heterocyclic chromone carboxamide derivatives.

2-Substituted chromones					3-Substituted chromones	
Compound	Yield	R	R ₁	R ₂	Compound	Yield
94	22%		H	H	95	35%
96	55%		H	H	97	25%
98	48%		H	H	99	10%
100	33%		H	H	101	45%
102	35%		H	H	103	22%
104	52%		H	H	105	47%

4.1.1 Synthesis of ester, carboxylic acid and formylchromone derivatives

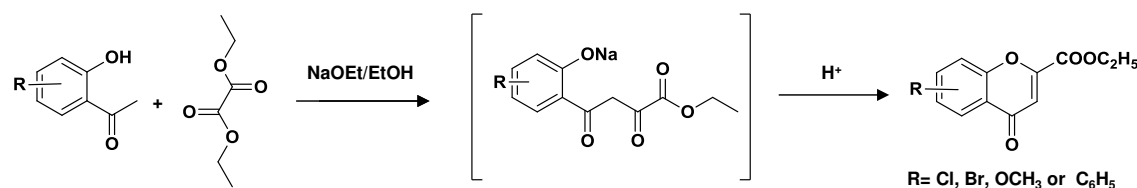
Some of the alkyl esters synthesised in this work (compounds 1-4, table 4.1.) were obtained by classical Fischer esterification (scheme 4.1 and article in section 3.7) from the commercially available chromone carboxylic acids and ethanol or propanol, in moderate to good yields (table 4.1.)



Scheme 4.1 Synthesis of ester chromone derivatives by Fisher esterification.

Additionally, the synthesis of the 6/7- substituted chromone esters (compounds 5, 6, 11 and 15, table 4.1) were obtained by Claisen condensation of the appropriate 2-hydroxyacetophenone with diethyl oxalate, in the presence of sodium ethoxide in

EtOH, followed by an intramolecular cyclisation, under acidic conditions (scheme 4.2 and article in section 3.7).

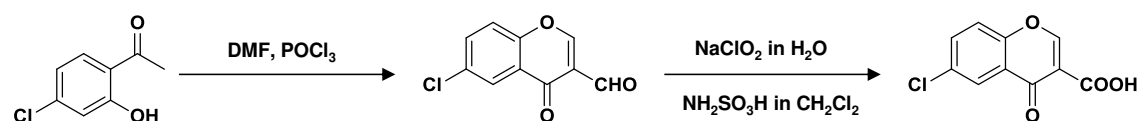


Scheme 4.2 Synthesis of ester chromone derivatives by Claisen condensation.

The good yield obtained (>60%, table 4.1) and the single-step purification process, consisting of a simple recrystallization from ethyl acetate, validates the selection of the method. After purification, this chromone ester was submitted to a hydrolytic process, following the procedure of Hadjeri *et al.* ^[306] (article in section 3.7), yielding the corresponding carboxylic acids (compounds 7, 8 and 17, table 4.1).

A different synthetic strategy was selected for the synthesis of 6-chloro-3-chromone carboxylic acid and (compound 9, table 4.1), since it was described that 3-chromone carboxylic acids can be easily obtained from 3-formylchromones ^[307].

Accordingly, 6-chloro-3-formylchromone (compound 10, table 4.1) was obtained *via* a Vilsmeier-Haack reaction, using 4-chloro-2-hydroxy acetophenone as the starting material, with a good yield (>70%, article in section 3.7.; scheme 4.3). The subsequent oxidation step, performed with sodium chlorite and sulfamic acid as oxidizing reagents, gave rise to the correspondent carboxylic acid in a moderate yield (48%, article in section 3.7; scheme 4.3).

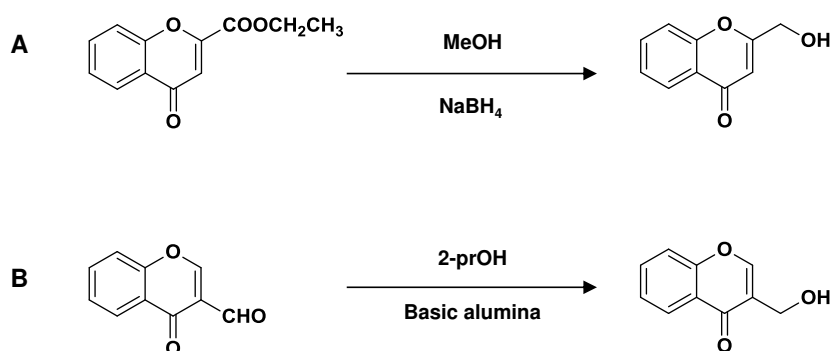


Scheme 4.3. Synthesis of 6-chloro-3-chromone carboxylic acid.

The commercial availability of the starting material and the simplicity of the reaction and its work-up, were the main reasons to adopt this strategy to obtain the intended chromone carboxylic acid derivative. This methodology (Vilsmeier-Haack reaction) was also used to obtain compounds 12 and 18 (table 4.1.) using the appropriate 2-hydroxyacetophenone as starting materials. These types of 2- and 3-chromone derivatives, namely the ester, formyl and the carboxylic acid derivatives were subsequently used as starting materials to obtain other type of functionalized chromones.

4.1.2 Synthesis of hydroxymethylchromone derivatives

The hydroxymethylchromone derivatives used along this project, namely the 2-hydroxymethylchromone and the 3-hydroxymethylchromone (compounds 13 and 14 respectively; table 4.1) were obtained by reduction processes from two different types of functionalized chromones: a chromone 2-ethyl ester derivative (synthesized by the method described in scheme 4.1) or the commercially available 3-formylchromone, respectively (scheme 4.4.).



Scheme 4.4. Synthesis of hydroxymethylchromone derivatives.

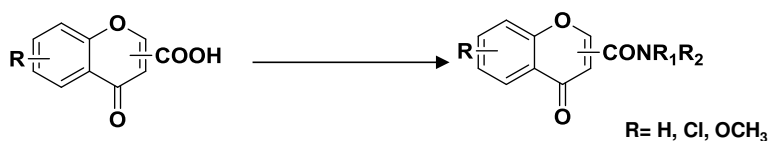
The 2-hydroxymethylchromone (scheme 4.4 A) was obtained by reducing the correspondent chromone ethyl ester using sodium borohydride (NaBH_4) in methanol that promotes the transformation of the ester into a hydroxyl function (article in section 3.7). It is noteworthy to mention that NaBH_4 is not a classic reagent for ester reduction under ambient conditions, mainly due to the slow reaction rate^[308]. In this particular case, the procedure was adopted from Payard *et al.*^[165] who have successfully obtained similar compounds in reasonable yields. The yields obtained in our studies are in accordance with those obtained by Payard *et al.*. These yields can somehow be explained by the presence in the chromone core of an α,β -unsaturated ketone system, which can react with NaBH_4 forming side products.

The synthesis of 3-hydroxymethylchromone (scheme 4.4 B) from 3-formylchromone was based on the work of Maturana *et al.*^[292], that used basic alumina in 2-propanol as reducing agent (article in section 3.7). The obtained yield for compound 14 (table 4.1) is in accordance with the reported by Maturana *et al.*.

4.1.3 Synthesis of amide chromone derivatives

The first synthetic approach used for the formation of the chromone carboxamides (table 4.2 and table 4.3) from chromone carboxylic acids (starting materials) involves the activation of the carboxylic acid function with phosphonium coupling reagents, and consequent formation of phosphonium reactive intermediates,

followed by a condensation reaction with aniline derivatives. (scheme 4.5.; articles in sections 3.1.- 3.8.)



Scheme 4.5. Synthesis of amide chromone derivatives.

The generation of the phosphonium intermediates was accomplished by using *O*-benzotriazol-1-yloxytris(dimethylamino)phosphonium hexafluorophosphate (BOP) (figure 4.1.) as a coupling agent, that was after substituted by *O*-benzotriazol-1-yloxytris(pyrrolidino)phosphonium hexafluorophosphate (PyBOP) (Fig. 4.1.), to avoid the generation of toxic hexamethylphosphoramide (HMPA), a by-product of BOP [309]. Another phosphonium coupling agent, bromotripyrrolidinophosphonium hexafluorophosphate (PyBrOP) (Fig. 4.1.), was used to obtain the tertiary amide reported in the work reprinted in section 3.7. In fact, it was described that BOP and PyBOP are not suitable coupling agents for condensation reactions with hindered aminoacids^[310]. As an alternative, the use of PyBrOP or chlorotripyrrolidinophosphonium hexafluorophosphate (PyClOP) (Fig. 4.1) is strongly advised. Therefore, the unproductive results obtained with PyBOP in the condensation of the chromone-2-carboxylic acid with the *N*-methyl aniline, was evaded by the use of PyBrOP (article in section 3.7).

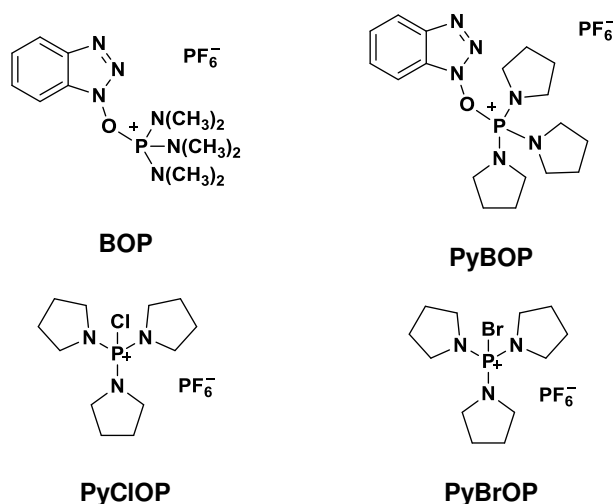


Figure 4.1. Phosphonium coupling agents.

Driven by the preliminary biological results, new chromone carboxamides were designed in order to progress the SAR studies, while costless, easy and eco-friendly reactions were sought for their synthesis. Although the amidation reaction promoted by phosphonium coupling reagents is a one-pot step synthesis, without the need of intermediate isolation, the high cost of the reagents, the laborious and time consuming purification steps boost the search of other synthetic strategies. It was found that the activation the chromone-2-carboxylic acid with phosphoryl chloride ($POCl_3$), gave rise to a rapid *in situ* formation of the acyl chloride intermediate, which without isolation is

used in the *N*-acylation step. In fact, after the subsequent addition of the intended amine derivative, and under microwave irradiation for a short period (5 min), several of the desired chromone carboxamides were obtained. The purification processes involves only filtration and recrystallization techniques (article in section 3.8.). However, despite the inherent advantages, this strategy revealed itself unproductive for the synthesis of chromone-3-carboxamides. Additional research is on progress to optimize the technique and attain good results with 3-substituted chromones.

4.1.4 Structural characterization of the chromone derivatives

All the synthesised compounds (tables 4.1, 4.2 and 4.3) were fully characterized by 1D NMR (^1H , ^{13}C and DEPT) techniques and electron impact mass spectrometry (EI/MZ). Additionally, 2D NMR (COSY, HMBC and HMQC) studies were also performed. A database for the unambiguous identification of the chromone-2-carboxamide library was successful attained using 1D and 2D NMR (article in section 3.8).

During the structural elucidation of the compounds of the chromone 3-carboxamide library some dilemmas arise due to the appearance of non-expected signals in the NMR spectra of all the compounds of the series, namely the splitting pattern of the NH of the carboxamide and of H-2 signals and also in the appearance of double signals in the region corresponding to the CONH and C-2 carbons (Table 2 of the article in section 3.3). To justify the presence of this type of signals in the spectra, a dynamic study was performed, using diverse spectroscopic and theoretical tools, which was reported on the paper in section 3.3. The data acquired in the NMR experiments as well as in theoretical approaches, gave rise to the hypothesis that a possible intramolecular hydrogen bond may be presented in solution, with the putative formation of tautomers. However, it seems also plausible the existence of amide rotamers in solution, as the amide function often demonstrates to have this property ^[311]. These hypotheses were investigated by performing focused NMR studies, like the use of deuterated water to evaluate the exchangeability of the proton and by the acquisition of the NMR data at temperatures higher than 300 K, to speed up the exchange of rotamers. Unfortunately the gathered data is still inconclusive and further investigations are still needed.

4.2 Chromone a valid scaffold for the development of MAO-B inhibitors

Since the introduction of L-deprenyl in 1975 as an antiparkinsonian drug the search for new of MAO-B inhibitors has been strengthened. As a result, rasagiline was

launched in 2006 for monotherapy in early Parkinson's disease or as an adjunct therapy in more advanced cases. Rasagiline has received singular attention not only due to its MAO-B inhibitory activity, but also for its neuroprotective properties. Although both mentioned drugs are highly potent selective inhibitors of MAO-B they are irreversible inhibitors, permanently deactivating the enzyme.

So, the development of selective and reversible MAO-B inhibitors is still an open issue and the goal of numerous medicinal chemistry programs. Accordingly, several privileged structures, such as pyrazoles, xanthenes, coumarins and hydrazine derivatives have been used in the process of discovery and development (chapter 1).

To validate the chromone structure as a scaffold for the development of new MAO-B inhibitors, we have selected for the first approach two functionalized chromones: chromone 2- and 3- carboxylic acids (article in section 3.1). To note that chromones without substituents doesn't not display MAO inhibitory activity^[212]. The results of the screening assays towards human MAO isoforms (*h*MAO-A and *h*MAO-B) showed that the presence and position of the COOH group on benzopyrone ring has a significant influence in the biological activity. In fact, when the COOH substituent is located in the position 3 of the benzopyrone ring a selective inhibition of *h*MAO-B isoform (IC_{50} *h*MAO-B 0.048 ± 0.0026 nM; SI >2083) was observed. In contrast, the chromone isomer, with the carboxylic function in position 2, has no activity for both MAO isoforms (article in section 3.1).

Molecular modeling and docking studies were at that point performed to assess the putative interactions between the chromone isomers and MAOs enzyme active sites that can explain the experimental data. These studies were performed in close collaboration with Stefano Alcaro's group, from the Department of Pharmacology, Faculty of Pharmacy, University "Magna Græcia" in Catanzaro, Italy.

The publication of the crystallographic structures of MAO-B in 2002^[312, 313] and MAO-A in 2004^[314] provided useful support tools to better understand the features that regulate the ligand recognition by both MAO isoforms. Apart from punctual differences in the amino acids sequences, since both human isoforms share approximately 70% of homology, one of the most relevant discoveries from the acquired x-ray data, was the structural differences of the active site of both isoforms, namely the bipartite cavity of *h*MAO-B against the monopartite cavity of *h*MAO-A^[315]. In fact, it was demonstrated that the active site of *h*MAO-B is formed by two hydrophobic cavities, the "substrate or catalytic cavity" and the "entrance cavity"^[312]. These two pockets are separated by four amino acids residues namely, Tyr326, Ile199, Leu171 and Phe168 and transient movements of these amino acids must occur for the ligand to reach the catalytic site of the enzyme^[312, 313, 315]. Furthermore, interactions with Ile199 and Tyr326 seem quite

important for inhibitor recognition by *h*MAO-B^[316]. The major differences regarding the active site of *h*MAO-B and *h*MAO-A have been identified, mainly the *h*MAO-B Ile199 and Tyr326 that are substituted in *h*MAO-A, by Phe208 and Ile335 respectively^[312].

The molecular docking data points out the existence of different interactions between the chromones and the active site of MAO isoforms, namely the presence of a hydrogen bond established between chromone 3-carboxylic acid and *h*MAO-B amino acid Tyr 326 (Fig. 4.2), that was not present in the docking process of chromone 2-carboxylic acid. This outcome was the engine for the design and development of a small chromone library, mainly based on chemical modifications similarly performed at positions 2 or 3 of the pyrone ring (tables 4.1. 4.2. and 4.3.) that was screened towards MAO isoforms. The results were reported in papers reprinted in sections 3.2., 3.3., and 3.4..

The preliminary SAR studies allow concluding that i) the modification of the carboxylic acid moiety by an ester or an alcohol function gives rise to inactive compounds (article in section 3.7.); ii) when the carboxylic acid was replaced by an alkyl/cycloalkyl or aryl amide function in position 3 of the chromone ring, several active compounds were obtained with a diverse inhibitory activity outline, although alkyl chromone carboxamides are less active than aryl ones (articles in sections 3.2., 3.3, and 3.4.); iii) the presence of a phenyl ring located on the 3-carboxamide side chain enhances MAO-B potency of inhibition (article in section 3.3.).

The overall data allow concluding that, in general, when the carboxamide substituent is allocated at position 3 of the chromone scaffold a *h*MAO-B inhibitory activity is noticed whereas the corresponding isomeric chromone-2- carboxamides are inactive in respect to both MAO isoforms. This tendency is similar to that obtained for the chromone carboxylic acids suggesting that the amide function can be also an important feature as it can also play a role in the establishment of a hydrogen bond with the active site of the enzyme.

After the preliminary SAR study the chromone carboxamide library was amplified to optimize the compound in potency and selectivity as a MAO-B

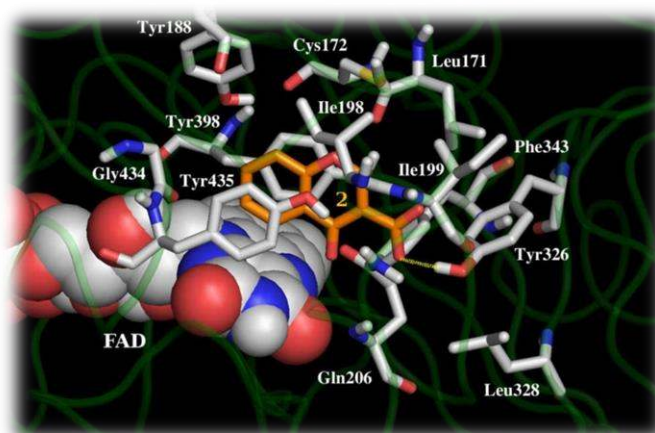
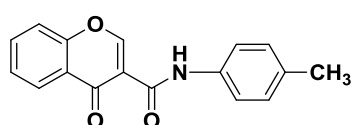


Figure 4.2. Virtual docking of chromone-3-carboxylic acid into the *h*MAO-B catalytic site (figure extracted from article in section 3.1).

inhibitor. Accordingly, the exocyclic aromatic ring was decorated with different type of

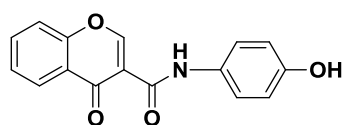
substituents located in different positions (see section 4.2). The data obtained so far confirms the superior activity and selectivity of all the chromone-3-carboxamide derivatives towards MAO-B isoform. Additionally, it was also concluded that the potency and selectivity of the chromone-3-carboxamides was modulated by substituents located in the *para* position of the exocyclic aromatic ring. The most promising compounds are highlighted in Fig. 4.3. Moreover, reversibility studies were performed over two of most promising chromones carboxamides (compounds 44 and 66, Fig. 4.3). These studies revealed that the mentioned chromone carboxamides behave as *quasi*-reversible MAO-B inhibitors (article in section 3.2.).

Compound 22



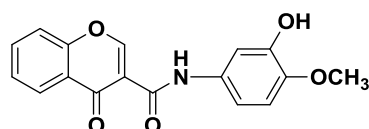
$h\text{MAO-B } IC_{50} (\mu\text{M}) = 0.068 \pm 0.0030$
 $SI > 1471$

Compound 44



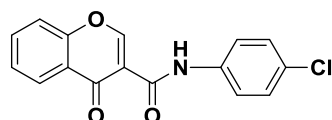
$h\text{MAO-B } IC_{50} (\mu\text{M}) = 0.064 \pm 0.0054$
 $SI = 74$

Compound 46



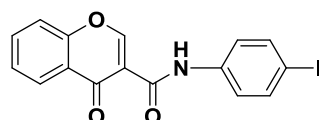
$h\text{MAO-B } IC_{50} (\mu\text{M}) = 0.0674 \pm 0.0032$
 $SI = 110$

Compound 66



$h\text{MAO-B } IC_{50} (\mu\text{M}) = 0.063 \pm 0.0042$
 $SI > 1585$

Compound 78



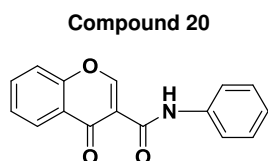
$h\text{MAO-B } IC_{50} (\mu\text{M}) = 0.069 \pm 0.0054$
 $SI > 1449$

Figure 4.3. Chemical structures of five of the best chromone-3 carboxamides and their inhibitory activity towards *h*MAO-B.

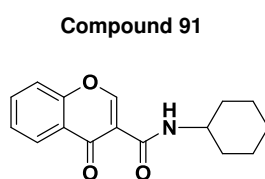
The theoretical calculated binding modes of *N*-phenyl, *N*-cyclohexyl *N*-propyl, (Fig. 4.4) and *N*-4'-chlorophenyl (compound 66, Fig. 4.3) chromone-3-carboxamides were visually inspected and similar interactions were found for all of the cited compounds (article in section 3.3).

The proposed binding modes of this type of chromone inhibitors reveal that the carboxamide side chain is located toward the FAD cofactor and the γ -pyrone ring located towards the pocket entrance. All the studied compounds showed a hydrogen bond interaction with Tyr326 residue involving either the ether present in the γ -pyrone ring (Compound 105, Fig. 4.4) and the sp^2 oxygen

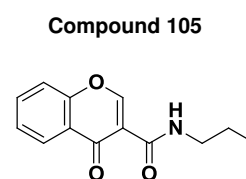
from the carboxamide moiety (compound 66, Fig. 4.3; compounds 20 and 91, Fig. 4.4). Remarkably, it was observed that all the studied compounds are somehow correlated with Cys172, an amino acid residue present in the entrance cleft of hMAO-B [312]. Focusing the attention in the *N*-(4-(chlorophenyl)-chromone-3-carboxamide (compound 66, Fig. 4.3), one of the most active hMAO-B inhibitors (article in section 3.2), it is possible to highlight the presence of hydrogen bonds with Cys172 and Tyr326 (Fig. 4.5) and other productive interactions of the hydrophobic side chain of the compound with Ile199, Pro102, Phe103, and Leu167.



*h*MAO-B IC_{50} (μ M) = 0.40 ± 0.022
SI > 250



*h*MAO-B IC_{50} (μ M) = 0.93 ± 0.062
SI > 107



*h*MAO-B IC_{50} (μ M) = 37.69 ± 1.68
SI > 2.7

Figure 4.4 Chemical structures of *N*-phenyl (compound 20), *N*-cyclohexyl (compound 91) and *N*-propyl (compound 105) chromone-3-carboxamides and their inhibitory activity towards hMAO-B.

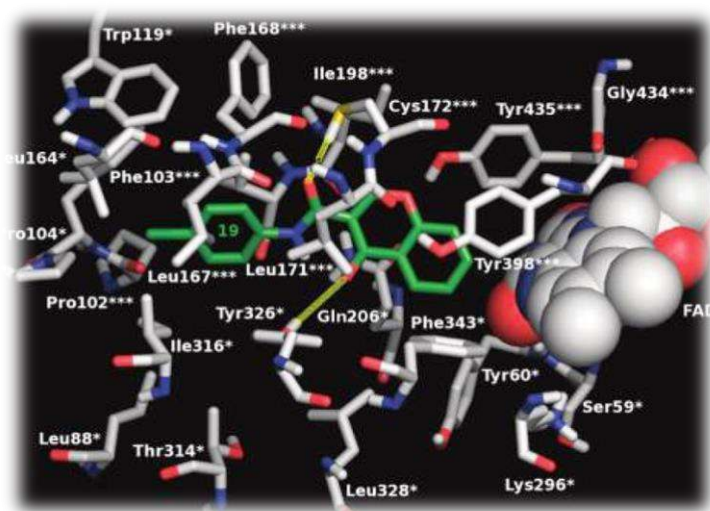


Figure 4.5 Virtual docking of *N*-(4-(chlorophenyl)-chromone-3-carboxamide into the hMAO-B catalytic site (figure extracted from article in section 3.2).

In summary, the molecular docking studies have shown that the productive interactions detected between the chromone-3-phenylcarboxamides and the *h*MAO-B isoform occur in non-conserved a.a. residues of the active site of *h*MAO-A isoform, a variance that can explain their selectivity towards *h*MAO-B isoform.

The overall data obtained in this rational drug discovery program allows to conclude that chromone-3-carboxamide is a valid scaffold for the development of MAO-B inhibitors and that a subsequent project of lead optimisation must be implemented to attain potent, selective and reversible MAO-B inhibitors.

4.3 Chromone a valid scaffold for the development of adenosine receptors ligands

One of the drug discovery approaches accepted at the present time as a putative solution to find an effective therapy for multifactorial pathoetiological diseases, such as neurodegenerative disorders and cancer, encompasses a change of the “one disease, one target, one molecule” paradigm. This new point of view embraces the concept of “promiscuous” drugs and consequently encloses the design and development of new drugs that act simultaneously in more than one target. Accordingly, and taking advantage of the MAO-B inhibition outline exhibited by chromone carboxamides, it was decided to perform the screening of the same chromone library towards other target. As adenosine receptors (ARs) are a recognized target for the development of drugs for the treatment of diverse maladies, namely in neurodegenerative diseases, as described in section 2.4 of this thesis, they have been selected to accomplish the objective. So, the affinity of the chromone ligands towards the four subtypes AR was evaluated. The data was first acquired by outsourcing with an academic research centre, and then by a fruitful collaboration with Professor Karl-Norbert Klotz, from the Institute of Pharmacology and Toxicology, University of Wurzburg. Consequently, the methods used to assess the AR binding capacity encompass different procedures, a fact that can explain the apparent data differences found in the published articles (articles in sections 3.5. and 3.6.).

One of the most glaring discrepancies is related with the data assessed for A_{2B} receptor. In fact, in one of the papers (article in section 3.5) the binding affinity was acquired using radioligand assays and in the other one (article in section 3.6) by the measurement of adenylyl cyclase activity (indirect method). The binding affinity data acquired for the other three receptors have been performed by radioligand competition experiments in both assays. Nevertheless, the type of cells and radioligands used in the cited assays was different (table 4.4).

Table 4.4. Radioligands binding assays conditions.

Adenosine receptor	Type of cells		Radioligands	
	Article in section 3.5	Article in section 3.6	Article in section 3.5	Article in section 3.6
A ₁	CHO transfected cells	CHO transfected cells	[³ H]DPCPX	[³ H]CCPA
A _{2A}	HeLa transfected cells		[³ H]ZM241385	[³ H]NECA
A ₃			[³ H]NECA	[³ H]HEMADO

Despite the pointed differences, and excluding the data acquired for A_{2B}, a comparative analysis for some chromone carboxamides disclosed the existence of the same structural trends: i) a higher affinity for A₃ AR subtype and ii) a higher selectivity for the A₃ AR subtype receptor for chromone-2-carboxamides.

In summary, the data acquired so far allow concluding that chromone carboxylic acids (the starting building blocks) display no significant binding affinity for all ARs and that the introduction of carboxamide type substituents result in compounds with a diverse affinity and selectivity profile towards human A₁, A_{2A} and A₃ ARs. In general, the introduction of a phenylcarboxamide substituent at position 2, with or without substituents in the exocyclic aromatic moiety (e.g. 3',4'-dimethoxyphenylcarboxamide) generates compounds that bind selectively to A₃ AR. However, one can highlight that when the phenylcarboxamide substituent is located at position 3 the compounds are generally more potent, but less selective.

Focusing our attention on the data described on the article in section 3.6., other significant SAR conclusions can be carried out. In general, it is possible to assume that the positions of the substituent on the pyran ring of the chromone scaffold, the type of amide (aromatic, cyclic or aliphatic) as well as the presence of electron donors or withdrawing groups on the exocyclic aromatic substituent have a marked effect on their binding affinity towards ARs.

A closer look through the results showed that, despite being more active, chromone-3-carboxamides are generally less selective than their corresponding isomers at position 2 (see tables 1 and 2 of the article in section 3.6.) and that in general, the presence of withdrawing groups causes a decrease or loss of the binding affinity towards A₃ ARs. Nevertheless, the presence of chlorine or nitro substituents at the *para* position of the chromone-3-phenylcarboxamides seems to improve the affinity for A_{2A} and A₃ ARs subtypes. The presence of electron donating groups at the exocyclic aromatic ring of the chromone carboxamides induced different performances

in the two isomeric series. In fact, all the chromone-2-phenylcarboxamides with donating groups displayed a significant binding affinity towards A_3 AR. The most remarkable improvement of potency is related with the introduction of a methoxy group, when compared to that of the non-substituted 2-phenylcarboxamide. Interestingly, the introduction of a hydroxy function at the *para* position of the exocyclic aromatic ring led to enhanced affinity binding towards A_{2A} AR, although with a reduced selectivity ratio. In contrast, the chromone-3-phenylcarboxamides with donating groups showed in general an improvement of their binding affinity potencies for all the ARs, when compared with the non-substituted one. An exception for this trend comprises the chromone-3-(4'-methoxyphenyl) carboxamide that only exhibits improvement in the binding affinity potency towards A_3 AR.

The overall results obtained with chromone carboxamide library allow concluding that this type of chromones can work as a valuable starting point for development of new ligands for A_3 AR. Some chromone carboxamides (Fig. 4.6) have an interesting binding affinity towards A_{2A} AR, despite the lack of selectivity regarding A_1 and A_3 ARs. It is expected that their optimisation can lead to the discovery of new ligands for this receptor subtype in a foreseeable future.

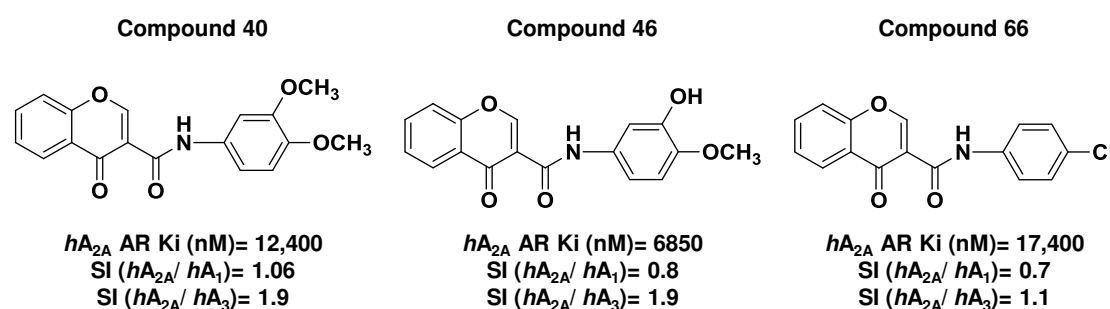


Figure 4.6. Chemical structures of three of the best chromone-3 carboxamides as A_{2A} AR ligands.

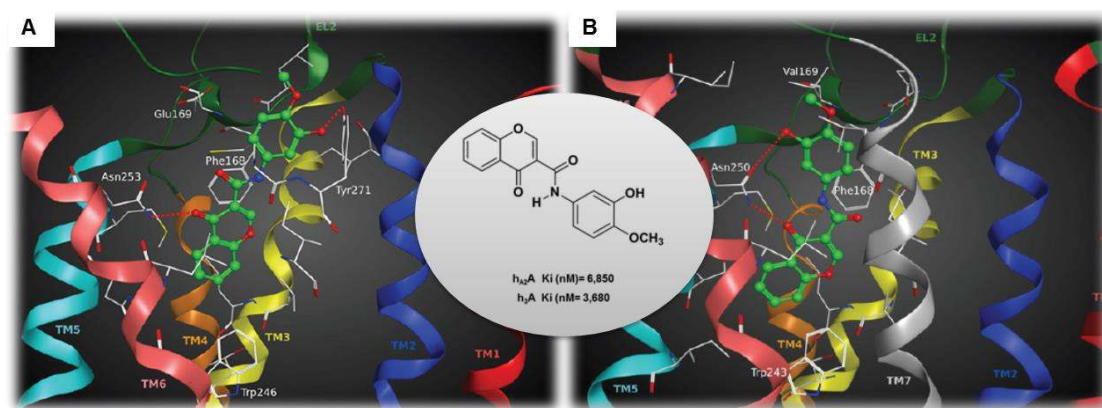


Figure 4.7. Hypothetical binding modes of one of our most active compound obtained after docking simulations: (A) inside the hA_{2A} AR binding site; (B) inside the hA_3 AR binding site. (Figure extracted from article in section 3.6)

The studies were also accomplished by a receptor-driven molecular modelling investigation performed in collaboration with the Molecular Modeling Section (MMS), Department of Pharmaceutical Sciences, University of Padua. It was concluded that in general chromone carboxamides exhibit different binding poses inside the binding pockets either of hA_{2A} or hA_3 ARs, a condition that can somehow explain the different K_i obtained in the pharmacological assays. This type of molecular docking studies (fig 4.7.) were thoroughly performed for one of the most active chromone carboxamide (compound 46, Fig. 4.6) towards A_{2A} and A_3 ARs subtypes in order to disclose the nature of interactions with the binding pocket of each receptor. Additionally, the *per residue* electrostatic and hydrophobic contributions were also calculated (article in section 3.6.).

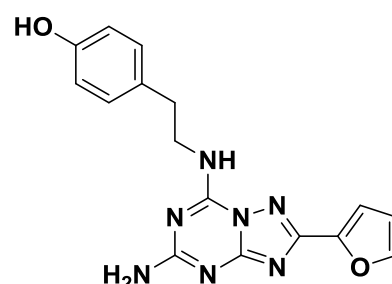


Figure 4.8. Chemical structure of ZM241385

The homology models, the mutagenesis studies and the A_{2A} AR recently determined crystallographic structure^[317] have brought to the light the existence of several amino acids residues that are important for ligand binding, namely Ile80, Val84, Leu85, Thr88, Gln89, Ile135, Leu167 (EL2), Phe168 (EL2), Asn181, Phe182, Val186, Trp246, Leu249, His250, Asn253, Ile274, Ser277, His278. Furthermore, the crystallographic structure of the hA_{2A} AR in complex with the potent and selective antagonist ZM241385 (Fig. 4.8) reinforced the importance of Glu169, His250, Asn253, Ile274, Phe168, Met177 and Leu249 amino acids residues in the binding of the ligand with the receptor^[317]. Interestingly, in the A_{2A} AR model used in our studies the most active chromone carboxamide revealed putative interactions with two key amino acid residues establishing an H-bond interaction with Asn253 and a stabilizing interaction

with Phe168 (EL2). In addition, a weak H-bond interaction with Tyr271 as well as hydrophobic interactions with some aa residues of the pocket, including Leu85, Trp246, Leu249, Tyr271 and Ile274, were also detected. However, no interaction with Glu169 (EL2) an important residue in ligand recognition was detected. The information gathered in the analysis of the electrostatic contribution *per residue* and in the hydrophobic interaction score patterns strengthen the hypothesis that the most stabilizing contributions are due the H-bond with Asn253 and the hydrophobic interactions of the ligand with Phe168 (EL2). The acquired data is of utmost significance for the optimisation step of this chromone carboxamide.

Despite the enormous advances in X-ray crystallography of proteins the high resolution structural information on the active and inactive states of GPCRs is still uncovered. In fact, the 3D structural information available so far for this type of receptors is still largely based on rhodopsin homology models^[317]. However, as previously mentioned, the recent publication of the crystal structure of the *hA_{2A}* AR in complex with a high-affinity subtype-selective antagonist, ZM241385 has provided a new template for the 3D structure of *hA₃* AR.

The homology model of the *hA₃* AR used in this work was built up by Moro and co-workers^[155, 318]. In accordance with the aim of project ligand binding studies were performed for the most active compound (the same used for *hA_{2A}* molecular docking studies, Fig. 4.7). The most important binding features were related with the presence of two H-bond interactions with Asn250 and Phe168 (EL2), and hydrophobic interactions between the ligand and some residues of the binding site, such as Leu91, Trp243, Leu246 and Leu264 (article in section 3.6.).

Comparing the data gathered for the *hA_{2A}* and the *hA₃* ARs one can infer that the electrostatic contribution associated to the Asn residue is much more prevalent for the *hA₃* AR ligand complex and in that way can compete with the stabilizing interaction with Phe168 found for *A_{2A}* AR ligand complex. This assumption is in accordance with the experimental data (*hA_{2A}* AR K_i (nM)= 6850 and *hA₃* AR K_i (nM)=3680) which showed a lower K_i value for *hA₃* AR.

As known in medicinal chemistry programs, the prerequisite of interdisciplinary artwork encompass a natural delay on the attainment of the results, a problematic that is aggravated when the project is focused on the discovery and development of dual-target drugs. So, when expecting data acquisition the chromone carboxamide library was amplified and the affinity of the ligands towards ARs was evaluated. In general, the new chromones display a superior affinity for *A₃* AR ligands and so this part of the unpublished work was reported in the thesis.

4.4 Chromone-2-carboxamide a valid scaffold for the development of A₃ AR ligands

Currently, a growing number of evidences related with all four AR subtypes as potential drug targets for cancer have been gathered, placing the A_{2A} and A₃ subtypes as the most promising ones^[319]. As adenosine plays a crucial role in the cell progression pathway, either during apoptosis or during cytostatic state, it has been postulated that high levels of extracellular adenosine can have a profound impact on the growth of solid tumours masses^[319]. Paradoxically, the drug discovery process performed so far encompasses either agonist or antagonist AR ligands and both of them have shown encouraging results^[320, 321]. As mentioned in section 2.4.2 the search for new A₃ AR agonists has been mainly based in adenosine and xanthine scaffolds, with other classes of compounds having a less significant expression in the drug discovery projects. However, the strategy to develop new A₃ AR antagonists involved also a diversity of scaffolds, such as flavonoids, 1,4-dihydropyridines and pyridine derivatives and isoquinoline and quinazoline derivatives^[322, 323].

On the other hand, it has been recently proposed that there is a significant inverse relationship between PD and certain types of cancers^[312, 314]. These two pathologies can be faced as the result of opposite abnormal cell signalling, with an irreversible cell death in PD and cell overproliferation resistant to death in carcinogenesis. The research in the field is now gathering evidences to attest the existence of an overlap between the molecular pathways implicated in these two distinct processes^[310, 311, 313].

Epidemiological studies have shown that some cancers, namely melanoma and breast cancer, occur frequently in PD patients, when compared with the controls^[324]. To note that the possibility of an increased risk of melanoma in PD patients associated with the L-Dopa therapy has being discarded over the years by the scientific community^[315] and that other variables, such as molecular, genetic and environmental factors are emerging as probable explanations for the epidemiological data^[317]. Albeit of the exact mechanisms underlying the observed cancer-PD association are not still fully understood, the study of the signalling pathways and mechanisms for both diseases can unveil new approaches in the discovery and development of new chemical entities as anti-cancer and/or as antiparkinsonian drugs. In fact, the work of Hebron *et. al.*^[318] that describes nilotinib, a drug approved by the US Food and Drug Administration (FDA) in 2007 to leukemia treatment, as a possible drug for Parkinson disease therapy was the pioneer.

In the search for dual-target compounds for PD based on the chromone scaffold it was observed that some compounds of the library displayed a noticeable affinity and

selectivity for A_3 AR subtype, and that when the library was amplified the new chromones exhibited a superior affinity for A_3 AR ligands (unpublished data). So, as mentioned before, this new data was included in the thesis and discussed.

As it was already mentioned in section 4.3 it was concluded that chromone 2-carboxamides were more selective for A_3 AR subtype than their isomers at position 3 and that the preliminary SAR studies have shown that the presence of electron donors or withdrawing groups on the aromatic exocyclic substituent modulate their affinity and selectivity towards the ARs. After the amplification of the chromone 2-carboxamide library and biological evaluation towards ARs a more well-founded SAR have been established. Some of the chemical modifications have been constructed on structural changes of the compounds highlighted in Fig. 4.9 involving the synthesis of their *ortho* and *meta* structural isomers (table 4.2).

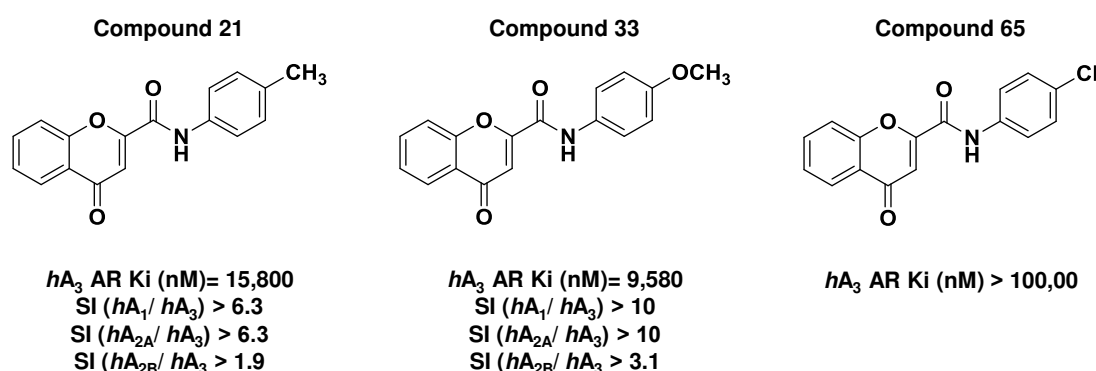
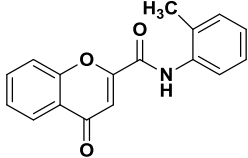
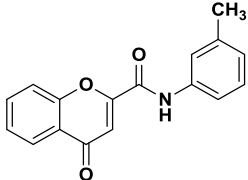
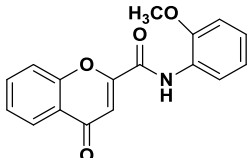
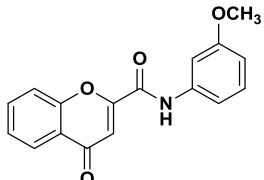
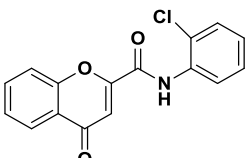
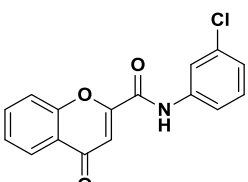


Figure 4.9. Chemical structures of mono substituted chromone-2-carboxamides, their corresponding hA_3 Ki and selective index (SI).

The binding affinity data of compounds 23, 25, 35, 37, 67 and 69 (table 4.5.) show that the location of the substituents, namely at *para* position of the exocyclic aromatic ring, are somewhat important for ligand recognition.

Table 4.5 Affinity (Ki, nM) of monosubstituted chromone-2-carboxamides in radioligand binding assays at $hARs$.

Compound	A ₁ AR Ki (nM)	A _{2A} AR Ki (nM)	A _{2B} AR Ki (nM)	A ₃ AR Ki (nM)
<div>23</div> 	>100,000	>100,000	>10,000	21,800 (17,300–27,500)
<div>25</div> 	>100,000	>100,000	>10,000	>100,000
<div>35</div> 	>100,000	>100,000	>10,000	>30,000
<div>37</div> 	>100,000	>30,000	>10,000	>30,000
<div>67</div> 	>100,000	>100,000	>10,000	>100,000
<div>69</div> 	>100,000	>100,000	>10,000	>100,000

Other structural modifications have been based on the results obtained for the compounds highlighted in figure 4.10, compound 45 (articles in sections 3.2 and 3.5) and the newly synthesised compounds (27 and 41) represented in table 4.6 were also evaluated as potential ligands for ARs and the (data is described in table 4.6.).

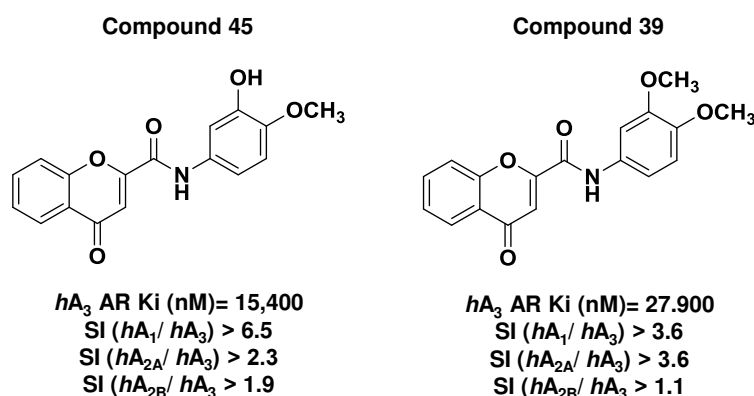
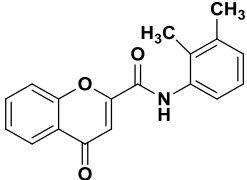
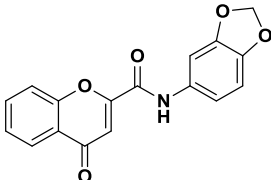
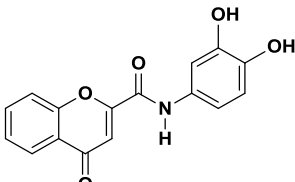


Figure 4.10. Chemical structures of di-exocyclic substituted chromone-2-carboxamides, their corresponding hA_3 Ki and selective index (SI).

Table 4.6. Affinity (Ki, nM) of disubstituted chromone-2-carboxamides in radioligand binding assays at $hARs$.

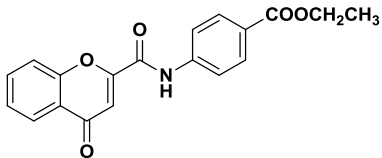
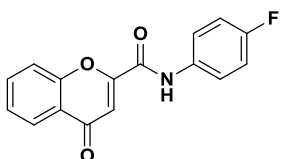
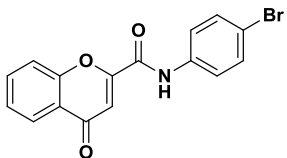
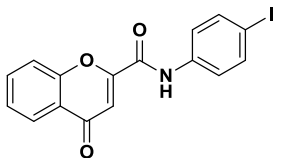
Compound	A_1 AR Ki (nM)	A_{2A} AR Ki (nM)	A_{2B} AR Ki (nM)	A_3 AR Ki (nM)
27		>100,000	>100,000	>10,000
41		>100,000	>100,000	>10,000
47		7,366 (4,290–12,700)	39,727 (32,099–49,168)	>10,000

Analysing the data reported in table 4.6., one can conclude that the modifications based on compound 47, which have two hydroxyl groups in *meta* and *para* positions of the exocyclic aromatic ring, were able to produce a compound with a better A_3 AR subtype binding profile, when compared with the compounds presented in figure 4.10. and with those described in Fig. 4.9. However, it is important to note that the selectivity index of this compound between A_1 AR and A_3 AR is only around 1.3 resulting in a loss of selectivity towards A_3 AR.

To inspect the role of electron donating and withdrawing groups on the binding affinity towards ARs, new chromone-2-carboxamides were synthesized (table 4.7. and 4.8.). The data obtained so far reinforces the hypothesis (article in section 3.6.) that the

presence of withdrawing groups in the exocyclic phenyl group (compounds 51, 63, 71 and 77, tables 4.7) has a negative effect in the binding affinity toward all ARs.

Table 4.7. Affinity (K_i , nM) of monosubstituted chromone-2-carboxamides with withdrawing groups in radioligand binding assays at *h*ARs.

Compound	A_1 AR K_i (nM)	A_{2A} AR K_i (nM)	A_{2B} AR K_i (nM)	A_3 AR K_i (nM)
51 	>100,000	>100,000	>10,000	>100,000
63 	>100,000	>100,000	>10,000	>100,000
71 	>100,000	>100,000	>10,000	>100,000
77 	>100,000	>100,000	>10,000	>100,000

Furthermore, the presence of a straight alkyl chain with a length higher than CH_3 (compounds 29 and 31, table 4.8) leads to a complete loss of activity towards A_3 AR subtype. Interestingly, the replacement of the OCH_3 (compound 33 table 4.2 and Fig. 4.9) by its bioisoster SCH_3 (compound 55, table 4.8.) or by a NH_2 group (compound 58, table 4.8) led to a total loss of activity for all the ARs.

To examine the importance of the existence of a secondary amide for the biological activity, tertiary chromone 2-carboxamides (compounds 81 and 100 table 4.9.) have been synthesised. However, a decrease or loss of binding affinity towards hA_3 AR (table 4.9.) was observed, when compared with monosubstituted *N*-phenyl chromone 2-carboxamide (K_i =14,200 nM, article in section 3.6).

Table 4.8. Affinity (K_i, nM) of monosubstituted chromone-2-carboxamides with donating groups in radioligand binding assays at hARs.

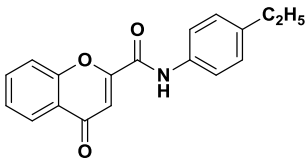
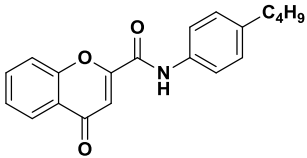
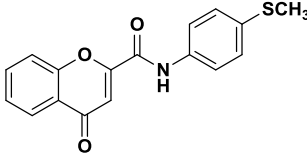
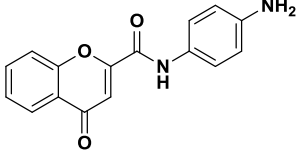
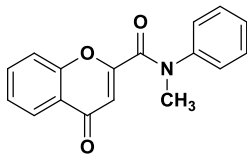
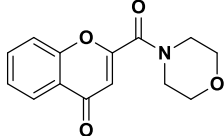
Compound	A ₁ AR K _i (nM)	A _{2A} AR K _i (nM)	A _{2B} AR K _i (nM)	A ₃ AR K _i (nM)
29 	>100,000	>100,000	>10,000	>30,000
31 	>100,000	>100,000	>10,000	>30,000
55 	>100,000	>100,000	>10,000	>100,000
58 	>10,000	>10,000	>10,000	>10,000

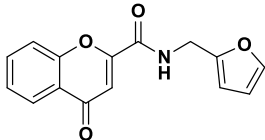
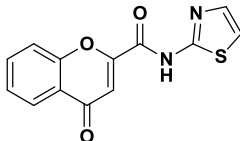
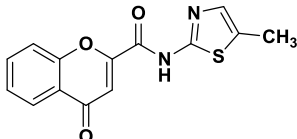
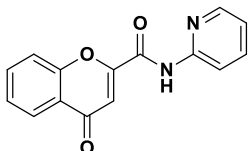
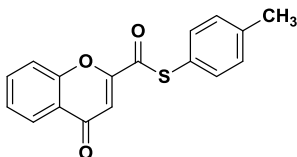
Table 4.9. Affinity (K_i, nM) of tertiary chromone-2-carboxamides in radioligand binding assays at hARs.

Compound	A ₁ AR K _i (nM)	A _{2A} AR K _i (nM)	A _{2B} AR K _i (nM)	A ₃ AR K _i (nM)
81 	>100,000	>100,000	>10,000	26,177 (21,177– 31,614)
100 	>100,000	>100,000	>10,000	>100,000

The replacement of the phenyl ring by other type of heteroaromatic rings gave rise to the compounds 92, 94, 96 and 98 (table 4.10). The results for the binding affinity assays (table 4.10) show that the introduction of a heterocyclic aromatic ring, directly linked to NH of the carboxamide (compounds 94, 96, 98) produced active but non selective ligands for A₁, A_{2A} and A₃ ARs. The presence of a CH₂ spacer between the carboxamide function and the exoheterocyclic ring (compound 92, table 4.9.) led to a

compound without affinity to A₃ and A_{2B} ARs but with affinity towards A₁ and A_{2A} ARs with a selective ratio A₁/A_{2A} of 0.7. This data and the results obtained for non-aromatic carboxamides (article in section 3.6) reinforce the hypothesis that the aromatic exocyclic ring is an important requisite for the binding affinity of chromone carboxamide ligands towards A₃ AR.

Table 4.10. Affinity (K_i, nM) of heterocyclic chromone-2-carboxamides in radioligand binding assays at hARs.

Compound	A ₁ AR K _i (nM)	A _{2A} AR K _i (nM)	A _{2B} AR K _i (nM)	A ₃ AR K _i (nM)
92 	11,976 (8,450– 17,000)	18,499 (11,700– 29,100)	>10,000	>100,000
94 	17,328 (11,400– 26,300)	15,092 (9,160– 24,900)	>10,000	11,923 (10,900– 13,100)
96 	8,178 (5600– 11,900)	10,354 (8,040– 13,300)	>10,000	1,307 (982– 1,740)
98 	10,203 (7,620– 13,700)	18,892 (13,300– 26,900)	>10,000	10,687 (8,610– 13,100)
102 	>100,000	>100,000	8,630 (5,740– 13,000)	8,214 (5,130– 13,100)

On the other hand, the modification of the carboxamide moiety (Compound 102, table 4.10) by introducing of a thio bioisostere, and maintenance of the substituent 4'-CH₃ on the phenyl exocyclic ring, led to a compound twice as potent for A₃ AR (K_i =8,630 nM) than compound 21 (K_i =15,800 nM) (Fig. 4.9) However, and despite the pronounced affinity potency improvement, a loss of specificity was observed as, surprisingly, a similar binding potency for A_{2B} AR (K_i =8,630 nM) (unpublished data) was noticed.

From the overall data obtained so far it is concluded that the type and position of the donor groups at the exocyclic phenyl ring of the chromone 2-carboxamides is constrained, as only 4'-CH₃ and the 4'-OCH₃ substituents are able to enhance the

affinity and specificity towards A_3 AR, when compared with the non-substituted *N*-phenyl chromone 2-carboxamide. In fact, the lack of binding affinity observed for the four positional isomers (compounds 29, 25, 35 and 37, table 4.5) corroborates the hypothesis that the location of substituents in the *para* position is vital to preserve the A_3 AR affinity. Interestingly, it was observed that the presence of two hydroxyl groups (compound 47, table 4.6.) at the exocyclic aromatic ring led to an enhancement of the binding affinity to A_3 AR. This compound is one of the most active compounds with a hA_3 AR $K_i=5,735$ nM being around 2.5 fold more potent than the non-substituted *N*-phenyl chromone 2-carboxamide (hA_3 AR $K_i= 14,200$ nM article in section 3.6). Finally, it is important to highlight the compound 96, the most potent compound so far tested, with an A_3 AR $K_i =1,307$ nM, being 6 and nearly 8 times more selective for A_3 than A_1 and A_{2A} , respectively.

Chapter 5

**Concluding remarks
and future
perspectives**

5.1 Concluding remarks and future perspectives

The discovery and development of a new drug is a long, laborious and demanding process. Its successful development generally relies on the availability of a continuous pipeline of novel molecules (New Chemical Entities, NCE's). However, a *de novo* drug discovery campaign has considerable drawbacks, mainly related to the challenge of selecting a satisfactory library for the establishment of preliminary structure–activity relationships. This process can be fast-tracked taking advantage of the concept of privileged structure. Despite the identification of many molecular frameworks performed so far, there is still a restricted number of core scaffolds and fragments for the design of chemical libraries directed for specific targets ^[13].

In this project, the chromone scaffold was validated as a useful framework for the development of new lead compounds for Parkinson disease. In this context, a pioneer dual-target (MAO-B and A_{2A} AR) drug discovery and development project based on the chromone scaffold has been implemented. To attain this goal, chromone libraries were planned and diversity-oriented synthetic strategies have been applied.

The results obtained so far highlight two promising chromone carboxamides (Fig. 5.1) that show potent and selective MAO-B inhibition and also display binding affinity towards A_{2A} AR.

The preliminary SAR studies, reinforced by the molecular modelling data, afford important clues to get-

up-and-go the research. In fact, it was demonstrated that, in general, only the chromone-3-carboxamide series present MAO-B inhibitory activity, and that some chromones display remarkable

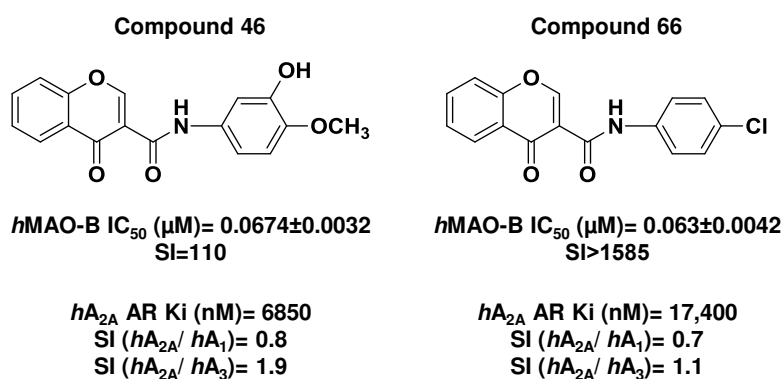


Figure 5.1. Chemical structures of two of the best chromone-3-carboxamides as inhibitors of hMAO-B isoform and as ligands of hA_{2A} ARs.

potency/selectivity ratios (Compound 22, $\text{IC}_{50} = 0.068 \pm 0.0030 \mu\text{M}$, $\text{SI} > 1471$; Compound 46 = $0.0674 \pm 0.0032 \mu\text{M}$ $\text{SI} = 110$; compound 66, $\text{IC}_{50} = 0.063 \pm 0.0042 \mu\text{M}$, $\text{SI} > 1585$ and compound 78, $\text{IC}_{50} = 0.069 \pm 0.0054 \mu\text{M}$ $\text{SI} > 1449$, to cite some). Interestingly, it was found that the two of the best chromone-3-carboxamides (Fig. 5.1.) displayed simultaneously affinity towards the A_{2A} AR subtype.

In a foreseeable future it will be important to perform fine molecular modifications in order to attain more robust SARs studies that hopefully will result in the

optimisation of above mentioned compounds. The improvement of either the A_{2A} AR potency as well as their selectivity towards this AR subtype is therefore a forthcoming aim in future research. Moreover, the results obtained for the chromone-2-carboxamides as selective ligands towards A₃ AR, provide a new scaffold for the development of new anti-cancer drugs. Therefore, efforts should also be performed to carry this particular research a step further. The introduction of substituent(s) on the aromatic chromone ring, bioisosteric replacements on the carboxamide moiety, and the modification of the substitution pattern on the exocyclic aromatic ring are some of the likely modifications that can be made.

Additionally, the balance between physicochemical and pharmacokinetic properties is not only a critical point in the design of new drugs, but also a feature of upmost importance in the design, synthesis and development of NCEs for neurodegenerative diseases. In fact, blood-brain barrier permeability is a crucial requirement to obtain centrally active drugs that are able to reach their target(s) within the CNS, making the development of these drugs a pressing and challenging endeavour. Accordingly, as a complement to the synthetic artwork and in order to enhance the preliminary SARs studies, screening assays will be important to attain several physicochemical and pharmacokinetic properties (e.g. solubility, permeability, metabolic stability) of the most promising compounds.

Bibliography

- [1] Wermuth C. G.; Ganellin C. R.; Lindberg P.; Mitscher L. A.; "Glossary of terms used in medicinal chemistry (IUPAC Recommendations 1998)". *Pure Appl. Chem.* **1998**, 70(5), 1129-1143.
- [2] Kornberg A.; "The two cultures: chemistry and biology". *Biochemistry* **1987**, 26(22), 6888-6891.
- [3] Imming P., in *The Practice of Medicinal Chemistry (Third Edition)* (Ed.: W. Camille Georges), Academic Press, New York, **2008**, pp. 63-72..
- [4] Drews J.; "Drug discovery: A historical perspective". *Science* **2000**, 287(5460), 1960-1964.
- [5] Lombardino J. G.; Lowe J. A.; "The role of the medicinal chemist in drug discovery - Then and now". *Nat. Rev. Drug Discov.* **2004**, 3(10), 853-862.
- [6] Chast F., in *The Practice of Medicinal Chemistry (Third Edition)* (Ed.: W. Camille Georges), Academic Press, New York, **2008**, pp. 1-62.
- [7] Walters W. P.; Green J.; Weiss J. R.; Murcko M. A.; "What Do Medicinal Chemists Actually Make? A 50-Year Retrospective". *J. Med. Chem.* **2011**, 54(19), 6405-6416.
- [8] Zavitz K. H.; Bartel P. L.; Hobden A. N., in *The Practice of Medicinal Chemistry (Third Edition)* (Ed.: W. Camille Georges), Academic Press, New York, **2008**, pp. 106-121..
- [9] Morphy R.; Kay C.; Rankovic Z.; "From magic bullets to designed multiple ligands". *Drug Discov. Today* **2004**, 9(15), 641-651.
- [10] Geldenhuys W. J.; Youdim M. B. H.; Carroll R. T.; Van der Schyf C. J.; "The emergence of designed multiple ligands for neurodegenerative disorders". *Prog. Neurobiol.* **2011**, 94(4), 347-359.
- [11] Satyanarayanajois S. D.; Hill R. A.; "Medicinal chemistry for 2020". *Future Med. Chem.* **2011**, 3(14), 1765-1786.
- [12] Horton D. A.; Bourne G. T.; Smythe M. L.; "The combinatorial synthesis of bicyclic privileged structures or privileged substructures". *Chem. Rev.* **2003**, 103(3), 893-930.
- [13] Welsch M. E.; Snyder S. A.; Stockwell B. R.; "Privileged scaffolds for library design and drug discovery". *Curr. Opin. Chem. Biol.* **2010**, 14(3), 347-361.
- [14] Parkinson's Disease Foundation, I. *Statistics on Parkinson's*. 2012 [cited 2012 30/11/2012]; http://www.pdf.org/en/parkinson_statistics].
- [15] De Lau, L. M. L.; Breteler M. M. B.; "Epidemiology of Parkinson's disease". *Lancet Neurol.* **2006**, 5(6), 525-535.

- [16] Fahn S.; Cohen G.; "The oxidant stress hypothesis in Parkinson's disease: Evidence supporting it". *Ann. Neurol.* **1992**, 32(6), 804-812.
- [17] Hauser D. N.; Hastings T. G.; "Mitochondrial dysfunction and oxidative stress in Parkinson's disease and monogenic parkinsonism". *Neurobiol. Dis.* **2013**, 51, 804-812.
- [18] Carlsson A.; "The occurrence, distribution and physiological role of catecholamines in the nervous system". *Pharmacol. Rev.* **1959**, 11(2, Part 2), 490-493.
- [19] Snyder S. H.; "Virtuoso design of drugs". *Nature* **1986**, 323(6086), 292-293.
- [20] Uversky V., in *Protein Misfolding, Aggregation, and Conformational Diseases*, Vol. 6 (Eds.: V. Uversky, A. Fink), Springer US, **2007**, pp. 61-110..
- [21] Tansey M. G.; McCoy M. K.; Frank-Cannon T. C.; "Neuroinflammatory mechanisms in Parkinson's disease: Potential environmental triggers, pathways, and targets for early therapeutic intervention". *Exp. Neurol.* **2007**, 208(1), 1-25.
- [22] Malkus K.; Tsika E.; Ischiropoulos H.; "Oxidative modifications, mitochondrial dysfunction, and impaired protein degradation in Parkinson's disease: how neurons are lost in the Bermuda triangle". *Mol. Neurodegener.* **2009**, 4(1), 24.
- [23] Schapira A. H.; Jenner P.; "Etiology and pathogenesis of Parkinson's disease". *Mov. Disord.* **2011**, 26(6), 1049-1055.
- [24] Bras J. M.; Singleton A.; "Genetic susceptibility in Parkinson's disease". *BBA-Mol. Basis Dis.* **2009**, 1792(7), 597-603.
- [25] Freire C.; Koifman S.; "Pesticide exposure and Parkinson's disease: Epidemiological evidence of association". *Neurotoxicology* **2012**, 33(5), 947-971.
- [26] Caudle W. M.; Guillot T. S.; Lazo C. R.; Miller G. W.; "Industrial toxicants and Parkinson's disease". *Neurotoxicology* **2012**, 33(2), 178-188.
- [27] Rodriguez-Oroz M. C.; Jahanshahi M.; Krack P.; Litvan I.; Macias R.; Bezard E.; Obeso J. A.; "Initial clinical manifestations of Parkinson's disease: features and pathophysiological mechanisms". *Lancet Neurol.* **2009**, 8(12), 1128-1139.
- [28] Blandini F.; Nappi G.; Tassorelli C.; Martignoni E.; "Functional changes of the basal ganglia circuitry in Parkinson's disease". *Prog. Neurobiol.* **2000**, 62(1), 63-88.
- [29] Juri C.; Rodriguez-Oroz M.; Obeso J. A.; "The pathophysiological basis of sensory disturbances in Parkinson's disease". *J. Neurol. Sci.* **2010**, 289(1-2), 60-65.

- [30] Wichmann T.; Smith Y.; Vitek J. L., in *Parkinson's Disease Diagnosis and Clinical Management, Vol. 1* (Eds.: Factor, W.J. Weiner S.A.), Demos Medical Publishing, LLC, New York, **2008**, pp. 245-267..
- [31] Cools R.; "Dopaminergic modulation of cognitive function-implications for L-DOPA treatment in Parkinson's disease". *Neurosci. Biobehav. R.* **2006**, 30(1), 1-23.
- [32] Schapira A. H. V.; Bezard E.; Brotchie J.; Calon F.; Collingridge G. L.; Ferger B.; Hengeler B.; Hirsch E.; Jenner P.; Noveck N. L.; Obeso J. A.; Schwarzschild M. A.; Spampinato U.; Davidai G.; "Novel pharmacological targets for the treatment of Parkinson's disease". *Nat. Rev. Drug Discov.* **2006**, 5(10), 845-854.
- [33] Rabey J. M.; Burns R. S., in *Parkinson's Disease Diagnosis and Clinical Management Vol. 1* (Eds.: Factor, W.J. Weiner S.A.), Demos Medical Publishing, LLC, New York, **2008**, pp. 257-273..
- [34] Muñoz P.; Huenchuguala S.; Paris I.; Segura-Aguilar J.; "Dopamine oxidation and autophagy". *Parkinsons Dis.* **2012**.
- [35] Darbin O.; "The aging striatal dopamine function". *Parkinsonism Relat. D.* **2012**, 18(5), 426-432.
- [36] Meiser J.; Weindl D.; Hiller K.; "Complexity of dopamine metabolism". *Cell Commun. Signal.* **2013**, 11(1), 34.
- [37] Tritsch N. X.; Sabatini B. L.; "Dopaminergic Modulation of Synaptic Transmission in Cortex and Striatum". *Neuron* **2012**, 76(1), 33-50.
- [38] Beaulieu J. M.; Gainetdinov R. R.; "The physiology, signaling, and pharmacology of dopamine receptors". *Pharmacol. Rev.* **2011**, 63(1), 182-217.
- [39] DeLong M.; Wichmann T.; "Update on models of basal ganglia function and dysfunction". *Parkinsonism Relat. D.* **2009**, Suppl 15, S237-S240.
- [40] Obeso J. A.; Marin C.; Rodriguez-Oroz C.; Blesa J.; Benitez-Temino B.; Mena-Segovia J.; Rodriguez M.; Olanow C. W.; "The basal ganglia in Parkinson's disease: current concepts and unexplained observations". *Ann. Neurol.* **2008**, 64 Suppl 2, S30-S46.
- [41] McAuley J. H.; "The physiological basis of clinical deficits in Parkinson's disease". *Prog. Neurobiol.* **2003**, 69(1), 27-48.
- [42] Nambu, A., in *Encyclopedia of Neuroscience* (Ed.: Larry, R.S.), Academic Press, Oxford, **2009**, pp. 111-117..
- [43] Obeso J.A.; Rodriguez-Oroz C.; Rodriguez M.; Lanciego J. L.; Artieda J.; Gonzalo N.; Olanow C. W.; "Pathophysiology of the basal ganglia in Parkinson's disease". *Trends Neurosci.* **2000**, 23, Suppl 1, S8-S19.

- [44] Nambu, A.; "Seven problems on the basal ganglia". *Curr. Opin. Neurobiol.* **2008**, 18(6), 595-604.
- [45] Jankovic J.; Aguilar L. G.; "Current approaches to the treatment of Parkinson's disease". *Neuropsychiatr. Dis. Treat.* **2008**, 4(4), 743-757.
- [46] Schapira A. H. V.; "Present and future drug treatment for Parkinson's disease". *J. Neurol. Neurosurg. Psychiatry* **2005**, 76(11), 1472-1478.
- [47] Nagatsu T.; Sawada M.; "L-dopa therapy for Parkinson's disease: Past, present, and future". *Parkinsonism Relat. Disord.* **2009**, 15, Suppl 1, S3-S8.
- [48] Nutt J. G.; Holford N. H. G.; "The response to levodopa in parkinson's disease: Imposing pharmacological law and order". *Ann. Neurol.* **1996**, 39(5), 561-573.
- [49] López I. C.; Ruiz P.J. G.; Del Pozo S. V. F.; Bernardos V. S.; " Motor complications in Parkinson's disease: Ten year follow-up study". *Mov. Disord.* **2010**, 25(16), 2735–2739.
- [50] Lang A. E.; Lees A.; "Levodopa". *Mov. Disord.* **2002**, 17, Suppl 4, S23-S37.
- [51] Barbeau A. M. H.; Botez M. I.; Joubert M.; "Levodopa combined with peripheral decarboxylase inhibition in Parkinson's disease". *Can. Med. Assoc. J.* **1972**, 106(11), 1169-1174.
- [52] Olanow C. W.; "Attempts to obtain neuroprotection in Parkinson's disease". *Neurology* **1997**, 49, Suppl 1, S26-33.
- [53] Weintraub D.; "Dopamine and impulse control disorders in Parkinson's disease". *Ann. Neurol.* **2008**, 64, Suppl 2, S93-S100.
- [54] Schapira A. H. V.; Olanow C. W.; "Drug selection and timing of initiation of treatment in early Parkinson's disease". *Ann. Neurol.* **2008**, 64 Suppl 2, S47-S55.
- [55] Lang A. E.; Lees A.; "Management of Parkinson's disease: An evidence-based review". *Mov. Disord.* **2002**, 17 Suppl 2, S52-S67.
- [56] Kincses Z. T.; Vecsei L.; "Pharmacological Therapy in Parkinson's Disease: Focus on Neuroprotection". *CNS Neurosci. Ther.* **2011**, 17(5), 345-367.
- [57] Schapira A. H.; Olanow C. W.; "Rationale for the use of dopamine agonists as neuroprotective agents in Parkinson's disease". *Ann. Neurol.* **2003**, 53 Suppl 3, S149-157.
- [58] Yoshioka M.; Tanaka K.-i.; Miyazaki I.; Fujita N.; Higashi Y.; Asanuma M.; Ogawa N.; "The dopamine agonist cabergoline provides neuroprotection by activation of the glutathione system and scavenging free radicals". *Neurosci. Res.* **2002**, 43(3), 259-267.

- [59] Ogawa N.; Tanaka K.-i.; Asanuma M.; Kawai M.; Masumizu T.; Kohno M.; Mori A.; "Bromocriptine protects mice against 6-hydroxydopamine and scavenges hydroxyl free radicals in vitro". *Brain Res.* **1994**, 657(1–2), 207-213.
- [60] Schapira A. H. V.; "Future directions in the treatment of Parkinson's disease". *Mov. Disord.* **2007**, 22, Suppl 17, S385-S391.
- [61] Singh N.; Pillay V.; Choonara Y. E.; "Advances in the treatment of Parkinson's disease". *Prog. Neurobiol.* **2007**, 81(1), 29-44.
- [62] Schapira A. H.; Agid Y.; Barone P.; Jenner P.; Lemke M. R.; Poewe W.; Rascol, O.; Reichmann H.; Tolosa, E.; "Perspectives on recent advances in the understanding and treatment of Parkinson's disease". *Eur. J. Neurol.* **2009**, 16(10), 1090-1099.
- [63] Mannisto P. T.; Kaakkola S.; "Catechol-O-methyltransferase (COMT): biochemistry, molecular biology, pharmacology, and clinical efficacy of the new selective COMT inhibitors". *Pharmacol. Rev.* **1999**, 51(4), 593-628.
- [64] Gordin, A.; Kaakkola S.; Teravainen H.; "Clinical advantages of COMT inhibition with entacapone - a review". *J. Neural Transm.* **2004**, 111(10-11), 1343-1363.
- [65] Burguera J. A.; Grandas F.; Horga de la Parte J. F.; Luquin R.; Marti F.; Matias-Guiu J.; Obeso J. A.; Kulisevsky J.; "Entacapone: is it useful as complimentary treatment with levodopa?". *Rev. Neurol.* **1999**, 28(8), 817-834.
- [66] Fénelon G.; Giménez-Roldán S.; Montastruc J. L.; Bermejo F.; Durif F.; Bourdeix I.; Péré J. J.; Galiano L.; Schadrack J.; "Efficacy and tolerability of entacapone in patients with Parkinson's disease treated with levodopa plus a dopamine agonist and experiencing wearing-off motor fluctuations. A randomized, double-blind, multicentre study". *J. Neural Transm.* **2003**, 110(3), 239-251.
- [67] Stocchi F.; De Pandis M. F.; "Utility of tolcapone in fluctuating Parkinson's disease". *Clin. Interv. Aging* **2006**, 1(4), 317-325.
- [68] Ceravolo, R.; Piccini P.; Bailey D. L.; Jorga K. M.; Bryson H.; Brooks D. J.; "¹⁸F-dopa PET evidence that tolcapone acts as a central COMT inhibitor in Parkinson's disease". *Synapse* **2002**, 43(3), 201-207.
- [69] Olanow, C. W.; "Tolcapone and Hepatotoxic Effects". *Arch. Neurol.* **2000**, 57(2), 263-267.
- [70] Reis J.; Encarnação I.; Gaspar A.; Morales A.; Milhazes N.; Borges F.; "Parkinson's disease management. part II discovery of MAO-B inhibitors based on nitrogen heterocycles and analogues". *Curr. Top. Med. Chem.* **2012**, 12(20), 2116-2130.

- [71] Rocha J. F.; Almeida L.; Falcão A.; Palma P. N.; Loureiro A. I.; Pinto R.; Bonifácio M. J.; Wright L. C.; Nunes T.; Soares-da-Silva P.; "Opicapone: a short lived and very long acting novel catechol-O-methyltransferase inhibitor following multiple-dose administration in healthy subjects". *Br. J. Clin. Pharmacol.* **2013**, 76(5):763-775.
- [72] Johnston J. P.; "Some observations upon a new inhibitor of monoamine oxidase in brain tissue". *Biochem. Pharmacol.* **1968**, 17(7), 1285-1297.
- [73] Keith F. T.; Sinead B.; Jeff O.; Sullivan;Gavin P. D.; Joe H.; "Monoamine Oxidases: Certainties and Uncertainties". *Curr. Med. Chem.* **2004**, 11(15), 1965-1982.
- [74] Youdim M. B.; Bakhle Y. S.; "Monoamine oxidase: isoforms and inhibitors in Parkinson's disease and depressive illness". *Br. J. Pharmacol.* **2006**, 147 Suppl 1, S287-S296.
- [75] Youdim M. B.; Edmondson D.; Tipton K. F.; "The therapeutic potential of monoamine oxidase inhibitors". *Nat. Rev. Neurosci.* **2006**, 7(4), 295-309.
- [76] Blesa J.; Phani S.; Jackson-Lewis V.; Przedborski S.; "Classic and New Animal Models of Parkinson's Disease". *J. Biomed. Biotechnol.* **2012**.
- [77] D'Amato R.; Lipman Z.; Snyder S.; "Selectivity of the Parkinsonian Neurotoxin MPTP: toxic metabolite MPP⁺ binds to neuromelanin". *Science* **1986**, 231, 987 - 989.
- [78] Foley P.; Gerlach M.; Youdim M. B.; Riederer P.; "MAO-B inhibitors: multiple roles in the therapy of neurodegenerative disorders?". *Parkinsonism Relat. Disord.* **2000**, 6(1), 25-47.
- [79] Takahata K.; Shimazu S.; Katsuki H.; Yoneda F.; Akaike A.; "Effects of selegiline on antioxidant systems in the nigrostriatum in rat". *J. Neural Transm.* **2006**, 113(2), 151-158.
- [80] Magyar, K.; Pálfi M.; Jenei V.; Szőko É.; "Deprenyl: From chemical synthesis to neuroprotection". **2006**, *J. Neural Transm.*, 71, Suppl, 143-156.
- [81] Cruickshank C. C.; Dyer K. R.; "A review of the clinical pharmacology of methamphetamine". *Addiction* **2009**, 104(7), 1085-1099.
- [82] Song M.-S.; Matveychuk D.; MacKenzie E. M.; Duchcherer M.; Mousseau D. D.; Baker G. B.; "An update on amine oxidase inhibitors: Multifaceted drugs". *Prog. Neuropsychopharmacol. Biol. Psychiatry* **2013**, 44, 118-124.
- [83] Birks J.; Flicker L.; "Selegiline for Alzheimer's disease". *Cochrane Database Syst Rev* **2003**(1), CD000442.

- [84] Kennedy B. P.; Ziegler M. G.; Alford M.; Hansen L. A.; Thal L. J.; Masliah E.; "Early and persistent alterations in prefrontal cortex MAO A and B in Alzheimer's disease". *J. Neural Transm.* **2003**, *110*(7), 789-801.
- [85] Rascol O.; Brooks D. J.; Melamed E.; Oertel W.; Poewe W.; Stocchi F.; Tolosa E.; "Rasagiline as an adjunct to levodopa in patients with Parkinson's disease and motor fluctuations (LARGO, Lasting effect in Adjunct therapy with Rasagiline Given Once daily, study): a randomised, double-blind, parallel-group trial". *Lancet* **2005**, *365*, 947-954.
- [86] Hanagasi H. A.; Gurvit H.; Unsalan P.; Horozoglu H.; Tuncer N.; Feyzioglu A.; Gunal D. I.; Yener G. G.; Cakmur R.; Sahin H. A.; Emre M.; "The effects of rasagiline on cognitive deficits in Parkinson's disease patients without dementia: A randomized, double-blind, placebo-controlled, multicenter study". *Mov. Disord.* **2011**, *26*(10), 1851-1858.
- [87] Youdim M. B.; Maruyama W.; Naoi M.; "Neuropharmacological, neuroprotective and amyloid precursor processing properties of selective MAO-B inhibitor antiparkinsonian drug, rasagiline". *Drugs Today* **2005**, *41*(6), 369-391.
- [88] Weinreb O.; Amit T.; Bar-Am, O.; Youdim B. M.; "Ladostigil: A Novel Multimodal Neuroprotective Drug with Cholinesterase and Brain-Selective Monoamine Oxidase Inhibitory Activities for Alzheimer's Disease Treatment". *Curr. Drug Targets* **2012**, *13*(4), 483-494.
- [89] Carradori S.; Secci D.; Bolasco A.; Chimenti P.; D'Ascenzio M.; "Patent-related survey on new monoamine oxidase inhibitors and their therapeutic potential". *Expert Opin. Ther. Pat.* **2012**, *22*(7), 759-801.
- [90] Syvalahti E. K.; Kunelius R.; Lauren L.; "Effects of antiparkinsonian drugs on muscarinic receptor binding in rat brain, heart and lung". *Pharmacol. Toxicol.* **1988**, *62*(2), 90-94.
- [91] LeWitt P. A.; Ward C. D.; Larsen T. A.; Raphaelson M. I.; Newman R. P.; Foster N.; Dambrosia J. M.; Calne D. B.; "Comparison of pergolide and bromocriptine therapy in parkinsonism". *Neurology* **1983**, *33*(8), 1009-1014.
- [92] Lees A.; "Alternatives to levodopa in the initial treatment of early Parkinson's disease". *Drugs Aging* **2005**, *22*(9), 731-740.
- [93] Olanow C. W.; Schapira A. H.; Agid, Y.; "Neuroprotection for Parkinson's disease: prospects and promises". *Ann. Neurol.* **2003**, *53 Suppl 3*, S1-2.
- [94] Katzenschlager R.; Sampaio C.; Costa J.; Lees A.; "Anticholinergics for symptomatic management of Parkinson's disease". *Cochrane Database Syst Rev* **2003**(2), CD003735.

- [95] Brocks D. R.; "Anticholinergic drugs used in Parkinson's disease: An overlooked class of drugs from a pharmacokinetic perspective". *J. Pharm. Pharm. Sci.* **1999**, 2(2), 39-46.
- [96] Robert S. M.; Albert C. M.; David C. P. M.; Robert R. Y. M.; "Amantadine in the Treatment of Parkinson's Disease". *JAMA* **1969**, 208(7), 1168-1170.
- [97] Calne D. B.; "Treatment of Parkinson's disease". *N. Engl. J. Med.* **1993**, 329(14), 1021-1027.
- [98] Adler C. H.; Stern M. B.; Vernon G.; Hurtig H. I.; "Amantadine in advanced Parkinson's disease: good use of an old drug". *J. Neurol.* **1997**, 244(5), 336-337.
- [99] Shannon K. M.; Goetz C. G.; Carroll V. S.; Tanner C. M.; Klawans H. L.; "Amantadine and Motor Fluctuations in Chronic Parkinson's Disease". *Clin. Neuropharmacol.* **1987**, 10(6), 522-526.
- [100] Goetz, C. G.; Koller W. C.; Poewe W.; Rascol O.; Sampaio C.; Brin M. F.; Lees A. J.; LeWitt P.; Lozano A.; Mizuno Y.; Nutt J.; Oertel W.; Olanow C. W.; Tolosa E.; "Amantadine and other antiglutamate agents". *Mov. Disord.* **2002**, 17 suppl 4, S13-S22.
- [101] Hallett P. J.; Standaert D. G.; "Rationale for and use of NMDA receptor antagonists in Parkinson's disease". *Pharmacol. Ther.* **2004**, 102(2), 155-174.
- [102] Davie C. A.; "A review of Parkinson's disease". *Br. Med. Bull.* **2008**, 86(1), 109-127.
- [103] Morelli M.; Carta A. R.; Jenner P., Vol. 193 (Eds.: C.N. Wilson, S.J. Mustafa), Springer Berlin Heidelberg, **2009**, pp. 589-615.
- [104] Xu, K.; Bastia E.; Schwarzschild M.; "Therapeutic potential of adenosine A_{2A} receptor antagonists in Parkinson's disease". *Pharmacol. Ther.* **2005**, 105(3), 267-310.
- [105] Svenningsson P.; Le Moine C.; Fisone G.; Fredholm B. B.; "Distribution, biochemistry and function of striatal adenosine A_{2A} receptors". *Prog. Neurobiol.* **1999**, 59(4), 355-396.
- [106] Sperlagh B.; Vizi E. S.; "The role of extracellular adenosine in chemical neurotransmission in the hippocampus and Basal Ganglia: pharmacological and clinical aspects". *Curr. Top. Med. Chem.* **2011**, 11(8), 1034-1046.
- [107] Fredholm B. B.; Ijzerman A. P.; Jacobson K. A.; Klotz K. N.; Linden J.; "International Union of Pharmacology. XXV. Nomenclature and classification of adenosine receptors". *Pharmacol. Rev.* **2001**, 53(4), 527-552.
- [108] Fredholm B. B.; "Adenosine receptors as drug targets". *Exp. Cell Res.* **2010**, 316(8), 1284-1288.

- [109] Zheng C. J.; Han L. Y.; Yap C. W.; Ji Z. L.; Cao Z. W.; Chen Y. Z.; "Therapeutic targets: progress of their exploration and investigation of their characteristics". *Pharmacol. Rev.* **2006**, *58*(2), 259-279.
- [110] Chen J. F.; Eltzschig H. K.; Fredholm B. B.; "Adenosine receptors as drug targets-what are the challenges?". *Nat. Rev. Drug Discov.* **2013**, *12*(4), 265-286.
- [111] Jacobson K. A.; Gao Z. G.; "Adenosine receptors as therapeutic targets". *Nat. Rev. Drug Discov.* **2006**, *5*(3), 247-264.
- [112] Jacobson K. A., in *Adenosine Receptors in Health and Disease*, Vol. 193 (Eds.: C.N. Wilson, S.J. Mustafa), Springer Berlin Heidelberg, **2009**, pp. 1-24.
- [113] Müller C. E.; Jacobson K. A.; "Recent developments in adenosine receptor ligands and their potential as novel drugs". *Biochim. Biophys. Acta* **2011**, *1808*(5), 1290-1308.
- [114] Gessi, S.; Merighi S.; Fazzi D.; Stefanelli A.; Varani K.; Borea P. A.; "Adenosine receptor targeting in health and disease". *Expert Opin Inv. Drugs* **2011**, *20*(12), 1591-1609.
- [115] Baraldi P. G.; Tabrizi M. A.; Gessi S.; Borea P. A.; "Adenosine receptor antagonists: Translating medicinal chemistry and pharmacology into clinical utility". *Chem. Rev.* **2008**, *108*(1), 238-263.
- [116] Jocham G.; Ullsperger M.; "Neuropharmacology of performance monitoring". *Neuroscience Biobehav.R.* **2009**, *33*(1), 48-60.
- [117] Hickey P.; Stacy M.; "Adenosine A_{2A} Antagonists in Parkinson's Disease: What's Next?". *Curr. Neurol. Neurosci. Rep.* **2012**, *12*(4), 376-385.
- [118] Xu K.; Bastia E.; Schwarzschild M.; "Therapeutic potential of adenosine A_{2A} receptor antagonists in Parkinson's disease". *Pharmacol. Ther.* **2005**, *105*(3), 267-310.
- [119] Rosin D. L.; Hettinger B. D.; Lee A.; Linden J.; "Anatomy of adenosine A_{2A} receptors in brain: morphological substrates for integration of striatal function". *Neurology* **2003**, *61 Suppl 6*, S12-S18.
- [120] Schiffmann S. N.; Fisone G.; Moresco R.; Cunha R. A.; Ferré S.; "Adenosine A_{2A} receptors and basal ganglia physiology". *Prog. Neurobiol.* **2007**, *83*(5), 277-292.
- [121] Muller C. E.; Ferre S.; in *Frontiers in CNS Drug Discovery in Blocking Striatal Adenosine A_{2A} Receptors: A New Strategy for Basal Ganglia Disorders*, Vol. 1 (Eds.: Atta-ur-Rahman, M.I. Choudhary), Bentham Science, **2010**.

- [122] Sebastião, A.; Ribeiro J., in *Adenosine Receptors in Health and Disease*, Vol. 193 (Eds.: C.N. Wilson, S.J. Mustafa), Springer Berlin Heidelberg, **2009**, pp. 471-534..
- [123] Diniz C.; Borges F.; Santana L.; Uriarte E.; Oliveira J. M.; Gonçalves J.; Fresco P.; "Ligands and therapeutic perspectives of adenosine A(2A) receptors". *Curr. Pharm. Des.* **2008**, 14(17), 1698-1722.
- [124] Baraldi P. G.; Tabrizi M. A.; Gessi S.; Borea P. A.; "Adenosine receptor antagonists: translating medicinal chemistry and pharmacology into clinical utility". *Chem. Rev.* **2008**, 108(1), 238-263.
- [125] Armentero M. T.; Pinna A.; Ferre S.; Lanciego J. L.; Muller C. E.; Franco R.; "Past, present and future of A(2A) adenosine receptor antagonists in the therapy of Parkinson's disease". *Pharmacol. Ther.* **2011**, 132(3), 280-299.
- [126] Shook B. C.; Jackson P. F.; "Adenosine A(2A) Receptor Antagonists and Parkinson's Disease". *ACS Chem. Neurosci.* **2011**, 2(10), 555-567.
- [127] ClinicalTrials.gov, Study of KW-6002 (Istradefylline) for the Treatment of Parkinson's Disease in Patients Taking Levodopa (6002-009), <http://clinicaltrials.gov/show/NCT00955526>..
- [128] Evans B. E.; Rittle K. E.; Bock M. G.; DiPardo R. M.; Freidinger R. M.; Whitter W. L.; Lundell G. F.; Veber D. F.; Anderson P. S.; "Methods for drug discovery: development of potent, selective, orally effective cholecystokinin antagonists". *J. Med. Chem.* **1988**, 31(12), 2235-2246.
- [129] Duarte C. D.; Barreiro E. J.; Fraga C. A.; "Privileged structures: a useful concept for the rational design of new lead drug candidates". *Mini Rev. Med. Chem.* **2007**, 7(11), 1108-1119.
- [130] DeSimone R. W.; Currie K. S.; Mitchell S. A.; Darrow J. W.; Pippin D. A.; "Privileged structures: applications in drug discovery". *Comb. Chem. High Throughput Screen* **2004**, 7(5), 473-494.
- [131] Klekota J.; Roth F. P.; "Chemical substructures that enrich for biological activity". *Bioinformatics* **2008**, 24(21), 2518-2525.
- [132] Lachance H.; Wetzel S.; Kumar K.; Waldmann H.; "Charting, navigating, and populating natural product chemical space for drug discovery". *J. Med. Chem.* **2012**, 55(13), 5989-6001.
- [133] Polanski J.; Kurczyk A.; Bak A.; Musiol R.; "Privileged structures - dream or reality: preferential organization of azanaphthalene scaffold". *Curr. Med. Chem.* **2012**, 19(13), 1921-1945.
- [134] Solomon V. R.; Lee H.; "Quinoline as a privileged scaffold in cancer drug discovery". *Curr. Med. Chem.* **2011**, 18(10), 1488-1508.

- [135] Ciapetti P.; Giethlen B., in *The Practice of Medicinal Chemistry (Third Edition)* (Ed.: W. Camille Georges), Academic Press, New York, **2008**, pp. 290-342.
- [136] Ko S. K.; Jang H. J.; Kim E.; Park S. B.; "Concise and diversity-oriented synthesis of novel scaffolds embedded with privileged benzopyran motif". *Chem. Commun.* **2006**, 28, 2962-2964.
- [137] Abu-Hashem A. A.; Youssef M. M.; "Synthesis of New Visnagen and Khellin Furochromone Pyrimidine Derivatives and Their Anti-Inflammatory and Analgesic Activity". *Molecules* **2011**, 16(3), 1956-1972.
- [138] Svendsen A. B.; Scheffer J. J. C.; "Natural products in therapy". *Pharm. World Sci.* **1982**, 4(4), 93-103.
- [139] Barnes P. J.; "Drugs for asthma". *Br. J. Pharmacol.* **2006**, 147suppl 1, S297-S303.
- [140] Felsten L. M.; Alikhan A.; Petronic-Rosic V.; "Vitiligo: A comprehensive overview: Part II: Treatment options and approach to treatment". *J. Am. Acad. Dermatol.* **2011**, 65(3), 493-514.
- [141] Berman B.; Ross R.; "Cromolyn". *Clin. Rev. Allergy Immunol.* **1983**, 1(1), 105-121.
- [142] Netzer N.; Küpper T.; Voss H.; Eliasson A.; "The actual role of sodium cromoglycate in the treatment of asthma—a critical review". *Sleep Breath.*, 1-6.
- [143] Mazzei M.; Balbi A.; Roma G.; Di Braccio M.; Leoncini G.; Buzzi E.; Maresca M.; "Synthesis and anti-platelet activity of some 2-(dialkylamino)chromones". *Eur. J. Med. Chem.* **1988**, 23(3), 237-242.
- [144] Mazzei M.; Sottofattori E.; Di Braccio M.; Balbi A.; Leoncini G.; Buzzi E.; Maresca M.; "Synthesis and antiplatelet activity of 2-(diethylamino)-7-ethoxychromone and related compounds". *Eur. J. Med. Chem.* **1990**, 25(7), 617-622.
- [145] Leoncini G.; Maresca M.; Colao C.; Buzzi E.; Mazzei M.; "Mode of action of 2-(diethylamino)-7-ethoxychromone on human platelets". *Cell Biochem. Funct.* **1991**, 9(2), 79-85.
- [146] Morris J.; Wishka D. G.; Lin A. H.; Humphrey W. R.; Wiltse A. L.; Gammill R. B.; Judge T. M.; Bisaha S. N.; Olds N. L.; "Synthesis and biological evaluation of antiplatelet 2-aminochromones". *J. Med. Chem.* **1993**, 36(14), 2026-2032.
- [147] Ceylan-Ünlüsoy, M.; Verspohl E. J.; Ertan R.; "Synthesis and antidiabetic activity of some new chromonyl-2,4-thiazolidinediones". *J. Enzyme Inhib. Med. Chem.* **2010**, 25(6), 784-789.
- [148] Puccetti L.; Fasolis G.; Vullo D.; Chohan Z. H.; Scozzafava A.; Supuran C. T.; "Carbonic anhydrase inhibitors. Inhibition of cytosolic/tumor-associated carbonic

- anhydrase isozymes I, II, IX, and XII with Schiff's bases incorporating chromone and aromatic sulfonamide moieties, and their zinc complexes". *Bioorg. Med. Chem. Lett.* **2005**, *15*(12), 3096-3101.
- [149] Al-Rashida M.; Ashraf M.; Hussain B.; Nagra S. A.; Abbas G.; "Discovery of new chromone containing sulfonamides as potent inhibitors of bovine cytosolic carbonic anhydrase". *Bioorg. Med. Chem.* **2011**, *19*(11), 3367-3371.
- [150] Lindell S. D.; Ort O.; Lümme P.; Klein R.; "The design and synthesis of novel inhibitors of NADH:ubiquinone oxidoreductase". *Bioorg. Med. Chem. Lett.* **2004**, *14*(2), 511-514.
- [151] Kumar A.; Singh B. K.; Sharma N. K.; Gyanda K.; Jain S. K.; Tyagi Y. K.; Baghel A. S.; Pandey M.; Sharma S. K.; Prasad A. K.; Jain S. C.; Rastogi R. C.; Raj H. G.; Watterson A. C.; Van der Eycken E.; Parmar V. S.; "Specificities of acetoxy derivatives of coumarins, biscoumarins, chromones, flavones, isoflavones and xanthenes for acetoxy drug: Protein transacetylase". *Eur. J. Med. Chem.* **2007**, *42*(4), 447-455.
- [152] Lee K. S.; Seo S. H.; Lee Y. H.; Kim H. D.; Son M. H.; Chung B. Y.; Lee J. Y.; Jin C.; Lee Y. S.; "Synthesis and biological evaluation of chromone carboxamides as calpain inhibitors". *Bioorg. Med. Chem. Lett.* **2005**, *15*(11), 2857-2860.
- [153] Kim S. H.; Lee Y. H.; Jung S. Y.; Kim H. J.; Jin C.; Lee Y. S.; "Synthesis of chromone carboxamide derivatives with antioxidative and calpain inhibitory properties". *Eur. J. Med. Chem.* **2011**, *46*(5), 1721-1728.
- [154] Inaba T.; Tanaka K.; Takeno R.; Nagaki H.; Yoshida C.; Takano S.; "Synthesis and Antiinflammatory Activity of 7-Methanesulfonylamino-6-phenoxychromones. Antiarthritic Effect of the 3-Formylamino Compound (T-614) in Chronic Inflammatory Disease Models". *Chem. Pharm. Bull.* **2000**, *48*(1), 131-139.
- [155] Gautam R.; Jachak S. M.; Kumar V.; Mohan C. G.; "Synthesis, biological evaluation and molecular docking studies of stellatin derivatives as cyclooxygenase (COX-1, COX-2) inhibitors and anti-inflammatory agents". *Bioorg. Med. Chem. Lett.* **2011**, *21*(6), 1612-1616.
- [156] Huang F. C.; Galembo R. A.; Poli G. B.; Learn K. S.; Morrisette M. M.; Johnson W. H.; Dankulich W. P.; Campbell H. F.; Carnathan G. W.; Van Inwegen R. G.; "Development of a novel series of (2-quinolinylmethoxy)phenyl-containing compounds as high-affinity leukotriene D4 receptor antagonists. 4. Addition of chromone moiety enhances leukotriene D4 receptor binding affinity". *J. Med. Chem.* **1991**, *34*(5), 1704-1707.

- [157] Zhang M. Q.; Wada Y.; Sato F.; Timmerman H.; "(Piperidinylalkoxy)Chromones - Novel Antihistamines with Additional Antagonistic Activity against Leukotriene D-4". *J. Med. Chem.* **1995**, 38(13), 2472-2477.
- [158] Brown F. J.; Bernstein P. R.; Cronk L. A.; Dosset D. L.; Hebbel K. C.; Maduskuie T. P.; Shapiro H. S.; Vacek E. P.; Yee Y. K.; Willard A. K.; Krell R. D.; Snyder D. W.; "Hydroxyacetophenone-Derived Antagonists of the Peptidoleukotrienes". *J. Med. Chem.* **1989**, 32(4), 807-826.
- [159] Nohara A.; Kuriki H.; Saijo T.; Ukawa K.; Murata T.; Kanno M.; Sanno Y.; "Studies on Antianaphylactic Agents -4- Synthesis and Structure-Activity-Relationships of 3-(4-Oxo-4*H*-1-Benzopyran)-3-Acrylic Acids, a New Series of Antiallergic Substances, and Some Related Compounds". *J. Med. Chem.* **1975**, 18(1), 34-37.
- [160] Nohara A.; Kuriki H.; Saijo T.; Sugihara H.; Kanno M.; Sanno Y.; "Studies on Antianaphylactic Agents -5- Synthesis of 3-(1*H*-Tetrazol-5-yl)Chromones, a New Series of Antiallergic Substances". *J. Med. Chem.* **1977**, 20(1), 141-145.
- [161] Ellis G. P.; Becket G. J. P.; Shaw D.; Wilson H. K.; Vardey C. J.; Skidmore I. F.; "Benzopyrones-14. Synthesis and anti-allergic properties of some N-tetrazolylcarboxamides and related compounds". *J. Med. Chem.* **1978**, 21(11), 1120-1126.
- [162] Nohara A.; Kuriki H.; Ishiguro T.; Saijo T.; Ukawa K.; Maki Y.; Sanno Y.; "Studies on Antianaphylactic Agents -6- Synthesis of Some Metabolites of 6-Ethyl-3-(1*H*-Tetrazol-5-yl)Chromone and Their Analogs". *J. Med. Chem.* **1979**, 22(3), 290-295.
- [163] Jadhav K. P.; Ingle D. B.; "Synthesis of 2-aryl-3-sulfonyl-6-methylchromones as PCA inhibitors". *Indian J. Chem. B* **1983**, 22(2), 150-153.
- [164] Mazzei M.; Balbi A.; Ermili A.; Sottofattori E.; Roma G.; Schiantarelli P.; Cadel S.; "Chemical and pharmacological research on pyran derivatives. XVI. Derivatives of 2-(dialkylamino)-7-methoxychrome with antiallergic activity". *// Farmaco Sci.* **1985**, 40(12), 895-908.
- [165] Payard M.; Mouysset G.; Tronche P.; Bastide P.; Bastide J.; "Research of Antiallergic Agents - 2-Hydroxymethylchromone and Structural Analogs". *Eur. J. Med. Chem.* **1985**, 20(2), 117-120.
- [166] Kuriki H.; Saijo T.; Maki Y.; Kanno M.; "Anti-allergic action of 6-ethyl-3-(1*H*-tetrazol-5-yl) chromone (AA-344) in rats". *Jpn J Pharmacol.* **1979**, 29(3), 385-397.

- [167] Lee G.; Swarbrick J.; Kiyohara G.; Payling D. W.; "Drug Permeation through Human-Skin .3. Effect of Ph on the Partitioning Behavior of a Chromone-2-Carboxylic Acid". *Int. J. Pharm.* **1985**, 23(1), 43-54.
- [168] Mazzei M.; Ermili A.; Balbi A.; "Chemical and pharmacological research on pyran derivatives. XVII - Synthesis of 2-(dialkylamino)-5-hydroxychromones and their transformation to derivatives of 2H-pyran[4,3,2-de]-1-benzopyran". // *Farmaco Sci.* **1986**, 41(8), 611-621.
- [169] Wells E.; Eady R. P.; Harper S. T.; Mather M. E.; Riley P. A.; "The anti-allergic effects of FPL 52694". *Int. Arch. Allergy Appl. Immunol.* **1985**, 76(2), 188-190.
- [170] Prakash O.; Kumar R.; Parkash V.; "Synthesis and antifungal activity of some new 3-hydroxy-2-(1-phenyl-3-aryl-4-pyrazolyl) chromones". *Eur. J. Med. Chem.* **2008**, 43(2), 435-440.
- [171] Ghotekar D. S.; Mandhane P. G.; Joshi R. S.; Bhagat S. S.; Gill C. H.; "Synthesis of Biologically Important Chromones and Pyrazolines". *Indian J. Heterocycl. Chem.* **2009**, 19(2), 101-104.
- [172] Hatzade K. M.; Taile V. S.; Gaidhane P. K.; Umare V. D.; Haldar A. G. M.; Ingle V. N.; "Synthesis and biological activities of new 7-O- β -D-glucopyranosyloxy- 3-(3-oxo-3-arylprop-1-enyl)-chromones". *Indian J. Chem. - Section B* **2009**, 48(11), 1548-1557.
- [173] Isaka M.; Sappan M.; Auncharoen P.; Srikitikulchai P.; "Chromone derivatives from the wood-decay fungus *Rhizina* sp. BCC 12292". *Phytochem. Lett.* **2010**, 3(3), 152-155.
- [174] Chohan Z. H.; Rauf A.; Naseer M. M.; Somra M. A.; Supuran C. T.; "Antibacterial, antifungal and cytotoxic properties of some sulfonamide-derived chromones". *J. Enzyme Inhib. Med. Chem.* **2006**, 21(2), 173-177.
- [175] Raj T.; Bhatia R. K.; Sharma R. K.; Gupta V.; Sharma D.; Ishar M. P. S.; "Mechanism of unusual formation of 3-(5-phenyl-3H-[1,2,4]dithiazol-3-yl)chromen-4-ones and 4-oxo-4H-chromene-3-carbothioic acid N-phenylamides and their antimicrobial evaluation". *Eur. J. Med. Chem.* **2009**, 44(8), 3209-3216.
- [176] Gohar A. K. M. N.; "Synthesis of several new chromones derivatives and their antibacterial activity". *Egyptian J. Chem.* **1990**, 31(3), 367-374.
- [177] Hatzade K.; Taile V.; Gaidhane P.; Ingle V.; "Synthesis, structural determination, and biological activity of new 7-hydroxy-3-pyrazolyl-4H-chromen-4-ones and their o- β -D-glucosides". *Turkish J. Chem.* **2010**, 34(2), 241-254.
- [178] Ali T. E. S.; Ibrahim M. A.; "Synthesis and antimicrobial activity of chromone-linked 2-pyridone fused with 1,2,4-triazoles, 1,2,4-triazines and 1,2,4-triazepines ring systems". *J. Braz. Chem. Soc.* **2010**, 21(6), 1007-1016.

- [179] Kumar S.; Koh J.; "Physiochemical, Optical and Biological Activity of Chitosan-Chromone Derivative for Biomedical Applications". *Int. J. Mol. Sci.* **2012**, *13*(5), 6102-6116.
- [180] Desideri N.; Conti C.; Mastromarino P.; Mastropaolo F.; "Synthesis and anti-rhinovirus activity of 2-styrylchromones". *Antiviral Chem. Chemother.* **2000**, *11*(6), 373-381.
- [181] Conti C.; Mastromarino P.; Goldoni P.; Portalone G.; Desideri N.; "Synthesis and anti-rhinovirus properties of fluoro-substituted flavonoids". *Antiviral Chem. Chemother.* **2005**, *16*(4), 267-276.
- [182] Rocha-Pereira J.; Cunha R.; Pinto D. C. G. A.; Silva A. M. S.; Nascimento M. S. J.; "(E)-2-Styrylchromones as potential anti-norovirus agents". *Biorg. Med. Chem.* **2010**, *18*(12), 4195-4201.
- [183] Park H. R.; Park K.-S.; Chong Y.; "2-Arylmethylaminomethyl-5,6-dihydroxychromone derivatives with selective anti-HCV activity". *Bioorg. Med. Chem. Lett.* **2011**, *21*(11), 3202-3205.
- [184] Kaye P. T.; Musa M. A.; Nchinda A. T.; Nocanda X. W.; "Novel Heterocyclic Analogues of the HIV-1 Protease Inhibitor, Ritonavir". *Synth. Commun.* **2004**, *34*(14), 2575-2589.
- [185] Yu D.; Chen C.-H.; Brossi A.; Lee K.-H.; "Anti-AIDS Agents. 60.† Substituted 3'R,4'R-Di-O-(-)-camphanoyl-2',2'-dimethyldihydropyrano[2,3-f]chromone (DCP) Analogues as Potent Anti-HIV Agents". *J. Med. Chem.* **2004**, *47*(16), 4072-4082.
- [186] Chen Y.; Cheng M.; Liu F. Q.; Xia P.; Qian K.; Yu D.; Xia Y.; Yang Z. Y.; Chen C. H.; Morris-Natschke S. L.; Lee K. H.; "Anti-AIDS agents 86. Synthesis and anti-HIV evaluation of 2',3'-seco-3'-nor DCP and DCK analogues". *Eur. J. Med. Chem.* **2011**, *46*(10), 4924-4936.
- [187] Park, J. H.; Lee S. U.; Kim S. H.; Shin S. Y.; Lee J. Y.; Shin C. G.; Yoo K. H.; Lee Y. S.; "Chromone and chromanone derivatives as strand transfer inhibitors of HIV-1 integrase". *Arch. Pharm. Res.* **2008**, *31*(1), 1-5.
- [188] Grażul M.; Kufelnicki A.; Wozniczka M.; Lorenz I.-P.; Mayer P.; Jóźwiak A.; Czyż M.; Budzisz E.; "Synthesis, structure, electrochemical properties, cytotoxic effects and antioxidant activity of 5-amino-8-methyl-4H-benzopyran-4-one and its copper(II) complexes". *Polyhedron* **2012**, *31*(1), 150-158.
- [189] Barath Z.; Radics R.; Spengler G.; Ocsosvski I.; Kawase M.; Motohashi N.; Shirataki Y.; Shah A.; Molnar J.; "Multidrug resistance reversal by 3-formylchromones in human colon cancer and human mdr1 gene-transfected mouse lymphoma cells". *In Vivo* **2006**, *20*(5), 645-649.

- [190] Nawrot-Modranka J.; Nawrot E.; Graczyk J.; "In vivo antitumor, in vitro antibacterial activity and alkylating properties of phosphorohydrazine derivatives of coumarin and chromone". *Eur. J. Med. Chem.* **2006**, 41(11), 1301-1309.
- [191] Huang W.; Liu M. Z.; Li Y.; Tan Y.; Yang G. F.; "Design, syntheses, and antitumor activity of novel chromone and aurone derivatives". *Biorg. Med. Chem.* **2007**, 15(15), 5191-5197.
- [192] Shaw A. Y.; Chang C.-Y.; Liao H.-H.; Lu P.-J.; Chen H.-L.; Yang C.-N.; Li H.-Y.; "Synthesis of 2-styrylchromones as a novel class of antiproliferative agents targeting carcinoma cells". *Eur. J. Med. Chem.* **2009**, 44(6), 2552-2562.
- [193] Singh P.; Kaur M.; Holzer W.; "Synthesis and evaluation of indole, pyrazole, chromone and pyrimidine based conjugates for tumor growth inhibitory activities - Development of highly efficacious cytotoxic agents". *Eur. J. Med. Chem.* **2010**, 45(11), 4968-4982.
- [194] Nam, D. H.; Lee K. Y.; Moon C. S.; Lee Y. S.; "Synthesis and anticancer activity of chromone-based analogs of lavendustin A". *Eur. J. Med. Chem.* **2010**, 45(9), 4288-4292.
- [195] Chen, Y.; Liu H.-R.; Liu H.-S.; Cheng M.; Xia P.; Qian K.; Wu P.-C.; Lai C.-Y.; Xia Y.; Yang Z.-Y.; Morris-Natschke S. L.; Lee K.-H.; "Antitumor agents 292. Design, synthesis and pharmacological study of S- and O-substituted 7-mercapto- or hydroxy-coumarins and chromones as potent cytotoxic agents". *Eur. J. Med. Chem.* **2012**, 49(0), 74-85.
- [196] Raj T.; Bhatia R. K.; kapur A.; Sharma M.; Saxena A. K.; Ishar M. P. S.; "Cytotoxic activity of 3-(5-phenyl-3H-[1,2,4]dithiazol-3-yl)chromen-4-ones and 4-oxo-4H-chromene-3-carbothioic acid N-phenylamides". *Eur. J. Med. Chem.* **2010**, 45(2), 790-794.
- [197] Donnelly D.; Geoghegan R.; O'Brien C.; Philbin E.; Wheeler T. S.; "Synthesis of heterocyclic-substituted chromones and related compounds as potential anticancer agents". *J. Med. Chem.* **1965**, 8(6), 872-875.
- [198] Khan K. M.; Ambreen N.; Hussain S.; Perveen S.; Iqbal Choudhary M.; "Schiff bases of 3-formylchromone as thymidine phosphorylase inhibitors". *Biorg. Med. Chem.* **2009**, 17(8), 2983-2988.
- [199] Budzisz E.; Graczyk-Wojciechowska J.; Zieba R.; Nawrot B.; "A new series of 2-substituted 3-phosphonic derivatives of chromone. Part II. Synthesis, in vitro alkylating and in vivo antitumour activity". *New J. Chem.* **2002**, 26(12), 1799-1804.
- [200] Walker E. H.; Pacold M. E.; Perisic O.; Stephens L.; Hawkins P. T.; Wymann M. P.; Williams R. L.; "Structural determinants of phosphoinositide 3-kinase

- inhibition by wortmannin, LY294002, quercetin, myricetin, and staurosporine". *Mol. Cell* **2000**, 6(4), 909-919.
- [201] Welling A.; Hofmann F.; Wegener J. W.; "Inhibition of L-type Ca(v)1.2 Ca²⁺ channels by 2,(4-morpholinyl)-8-phenyl-4H-1-benzopyran-4-one (LY294002) and 2-[1-(3-dimethyl-aminopropyl)-5-methoxyindol-3-yl]-3-(1H-indol-3-yl) maleimide (Go6983)". *Mol. Pharmacol.* **2005**, 67(2), 541-544.
- [202] Frazzetto M.; Suphioglu C.; Zhu J.; Schmidt-Kittler O.; Jennings I. G.; Cranmer S. L.; Jackson S. P.; Kinzler K. W.; Vogelstein B.; Thompson P. E.; "Dissecting isoform selectivity of PI3K inhibitors: the role of non-conserved residues in the catalytic pocket". *Biochem. J.* **2008**, 414, 383-390.
- [203] Gunn R.; Hailes H.; "Insights into the PI3-K-PKB-mTOR signalling pathway from small molecules". *J. Chem. Biol.* **2008**, 1(1-4), 49-62.
- [204] Forghieri M.; Laggner C.; Paoli P.; Langer T.; Manao G.; Camici G.; Bondioli L.; Prati F.; Costantino L.; "Synthesis, activity and molecular modeling of a new series of chromones as low molecular weight protein tyrosine phosphatase inhibitors". *Bioorg. Med. Chem.* **2009**, 17(7), 2658-2672.
- [205] Ishar M. P. S.; Singh G.; Singh S.; Sreenivasan K. K.; Singh G.; "Design, synthesis, and evaluation of novel 6-chloro-/fluorochromone derivatives as potential topoisomerase inhibitor anticancer agents". *Bioorg. Med. Chem. Lett.* **2006**, 16(5), 1366-1370.
- [206] Recanatini M.; Bisi A.; Cavalli A.; Belluti F.; Gobbi S.; Rampa A.; Valenti P.; Palzer M.; Paluszczak A.; Hartmann R. W.; "A New Class of Nonsteroidal Aromatase Inhibitors: Design and Synthesis of Chromone and Xanthone Derivatives and Inhibition of the P450 Enzymes Aromatase and 17 α -Hydroxylase/C17,20-Lyase". *J. Med. Chem.* **2001**, 44(5), 672-680.
- [207] Peixoto, F.; Barros A. I. R. N. A.; Silva A. M. S.; "Interactions of a new 2-styrylchromone with mitochondrial oxidative phosphorylation". *J. Biochem. Mol. Toxicol.* **2002**, 16(5), 220-226.
- [208] Huang W.; Ding Y.; Miao Y.; Liu M. Z.; Li Y.; Yang G. F.; "Synthesis and antitumor activity of novel dithiocarbamate substituted chromones". *Eur. J. Med. Chem.* **2009**, 44(9), 3687-3696.
- [209] Martorana A.; Mori F.; Esposito Z.; Kusayanagi H.; Monteleone F.; Codeca C.; Sancesario G.; Bernardi G.; Koch G.; "Dopamine modulates cholinergic cortical excitability in Alzheimer's disease patients". *Neuropsychopharmacol.* **2009**, 34(10), 2323-2328.

- [210] Mitchell R. A.; Herrmann N.; Lanctôt K. L.; "The Role of Dopamine in Symptoms and Treatment of Apathy in Alzheimer's Disease". *CNS Neurosci. Ther.* **2011**, 17(5), 411-427.
- [211] Brühlmann C.; Ooms F.; Carrupt P. A.; Testa B.; Catto M.; Leonetti F.; Altomare C.; Carotti A.; "Coumarins derivatives as dual inhibitors of acetylcholinesterase and monoamine oxidase". *J. Med. Chem.* **2001**, 44(19), 3195-3198.
- [212] Legoabe L. J.; Petzer A.; Petzer J. P.; "Selected chromone derivatives as inhibitors of monoamine oxidase". *Bioorg. Med. Chem. Lett.* **2012**, 22(17), 5480-5484.
- [213] Legoabe, L. J.; Petzer A.; Petzer J. P.; "Selected C7-substituted chromone derivatives as monoamine oxidase inhibitors". *Bioorg. Chem.* **2012**, 45(0), 1-11.
- [214] Legoabe, L. J.; Petzer A.; Petzer J. P.; "Inhibition of monoamine oxidase by selected C6-substituted chromone derivatives". *Eur. J. Med. Chem.* **2012**, 49(0), 343-353.
- [215] Erickson R. H.; Natalie K. J.; Bock W.; Lu Z. J.; Farzin F.; Sherrill R. G.; Meloni D. J.; Patch R. J.; Rzesotarski W. J.; Clifton J.; Pontecorvo M. J.; Bailey M. A.; Naper K.; Karbon W.; "(Aminoalkoxy)Chromones - Selective Sigma Receptor Ligands". *J. Med. Chem.* **1992**, 35(9), 1526-1535.
- [216] Price W. A.; Silva A. M. S. S.; Cavaleiro J. A. S.; "2-Styrylchromones: Biological Action, Synthesis and Reactivity". *Heterocycles* **1993**, 36(11), 2601-2612.
- [217] Santos, C.M. M.; Silva A. M. S.; Cavaleiro J.A. S.; "Synthesis of New Hydroxy-2-styrylchromones". *Eur. J. Org. Chem.* **2003**, 2003(23), 4575-4585.
- [218] Silva A. M. S.; Pinto D. C. G. A.; Cavaleiro J. A. S.; Levai A.; Patonay T.; "Synthesis and reactivity of styrylchromones". *Arkivoc* **2004**, 2004(7), 106-123.
- [219] Gomes A.; Neuwirth O.; Freitas M.; Couto D.; Ribeiro D.; Figueiredo A. G. P. R.; Silva A. M. S.; Seixas R. S. G. R.; Pinto D. C. G. A.; Tomé A. C.; Cavaleiro J. A. S.; Fernandes E.; Lima J. L. F. C.; "Synthesis and antioxidant properties of new chromone derivatives". *Bioorg.; Med. Chem.* **2009**, 17(20), 7218-7226.
- [220] Königs P.; Neumann O.; Kataeva O.; Schnakenburg G.; Waldvogel S. R.; "Convenient Synthesis of 3-Cinnamoyl-2-styrylchromones: Reinvestigation of the Baker–Venkataraman Rearrangement". *Eur. J. Org. Chem.* **2010**, 2010(33), 6417-6422.
- [221] Okombi S.; Schmidt J.; Mariotte A.-M.; Perrier E.; Boumendjel A.; "A One-Step Synthesis of 2-Alkyl-5-hydroxychromones and 3-Alkoyl-2-alkyl-5-hydroxychromones". *Chem. Pharm. Bull.* **2005**, 53(11), 1460-1462.

- [222] Reddy B. P.; Krupadanam G. L. D.; "The synthesis of 8-allyl-2-styrylchromones by the modified baker-venkataraman transformation". *J. Heterocycl. Chem.* **1996**, 33(6), 1561-1565.
- [223] Riva C.; De Toma C.; Donadel L.; Boi C.; Pennini R.; Motta G.; Leonardi A.; "New DBU (1,8-Diazabicyclo[5.4.0]undec-7-ene) Assisted One-Pot Synthesis of 2,8-Disubstituted 4H-1-Benzopyran-4-ones". *Synthesis* **1997**, 1997(02), 195-201.
- [224] Lan-Ping, Z.; Ya-lou W.; "Facile Synthesis of 5-Hydroxy-2-(2-phenylethyl)chromone". *Chem. Res. Chin. Univ.* **2010**, 26(2), 245-248.
- [225] Castañeda I. C. H.; Ulic S. E.; Védova C. O. D.; Metzler-Nolte N.; Jios J. L.; "One-pot synthesis of 2-trifluoromethylchromones". *Tetrahedron Lett.* **2011**, 52(13), 1436-1440.
- [226] Lacova M.; El-Shaaer H.; Loos D.; Matulova M.; Chovancova J.; Furdik M.; "Evaluation of Effect of Microwave Irradiation on Syntheses and Reactions of Some New 3-Acyl-methylchromones". *Molecules* **1998**, 3(3), 120-131.
- [227] Devitt, P. F.; Timoney A.; Vickars M. A.; "Synthesis of Heterocyclic-Substituted Chromones and Chalcones". *The Journal of Organic Chemistry* **1961**, 26(12), 4941-4944.
- [228] Geen, G. R.; Giles R. G.; Grinter T. J.; Hayler J. D.; Howie S. L. B.; Johnson G.; Mann I. S.; Novack V. J.; Oxley P. W.; Quick J. K.; Smith N.; "A Direct and High Yielding Route to 2-(5-Tetrazolyl) Substituted Benzopyran-4-ones: Synthesis of Pranlukast". *Synth. Commun.* **1997**, 27(6), 1065-1073.
- [229] Ji, J.-H. Y. Y.-S. Y. R.-Y.; "A Mild and Efficient Procedure for the Preparation of Chromone-2-carboxylates". *Chin. Chem. Lett.* **2006**, 17(8), 1005-1008.
- [230] Dyrager C.; Möllers L. N.; Kjäll L. K.; Alao J. P.; Dinér P.; Wallner F. K.; Sunnerhagen P.; Grøtli M.; "Design, Synthesis, and Biological Evaluation of Chromone-Based p38 MAP Kinase Inhibitors". *J. Med. Chem.* **2011**, 54(20), 7427-7431.
- [231] Ellis G. P., in *Chemistry of Heterocyclic Compounds*, John Wiley & Sons, Inc., **2008**, pp. 495-555..
- [232] Banerji A.; Goomer N. C.; "A New Synthesis of Flavones". *Synthesis* **1980**, 1980(11), 874-875.
- [233] Hirao I.; Yamaguchi M.; Hamada M.; "A Convenient Synthesis of 2- and 2,3-Substituted 4H-Chromen-4-ones". *Synthesis* **1984**, 1984(12), 1076-1078.
- [234] Kaye P. T.; Nchinda A. T.; Gray C. A.; "Chromone studies. Part 11. Synthesis and electron-impact mass spectrometric study of granulysin and side-chain analogues". *J. Chem. Res.(Syn.)* **2002**, 2002(7), 321-325.

- [235] Ellis G. P.; Barker G.; in *Progress in Medicinal Chemistry, Vol. Volume 9* (Eds.: G.P. Ellis, G.B. West), Elsevier, **1973**, pp. 65-116..
- [236] Appleton R. A.; Bantick J. R.; Chamberlain T. R.; Hardern D. N.; Lee T. B.; Pratt A. D.; "Antagonists of slow reacting substance of anaphylaxis. Synthesis of a series of chromone-2-carboxylic acids". *J. Med. Chem.* **1977**, *20*(3), 371-379.
- [237] Hosseinimehr S. J.; Shafiee A.; Mozdarani H.; Akhlagpour S.; Froughizadeh M.; "Radioprotective effects of 2-imino-3-[(chromone-2-yl)carbonyl] thiazolidines against gamma-irradiation in mice". *J. Radiat. Res.* **2002**, *43*(3), 293-300.
- [238] Hadjeri M.; Barbier M.; Ronot X.; Mariotte A.-M.; Boumendjel A.; Boutonnat J.; "Modulation of P-Glycoprotein-Mediated Multidrug Resistance by Flavonoid Derivatives and Analogues". *J. Med. Chem.* **2003**, *46*(11), 2125-2131.
- [239] Li N.-G.; Shi Z.-H.; Tang Y.-P.; Ma H.-Y.; Yang J.-P.; Li B.-Q.; Wang Z.-J.; Song S.-L.; Duan J.-A.; "Synthetic strategies in the construction of chromones". *J. Heterocycl. Chem.* **2010**, *47*(4), 785-799.
- [240] Lee K. S.; Seo S. H.; Lee Y. H.; Kim H. D.; Son M. H.; Chung B. Y.; Lee J. Y.; Jin C.; Lee Y. S.; "Synthesis and biological evaluation of chromone carboxamides as calpain inhibitors". *Bioorg. Med. Chem. Lett.* **2005**, *15*(11), 2857-2860.
- [241] Hosseinimehr S. J.; Emami S.; Taghdisi S. M.; Akhlaghpour S.; "5,7-Dihydroxychromone-2-carboxylic acid and its transition-metal (Mn and Zn) chelates as non-thiol radioprotective agents". *Eur. J. Med. Chem.* **2008**, *43*(3), 557-561.
- [242] Looker J. H.; McMechan J. H.; Mader J. W.; "An amine solvent modification of the Kostanecki-Robinson reaction. Application to the synthesis of flavonols". *J. Org. Chem.* **1978**, *43*(12), 2344-2347.
- [243] Irgashev R. A.; Sosnovskikh V. Y.; Kalinovich N.; Kazakova O.; Röschenhalter G.-V.; "Methyl 2-methoxytetrafluoropropionate as a synthetic equivalent of methyl trifluoropyruvate in the Claisen condensation. The first synthesis of 2-(trifluoroacetyl)chromones and 5-aryl-2-hydroxy-2-(trifluoromethyl)furan-3(2H)-ones". *Tetrahedron Lett.* **2009**, *50*(34), 4903-4905.
- [244] Costantino L.; Rastelli G.; Gamberini M. C.; Vinson J. A.; Bose P.; Iannone A.; Staffieri M.; Antolini L.; Del Corso A.; Mura U.; Albasini A.; "1-Benzopyran-4-one Antioxidants as Aldose Reductase Inhibitors". *J. Med. Chem.* **1999**, *42*(11), 1881-1893.
- [245] Kumar, R.; Johar R.; Aggarwal A. K., "Synthesis, structural elucidation and antimicrobial effectiveness of coordination entities of cobalt (II) and nickel (II) derived from 9,17-diaza-2,6,11,15-tetrathia-1,7,10,16-(1,2)-tetrabenzencyclooctadecaphan-8,17-diene". *Eur. J. Chem.* **2012**, *3*(1), 57-64.

- [246] Mozingo R.; "2-Ethylchromone". *Org. Synth. Coll.* **1955**, *III*, 387.
- [247] Sonar A. S.; Dandale S. G.; Solanki P. R.; "A Facile Microwave Assisted Synthesis and Antimicrobial Activity of Some Active Intermediates ". *J. Chem. Pharm. Res.* **2011**, *3*(6), 752-758.
- [248] Li J.-J.; Corey E. J.; in *Name Reactions in Heterocyclic Chemistry*, John Wiley & Sons, Inc., **2005**, pp. 495-543..
- [249] Shokol T. V.; Turov A. V.; Khilya V. P.; "2-R-7-Hydroxy-8-methyl-3-(2-quinolyl)chromones". *Chem. Heterocycl. Comp.* **2005**, *41*(3), 354-361.
- [250] Frasinuk M.; Khilya V.; "Chemistry of hetero analogs of isoflavones 26. Synthesis of 2-alkyl derivatives of 3-(thiazol-2-yl)-and 3-(benzothiazol-2-yl)chromones". *Chem. Heterocycl. Comp.* **2008**, *44*(6), 666-670.
- [251] Javed T.; Kahlon S. S.; "Multi-step synthesis of benzopyranones via a key step involving reaction of the intermediate compound with phenyltrimethylammonium tribromide". *J. Heterocycl. Chem.* **2002**, *39*(4), 627-630.
- [252] Nohara A.; Umetani T.; Sanno Y.; "Studies on antianaphylactic agents—I : A facile synthesis of 4-oxo-4H-1-benzopyran-3-carboxaldehydes by Vilsmeier reagents". *Tetrahedron* **1974**, *30*(19), 3553-3561.
- [253] Vasselin D. A.; Westwell A. D.; Matthews C. S.; Bradshaw T. D.; Stevens M. F. G.; "Structural Studies on Bioactive Compounds. 40.1 Synthesis and Biological Properties of Fluoro-, Methoxyl-, and Amino-Substituted 3-Phenyl-4H-1-benzopyran-4-ones and a Comparison of Their Antitumor Activities with the Activities of Related 2-Phenylbenzothiazoles". *J. Med. Chem.* **2006**, *49*(13), 3973-3981.
- [254] Ali, M. M.;Sana S.;Tasneem;Rajanna K. C.;Saiprakash P. K.; "Ultrasonically Accelerated Vilsmeier Haack Cyclisation and Formylation Reactions". *Synth. Commun.* **2002**, *32*(9), 1351-1356.
- [255] Borrell J. I.; Teixidó J.; Schuler E.; Michelotti E.; "Solid-supported synthetic equivalents of 3-formylchromone and chromone". *Tetrahedron Lett.* **2001**, *42*(31), 5331-5334.
- [256] Dorofeenko G. N.; Tkachenko V. V.; "Synthesis of 4-alkoxybenzopyrylium salts and chromones". *Chem. Heterocycl. Comp.* **1972**, *8*(8), 935-938.
- [257] Jaen J. C.; Wise L. D.; Heffner T. G.; Pugsley T. A.; Meltzer L. T.; "Dopamine autoreceptor agonists as potential antipsychotics. 2. (Aminoalkoxy)-4H-1-benzopyran-4-ones". *J. Med. Chem.* **1991**, *34*(1), 248-256.
- [258] Lubbe M.; Appel B.; Flemming A.; Fischer C.; Langer P.; "Synthesis of 7-hydroxy-2-(2-hydroxybenzoyl)benzo[c]chromen-6-ones by sequential

- application of domino reactions of 1,3-bis(silyl enol ethers) with benzopyrylium triflates". *Tetrahedron* **2006**, 62(50), 11755-11759.
- [259] Ellis G. P.; in *Chemistry of Heterocyclic Compounds*, John Wiley & Sons, Inc., **1977**, pp. 495-555..
- [260] Bolós J.; Gubert S.; Anglada L.; Planas J. M.; Burgarolas C.; Castelló J. M.; Sacristán A.; Ortiz J. A.; "7-[3-(1-Piperidinyl)propoxy]chromenones as Potential Atypical Antipsychotics". *J. Med.Chem.* **1996**, 39(15), 2962-2970.
- [261] Oyman U.; Gunaydin K.; "Condensation of Ethyl Acetoacetate with Naphthalene-Diols. The Synthesis of some Novel Coumarins and Chromones. Part 1". *Bull. Soc. Chim. Belg.* **1994**, 103(12), 763-764.
- [262] Li J. J.; Corey E. J.; in *Name Reactions in Heterocyclic Chemistry II*, John Wiley & Sons, Inc., **2011**, pp. 401-513..
- [263] Fillion E.; Dumas A. M.; Kuropatwa B. A.; Malhotra N. R.; Sitler T. C.; "Yb(OTf)₃-Catalyzed Reactions of 5-Alkylidene Meldrum's Acids with Phenols: One-Pot Assembly of 3,4-Dihydrocoumarins, 4-Chromanones, Coumarins, and Chromones". *J. Org. Chem.* **2005**, 71(1), 409-412.
- [264] Obrecht D.; "Acid-Catalyzed Cyclization Reactions of Substituted Acetylenic Ketones: A new Approach for the Synthesis of 3-Halofurans, Flavones, and Styrylchromones". *Helv. Chim. Acta* **1989**, 72(3), 447-456.
- [265] Kumar P.; Bodas M. S.; "A Novel Synthesis of 4H-Chromen-4-ones via Intramolecular Wittig Reaction". *Org. Lett.* **2000**, 2(24), 3821-3823.
- [266] Jung, J.-C.; Min J.-P.; Park O.-S.; "A Highly Practical Route to 2-Methylchromones from 2-Acetoxybenzoic Acids". *Synth. Commun.* **2001**, 31(12), 1837-1845.
- [267] Nixon N. S.; Scheinmann F.; Suschitzky J. L.; "Heterocyclic syntheses with allene-1,3-dicarboxylic esters and acids : new chromene, chromone, quinolone, α -pyrone and coumarin syntheses". *Tetrahedron Lett.* **1983**, 24(6), 597-600.
- [268] Pochat F.; L'Haridon P.; "New Substituted Derivatives of Benzopyran and Chromone". *Synth. Commun.* **1998**, 28(6), 957-962.
- [269] Athanasellis G.; Melagraki G.; Afantitis A.; Makridima K.; Igglessi-Markopoulou O.; "A simple synthesis of functionalized 2-amino-3-cyano-4-chromones by application of the N-hydroxybenzotriazole methodology". *Arkivoc* **2006**, 2006(10), 28-34.
- [270] Yang Q.; Alper H.; "Synthesis of Chromones via Palladium-Catalyzed Ligand-Free Cyclocarbonylation of o-Iodophenols with Terminal Acetylenes in Phosphonium Salt Ionic Liquids". *J. Org. Chem.* **2010**, 75(3), 948-950.

- [271] Lin C.-F.; Lu W.-D.; Wang I. W.; Wu M.-J.; "Synthesis of 2-(Diarylmethylene)-3-benzofuranones Promoted via Palladium-Catalyzed Reactions of Aryl iodides with 3-Aryl-1-(2- tert-butyldimethyl-silyloxy)phenyl-2-propyn-1-ones". *Synlett* **2003**, 2003(13), 2057-2061.
- [272] Liang B.; Huang M.; You Z.; Xiong Z.; Lu K.; Fathi R.; Chen J.; Yang Z.; "Pd-Catalyzed Copper-Free Carbonylative Sonogashira Reaction of Aryl Iodides with Alkynes for the Synthesis of Alkynyl Ketones and Flavones by Using Water as a Solvent". *J. Org. Chem.* **2005**, 70(15), 6097-6100.
- [273] Wen L.; Zhang H.; Lin H.; Shen Q.; Lu L.; "A facile synthetic route to 2-trifluoromethyl-substituted polyfunctionalized chromenes and chromones". *J. Fluorine Chem.* **2012**, 133(0), 171-177.
- [274] Vedachalam S.; Zeng J.; Gorityala B. K.; Antonio M.; Liu X.-W.; "N-Heterocyclic Carbene-Catalyzed Intramolecular Aldehyde–Nitrile Cross Coupling: An Easy Access to 3- Aminochromones". *Org. Lett.* **2010**, 12(2), 352-355.
- [275] Vedachalam S.; Wong Q.-L.; Maji B.; Zeng J.; Ma J.; Liu X.-W.; "N-Heterocyclic Carbene Catalyzed Intramolecular Hydroacylation of Activated Alkynes: Synthesis of Chromones". *Adv. Synth. Catal.* **2011**, 353(2-3), 219-225.
- [276] Kapoor R. P.; Singh O. V.; Garg C. P.; "Dehydrogenation of Chromanones Using DMSO-I₂-H₂SO₄ and DMSO-I₂ Systems - a Convenient Route for the Synthesis of Chromones". *J. Indian Chem. Soc.* **1991**, 68(6), 367-368.
- [277] Hila J. E.; Tsitinitsamis M.; Hamon M.; Delcroix J. P.; "Oxidation of 4-Chromanol and 4-Chromanone by Vanadium Pentoxide in Sulfuric-Acid 2.5 M". *Analusis* **1982**, 10(5), 220-224.
- [278] Shanker C. G.; Mallaiah B. V.; Srimannarayana G.; "Dehydrogenation of Chromanones and Flavanones by 2,3-Dichloro-5,6-Dicyano-1,4-Benzoquinone (Ddq) - a Facile Method for the Synthesis of Chromones and Flavones". *Synthesis-Stuttgart* **1983**(4), 310-311.
- [279] Clarke D. S.; Gabbutt C. D.; Hepworth J. D.; Heron B. M.; "Synthesis of 3-alkenyl-2-arylchromones and 2,3-dialkenylchromones via acid-catalysed retro-Michael ring opening of 3-acylchroman-4-ones". *Tetrahedron Lett.* **2005**, 46(33), 5515-5519.
- [280] Sosnovskikh V. Y.; Irgashev R. A.; "A novel and convenient synthesis of 3-(polyhaloacyl)chromones using diethoxymethyl acetate". *Synlett* **2005**(7), 1164-1166.
- [281] Sosnovskikh V. Y.; Irgashev R. A.; Barabanov M. A.; "3-(Polyhaloacyl)chromones and their Hetero Analogues: Synthesis and Reactions with Amines". *Synthesis* **2006**, 2707-2718.

- [282] Singh O. V.; George V.; "Thallium(III) P-Tosylate Mediated Oxidative Rearrangement in Substituted Chromanones - a Novel-Approach to the Synthesis of Substituted Chromones and Tetrahydroxanthones". *Indian J. Chem. - Section B* **1995**, 34(10), 856-864.
- [283] Santhosh K. C.; Balasubramanian K. K.; "A Facile Synthesis of 3-Alkylchromanones and Chromones". *Tetrahedron Lett.* **1991**, 32(52), 7727-7730.
- [284] Mandal P. V.; Venkateswaran R.; "Lewis Acid-catalysed Facile Elimination of the Diazo Group in 3-Diazo chromanones. Novel Conversion of Chromanones into Chromones". *J. Chem. Res. Syn* **1998**(2), 88-89.
- [285] Bayer V.; Pastor R. E.; Cambon A. R.; "Synthesis of 2-F-Alkyl Chromones and Evidence of Their Reaction Intermediates". *J. Fluorine Chem.* **1982**, 20(4), 497-505.
- [286] Patonay T.; Dinya Z.; Levai A.; Molnar D.; "Reactivity of alpha-arylidene benzoheteracyclanone dibromides toward azide ion: an effective approach to 3-(alpha-substituted-benzyl)chromones and 1-thiochromones". *Tetrahedron* **2001**, 57(14), 2895-2907.
- [287] Venkati M.; Krupadanam G. L. D.; "A new synthesis of cis-3-substituted chroman-4-ols". *Synth. Commun.* **2002**, 32(14), 2227-2235.
- [288] Fridén-Saxin M.; Pemberton N.; Silva A. K.; Dyrager C.; Friberg A.; Grøtli M.; Luthman K.; "Synthesis of 2-Alkyl-Substituted Chromone Derivatives Using Microwave Irradiation". *J. Org. Chem.* **2009**, 74(7), 2755-2759.
- [289] Rode M.; Gupta R. C.; Karale B. K.; Rindhe S. S.; "Synthesis and characterization of some substituted chromones as an anti-infective and antioxidant agents". *J. Heterocycl. Chem.* **2008**, 45(6), 1597-1602.
- [290] Walenzyk T.; Carola C.; Buchholz H.; König B.; "Chromone derivatives which bind to human hair". *Tetrahedron* **2005**, 61(31), 7366-7377.
- [291] Baziard-Mouysset G.; Younes S.; Labssita Y.; Payard M.; Caignard D.-H.; Rettori M.-C.; Renard P.; Pfeiffer B.; Guardiola-Lemaitre B.; "Synthesis and structure-activity relationships of novel 2-amino alkyl chromones and related derivatives as a site-selective ligands". *Eur. J. Med. Chem.* **1998**, 33(5), 339-347.
- [292] Araya-Maturana R.; Heredia-Moya J.; Pessoa-Mahana H.; Weiss-López B.; "Improved Selective Reduction of 3-Formylchromones Using Basic Alumina and 2-Propanol". *Synth. Commun.* **2003**, 33(18), 3225-3231.
- [293] Ishizuka N.; Matsumura K.-I.; Sakai K.; Fujimoto M.; Mihara S.-I.; Yamamori T.; "Structure-Activity Relationships of a Novel Class of Endothelin-A Receptor

- Antagonists and Discovery of Potent and Selective Receptor Antagonist, 2-(Benzo[1,3]dioxol-5-yl)-6-isopropoxy-4-(4-methoxyphenyl)-2H-chromene-3-carboxylic Acid (S-1255). 1. Study on Structure–Activity Relationships and Basic Structure Crucial for ETA Antagonism". *J. Med. Chem.* **2002**, 45(10), 2041-2055.
- [294] Sosnovskikh V. Y.; Irgashev R. A.; "Uncatalyzed addition of indoles and N-methylpyrrole to 3-formylchromones: synthesis of (chromon-3-yl)bis(indol-3-yl)methanes and E-2-hydroxy-3-(1-methylpyrrol-2-ylmethylene)chroman-4-ones under solvent-free conditions". *Tetrahedron Lett.* **2007**, 48(42), 7436-7439.
- [295] Terzidis M.; Tsoleridis C. A.; Stephanidou-Stephanatou J.; "Reaction of chromone-3-carboxaldehydes with TOSMIC: synthesis of 4-(2-hydroxybenzoyl)pyrroles". *Tetrahedron* **2007**, 63(33), 7828-7832.
- [296] Mohammed-Musthafa T. N.; Siddiqui Z.; Husain F.; Ahmad I.; "Microwave-assisted solvent-free synthesis of biologically active novel heterocycles from 3-formylchromones". *Med. Chem. Res.* **2011**, 20(9), 1473-1481.
- [297] El-Shaaer H. M.; Foltínová P.; Lácová M.; Chovancová J.; Stankovičová H.; "Synthesis, antimicrobial activity and bleaching effect of some reaction products of 4-oxo-4H-benzopyran-3-carboxaldehydes with aminobenzothiazoles and hydrazides". *Il Farmaco* **1998**, 53(3), 224-232.
- [298] Tsao L.; Chzhan L.; Lyu T.; "Synthesis of 3-(3'-Acetyl-5'-aroyl-1',3',4'-oxadiazolyl-2')-chromones". *Chem. Nat. Compd.* **2001**, 37(4), 311-314.
- [299] Cao L.; Wang W.; "Synthesis of 3-(5-Aryl-1,3,4-oxadiazol-2-yl)chromones". *Chem. Heterocycl. Comp.* **2003**, 39(8), 1072-1075.
- [300] Cao, L.;Zhang L.;Liu J. J.; "Synthesis of 3-(3-Acetyl-5-aryl-2,3-dihydro-1,3,4-oxadiazol-2-yl)chromones". *Chem. Heterocycl. Comp.* **2004**, 40(2), 214-218.
- [301] Kaspentakis G. C.; Tsoleridis C. A.; Stephanidou-Stephanatou J.; "Reaction of 3-formylchromone-N-benzoylhydrazone with ketenes. Synthesis and structural studies of chromone 1,3,4-oxadiazolines". *J. Heterocycl. Chem.* **2007**, 44(2), 425-430.
- [302] Diwakar S. D.; Joshi R. S.; Gill C. H.; "Synthesis and in vitro antibacterial assessment of novel chromones featuring 1,2,4-oxadiazole". *J. Heterocycl. Chem.* **2011**, 48(4), 882-887.
- [303] Kumar S.; Singh B. K.; Pandey A. K.; Kumar A.; Sharma S. K.; Raj H. G.;Prasad A. K.; Eycken E. V.; Parmar V. S.; Ghosh B.; "A chromone analog inhibits TNF- α induced expression of cell adhesion molecules on human endothelial cells via blocking NF- κ B activation". *Biorg. Med. Chem.* **2007**, 15(8), 2952-2962.

- [304] Siddiqui Z. N.; Musthafa T. N. M.; "An efficient and novel synthesis of chromonyl chalcones using recyclable Zn(I-proline)₂ catalyst in water". *Tetrahedron Lett.* **2011**, 52(31), 4008-4013.
- [305] Patonay T.; Kiss-Szikszai A.; Silva V. M. L.; Silva A. M. S.; Pinto D. C. G. A.; Cavaleiro J. A. S.; Jekő J.; "Microwave-Induced Synthesis and Regio- and Stereoselective Epoxidation of 3-Styrylchromones". *Eur. J. Org. Chem.* **2008**, 2008(11), 1937-1946.
- [306] Hadjeri M.; Barbier M.; Ronot X.; Mariotte A. M.; Boumendjel A.; Boutonnat J.; "Modulation of P-glycoprotein-mediated multidrug resistance by flavonoid derivatives and analogues". *J. Med. Chem.* **2003**, 46(11), 2125-2131.
- [307] Sabitha G.; "3-Formylchromone as a versatile synthon in heterocyclic chemistry". *Aldrichim. Acta* **1996**, 29, 13-25.
- [308] Smith M. B.; March J.; in *March's Advanced Organic Chemistry*, John Wiley & Sons, Inc., **2006**, pp. 1703-1869..
- [309] Mazzei M.; Ermili A.; Balbi A.; "Chemical and pharmacological research on pyran derivatives. XVII - Synthesis of 2-(dialkylamino)-5-hydroxychromones and their transformation to derivatives of 2H-pyran[4,3,2]-1-benzopyran". // *Farmaco* **1986**, 41(8), 611-621.
- [310] Du L.; Pertsemliadis A.; "Cancer and neurodegenerative disorders: pathogenic convergence through microRNA regulation". *J. Mol. Cell. Biol.* **2011**.
- [311] West A. B.; Dawson V. L.; Dawson T. M.; "To die or grow: Parkinson's disease and cancer". *Trends Neurosci.* **2005**, 28(7), 348-352.
- [312] D'Amelio M.; Ragonese P.; Sconzo G.; Aridon P.; Savettieri G.; "Parkinson's Disease and Cancer". *Ann. N. Y. Acad. Sci.* **2009**, 1155(1), 324-334.
- [313] Devine M. J.; Plun-Favreau H.; Wood N. W.; "Parkinson's disease and cancer: two wars, one front". *Nat. Rev. Cancer* **2011**, 11(11), 812-823.
- [314] Bajaj A.; Driver J.; Schernhammer E.; "Parkinson's disease and cancer risk: a systematic review and meta-analysis". *CCC* **2010**, 21(5), 697-707.
- [315] Fiala K. H.; Whetteckey J.; Manyam B. V.; "Malignant melanoma and levodopa in Parkinson's disease: causality or coincidence?". *Parkinsonism Relat. Disord.* **2003**, 9(6), 321-327.
- [316] Tianhong L.; Yanxin S.; An X.; "Integration of large scale fertilizing models with GIS using minimum unit". *Environ. Model. Software* **2003**, 18(3), 221-229.
- [317] Pan T.; Li X.; Jankovic J.; "The association between Parkinson's disease and melanoma". *Int. J. Cancer* **2011**, 128(10), 2251-2260.
- [318] Hebron M. L.; Lonskaya I.; Moussa C. E. H.; "Nilotinib reverses loss of dopamine neurons and improves motor behavior via autophagic degradation of

- α -synuclein in parkinson's disease models". *Hum. Mol. Genet.* **2013**, 22(16), 3315-3328.
- [319] Fishman P.; Bar-Yehuda S.;Synowitz M.;Powell J. D.;Klotz K. N.;Gessi S.;Borea P. A.; "Adenosine receptors and cancer". *Handb. Exp. Pharmacol.* **2009**(193), 399-441.
- [320] Jacobson K. A.; Klutz A. M.; Tosh D. K.;Ivanov A. A.; Preti D.; Baraldi P. G.; "Medicinal chemistry of the A3 adenosine receptor: agonists, antagonists, and receptor engineering". *Handb. Exp. Pharmacol.* **2009**(193), 123-159.
- [321] Fishman P.; Bar-Yehuda S.;Varani K.;Gessi S.;Merighi S.;Borea P., in *A3 Adenosine Receptors from Cell Biology to Pharmacology and Therapeutics* (Ed.: P.A. Borea), Springer Netherlands, **2010**, pp. 301-317.
- [322] Jacobson K.; Gao Z.-G.;Tosh D.; Sanjayan G.; Castro S.; in *A3 Adenosine Receptors from Cell Biology to Pharmacology and Therapeutics* (Ed.: P.A. Borea), Springer Netherlands, **2010**, pp. 93-120.
- [323] Baraldi P.; Romagnoli R.; Saponaro G.; Baraldi S.; Tabrizi M.;Preti D.; in *A3 Adenosine Receptors from Cell Biology to Pharmacology and Therapeutics* (Ed.: P.A. Borea), Springer Netherlands, **2010**, pp. 121-147.
- [324] Rugbjerg K.; Friis S.; Lassen C. F.; Ritz B.; Olsen J. H.; "Malignant melanoma, breast cancer and other cancers in patients with Parkinson's disease". *Int. J. Cancer* **2012**, 131(8), 1904-1911.